INFORMATION TO USERS

This manuscript has been reproduced from the microfilm master. UMI films the text directly from the original or copy submitted. Thus, some thesis and dissertation copies are in typewriter face, while others may be from any type of computer printer.

The quality of this reproduction is dependent upon the quality of the copy submitted. Broken or indistinct print, colored or poor quality illustrations and photographs, print bleedthrough, substandard margins, and improper alignment can adversely affect reproduction.

In the unlikely event that the author did not send UMI a complete manuscript and there are missing pages, these will be noted. Also, if unauthorized copyright material had to be removed, a note will indicate the deletion.

Oversize materials (e.g., maps, drawings, charts) are reproduced by sectioning the original, beginning at the upper left-hand corner and continuing from left to right in equal sections with small overlaps.

Photographs included in the original manuscript have been reproduced xerographically in this copy. Higher quality 6" x 9" black and white photographic prints are available for any photographs or illustrations appearing in this copy for an additional charge. Contact UMI directly to order.

ProQuest Information and Learning
300 North Zeeb Road, Ann Arbor, MI 48106-1346 USA
800-521-0600

INSTABILITY AND FINGERING OF DNAPL BELOW THE WATER TABLE

by

Alexandre Tartakovski

A Dissertation Submitted to the Faculty of the

DEPARTMENT OF HYDROLOGY AND WATER RESOURCES

In Partial Fulfillment of the Requirements
For the Degree of

DOCTOR OF PHILOSOPHY
WITH A MAJOR IN HYDROLOGY

In the Graduate College

THE UNIVERSITY OF ARIZONA

2002

THE UNIVERSITY OF ARIZONA ®
GRADUATE COLLEGE

As members of the Final Examination Committee, we certify that we have read the dissertation prepared by Alexandre Miron Tartakovski

entitled Instability and fingering of Dense Non-Aqueous Phase Liquid below the water table

and recommend that it be accepted as fulfilling the dissertation requirement for the Degree of Doctor of Philosophy

Shlomo P Neuman	2/25/02 Date
Tian-Chyi J Yeh	2/25/02 Date
Thomas Maddock III	2/25/02 Date
A. Eduardo Saez	2/25/02 Date
Roberto Guzman	2/25/02 Date

Final approval and acceptance of this dissertation is contingent upon the candidate's submission of the final copy of the dissertation to the Graduate College.

I hereby certify that I have read this dissertation prepared under my direction and recommend that it be accepted as fulfilling the dissertation requirement.

Dissertation Director — 2/25/02 Date

Shlomo P. Neuman

STATEMENT BY AUTHOR

This dissertation has been submitted in partial fulfillment of requirements for an dvanced degree at The University of Arizona and is deposited in the University Library to be made available to borrowers under rules of the Library.

Brief quotations from this dissertation are allowable without special permission, provided that accurate acknowledgment of source is made. Requests for permission for extended quotation from or reproduction of this manuscript in whole or in part may be granted by the head of the major department or the Dean of the Graduate College when in his or her judgment the proposed use of the material is in the interests of scholarship. In all other instances, however, permission must be obtained from the author.

SIGNED: 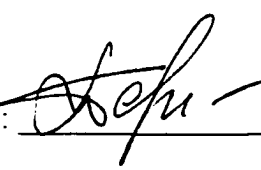

ACKNOWLEDGMENTS

I am grateful to my advisor Dr. Shlomo Neuman, who has provided me generous financial and moral support in the past four years. I am indebted for his guidance and patience. Dr. Neuman carefully edited every word of this dissertation. This research was supported through Dr. Neuman by the EPA STAR Program Grant NR 836157-01-1.

I would like to express my gratitude to my other committee members, Drs. Tian-Chyi J Yeh, Tom Maddock III, Eduardo Saez and Roberto Guzman for their editing of an original draft of this dissertation.

I am especially thankful to my brother, Daniel Tartakovsky for his advice and encouragement.

I also would like to thank Dr. David Kessler for providing valuable comments and suggestions on this research.

My study has benefited from discussions among my officemates and friends: Yunjung Hyun, Abel Hernandez, Wenbin Wang, Velimir Vesselinov, Walter Illman, Donghai Wang and Ming Ye.

Finally, my gratitude to my wife, Guzel and daughter, Masha for their infinite patience and support.

DEDICATION

To

My parents Nina and Miron Tartakovsky

My wife Guzel

And

My daughter Maria

TABLE OF CONTESTS

TABLE OF CONTENT - *Continued*

TABLE OF CONTENT - *Continued*

TABLE OF CONTENT - *Continued*

LIST OF FIGURES

LIST OF FIGURES-*Continued*

LIST OF FIGURES-*Continued*

LIST OF FIGURES-*Continued*

LIST OF FIGURES-*Continued*

LIST OF FIGURES-*Continued*

LIST OF FIGURES-*Continued*

ABSTRACT

We analyze the movement of DNAPL in a three-dimensional randomly heterogeneous porous medium, saturated with water, that is initially pooled above a water table or flows at a constant flux. We consider the front to form a sharp boundary at which the capillary pressure head, assumed equal to the entry pressure head of DNAPL, is prescribed either deterministically or randomly; treat log conductivity as a statistically homogeneous random field with given mean, variance and covariance; cast the corresponding boundary-value problem in the form of an integro-differential equation, in which the parameters and domain of integration are random; expand this equation in a Taylor series about the mean position of the front; and take ensemble mean. To quantify the predictive uncertainty associated with this mean solution, we develop a set of integro-differential equations for the corresponding second ensemble moments. We solve the resulting moment equations analytically and numerically in one and two dimensions to second order in the standard deviation of log conductivity. A comparison of our one-dimensional solutions with the results of Monte Carlo simulations verifies its accuracy. We also show that a probabilistic analysis of wetting front instability due to Chen and Neuman (1996) applies to a DNAPL front.

CHAPTER 1

INTRODUCTION

1.1 DNAPL behavior in porous media

Chlorinated organic solvents such as TCE and PCE are among the most ubiquitous and problematic groundwater contaminants. They usually enter the subsurface in the form of organic liquids which exhibit low miscibility with water and are heavier (denser), thereby forming a separate dense non-aqueous phase liquid (DNAPL). Being heavier and less viscous than water, DNAPLs have high downward mobility and thus tend to penetrate deep below the water table (Pankow and Cherry, 1996). Their downward movement tends to be unstable and to occur in the form of rapidly advancing narrow fingers (Schwille, 1988).

Though instability and fingering may occur in uniform porous media due to differences in density and viscosity between DNAPL and water across their interface, in non-uniform porous and fractured media they tend to develop preferentially along fractures or channels of elevated permeability. A recent review by Chen et al. (1995) shows that little is known about the manner in which medium heterogeneity affects the development and propagation of unstable fingers between immiscible fluids.

When DNAPLs encounter resistance to downward flow, they spread laterally over low permeability layers and lenses to form shallow pools of free-product, which may be laterally extensive. Though chlorinated solvents are non-wetting on mineral surfaces

relative to water, their interfacial tension with water is low enough to allow penetration into narrow pores and fractures, with relative ease. Upon contact with ground water, DNAPLs dissolve slowly to form plumes of dissolved contaminants, thus forming a long-term source of groundwater contamination. In fractured porous media such as clays, shales and sandstones, much of the DNAPL can end up in dissolved and/or sorbed state within blocks of porous matrix. Together such free-phase, residual, and porous matrix sources can feed large contaminant plumes for decades or centuries.

The distribution of DNAPLs within the source area(s) of contaminant plume(s) is extremely complex. Major deflection in DNAPL movement, and the formation of unstable fingers, often take place due to subtle micro-stratigraphic and micro-structural variation which are seldom resolved at site investigation. Hence, standard methods of site investigation and analysis rarely provide the level of detail needed to generate a reliable picture of the nature and extent of DNAPL below the water table. Such a picture is, however, essential for a detailed analysis of past or future DNAPL migration and for the cost-effective design of remedial measures. The complexity of unresolved small-scale heterogeneities renders the deterministic prediction of DNAPL pathways impossible; even estimates of total DNAPL mass are typically subject to errors of several orders of magnitude. Stochastic methods of analysis should allow accounting for disparities between scales of field investigation and smaller scales at which instabilities and fingers typically develop. Therefore, this work focuses on the question of how random, multiscale heterogeneities in medium properties affect unstable DNAPL migration below the water table.

Instability during immiscible displacement of one fluid by another in porous and fractured media is triggered by unfavorable differences between the viscosities and densities of the two fluids. Viscous forces have a stabilizing influence when a more viscous fluid displaces a less viscous fluid, and a destabilizing influence when a less viscous fluid displaces a more viscous fluid. Both effects increase with the mean propagation speed of the interface. Gravity has a stabilizing influence when the denser fluids is at the bottom, and a destabilizing influence otherwise, regardless of mean flow direction or speed (Chen et al. 1995).

When both viscous and gravitational forces act to stabilize the interface, it is unconditionally stable. When both of these forces act to destabilizing the interface, it is unconditionally unstable. When viscosity is stabilizing and gravity is destabilizing, the interface is stable provided that its mean speed exceeds some critical value. When viscosity is destabilizing and gravity is stabilizing, the interface is stable on condition that its mean speed is below a critical value (Chen et al. 1995).

During the downward propagation of a DNAPL front in a water-saturated subsurface environment, both viscosity and gravity act to destabilize the front. Surface tension has a stabilizing effect on the interface between two immiscible fluids in all cases. Suppose that the interface is perturbed slightly into a composite wave form containing diverse wave lengths (and spatial frequencies) of very small amplitude. If the interface is unstable and there is no surface tension, the amplitudes of all these perturbations (incipient fingers) can initially grow at rates that increase as their wavelengths decrease (frequencies increase). If surface tension is active, only perturbations with wavelength

above some critical value (frequencies below some critical value) can grow, all others decay. The critical wavelength increases with surface tension. The fastest growing perturbation has a wavelength that exceeds critical by a constant factor. The corresponding fingers appear first, and then dominate their neighbors. Smaller fingers often coalesce into one or more dominant finger (Chen et al. 1995).

Under uniform mean flow in homogeneous media, established fingers tend to elongate linearly with time (Chuoke et al. 1959, Gupta et al. 1974). Their rate of elongation increases with mean flow rate and viscosity contrast but decreases with surface tension (Saffman-Taylor, 1958, Chuoke et al. 1959).

Shielding occurs when larger fingers outgrow their smaller neighbors and spread laterally to inhibit their growth. The widening of dominant fingers by shielding reduces surface tension, which may render them unstable. This, in turn, may cause the fingers to split (bifurcate) at their tips into narrower branches, which widen, become unstable, and so on. The cycle of shielding, spreading and splitting may repeat itself periodically (Park and Homsy, 1985; Maxworthy, 1987 and others).

When capillary action is weak and/or mean flow rate is high, bifurcation may continue to yield a contorted, dendritic interface with random fractal geometry (Chang et al. 1994).

Spatial variations in permeability are conducive to the preferential development of fingers along paths of least resistance to flow. Instability in such heterogeneous media may occur under conditions that would not be favorable for the development of fingers in uniform media. This is true on the pore scale, on the laboratory scale, and on the field scale. Experiments by Schwille (1988) have shown that when DNAPL penetrates from

coarse-grained to an underlying fine-grained layer, it propagates downward in the form of narrow, irregular fingers.

1.2 Review of recent experimental work

Recent reviews of experimental works related to instability and fingering during immiscible displacement were published by Chen et al. (1995) and de Rooij (2000). Their reviews indicate that both wetting fronts in unsaturated soils, and DNAPL fronts in saturated porous media, exhibit classic front instability and fingering as described earlier. Here we summarize briefly some additional experimental work done in the last few years.

Longino and Kuper (1999) studied the retention capacity of natural, rough wall fractures by injecting perchlorethylene (PCE) into fractured limestone samples. They found strong correlation between retention capacity (portion of fracture void volume occupied by nonwetting fluid) and capillary number.

Glass et al. (2000) found experimentally that in a heterogeneous soil, gravity can have a stabilizing effect on a DNAPL front (when downward moving DNAPL encounters a capillary barrier with higher DNAPL entry pressure, it temporary stops creating horizontal pools until the pressure difference across the front exceeds the DNAPL entry pressure). According to the authors "nonwetting invasion occurs as a sequence of gravity-stabilized-destabilized displacements within the heterogeneous media. Pore-scale gravity destabilized DNAPL fingers occur in all units as they are entered (by DNAPL), but they

are overwritten by macroscopic gravity-stabilized displacement behind capillary barriers that create backward growing macroscopic pools."

Sililo and Tellam (2000) conducted experiments on wetting front instability in layered sand. They found that (1) stratification tends to enhance rather than dissipate fingering; (2) in discontinuously layered systems, funneling influences the location of fingers; (3) in multilayered systems, lateral flow on top of fine-grained layers promotes greater flux (and more fingers) in the down-dip direction; (4) in systems where a top fine-grained layer has variable thickness finger frequency and the amount of flow will be greatest where the fine-grained layer is thinnest; (5) surface depressions in an upper fine-grained layer will concentrate flow, with fingers forming below such areas; and (6) in systems where an upper fine-grained layer has macropores, the latter will concentrate water flow and fingers will form directly below these zones. Sililo and Tellam found that fingers could persist in the same locations from one recharge event to another.

Zhang and Smith (2001) observed that vertical displacement of water by ponded, less viscous DNAPL is unstable, confirming the destabilizing effect of gravity. They also observed that fingering does not commence until the pressure difference across the fluid interface exceeds the DNAPL entry pressure.

Difficulties in reproducing experiments with immiscible fronts across different but essentially identical samples of the same granular material were reported by van Dam et al. (1994). Similar difficulties were reported by Hollenback and Jensen (1998) in reproducing measurements on a single sample sequentially in time. Discrepancies were found also between soil properties (retention capacity, capillary pressure, relative

permeability) measured during immiscible displacement using different methods (e.g., Stolte et al. 1994) and at different scales (e.g., Kasteell et al. 1999).

Mortensen et al. (2001) attributed this lack of reproducibility to "slight differences in initial conditions, internal sample heterogeneity, contact between sample and boundary conditions, microbial growth, changing fluid-fluid-solid contact angles, swelling and consolidation of the sample, disturbances in experiments while making measurements".

1.3 Continuum or pore scale approach?

Hydrologic properties show spatial variations on various scales: on the laboratory scale due to variations in pore size and geometry and on the field scale due to depositional irregularity and fracturing. Theories of flow in porous media are generally based on and supported by laboratory experiments.

At the pore scale, fluid flow is governed by the Navier-Stokes equation. However, it is not practical to describe flow in all individual pores of the medium mathematically. In practice, one is interested mainly in average, macroscopic descriptions of flow over volumes of the medium that allow measurement of system parameters and states. Details of flow on scales smaller than such macroscopic support volumes are ignored. Parameters and states measured or defined on macroscopic support volumes are ascribed to the center of the volume and considered to be functions of space, defined over a continuum of such points.

Heterogeneity depends on the size of the support volume. Soil properties measured on a small support scale may exhibit rapid and large spatial fluctuations; both the frequency and the amplitude of these fluctuations diminish as the support volume increases.

Based on experiments by Glass et al. (2000), it was suggested by Glass et al. (2001) that it would be difficult to simulate a nonwetting invasion process using porous continuum approaches. The experiments have revealed "a nonwetting invasion structure as a set of macroscopic pools connected by pore-scale fingers". Glass et al. (2000) questioned "whether two-face, porous continuum scale modeling would be able to capture the unstable lithology-driven migration behavior found in our (Glass et al. 2000) experiments, given the intrinsic pore-scale nature of finger formation and propagation, together with the local nature of the failure of capillary barriers." Glass et al. (2000) identified the length scales that describe such pools and finger geometry. Glass et al. (2001) proposed a growth model that assembles these length scales and allows one to model nonwetting phase migration in a heterogeneous medium. Based on good agreement between simulated and observed results, Glass (2001) argued that near pore scale simulation approaches capture better the complexity of immiscible displacement than do models based on traditional continuum approaches.

Yet classical porous continuum approaches (Saffman and Taylor, 1958; Chuoke et al. 1959; Raats 1973; Philip 1976; Neuman 1982; Chen and Neuman 1996; Wang et al. 1998b; Smith and Zhang 2001, Tartakovsky and Winter 2001; and many others) have proven successful in predicting such fundamental characteristics of immiscible displacement as the onset of instability, mean distance between adjacent fingers, shape

and mean propagation rate of fingers, etc. We shall therefore base our discussion on the standard porous continuum approach.

1.4 Theoretical analyses of immiscible displacement based on continuum approach

Most analyses of immiscible displacement are based on the assumption that a sharp front forms between the two fluids. Recent reviews of theories related to instability and fingering during immiscible displacement is given by Chen et al. (1995) and de Rooij (2000).

One of the earliest analyses of front instability in a Hele-Shaw cell (an analogue of an ideal fracture) is that by Saffman and Taylor (1958).

Consider a fracture of infinite extent and constant aperture b (Figure 1.1). Two immiscible fluids, 1 and 2, completely fill the gap between the fracture wall. The fluids are separated by a sharp front coinciding with the x axis. The y axis is perpendicular to the front, pointing upward. Assume that at time t=0 the interface is perturbed slightly into a wave form. A single harmonic of this wave can be described by $y = \eta(x,t) = \varepsilon \exp(inx + \sigma t)$, where $i = \sqrt{-1}$, n is a wave number, ε is a small positive constant, and σ is a growth factor. The wave grows in magnitude (the front becomes unstable) if σ is positive, and diminishes (the front is stable) if σ is negative. One of the difficulties in predicting the dynamics of the fingering process is describing correctly fluid pressure variations across the interface (Glass et al., 1991). To do so, Saffman-

Taylor (1958) employed Laplace's formula which for sufficiently small wave amplitudes can be written as

$$p_1 - p_2 = T\frac{\partial^2 \eta}{\partial x^2} \pm \frac{2T\cos\theta}{b}. \tag{1.1}$$

Here T is a surface tension coefficient, θ is contact angle between fracture wall and wetting fluid, and the sign is positive or negative depending on whether 2 or 1 is the wetting fluid. This lead Saffman and Taylor (1958) to the following instability criterion

$$\left(\frac{\mu_1}{k_1} + \frac{\mu_2}{k_2}\right)\frac{\sigma}{n} = \left(\frac{\mu_1}{k_1} - \frac{\mu_2}{k_2}\right)U + (\rho_1 - \rho_2)g - Tn^2 \tag{1.2}$$

where μ_1 and μ_2 are the viscosities of fluids 1 and 2, ρ_1 and ρ_2 are their densities, k_i are permeabilities which in the case of an ideal fracture are equal to $b^2/12$, and U is the front velocity.

For σ to be positive so as to cause the wave to grow, one must have

$$\left(\frac{\mu_1}{k_1} - \frac{\mu_2}{k_2}\right)U + (\rho_1 - \rho_2)g - Tn^2 > 0 \tag{1.3}$$

This is similar to a criterion derived earlier by Hill (1952) except that it accounts for surface tension.

Chuoke et al. (1959) extended the analysis of Saffman and Taylor to porous media and obtained an instability criterion similar to (1.2). However, instead of (1.1) he wrote

$$p_1 - p_2 = T^*\nabla^2\eta + p_c(t) \tag{1.4}$$

where T^* is an effective (macroscopic) surface tension coefficient and $p_c(t)$ is related to cappilary pressure drop across microscopic interfaces but does not depend on the

curvature of the macroscopic interface, only on time. Chuoke et al. based their concept of T^* on heuristic energy arguments. By matching wavelengths predicted by their theory to measured wavelength during the displacement of oil by water in a medium of glass beads, Chuoke et al. determined that $T^*=CT$ where C=7.6.

Raats (1973) studied the instability of a sharp Green and Ampt (1911) wetting front during infiltration into a dry soil. He noted (based on intuition) that the wetting front would break up into fingers if the velocity of the front would increase with depth L ($dU/dL < 0$). He also noted that infiltration of water into a soil without the possibility of air escaping would lead to an unstable front with downward moving fingers of water interspaced with fingers of air moving up.

Philip (1975) combined the work of Saffman and Taylor (1958) and Raats (1973) by applying linear stability analysis to Green-Ampt infiltration. He placed Raats's (1973) analysis on a more rigorous footing. According to Philip's criterion, a front is unstable if the gradient of pressure head immediately above it opposes the flow:

$$\frac{1}{\rho g}\frac{\partial p}{\partial z} < 0 \tag{1.5}$$

where z is the vertical coordinate (positive upwards). A continuous or sudden increase in permeability with depth across the wetting front tends to destabilize it. Wang et al. (1998b) tested the theories of Raats and Philip experimentally (in homogeneous porous medium) and found them to apply to wetting fronts in most cases.

Neuman (1982) and Neuman and Chen (1996) generalized the works of Saffman and Taylor (1958) and Chuoke et al. (1973) to arbitrary fracture, mean flow, and fluid

interface orientations. Their generalized analyses show that the front is not necessarily perpendicular and fingers do not necessarily extend parallel to the direction of mean flow.

Yortstos and Huang (1986) investigated theoretically the effect of capillarity on the stability of a sharp front between immiscible fluids in a porous medium by use of step initial profile saturation in two-phase flow equations. They derived an estimate for T^* that is proportional to T, inversely proportional to the capillary number and depends on the relative permeability, mobility, and capillary-pressure characteristics of the system. Their estimate is in good agreement with that of Chuoke et al. (1959).

Wang et al. (1998c) extended the analysis of Chuoke et al. (1959) to 24 possible combinations of wetting/non-wetting fluids, density and viscosity contrasts and flow directions, obtaining a separate stability criterion for each. All criteria were cast in the form of either a minimum or maximum infiltration rate that would result in instability. Front instability was shown to be a function of medium wettability by the driving fluids, differences in density and viscosity between the fluids, interfacial tension, and flow direction relative to gravity. They showed that fingers initiate and propagate according to the spatial and temporal distribution of fluid entry pressure in the porous medium.

Du et al. (2001) investigated the stability of a gradual (transitional; not sharp) wetting front by perturbing in three-dimensions a traveling wave solution (describing stable flow) of the one-dimensional vertical Richards' flow equation. Their solution shows that, depending on initial conditions, the initial perturbation (1) may decay monotonically with time; (2) may not decay but its downward velocity may be less than that of the unperturbed front so that flow behind the unperturbed front would gradually overwhelm

the fingers to render flow stable; (3) may grow with time and have a downward velocity greater than that of the stable front, causing fingers to grow ahead of the stable front so as to render it unstable. Yao and Hendrickx (2001) verified the stability analysis of Du et al. (2001) and found that it can be used for the assessment of wetting front instabilities in homogeneous soils over a wide range of nonponding infiltration rates.

Nizovtsev et al. (1998) inferred the (in)stability of an experimentally produced wetting front from its fractal properties.

Smith and Zhang (2001) used fractal concept to determine T^* and to evaluate its use for predicting the wavelength of fingers during DNAPL infiltration into an initially water-saturated homogeneous porous medium. The predicted wavelengths were close to those observed.

1.5 Effect of heterogeneity on immiscible displacement

In natural soils and rocks the front instability phenomenon is strongly colored by systematic and random spatial variations in macroscopic medium properties.

Despite notable progress in obtaining analytical solutions describing groundwater flow in randomly heterogeneous domains with fixed boundaries, there are virtually no studies on flow with moving time-dependent surfaces. Stochastic averaging of flow and transport equations has typically dealt either with flows in infinite domains (e.g. Winter et al. 1984; Dagan 1989;Yeh 1992: Indelman 1996; Christakos and Hristopulos 1997), or with flows

in domains bounded by Dirichlet or Neumann boundaries (e.g. Dagan 1989; Neuman and Orr 1993; Tartakovsky and Neuman 1998; Guadagnini and Neuman 1999, Zhang 2002).

A stochastic analysis of wetting front instability in randomly stratified soils has been published by Chen and Neuman (1996). Their work is closely related to earlier deterministic analyses by Raats (1973) and especially Philip (1975). The authors derived a probabilistic criterion for the onset of wetting front instability by treating the front as a sharp boundary and taking the natural log hydraulic conductivity, $Y=\ln K$, to be a random multivariate Gaussian function of space. Whereas the mean, $\overline{Y}$, of this function may exhibit a spatial drift, its fluctuations $Y' = Y - \overline{Y}$ about the mean are statistically homogeneous with zero mean, $\overline{Y'} \equiv 0$ and constant variance σ_Y^2 and spatial correlation scale I_Y. The authors obtained closed-form expressions for the probability of instability and for the mean critical wave number, both directly and via a first-order reliability method. They then used Monte Carlo simulations to verify their analytical solutions and to determine the mean maximum rate of incipient finger growth and corresponding mean wave number. Chen and Neuman found that random fluctuations in soil permeability may have either a stabilizing or a destabilizing effect on a wetting front, depending on the spatial trend, variance and spatial correlation scale of log hydraulic conductivity.

Gau et al. (1998) analyzed conditions for the onset of instability of a sharp front in a randomly heterogeneous porous medium. They equated instability with a growth in front variance with time, and developed criteria required for such growth to occur. In Chapter 4 of this dissertation we show that the variance of front position always increases with time, reflecting a growing uncertainty about the position of the front. Such growth does not

necessarily imply front instability. On the other hand, a deterministic front having zero variance can be unstable under certain conditions.

Shariati and Yortsos (2001) have addressed the effect of nonrandom stratification on the stability of miscible fronts.

1.6 Finger evolution

Linear instability analysis does not provide information about finger evolution. To address this important issue Saffman and Taylor (1958) analyzed the penetration rate and shape of a finger in a Hele-Shaw cell by assuming that the displacing fluid has negligible viscosity compared to displaced fluid and that the effects of gravity and surface tension are unimportant. They obtained parametric solution for constant front velocity

$$x = \frac{1-\lambda}{\pi} \ln\left(1+\cos\frac{\pi y}{\lambda}\right) \tag{1.6}$$

where x is distance, λ is half the finger width, y is the transverse coordinate and the channel has unit half width. Here λ can vary theoretically between 0 and 1. In experiments, the authors observed only one λ for any given capillary number. At large velocities, the observed shape was in good agreement with the calculated shape when λ was set equal to ½.

Mineev-Weinstein and Dawson (1994) used conformal mapping to study analytically the evolution of a two-dimensional interface in the absence of surface tension and gravity. Their solution holds for asymmetric initial fronts and reproduces such features of

viscous fingering as screening and tip splitting. A weak point of conformal mapping is that it is based on Laplace's equation and so cannot be applied to heterogeneous media. The same holds true for the Saffman-Taylor solution, which was obtained using potential and stream functions.

A major difficulty in analyzing unstable fronts arise from the fact that equations describing immiscible displacement are non-linear due to a moving boundary. To overcome this Li et al. (1983) derived integro-differential equations for the evolution of Saffman-Taylor type fingers

$$M + d_0 \int_{\gamma(t)} k(\mathbf{y}) \nabla_y G(\mathbf{x},\mathbf{y}) \cdot \mathbf{n} d\mathbf{y} = \int_{\gamma(t)} V_n(\mathbf{y},t) G(\mathbf{x},\mathbf{y}) d\mathbf{y} \tag{1.7}$$

$$\int_{\gamma(t)} V_n(\mathbf{y},t) d\mathbf{y} = Q \tag{1.8}$$

Here d_0 is capillary number, $k(\mathbf{y})$ is the curvature of the front γ, V_n is the normal velocity of the front, Q is the flow rate (prescribed at infinity), $\mathbf{n}$ is a unit vector normal to γ and M is a constant determined on the basis of (1.8).

The Green's function G satisfies (Kessler *et al.*, 1986)

$$\nabla_y^2 G(\mathbf{x},\mathbf{y}) + \delta(\mathbf{x}-\mathbf{y}) = 0 \qquad \mathbf{y},\mathbf{x} \in \Omega_T \tag{1.9}$$

subject to

$$\mathbf{n}(\mathbf{x}) \cdot \nabla_x G(\mathbf{x},\mathbf{y}) = 0 \qquad \mathbf{x} \in walls \tag{1.10}$$

$$G(\mathbf{x},\mathbf{y}) = 0 \qquad z_x \to -\infty \tag{1.11}$$

where z_x is the component of the coordinate vector $\mathbf{x}$ in the direction of flow. As G is defined on the entire domain Ω_T including regions occupied by both immiscible fluids, it

does not depend on front position. The solution assumes dependence of capillary pressure at γ on d_0 and $k(y)$, but disregards gravity. With some modification (introduced in Chapter 2) these equations can be used to describe front propagation in three-dimensional heterogeneous porous media.

Readers interested in additional references to unstable fronts should consult the book by Pierre (1997) and review papers of Chen et al. (1995) and de Rooij (2000).

When conductivity is random, the flow equations are stochastic and their solution is uncertain. To address this, Tartakovsky (2000) and Tartakovsky and Winter (2001) developed integro-differential equations similar to Li et al. (1983) for leading statistical moments of a horizontal wetting front in a three-dimensional, randomly heterogeneous soil. They did so by treating log hydraulic conductivity as a statistically homogeneous random field with given mean, variance and covariance, recasting the governing stochastic differential equations in integro-differential form and averaging them in probability space to obtain leading-order ensemble moment equations for the mean and variance of front evolution with time.

1.7 Some gaps in existing knowledge

Despite impressive progress in the understanding of unstable flow, significant gaps in knowledge remain (de Rooij, 2000).

Details of front evolution, especially in the field, remain largely obscure. Under laboratory conditions (uniform materials, level layering), finger size and spacing may be

determined entirely by the properties of the medium and the flow. In the field, on the other hand, local heterogeneities in the top few centimeters of the soil together with microtopography may determine in which direction infiltrating water flows and how much water a finger receives (de Rooij, 2000).

Commenting on the effect of heterogeneity on front instability, de Rooij (2000) notes that "whether soil heterogeneity increases or decreases the tendency of the immiscible front to become unstable has only been tentatively investigated. Obviously, this issue is highly relevant for field conditions. Once an unstable front has formed in a heterogeneous soil, the combined effect of soil heterogeneity and front instability needs to be considered to allow reliable modeling of field scale solute transport. So far, very few studies have tackled this issue, and no definite conclusions can be drawn. It is conceivable that in a particular field, depending on the conditions, either heterogeneity or fingered flow is so dominant that the effect of the other process is masked; but when the conditions change both process might reinforce each other, leading to even more enhanced solute leaching than would be expected on the basis of the separate processes alone."

In this work we address some of these issues, particularly the effect of heterogeneity on unstable DNAPL and wetting fronts.

1.8 Scope of this study

Based on the sharp front approximation, we derive in Chapter 2 stochastic equations and boundary conditions that control DNAPL propagation in randomly heterogeneous

saturated porous media. We propose a new moment approach to the analysis of these stochastic equations by converting them into integro-differential equations similar (but not identical) to those of Tartakovsky and Winter (2001).

In Chapter 3 we extend Philip's (1975) wetting front instability analysis to that of a DNAPL front and show that a probabilistic analysis of wetting front instability due to Chen and Neuman (1996) applies to the latter.

Chapter 4 presents one-dimensional analytical solutions of moment equations derived in Chapter 2 and their comparison with Monte Carlo simulations.

In Chapter 5 we develop two-dimensional numerical solutions of moment equations derived in Chapter 2, without considering gravity.

Conclusions are present in Chapter 6. Lengthy mathematical derivations are deferred in Appendices.

CHAPTER 2

THREE-DIMENSIONAL DNAPL FRONT

2.1. Problem definition

We analyze the downward movement of DNAPL in a three-dimensional randomly heterogeneous porous domain Ω_T, saturated with water. DNAPL is initially pooled to a height H_0 above the water table (Fig. 2.1) or flows at a constant flux Q.

We consider in detail the first case and present equations for the prescribed flux case whose derivation is very similar.

2.2. Front propagation under constant head

Let the water table be situated at the origin of the vertical coordinate z, defined to be positive downward. DNAPL with viscosity μ_D much larger than that of water μ_W ($\mu_D \gg \mu_W$) penetrates below the water table where it forms a sharp boundary, γ. It occupies a flow domain $\Omega(\Omega \subset \Omega_T)$ bounded by γ and a combination of Direchlet boundary segments, Γ_D, and Neumann boundary segments, Γ_N. Outside of Ω the saturation of DNAPL is taken to be zero. Inside Ω the saturation of DNAPL is $s_D = 1 - s_{rW}$, where s_{rW} is the saturation of residual water, treated here as being immobile. Assuming that s_{rW} is a constant, the transient flow of DNAPL is governed by Darcy's law and the mass conservation principle,

$$\mathbf{q}_D(\mathbf{x},t) = -K_D(\mathbf{x})\nabla h_D(\mathbf{x},t) \qquad \nabla \bullet \mathbf{q}_D(\mathbf{x},t) = 0 \qquad \mathbf{x} \in \Omega,\ t > 0 \tag{2.1}$$

where $\mathbf{x}(x_x, y_x, z_x)$ is a coordinate vector, t is time, $K_D = k\rho_D g/\mu_D$ is DNAPL conductivity and $h_D(\mathbf{x},t) = P_D(\mathbf{x},t)/\rho_D g - z_x$. We express the intrinsic permeability of DNAPL as $k = \hat{k}k_{RD}(s_D)$ where $\hat{k}$ is intrinsic permeability of the porous medium and k_{RD} is relative permeability of DNAPL, which depends on s_D. Since we take s_D to be a deterministic constant so is k_{RD} a deterministic constant.

In general the conductivity K_D is a second-rank tensor, but here we take it to be a random scalar function $K_D(\mathbf{x}) = \overline{K}(\mathbf{x}) + K'(\mathbf{x})$ with mean $\overline{K}(\mathbf{x})$ and fluctuation $K'(\mathbf{x})$ having zero mean, $\overline{K'}(\mathbf{x}) = 0$, variance $\sigma_K^2(\mathbf{x})$ and covariance function $C_K(\mathbf{x},\mathbf{y})$. We assume that the mean, variance and covariance of $\hat{k}$ can be estimated from, and conditioned on, field measurements of $\hat{k}$ by geostatistical methods [e.g. Neuman, 1984]. Spatial drift and/or conditioning may render $K_D(\mathbf{x})$ statistically nonhomogeneous.

Let the water table (WT) be located at z=0 and remain at reference absolute pressure $P_w(x, y, 0) = P_0$. Consider fluid pressures in the DNAPL pool to be hydrostatic,

$$P_w(x_x, y_x, z_x) = P_0 + \rho_w g z_x \tag{2.2}$$

$$P_D(x_x, y_x, z_x) = P_D(x_x, y_x, 0) + \rho_D g z_x \tag{2.3}$$

The top of the DNAPL pool is taken to remain at a known and deterministic depth z=-H_0. At this depth, capillary pressure is assumed to be $P_C(-H_0) = P_D(-H_0) - P_w(-H_0) \equiv 0$. Considering (2.2) and (2.3), this implies

$$P_D(x, y, 0) = P_0 + (\rho_D - \rho_w)gH_0 \tag{2.4}$$

At the front we take the capillary pressure to be equal to the DNAPL entry pressure into a water-saturated medium, $P_C(\mathbf{x}_\gamma) \equiv P_E$.

Analyses based on the sharp front approximation (which effectively disregards front thickness) have been reasonably successful in predicting the onset of instability under a variety of laboratory and field conditions (for example Saffman and Taylor, 1958).

Methods to determine P_E on the basis of moisture retention and relative conductivity characteristics of uniform and heterogeneous soils have been reviewed by Chen and Neuman (1996). These authors found that, in a randomly stratified soil, variations in effective entry pressure have a negligible effect on the onset of wetting front instability. We therefore take P_E to be a deterministic constant.

Next we assume that water pressure at the front is not affected by DNAPL and remains hydrostatic,

$$P_W(\mathbf{x},t) = P_0 + \rho_W g z_x(t) \qquad \mathbf{x} \in \gamma(t) \tag{2.5}$$

Hence DNAPL pressure at the front is

$$P_D(\mathbf{x},t) = P_E + P_0 + \rho_W g z_x(t) \qquad \mathbf{x} \in \gamma(t) \tag{2.6}$$

With this, the governing equation and the boundary conditions that control DNAPL penetration below the water table can be stated in terms of modified head $h=h_D-a$ as

$$\nabla\cdot\left(K_D(\mathbf{x})\nabla h(\mathbf{x},t)\right) = 0 \qquad \mathbf{x}\in\Omega,\ t>0 \tag{2.7}$$

$$\mathbf{n}(\mathbf{x},t)\cdot\left(K_D(\mathbf{x})\nabla h(\mathbf{x},t)\right) = 0 \qquad \mathbf{x}\in\Gamma_N \tag{2.8}$$

$$h(\mathbf{x},t) = H - a \qquad z_x = 0 \tag{2.9}$$

$$h(\mathbf{x},t) = -bz_x \qquad -\mathbf{n}(\mathbf{x},t)\cdot\left(K_D(\mathbf{x})\nabla h(\mathbf{x},t)\right) = \theta V_n(\mathbf{x},t) \qquad \mathbf{x}\in\gamma(t) \tag{2.10}$$

where $a = \frac{P_0 + P_E}{\rho_D g}$; $b = \frac{\rho_D - \rho_W}{\rho_D}$; $H = \frac{P_0}{\rho_D g} + bH_0$; $\theta = s_D n$ is volumetric DNAPL content; n is porosity; and V_n is the normal velocity of the moving boundary γ,

$$V_n(\mathbf{x},t) = \frac{d\mathbf{x}}{dt} \bullet \mathbf{n}(\mathbf{x},t) \qquad \mathbf{x} \in \gamma(t) \tag{2.11}$$

As long as the front has a unique depth at any horizontal position, $\xi(x_x, y_x, t) \equiv z_x \,|\, \mathbf{x} \in \gamma(t)$, V_n can be defined as (Neuman and Whitherspoon, 1970b)

$$V_n(\mathbf{x},t) = \frac{\partial \xi(x_x, y_x, t)}{\partial t} n_z(x,t) \tag{2.12}$$

where n_z is the vertical component of $\mathbf{n}$.

As K_D is random, equations (2.1) and (2.8) – (2.11) are stochastic and their solution is uncertain. Our aim is to solve them in terms of leading moments of $h(\mathbf{x},t)$, its gradient and $\xi(x_x, y_x, t)$.

2.3. Integral moment equations

Equations (2.1) and (2.8) – (2.11) are non-linear due to the presence of a moving boundary, γ. It helps recasting them in the form of an integral equation (Appendix A),

$$h(\mathbf{x},t) = -(H-a)\int_{\Gamma_D} \bar{K}(\mathbf{y})\mathbf{n}(\mathbf{y})\bullet\nabla_{\mathbf{y}}G(\mathbf{y},\mathbf{x})d\mathbf{y}$$

$$-\int_{\gamma(t)} \left[\theta V_n(\mathbf{y},t)G(\mathbf{y},\mathbf{x}) - \bar{K}(\mathbf{y})b\xi(x_y,y_y;t)\mathbf{n}(\mathbf{y},t)\bullet\nabla_{\mathbf{y}}G(\mathbf{y},\mathbf{x})\right]d\mathbf{y} \qquad (2.13)$$

$$-\int_{\Omega(t)} K'(\mathbf{y})\nabla_{\mathbf{y}}h(\mathbf{y},t)\bullet\nabla_{\mathbf{y}}G(\mathbf{y},\mathbf{x})d\mathbf{y}$$

Here $G(\mathbf{y},\mathbf{x})$ is a deterministic Green's function defined as

$$\nabla_{\mathbf{y}}\bullet\left[\bar{K}(\mathbf{y})\nabla_{\mathbf{y}}G(\mathbf{y},\mathbf{x})\right] + \delta(\mathbf{y}-\mathbf{x}) = 0 \qquad \mathbf{y},\mathbf{x}\in\Omega_T \qquad (2.14)$$

subject to homogeneous boundary conditions

$$G(\mathbf{y},\mathbf{x}) = 0 \qquad \mathbf{y}\in\Gamma_D \qquad (2.15)$$

$$\mathbf{n}(\mathbf{y})\bullet\nabla_{\mathbf{y}}G(\mathbf{y},\mathbf{x}) = 0 \qquad \mathbf{y}\in\Gamma_N \qquad (2.16)$$

The domain Ω_T over which $G(\mathbf{y},\mathbf{x})$ is defined extends below the moving front and G is therefore independent of this front. This is a major advantage, which forms a key element of our solution. The latter is based on a perturbation of (2.13).

2.4. Perturbation analysis

In (2.13) we expand K_D and all quantities that depend on it in powers of σ_Y, the standard deviation of Y=lnK_D, according to

$$K_D(z) = e^{\bar{Y}(z)}e^{Y'(z)} = K_G(1+Y'(z)+\frac{Y'^2(z)}{2}+\ldots) \qquad (2.17)$$

where $K_G = \exp\bar{Y}$ is the geometric mean of K_D.

Taking the ensemble mean of (2.17) gives

$$\overline{K}(z) = K_G\left(1+\frac{\sigma_Y^2}{2}+\ldots\right) \tag{2.18}$$

Subtracting (2.18) from (2.17) yields

$$K'(z) = K_D(z) - \overline{K}(z) = K_G\left(Y'(z)+\frac{Y'^2(z)}{2}-\frac{\sigma_Y^2(z)}{2}+\ldots\right) \tag{2.19}$$

Correspondingly,

$$h(z) = h^{(0)}(z)+h^{(1)}(z)+h^{(2)}(z)+\ldots \tag{2.20}$$

$$\xi = \xi^{(0)}+\xi^{(1)}+\xi^{(2)}+\ldots \tag{2.21}$$

$$V_n = V_n^{(0)}+V_n^{(1)}+V_n^{(2)}+\ldots \tag{2.22}$$

where the superscripts indicate order of expansion in Y' or, more precisely, in σ_Y. It follows that, to leading orders of approximation, the ensemble mean of (2.13) is (Appendix B),

$$h^{(0)}(\mathbf{x},t) = -(H-a)\int_{\Gamma_D} K_G(\mathbf{y})\nabla_y G^{(0)}(\mathbf{y},\mathbf{x})\cdot\mathbf{n}(\mathbf{y})d\mathbf{y}$$

$$-\theta\int_{y^{(0)}(t)} V_n^{(0)}(\mathbf{y},t)G^{(0)}(\mathbf{y},\mathbf{x})d\mathbf{y}$$

$$+b\int_{y^{(0)}(t)} K_G(\mathbf{y})\xi^{(0)}(x_y,y_y;t)\nabla_y G^{(0)}(\mathbf{y},\mathbf{x})\cdot\mathbf{n}(\mathbf{y},t)d\mathbf{y} \tag{2.23}$$

$$\overline{h}^{[1]} = h^{(0)} \quad (\overline{h}^{(1)} \equiv 0) \tag{2.24}$$

$$\overline{h}^{[2]}(\mathbf{x},t) = -(H-a)\int_{\Gamma_D} K_G(\mathbf{y})\mathbf{n}(\mathbf{y})\bullet\nabla_{\mathbf{y}}G^{(0)}(\mathbf{y},\mathbf{x})d\mathbf{y}$$

$$-\theta\int_{\gamma^{[2]}(t)}\left(\overline{V}_n^{[2]}(\mathbf{y},t)G^{(0)}(\mathbf{y},\mathbf{x}) - \frac{\sigma_Y^2}{2}V_n^{(0)}(\mathbf{y},t)G^{(0)}(\mathbf{y},\mathbf{x})\right)d\mathbf{y}$$

$$+b\int_{\gamma^{[2]}(t)} K_G(\mathbf{y})\overline{\xi}^{[2]}(x_{\mathbf{y}},y_{\mathbf{y}},t)\mathbf{n}(\mathbf{y},t)\bullet\nabla_{\mathbf{y}}G^{(0)}(\mathbf{y},\mathbf{x})d\mathbf{y} \qquad (2.25)$$

$$+\int_{\Omega^{(0)}(t)} K_G(\mathbf{y})\mathbf{r}^{[2]}(\mathbf{y},t)\bullet\nabla_{\mathbf{y}}G^{(0)}(\mathbf{y},\mathbf{x})d\mathbf{y}$$

$$-\int_{\gamma^{(0)}(t)} K_G(\mathbf{y})C_{Y\gamma}^{[2]}(\mathbf{y},x_{\mathbf{y}},y_{\mathbf{y}},t)\nabla_{\mathbf{y}}h^{(0)}(\mathbf{y},t)\bullet\nabla_{\mathbf{y}}G^{(0)}(\mathbf{y},\mathbf{x})d\mathbf{y}$$

where superscripts (i) denote quantities that contain strictly i-th order terms, superscripts $[i]$ denote quantities that contain terms up to order i, $\gamma^{(i)}$ and $\gamma^{[i]}$ are fronts corresponding to $\xi^{(i)}$ and $\xi^{[i]}$, and $\mathbf{r}^{[2]}(\mathbf{x}) = -\overline{Y'(\mathbf{x})\nabla h'(\mathbf{x})}^{[2]}$ is a second-order approximation of "residual flux".

The residual flux is obtained by operating on (2.13) with the stochastic differential operator $K'(\mathbf{x})\nabla_{\mathbf{x}}$, taking ensemble mean, and retaining terms of order σ_Y^2 (Appendix C):

$$\mathbf{r}(\mathbf{x},t)^{[2]} = \theta\int_{\gamma^{(0)}(t)} C_{YV_n}^{[2]}(\mathbf{x};\mathbf{y},t)\nabla_{\mathbf{x}}G^{(0)}(\mathbf{y},\mathbf{x})d\mathbf{y}$$

$$-b\int_{\gamma^{(0)}(t)} K_G(\mathbf{y})C_{Y\gamma}^{[2]}(\mathbf{x};\mathbf{y},t)\mathbf{n}(\mathbf{y},t)\bullet\nabla_{\mathbf{y}}\nabla_{\mathbf{x}}G^{(0)}(\mathbf{y},\mathbf{x})d\mathbf{y} \qquad (2.26)$$

$$+\int_{\Omega^{(0)}(t)} K_G(\mathbf{y})C_Y^{[2]}(\mathbf{x},\mathbf{y})\nabla_{\mathbf{y}}h^{(0)}(\mathbf{y},t)\bullet\nabla_{\mathbf{y}}\nabla_{\mathbf{x}}G^{(0)}(\mathbf{y},\mathbf{x})d\mathbf{y}$$

and $C_Y(\mathbf{x},\mathbf{y}) = \overline{Y'(\mathbf{x})Y'(\mathbf{y})}$.

The second-order covariance $C_{Y\gamma}^{[2]}(\mathbf{z},x_{\mathbf{x}},y_{\mathbf{x}},t)$ is obtained by evaluating (2.13) at the front, multiplying by $Y'(\mathbf{z})$, taking average, and retaining terms of order σ_Y^2 (Appendix D):

$$bC_{Y\gamma}^{[2]}(\mathbf{z};x_{\mathrm{x}},y_{\mathrm{x}},t)=\int_{\Omega^{(0)}(t)}K_G(\mathbf{y})C_{Y}^{[2]}(\mathbf{z},\mathbf{y})\nabla_{\mathrm{y}}h^{(0)}(\mathbf{y},t)\bullet\nabla_{\mathrm{y}}G^{(0)}\left(\mathbf{y};x_{\mathrm{x}},y_{\mathrm{x}},\xi(x_{\mathrm{x}},y_{\mathrm{x}},t)\right)d\mathbf{y}$$

$$+\theta\int_{\gamma^{(0)}(t)}C_{YV_n}^{[2]}(\mathbf{z};\mathbf{y},t)G^{(0)}\left(\mathbf{y},x_{\mathrm{x}},y_{\mathrm{x}},\xi(x_{\mathrm{x}},y_{\mathrm{x}},t)\right)d\mathbf{y} \tag{2.27}$$

$$-b\int_{\gamma^{(0)}(t)}K_G(\mathbf{y})C_{Y\gamma}^{[2]}(\mathbf{z};\mathbf{y},t)\mathbf{n}(\mathbf{y},t)\bullet\nabla_{\mathrm{y}}G^{(0)}\left(\mathbf{y},x_{\mathrm{x}},y_{\mathrm{x}},\xi(x_{\mathrm{x}},y_{\mathrm{x}},t)\right)d\mathbf{y}$$

The second –order covariance $C_{YV_n}^{[2]}(\mathbf{x};x_{\mathrm{y}},y_{\mathrm{y}},t)$ is given by

$$C_{YV_n}^{[2]}(\mathbf{x};x_{\mathrm{y}},y_{\mathrm{y}},t)=\overline{Y'^{(1)}(\mathbf{x})V_n^{(1)}(x_{\mathrm{y}},y_{\mathrm{y}},t)}$$

$$=\frac{\partial C_{Y\gamma}^{[2]}(\mathbf{x};x_{\mathrm{y}}y_{\mathrm{y}},t)}{\partial t}n_z\left(x_{\mathrm{y}},y_{\mathrm{y}},t\right) \tag{2.28}$$

From (2.10) it follows that

$$\overline{h}(\mathbf{x},t)^{[t]}=-b\overline{\xi}(x_{\mathrm{x}},y_{\mathrm{x}},t)^{[t]}\qquad z_{\mathrm{x}}=\overline{\xi}(x_{\mathrm{x}},y_{\mathrm{x}},t)^{[t]} \tag{2.29}$$

where $\overline{h}(\mathbf{x},t)^{[t]}$ is given to zero and second order by (2.23) and (2.25), respectively. According to (2.11),

$$\overline{V}_n(\mathbf{x},t)^{[t]}=\frac{\partial\overline{\xi}(x_{\mathrm{x}},y_{\mathrm{x}},t)^{[t]}}{\partial t}n_z(\mathbf{x},t) \tag{2.30}$$

The second-order covariance $C_{\gamma}^{[2]}(x_{\mathrm{x}},y_{\mathrm{x}},\tilde{t};x_{\mathrm{y}},y_{\mathrm{y}},t)=\overline{\xi'(x_{\mathrm{x}},y_{\mathrm{x}},\tilde{t})\xi'(x_{\mathrm{y}},y_{\mathrm{y}},t)}^{[2]}$ is obtained by evaluating (2.13) at the front, multiplying by $\xi'(x_{\mathrm{x}},y_{\mathrm{x}},t)$, and taking average (Appendix E):

$$bC_{\gamma}^{[2]}(x_x,y_x,\tilde{t};x_x,y_x,t)=\theta\int_{\gamma^{(0)}(t)}C_{\gamma V_n}^{[2]}(x_x,y_x,\tilde{t};x_y,y_y,t)G^{(0)}\left(\mathbf{y};x_x,y_x,\xi(x_x,y_x,t)\right)d\mathbf{y}$$

$$-b\int_{\gamma^{(0)}(t)}K_G(\mathbf{y})C_{\gamma}^{[2]}(x_x,y_x,\tilde{t};x_y,y_y,t)\mathbf{n}(\mathbf{y},t)\bullet\nabla_y G^{(0)}\left(\mathbf{y};x_x,y_x,\xi(x_x,y_x,t)\right)d\mathbf{y} \tag{2.31}$$

$$+\int_{\Omega^{(0)}(t)}K_G(\mathbf{y})C_{\gamma\gamma}^{[2]}(\mathbf{y};x_x,y_x,t)\nabla_y h^{(0)}(\mathbf{y},t)\bullet\nabla_y G^{(0)}\left(\mathbf{y};x_x,y_x,\xi(x_x,y_x,t)\right)d\mathbf{y}$$

where

$$C_{\gamma V_n}^{[2]}(x_y,y_y,\tilde{t};x_z,y_z,t)=\frac{\partial C_{\gamma}^{[2]}(x_y,y_y,\tilde{t};x_z,y_z,t)}{\partial t}n_z(\mathbf{z}) \tag{2.32}$$

The variance $\left[\sigma_{\gamma}^2\right]^{[2]}$ of front positions corresponds to the limit of (2.31) as $\tilde{t}\to t$.

Similarly, the variance of hydraulic head, $\left[\sigma_h^2(\mathbf{x},t)\right]^{[2]}=\overline{h'(\mathbf{x},t)h'(\mathbf{x},t)}^{[2]}$, is given by (Appendix F):

$$\left[\sigma_h^2(\mathbf{x},t)\right]^{[2]}=-\theta\int_{\gamma^{[1]}(t)}C_{hV}^{[2]}\left(\mathbf{x};x_y,y_y,t\right)G^{(0)}(\mathbf{y},\mathbf{x})d\mathbf{y}$$

$$+b\int_{\gamma^{(0)}(t)}K_G(\mathbf{y})C_{h\gamma}^{[2]}\left(\mathbf{x};x_y,y_y,t\right)\mathbf{n}(\mathbf{y},t)\bullet\nabla_y G^{(0)}(\mathbf{y},\mathbf{x})d\mathbf{y} \tag{2.33}$$

$$-\int_{\Omega^{(0)}(t)}K_G(\mathbf{y})C_{hV}^{[2]}(\mathbf{x},\mathbf{y})\nabla_y h^{(0)}(\mathbf{y},t)\bullet\nabla_y G^{(0)}(\mathbf{y},\mathbf{x})d\mathbf{y}$$

where the cross-covariance $C_{hV}^{[2]}\left(\mathbf{x};x_y,y_y,t\right)=\overline{h'(\mathbf{x})V'\left(x_y,y_y,\xi^{(0)}(x_y,y_y,t)\right)}^{[2]}$ is given by

$$C_{hV_n}^{[2]}\left(\mathbf{x};x_y,y_y t\right)=\frac{\partial C_{h\gamma}^{[2]}\left(\mathbf{x};x_y,y_y,t\right)}{\partial t}n_z(\mathbf{y}). \tag{2.34}$$

The cross-covariance $C_{h\gamma}^{[2]}\left(\mathbf{x};x_y,y_y,t\right)=\overline{h'(\mathbf{x})\xi'(x_y,y_y,t)}^{[2]}$ is given by

$$
\begin{aligned}
&C^{[2]}_{h\gamma}(\mathbf{x},x_z,y_z,t) = \\
&-\theta \int_{\gamma^{(0)}(t)} C^{[2]}_{\gamma V_n}(x_z,y_z,t;x_y,y_y,t)G^{(0)}(\mathbf{y},\mathbf{x})d\mathbf{y} \\
&+b \int_{\gamma^{(0)}(t)} K_G(\mathbf{y})C^{[2]}_{\gamma}(x_z,y_z,t;x_y,y_y,t)\mathbf{n}(\mathbf{y},t)\bullet\nabla_y G^{(0)}(\mathbf{y},\mathbf{x})d\mathbf{y} \\
&-\int_{\Omega^{(0)}(t)} K_G(\mathbf{y})C^{[2]}_{\gamma\gamma}(\mathbf{y},t;x_z,y_z,t)\nabla_y h^{(0)}(\mathbf{y},t)\bullet\nabla_y G^{(0)}(\mathbf{y},\mathbf{x})d\mathbf{y}
\end{aligned}
\tag{2.35}
$$

The cross-covariance $C^{[2]}_{h\gamma}(\mathbf{x},\mathbf{z}) = \overline{h'(\mathbf{x})\gamma'(\mathbf{z})}^{[2]}$ is given by

$$
\begin{aligned}
&C^{[2]}_{h\gamma}(\mathbf{x},\mathbf{z}) = \\
&-\theta \int_{\gamma^{(0)}(t)} C^{[2]}_{\gamma V_n}(\mathbf{z};x_y,y_y,t)G^{(0)}(\mathbf{y},\mathbf{x})d\mathbf{y} \\
&+b \int_{\gamma^{(0)}(t)} K_G(\mathbf{y})C^{[2]}_{\gamma\gamma}(\mathbf{z};x_y,y_y,t)\mathbf{n}(\mathbf{y},t)\bullet\nabla_y G^{(0)}(\mathbf{y},\mathbf{x})d\mathbf{y} \\
&-\int_{\Omega^{(0)}(t)} K_G(\mathbf{y})C^{[2]}_{\gamma}(\mathbf{z},\mathbf{y})\nabla_y h^{(0)}(\mathbf{y},t)\bullet\nabla_y G^{(0)}(\mathbf{y},\mathbf{x})d\mathbf{y}
\end{aligned}
\tag{2.36}
$$

The normal velocity covariance $C^{[2]}_{V_n}(x_y,y_y,\tilde{t};x_z,y_z,t) = \overline{V'_n(x_y,y_y,\tilde{t})V'_n(x_z,y_z,t)}^{[2]}$ is given by

$$
C^{[2]}_{V_n}(x_y,y_y,\tilde{t};x_z,y_z,t) = \frac{\partial C^{[2]}_{\gamma V_n}(x_y,y_y,\tilde{t};x_z,y_z,t)}{\partial\tilde{t}} n_z(\mathbf{y}) \tag{2.37}
$$

The second-order velocity variance $\left[\sigma^2_{V_n}\right]^{[2]}$ is obtained by taking the limit $(x_y,y_y,\tilde{t}) \to (x_z,y_z,t)$.

2.5 Flux driven front propagation

Next we consider a front γ driven by a constant flux Q. Here the transient flow of DNAPL in Ω is governed by

$$\nabla\cdot\left(K_D(\mathbf{x})\nabla h(\mathbf{x},t)\right)=0 \qquad \mathbf{x}\in\Omega,\ t>0 \tag{2.38}$$

subject to the boundary conditions,

$$\mathbf{n}(\mathbf{x},t)\cdot\left(K_D(\mathbf{x})\nabla h(\mathbf{x},t)\right)=0 \qquad \mathbf{x}\in\Gamma_N \tag{2.39}$$

$$-\mathbf{n}(\mathbf{x},t)\cdot\left(K_D(\mathbf{x})\nabla h(\mathbf{x},t)\right)=Q \qquad z_{\mathbf{x}}=0 \tag{2.40}$$

$$h(\mathbf{x},t)=-bz_{\mathbf{x}} \qquad -\mathbf{n}(\mathbf{x},t)\cdot K_D(\mathbf{x})\nabla h(\mathbf{x},t)=\theta V_n(\mathbf{x},t) \qquad \mathbf{x}\in\gamma(t) \tag{2.41}$$

In analogy to (2.23)-(2.25), the leading moments of h are

$$h^{(0)}(\mathbf{x},t)=-Q\int_{\Gamma_{N1}}G^{(0)}(\mathbf{y},\mathbf{x})d\mathbf{y}-\theta\int_{\gamma^{(0)}(t)}V_n^{(0)}(\mathbf{y},t)G^{(0)}(\mathbf{y};\mathbf{x})d\mathbf{y}$$

$$+b\int_{\gamma^{(0)}(t)}K_G(\mathbf{y})\xi^{(0)}(x_{\mathbf{y}},y_{\mathbf{y}};t)\nabla_{\mathbf{y}}G^{(0)}(\mathbf{y},\mathbf{x})\cdot\mathbf{n}(\mathbf{y},t)d\mathbf{y} \tag{2.42}$$

$$\overline{h}^{[1]}=h^{(0)} \quad (\overline{h}^{(1)}\equiv 0) \tag{2.43}$$

$$\overline{h}^{[2]}(\mathbf{x},t) = -Q\int_{\Gamma_{N1}} G^{[2]}(\mathbf{y},\mathbf{x})d\mathbf{y}$$
$$-\theta\int_{\gamma^{[2]}(t)}\left(\overline{V}_n^{[2]}(\mathbf{y},t)G^{(0)}(\mathbf{y},\mathbf{x}) - \frac{\sigma_Y^2}{2}V_n^{(0)}(\mathbf{y},t)G^{(0)}(\mathbf{y},\mathbf{x})\right)d\mathbf{y}$$
$$+b\int_{\gamma^{[2]}(t)} K_G(\mathbf{y})\overline{\xi}^{[2]}(x_y,y_y;t)\mathbf{n}(\mathbf{y},t)\bullet\nabla_y G^{(0)}(\mathbf{y},\mathbf{x})d\mathbf{y} \qquad (2.44)$$
$$+\int_{\Omega^{(0)}(t)} K_G(\mathbf{y})\mathbf{r}^{[2]}(\mathbf{y},t)\bullet\nabla_y G^{(0)}(\mathbf{y},\mathbf{x})d\mathbf{y}$$
$$-\int_{\gamma^{(0)}(t)} K_G(\mathbf{y})C_{Y\gamma}^{[2]}(\mathbf{y};x_y,y_y,t)\nabla_y h^{(0)}(\mathbf{y},t)\bullet\nabla_y G^{(0)}(\mathbf{y},\mathbf{x})d\mathbf{y}$$

where $G(\mathbf{y},\mathbf{x})$ is a deterministic Green's function that satisfies

$$\nabla_y\bullet\left[\overline{K}(\mathbf{y})\nabla_y G(\mathbf{y},\mathbf{x})\right] + \delta(\mathbf{y}-\mathbf{x}) = 0 \qquad \mathbf{y},\mathbf{x}\in\Omega_T \qquad (2.45)$$

subject to the boundary conditions

$$\mathbf{n}(\mathbf{y})\bullet\nabla_y G(\mathbf{y},\mathbf{x}) = 0 \qquad \mathbf{y}\in\Gamma_{N1} \qquad (2.46)$$

$$\mathbf{n}(\mathbf{y})\bullet\nabla_y G(\mathbf{y},\mathbf{x}) = 0 \qquad \mathbf{y}\in\Gamma_N \qquad (2.47)$$

Due to our choice of deterministic boundary conditions, the expressions for moments remain the same as in the prescribed head case. Their values, however, are different due to our redefinition of the Green's function.

The zero-order approximation of the mean hydraulic head, $h^{(0)}(\mathbf{x},t)$, satisfies a standard boundary-value problem with moving boundaries for a medium with known properties, driven by deterministic functions. Nonlocality of the mean flow problem manifests itself solely in second-order (and higher) terms.

CHAPTER 3

PROBABILITY CRITERION FOR INSTABILITY

3.1 Criterion for instability

In this chapter we present a stochastic analysis of DNAPL front instability during infiltration into a randomly stratified saturated porous medium. A probability criterion for the onset of wetting front instability during surface water infiltration into a randomly stratified partially saturated soil was first derived by Chen and Neuman (1995). They studied the probability of instability and mean critical wave number by combining Philip's (1975) stability analysis with first-order reliability theory. They then verified the results by Monte Carlo simulation. In this chapter we show that it is possible to apply exactly the same probability criterion to the onset of DNAPL front instability. The wetting front can be considered as a special case of the model described in Chapter 2 with $b=(\rho_D-\rho_{ir})/\rho_D=1$, where in case of a wetting front ρ_D would represent water density and ρ_{ir} air density. To be consistent with Chen and Neuman (1996) we define the vertical coordinate z as having its origin at the water table and pointing upward (everywhere else in this dissertation z is defined to be positive downward).

The one-dimensional versions of (2.1), (2.3) and (2.6) are

$$q_D(z)=-\frac{k(z)}{\mu_D}\frac{d}{dz}\left(P_D(z)+z\rho_D g\right) \qquad -L\le z\le 0 \tag{3.1}$$

$$P_D(0)=P_0+(\rho_D-\rho_w)gH \tag{3.2}$$

$$P_D(-L)=P_c(-L)+P_w(-L)=P_E+P_w(0)+L\rho_w g \tag{3.3}$$

where L is vertical front position.

Let the horizontal front $z=-L(t)$ at reference time t_0 be perturbed slightly into a three-dimensional wave form,

$$z(x,y,t) = -L + \varepsilon(t)\sin(nx+\tau)\sin(my+\delta) \tag{3.4}$$

where $\varepsilon(t)$ is a small positive amplitude, n and m are wave numbers corresponding to x and y, respectively, and τ and δ are corresponding phase shifts. Clearly, the front becomes unstable if $d\varepsilon/dt>0$ and stable otherwise.

In a manner similarly to Philip (1975) a criterion of instability can be obtained (Appendix G) as

$$G < 0 \tag{3.5}$$

where G is vertical DNAPL pressure head gradient immediately above front,

$$G \equiv \frac{1}{\rho_D g}\frac{dP_D}{dz}_{z=-L} = \frac{1}{k(-L)\int_0^{-L}\frac{dz}{k(z)}}\left[\frac{P_E}{\rho_D g} - (1-\frac{\rho_w}{\rho_D})(L+H)\right] - 1 \tag{3.6}$$

In other words, instability can develop only if the pressure gradient immediately above the front is negative, i.e., the pressure head increase downward. When the pressure head immediately above the wetting front is uniform or increases upward, the front remains stable. Stated otherwise, when the pressure gradient immediately above the front assists its descent, the flow is unstable. This is due to the fact that gravity acts to destabilize and viscosity to stabilize the front. When the pressure gradient assists front descent, it enhances the stabilizing viscous effect relative to that of gravity: the reverse is true when it opposes front descent.

Note that if we define z to be positive downward, the front will be unstable when $G>0$. (3.7)

According to Philip (1975) the effect of surface tension T at the DNAPL-water interface adds a curvature to the original plane front and produces a perturbation in P_E. It introduces an additional condition of instability (Appendix G),

$$M < M_c = \sqrt{-\frac{\theta(\rho_D - \rho_w)gG}{T}} \tag{3.8}$$

where $M = \sqrt{m^2 + n^2}$ is a wave number.

Using an approximation proposed by Philip (Appendix 3.1) the wave number, M_m, for the most unstable disturbance is given by

$$M_m = \frac{M_c}{\sqrt{3}} \tag{3.9}$$

3.2 Stochastic analysis of front instability

We consider a stratified medium in which $k(z)$ changes with elevation in a random manner. We assume that $Y(z)=\ln k(z)$ is a Gaussian field, $Y(z) = \bar{Y}(z) + Y'(z)$, with mean, $\bar{Y}$ and fluctuation $Y'(z)$ having zero-mean, $\overline{Y'(z)} = 0$, and an exponential covariance,

$$C_Y(\Delta z) = \sigma_Y^2 \exp\left(-\frac{\Delta z}{l_Y}\right) \tag{3.10}$$

where l_Y is the spatial autocorrelation scale of Y, σ_Y^2 is the variance, and Δz is a vertical separation distant.

When $k(z)$ changes randomly, so does G. We shall speak of the probability $P(G<0)$ that instability may develop under given condition. Due to the nonlinear relationship between G and K, $P(G<0)$ cannot be evaluated in closed form under general conditions. Instead, following Chen and Neuman (1996), we present a closed form solution for large L/I_Y, develop an approximate solution for small L/I_Y by means of first-order reliability theory, and evaluate the mean critical wave number for both cases. We do so for both statistically homogeneous Gaussian log conductivity field, with constant $\overline{Y}$ and for $\overline{Y}$ that varies with depth.

3.2.1 Probability of instability, $P(G<0)$

Under the previous assumptions we can express the permeability field as

$$k(z)=e^{Y(z)}=e^{\overline{Y}}e^{Y'(z)} \tag{3.11}$$

Substitution of (3.11) into expression for G yields

$$\begin{aligned} G &= \frac{1}{e^{\overline{Y}}e^{Y'(L)}\int_0^L \frac{d\xi}{e^{\overline{Y}}e^{Y'(\xi)}}}\left[-\psi_E+(1-\frac{\rho_w}{\rho_D})(L+H)\right]-1 \\ &= \frac{G_u+1}{\Gamma\Sigma}-1 \end{aligned} \tag{3.12}$$

$$\text{where}\quad G_u=\frac{H(1-\frac{\rho_w}{\rho_D})-L\frac{\rho_w}{\rho_D}-\psi_E}{L}, \tag{3.13}$$

$$\Gamma=e^{Y'(L)}, \tag{3.14}$$

$$\Sigma = \frac{1}{L}\int_0^L e^{-Y'(\xi)}d\xi \tag{3.15}$$

$$\psi_E = P_E / \rho_D g \tag{3.16}$$

Note that G_u represents G in a uniform medium and ψ_E is an entry pressure head. Our expression for G looks exactly like that of Chen and Neuman (1996), thus allowing us to apply their results to our case.

3.2.2 Closed form solution for large L/I_Y

It was shown by Chen and Neuman (1996) that for large L/I_Y (in their case L/I_Y >40) we can replace Σ in (3.12) by its mean value, $\Sigma = \overline{\Sigma} = \exp(\frac{\sigma_Y^2}{2})$. Treating ψ_E as a constant, the probability of instability is (Appendix 3.2)

$$P(G<0) = \frac{1}{2}\left\{1 + erf\left[\frac{\sigma_Y}{2\sqrt{2}} - \frac{\ln(G_u+1)}{\sqrt{2}\sigma_Y}\right]\right\} \tag{3.17}$$

This implies that:

a) When $\sigma_Y^2 = 0$

if $G_u \geq 0$, then $P(G<0) = \frac{1}{2}(1 + erf[-\infty]) = 0$

if $G_u < 0$, then $P(G<0) = \frac{1}{2}(1 + erf[\infty]) = 1$

The DNAPL front is either stable or unstable when the medium is uniform.

b) When $\sigma_y^2 > 2\ln(1+G_u)$, *erf*(x>0)>0 and $P(G<0)>0.5$.

c) When $\sigma_y^2 < 2\ln(1+G_u)$, *erf*(x<0)<0 and $P(G<0)<0.5$.

d) When $G_u \geq 0, P(G<0)$ increases monotonically from 0 to 1 as σ_y^2 increase (Figure 3.1a); the probability of instability increases with heterogeneity when the front is uniformly stable.

e) When $G_u < 0, P(G<0) > 0.5$; the probability of instability first decreases from 1 and then increases back to 1 as σ_y^2 increases, with a minimum when *erf*(0)=0 (Figure 3.1b).

f) When G_u approaches 0,

$$P(G<0) = \frac{1}{2}\left\{1+erf\left[\frac{\sigma_y}{2\sqrt{2}}\right]\right\}$$

Figures 3.1(a) and 3.1(b) compare the probability of instability computed analytically and by Monte Carlo simulation for prescribed ψ_E at L/I_Y=40 given two values of G_u (Chen and Neuman, 1996). The two solutions are close for $\sigma_Y^2 \leq 2$ but differ for larger variance.

Next allow ψ_E to vary randomly as:

$$\psi_c(z) = -bk^{-1/2}(z) \tag{3.18}$$

where $b = -\psi_c^* k^{*1/2}$, ψ^*, k^* are reference values (Philip, 1975).

Then it was shown by Chen and Neuman (1996), (Appendix H), that the probability of instability is

$$P(G<0)=P(G'>0)=P(k>K_0)=P(\ln k>\ln K_0), \tag{3.19}$$

where $\ln k \equiv Y$, and K_0 is given by

$$K_0=\begin{cases}(\sqrt[3]{P+\sqrt{Q}}+\sqrt[3]{P-\sqrt{Q}})^2, & \text{if } Q>0\\ (\sqrt[3]{P+\sqrt{Q}i}+\sqrt{P-\sqrt{Q}i})^2, & \text{if } Q<0\end{cases} \tag{3.20}$$

where $P=b/(2LB)$, $Q=\dfrac{b^2}{4L^2B^2}-\dfrac{(G_E+1)^3}{27B^3}$ and $B=\exp\left(-\bar{Y}+\sigma_Y^2/2\right)$.

Figures 3.1(c) and 3.1(d) (Chen and Neuman, 1996) compare the probability of instability computed this way and by Monte Carlo simulation for random ψ_E based on b=8.16$(m^3/d)^{1/2}$ when L/I_Y=40. We again see excellent agreement between Monte Carlo and analytical results for $\sigma_Y^2 \le 2$, and satisfactory agreement for larger variance.

3.2.3 Reliability solution for small L/I_Y

It was shown by Chen and Neuman (1996) that when $L/I_Y<40$, Σ may vary significantly about the mean. To handle this situation, Chen and Neuman used reliability theory.

According to the first-order reliability method FORM, one can express the probability of instability as

$$P=1-\Phi(\delta), \tag{3.21}$$

where Φ is the cumulative normal distribution function, δ is a reliability index defined as $\delta = \mu_g / \sigma_g$. μ_g and σ_g are the mean and standard deviation of a performance function $g(x)$, that is less than zero, by definition, in the case of instability.

Chen and Neuman have shown that when capillary pressure at the front is prescribed, one can define g as

$$g = \ln(1+G) = \ln(1+G_u) - Y(L) - \tilde{Y} \tag{3.22}$$

and

$$\delta = \frac{\ln(1+G_u) - \overline{Y} - \overline{\tilde{Y}}}{\sqrt{\sigma_Y^2 + \sigma_{\tilde{Y}}^2 + 2\rho\sigma_Y\sigma_{\tilde{Y}}}} \tag{3.23}$$

where $\tilde{Y} = \ln \tilde{k}$, $\tilde{k} = \frac{1}{L}\int_0^L \frac{1}{k(\xi)} d\xi$ and $\rho = \frac{C_{Y\tilde{Y}}}{\sigma_Y \sigma_{\tilde{Y}}}$ is the cross-correlation coefficient.

An expression for the cross-covariance $C_{Y\tilde{Y}}$ is given in Appendix H

For the case where capillary pressure head at the front is random, Chen and Neuman obtained a performance function

$$g(Z) = \left(\frac{b}{L} e^{-\frac{1}{2}(\sigma_Y Z_1 + \overline{Y})} + G_E + 1 \right) \exp(-\sigma_Y Z_1 - \rho\sigma_{\tilde{Y}} Z_1 - \sqrt{1-\rho^2}\sigma_{\tilde{Y}} Z_2 - \overline{Y} - \overline{\tilde{Y}}) - 1 \tag{3.24}$$

where Z_1 and Z_2 are two components of the vector Z:

$$Z = L^{-1} D^{-1} (Y - M), \tag{3.25}$$

where L is the lower triangle matrix obtained by Choleski decomposition of the correlation matrix $R = LL^T$ of Y

$$L = \begin{bmatrix} 1 & 0 \\ \rho & \sqrt{1-\rho^2} \end{bmatrix}, \tag{3.26}$$

D is a diagonal matrix, such that D_{nn} is the variance of the vector $\mathbf{Y}=(Y(L), \tilde{Y})^T$, and M is a vector with components that represent the mean of $\mathbf{Y}$: $\bar{Y}$ and $\bar{\tilde{Y}}$. G_E is given by (IV.30). The reliability index, δ, now can be determined by a search algorithm.

Figures 3.2(a) and 3.2(b) (Chen and Neuman, 1996) compare the probability of instability computed analytically and by Monte Carlo simulation for constant ψ_E and 3.2(c) and 3.2(d) – for random ψ_E when L/I_Y=40 at two different values of G_u. We can see excellent agreement between Monte Carlo and analytical results for σ_Y^2 values from 10^{-5} to 10^2.

3.2.4 Vertical drift in permeability

Consider the case where the mean log permeability varies linearly with depth according to $\bar{Y}(\xi) = \bar{Y}(L) + s(\xi - L)$, where s is slope, positive when $\bar{Y}(\xi)$ increases with depth and negative when it decreases. Then according to Chen and Neuman

$$\bar{\tilde{k}} = ce^{-\bar{Y}(L)+\sigma_Y^2}, \tag{3.27}$$

$$\sigma_{\tilde{k}}^2 = \frac{e^{-2\bar{Y}+\sigma_Y^2}}{sL}\left(\frac{1}{L}\int_0^L \left(e^{2sL-s\xi} - e^{s\xi}\right)e^{C_Y(\xi)}d\xi - sLc^2\right) \tag{3.28}$$

$$C_{k\tilde{k}} = e^{\sigma_Y^2}\left(\frac{1}{L}\int_0^L e^{s\xi}e^{-C_Y(\xi)}d\xi - c\right) \tag{3.29}$$

where $c = \left(e^{sL} - 1\right)/(sL)$.

Assuming that $\tilde{Y} = \ln \tilde{k}$ is normal, one obtains

$$\bar{\tilde{Y}} = -\bar{Y} + \frac{\sigma_Y^2}{2} - \frac{\sigma_{\tilde{Y}}^2}{2} + \ln c \tag{3.30}$$

$$\sigma_{\tilde{Y}}^2 = \ln\left(\frac{1}{sLc^2}\frac{1}{L}\int_0^L \left(e^{2sL-s\xi} - e^{s\xi}\right) e^{C_Y(\xi)} d\xi\right) \tag{3.31}$$

$$C_{Y\tilde{Y}} = \ln\left(\frac{1}{cL}\int_0^L e^{s\xi} e^{-C_Y(\xi)} d\xi\right) \tag{3.32}$$

Using these expressions in FORM, Chen and Neuman obtained the probability of instability in the presence of vertical drift in permeability that agrees well with Monte Carlo simulation.

3.2.5 Mean critical wave number

When $G < 0$, one can rewrite (3.8) as

$$M_c = \sqrt{\frac{\theta(\rho_D - \rho_w)g}{T}}\sqrt{-G} \tag{3.33}$$

According to our model θ is a constant, and so is $\sqrt{\frac{\theta(\rho_D - \rho_w)g}{T}}$. Taking the mean of (3.33) yields

$$E[M_c] = \sqrt{\frac{\theta(\rho_D - \rho_w)g}{T}} E\left[\sqrt{-G}\right] \tag{3.34}$$

The normalized mean critical wave number is then

$$\frac{E[M_c]}{\sqrt{\frac{\theta(\rho_D-\rho_w)g}{T}}} = E\left[\sqrt{-G}\right] = \int_{-\infty}^{0}\sqrt{-G}f(-G)d(-G)$$

$$= \int_{-\infty}^{0}\sqrt{-G}dF(-G) \tag{3.35}$$

where f is a probability distribution function and F is cumulative distribution function.

(3.35) can be estimated numerically.

CHAPTER 4

ANALYTICAL SOLUTION IN ONE DIMENSION

Here we solve a one-dimensional version of the moment equations obtained in Chapter 2 for front depth $\xi(t)$ within a vertical depth interval $x \in (0,l)$ where $l > \xi$. For this we take $Y(x)$ to have a constant mean, $\bar{Y}$, and an exponential covariance,

$$C_Y\left(|x-y|\right) = \sigma_Y^2 \exp\left(-\frac{|x-y|}{l_Y}\right) \tag{4.1}$$

where l_Y is the spatial autocorrelation scale of Y. The auxiliary function $G_K(x,y) = \bar{K}G(x,y)$ satisfies the equation

$$\frac{\partial^2 G_K(x,y)}{\partial x^2} + \delta(x-y) = 0 \qquad 0 \le x, \quad y \le l \tag{4.2}$$

and is given in Appendix I by

$$G_K(x,y) = -(x-y)\mathrm{H}(x-y) + \alpha(y)x + \beta(y) \tag{4.3}$$

where H is the Heaviside function and $\alpha(y)$ and $\beta(y)$ are arbitrary functions to be determined from boundary conditions .

4.1 Front propagation under a fixed head boundary condition in the presence of gravity

Here we consider a front driven by a constant head boundary condition in the presence of gravity. We prescribe

$h=H-a$ at $x=0$ (4.4)

while maintaining

$h=-b\xi(t)$ at $x=\xi(t)$ (4.5)

In this case G_K is subject to the homogeneous boundary conditions

$G_K(x,y)=0 \qquad x=0$ (4.6)

$G_K(x,y)=0 \qquad x=l$ (4.7)

Evaluating (4.3) at $x=0$ gives

$\beta(y)\equiv 0$ (4.8)

and evaluating (4.3) at $x=l$ yields

$-l+y+\alpha(y)l=0$ (4.9)

From here $\alpha(y)$ can be found as

$$\alpha(y)=\frac{l-y}{l} \tag{4.10}$$

Substituting $\alpha(y)$ and $\beta(y)$ into (4.3) leads to

$$G_K(x,y)=-(x-y)\mathrm{H}(x-y)+\frac{l-y}{l}x \tag{4.11}$$

Substituting (4.11) into the one-dimensional version of (2.13) and evaluating at $x=\xi$ yields (Appendix J)

$$0=\theta\frac{d\xi(t)}{dt}\xi(t)+\bar{K}\left[a-H-b\xi(t)\right]+\int_0^{\xi(t)}K'(y)\frac{\partial h(y,t)}{\partial y}dy \tag{4.12}$$

Expanding the integral in a Taylor series around $\bar{\xi}(t)$ gives

$$\begin{aligned}0&=\theta\frac{d\xi(t)}{dt}\xi(t)+\bar{K}\left[a-H-b\xi(t)\right]\\&+\int_0^{\bar{\xi}(t)}K'(y)\frac{\partial h(y,t)}{\partial y}dy+\xi'(t)K'(y)\frac{\partial h(y,t)}{\partial y}\bigg|_{y=\bar{\xi}(t)}+\ldots\end{aligned} \tag{4.13}$$

The mean of (4.13) is, to leading orders of approximation,

$$\frac{\theta}{K_G}\frac{d\xi^{(0)}(t)}{dt}=b+\frac{H-a}{\xi^{(0)}(t)} \tag{4.14}$$

and

$$\begin{aligned}&\theta\xi^{(0)}\frac{d\bar{\xi}^{(2)}}{dt}+\bar{\xi}^{(2)}\left(\theta\frac{d\xi^{(0)}}{dt}-bK_G\right)\\&=-\frac{\theta}{2}\frac{d\left[\sigma_\xi^2\right]^{(2)}}{dt}+\left(H-a+b\xi^{(0)}\right)K_G\frac{\sigma_Y^2}{2}\\&+\int_0^{\xi^{(0)}}r^{(2)}(y,t)dy-K_GC_{Y\xi}^{(2)}(\xi^{(0)},t)\frac{\partial h^{(0)}(y,t)}{\partial y}\bigg|_{y=\xi^{(0)}}\end{aligned} \tag{4.15}$$

Multiplying (4.13) by ξ' and taking the mean yields, to leading order,

$$\begin{aligned}&\frac{\theta}{2}\xi^{(0)}\frac{d\left[\sigma_\xi^2(t)\right]^{(2)}}{dt}+\left(\theta\frac{d\xi^{(0)}}{dt}-K_Gb\right)\left[\sigma_\xi^2(t)\right]^{(2)}\\&\qquad=-K_G\int_0^{\xi^{(0)}}C_{Y\xi}^{(2)}(y,\xi^{(0)})\frac{\partial h^{(0)}(y,t)}{\partial y}dy\end{aligned} \tag{4.16}$$

Expressions (4.14) - (4.16) are ordinary differential equations for $\xi^{(0)}$, $\xi^{(2)}$ and $\left[\sigma_{\xi}^{2}\right]^{(2)}$ respectively. All three are subject to zero initial conditions.

4.1.1 Zero-order mean front

Integrating (4.14) yields an implicit solution for $\xi^{(0)}$ (Appendix K),

$$\frac{K_G}{\theta}t = \frac{1}{b}\left[\xi^{(0)} - \frac{H-a}{b}\ln\left(\frac{b\xi^{(0)}}{H-a}+1\right)\right] \tag{4.17}$$

4.1.2 Zero-order mean head and its gradient

The zero-order mean head is given in Appendix L

$$h^{(0)}(x,t) = H - a - \left(b\xi^{(0)}(t) + H - a\right)\frac{x}{\xi^{(0)}(t)} \tag{4.18}$$

The zero-order mean head gradient is obtained by taking the derivative of (4.18) with respect to z,

$$\frac{\partial h^{(0)}(x,t)}{\partial x} = -\frac{b\xi^{(0)}(t) + H - a}{\xi^{(0)}(t)} \tag{4.19}$$

4.1.3 Cross-covariance $C_{Y\xi}$

As a prerequisite for solving (4.15) and (4.16), one must first solve an ordinary differential equation for $C_{Y\xi}^{(2)}$ that is derived in Appendix M,

$$\theta\xi^{(0)}(t)\frac{\partial C_{Y\xi}^{(2)}(x,t)}{\partial t}+\left(\theta\frac{d\xi^{(0)}(t)}{dt}-K_G b\right)C_{Y\xi}^{(2)}(x,t)$$
$$=K_G\left(b+\frac{H-a}{\xi^{(0)}(t)}\right)\int_0^{\xi^{(0)}(t)}C_Y^{(2)}(x,y)dy \tag{4.20}$$

The solution of this equation, subject to initial condition $C_{Y\xi}^{(2)}(x,0)=0$, is given in Appendix M:

$$C_{Y\xi}^{(2)}(x,\xi^{(0)})=\sigma_Y^2 l_Y\frac{b\xi^{(0)}+H-a}{b\xi^{(0)}}$$

$$\left[e^{-\frac{bx+H-a}{bl_Y}}\left\{Ei\left(\frac{bx+H-a}{bl_Y}\right)-Ei\left(\frac{H-a}{bl_Y}\right)\right\}-e^{-\frac{x}{l_Y}}\ln\frac{bx+H-a}{H-a}\right.$$

$$\left.+\left(2-e^{-x/l_Y}\right)\ln\frac{b\xi^{(0)}+H-a}{bx+H-a}-e^{\frac{bx+H-a}{bl_y}}\left\{Ei\left(-\frac{b\xi^{(0)}+H-a}{bl_y}\right)-Ei\left(-\frac{bx+H-a}{bl_y}\right)\right\}\right] \tag{4.21}$$

where $Ei(\alpha y)=\int\frac{e^{\alpha y}}{y}dy$ is the exponential integral (Gradshteyn and Ryzhik 1994, p.113, 2.325).

4.1.4 Residual flux

To solve (4.15) and (4.16), an expression for the residual flux is required. It is given in Appendix N as

$$r^{(2)}(x) = K_G \frac{\partial C_{Y\xi}^{(2)}(x,\xi^{(0)})}{\partial \xi^{(0)}} \frac{b\xi^{(0)} + H - a}{\xi^{(0)}} - K_G \sigma_Y^2 \frac{b\xi^{(0)} + H - a}{\xi^{(0)}} \tag{4.22}$$

where $\partial C_{Y\xi}^{(2)}(x,\xi^{(0)})/\partial \xi^{(0)}$ is given in Appendix N.

4.1.5 Front variance

The solution of (4.16) is given in Appendix O,

$$\left[\sigma_\xi^2(t)\right]^{(2)} = 2\left(\frac{b\xi^{(0)}(t) + H - a}{\xi^{(0)}(t)}\right)^2 \int_0^{\xi^{(0)}(t)} \frac{\int_0^x C_{Y\xi}^{(2)}(y,x)dy}{(bx + H - a)^2} dx \tag{4.23}$$

where the integral of the cross-covariance $C_{Y\xi}^{(2)}$ is given in Appendix P as

$$\int_0^x C_{Y\xi}^{(2)}(y,\xi^{(0)})dy = \sigma_Y^2 l_r^2 \frac{b\xi^{(0)}+H-a}{b\xi^{(0)}}$$

$$\left[-e^{-\frac{bx+H-a}{bl_Y}} Ei\left(\frac{bx+H-a}{bl_Y}\right)+Ei\left(\frac{H-a}{bl_Y}\right)e^{-\frac{bx+H-a}{bl_Y}}\right.$$

$$-\ln\frac{H-a}{bl_Y}e^{-\frac{x}{l_Y}}+2\ln\frac{b\xi^{(0)}+H-a}{bl_Y}\frac{x}{l_Y}$$

$$-2\frac{bx+H-a}{bl_y}\ln\frac{bx+H-a}{bl_y}+2\frac{H-a}{bl_y}\ln\frac{H-a}{bl_y}+2\frac{x}{l_y}$$

$$+\ln\frac{b\xi^{(0)}+H-a}{bl_Y}e^{-x/l_Y}-\ln\frac{b\xi^{(0)}+H-a}{bl_Y}$$

$$-Ei\left(-\frac{b\xi^{(0)}+H-a}{bl_y}\right)e^{\frac{bx+H-a}{bl_y}}+Ei\left(-\frac{b\xi^{(0)}+H-a}{bl_y}\right)e^{\frac{H-a}{bl_y}}$$

$$\left.+e^{\frac{bx+H-a}{bl_Y}}Ei\left(-\frac{bx+H-a}{bl_Y}\right)-e^{\frac{H-a}{bl_Y}}Ei\left(-\frac{H-a}{bl_Y}\right)+\ln\frac{H-a}{bl_Y}\right] \qquad (4.24)$$

4.1.6 Second-order mean front position

The solution of (4.15) is given in Appendix Q:

$$\bar{\xi}^{(2)}\left(\xi^{(0)}(t)\right)=\frac{b\xi^{(0)}(t)+H-a}{\xi^{(0)}(t)}\int_0^{\xi^{(0)}(t)}\frac{xR(x)}{bx+H-a}dx \qquad (4.25)$$

where

$$R(x)=-\frac{1}{(x)^2}\int_0^x C_{Y\xi}^{(2)}(y,x)dy+\frac{1}{(x)^2}\frac{H-a}{bx+H-a}\left[\sigma_\xi^2\right]^{(2)}-\frac{\sigma_Y^2}{2}$$
$$+\frac{1}{x}\frac{d}{dx}\left(\int_0^x C_{Y\xi}^{(2)}(y,x)dy\right) \tag{4.26}$$

$\int_0^x C_{Y\xi}^{(2)}(y,x)dy$ and $\frac{d}{dx}\left(\int_0^x C_{Y\xi}^{(2)}(y,x)dy\right)$ are given in Appendix P and Appendix Q, respectively.

4.1.7 Second-order mean head and its gradient

Substitution of (4.22) into (L.15) yields

$$\bar{h}^{(2)}(x,t)=-x\frac{b\xi^{(0)}(t)+H-a}{\xi^{(0)}(t)}\frac{d\bar{\xi}^{(2)}\left(\xi^{(0)}(t)\right)}{d\xi^{(0)}(t)}-x\frac{\sigma_Y^2}{2}\frac{b\xi^{(0)}(t)+H-a}{\xi^{(0)}(t)}$$
$$+\frac{b\xi^{(0)}(t)+H-a}{\xi^{(0)}(t)}\frac{\partial}{\partial\xi^{(0)}(t)}\left(\int_0^x C_{Y\xi}^{(2)}\left(y,\xi^{(0)}(t)\right)dy\right) \tag{4.27}$$

where $\frac{d\bar{\xi}^{(2)}\left(\xi^{(0)}(t)\right)}{d\xi^{(0)}(t)}$ and $\frac{\partial}{\partial\xi^{(0)}(t)}\left(\int_0^x C_{Y\xi}^{(2)}\left(y,\xi^{(0)}(t)\right)dy\right)$ are given in Appendix Q.

The second-order mean head gradient is obtained from (L.15) in Appendix L:

$$\frac{\partial\bar{h}^{(2)}(x,t)}{\partial x}=-\frac{b\xi^{(0)}(t)+H-a}{\xi^{(0)}(t)}\frac{d\bar{\xi}^{(2)}\left(\xi^{(0)}(t)\right)}{d\xi^{(0)}(t)}+\frac{\sigma_Y^2}{2}\frac{b\xi^{(0)}(t)+H-a}{\xi^{(0)}(t)}+\frac{1}{K_G}r^{(2)}(x,t) \tag{4.28}$$

Substitution (4.22) into (4.28) yields

$$\frac{\partial\bar{h}^{(2)}(x,t)}{\partial x}=-\frac{b\xi^{(0)}(t)+H-a}{\xi^{(0)}(t)}\left(\frac{d\bar{\xi}^{(2)}\left(\xi^{(0)}(t)\right)}{d\xi^{(0)}(t)}+\frac{\sigma_Y^2}{2}-\frac{\partial C_{Y\xi}^{(2)}(x,\xi^{(0)})}{\partial\xi^{(0)}}\right) \tag{4.29}$$

Another way to find the mean head gradient at the front is through direct averaging of the second boundary condition in (2.9):

$$-\bar{K}\frac{\partial \bar{h}}{\partial x}\bigg|_{x=\xi} + r(\xi) = \theta\frac{d\bar{\xi}}{dt} \tag{4.30}$$

From here the zero-order head gradient is

$$\frac{\partial h^{(0)}}{\partial x}\bigg|_{x=\xi} = -\frac{\theta}{K_G}\frac{d\xi^{(0)}}{dt} \tag{4.31}$$

Substitution of (4.14) into (4.31) yields

$$\frac{\partial h^{(0)}}{\partial x}\bigg|_{x=\xi} = -\frac{b\xi^{(0)}(t) + H - a}{\xi^{(0)}(t)} \tag{4.32}$$

that is the same as (4.33).

The second-order mean head gradient is

$$\frac{\partial \bar{h}^{(2)}}{\partial x}\bigg|_{x=\xi} = -\frac{\theta}{K_G}\frac{d\bar{\xi}^{(2)}}{dt} - \frac{\sigma_Y^2}{2}\frac{\partial \bar{h}^{(0)}}{\partial x}\bigg|_{x=\xi} + \frac{r^{(2)}(\xi^{(0)})}{K_G} \tag{4.34}$$

After changing the variable of integration $\frac{d}{dt} = \frac{d}{d\xi^{(0)}}\frac{d\xi^{(0)}}{dt}$ and substituting of (4.14) and (4.19), (4.34) becomes the same as (4.28).

Note that the zero-order head gradient does not depend on x, thus corresponding to one-dimensional flow in a homogeneous porous medium. On the other hand the second-order mean gradient varies with x, reflecting the heterogeneous nature of the medium.

4.1.8 Variance of head gradient

A second-order approximation for the variance of head gradient is given in Appendix R:

$$\left[\sigma^2_{dh/dx}\left(\xi^{(0)}(t)\right)\right]^{(2)} = -2\left(\frac{b\xi^{(0)}(t)+H-a}{\xi^{(0)}(t)}\right)^2 \left.\frac{\partial C^{(2)}_{Y\xi}(x,\xi^{(0)}(t))}{\partial \xi^{(0)}}\right|_{x=\xi^{(0)}} + \sigma^2_Y\left(\frac{b\xi^{(0)}(t)+H-a}{\xi^{(0)}(t)}\right)^2$$
$$+\frac{b\xi^{(0)}(t)+H-a}{\xi^{(0)}(t)}\frac{H-a}{\left(\xi^{(0)}(t)\right)^2}C^{(2)}_{Y\xi}(\xi^{(0)}(t),\xi^{(0)}(t))$$
$$+\frac{1}{2}\left(\frac{b\xi^{(0)}(t)+H-a}{\xi^{(0)}(t)}\right)^2 \frac{d^2\left[\sigma^2_\xi\left(\xi^{(0)}(t)\right)\right]^{(2)}}{d\xi^{(0)}(t)^2} - \frac{1}{2}\frac{b\xi^{(0)}(t)+H-a}{\xi^{(0)}(t)}\frac{H-a}{\left(\xi^{(0)}(t)\right)^2}\frac{d\left[\sigma^2_\xi\left(\xi^{(0)}(t)\right)\right]^{(2)}}{d\xi^{(0)}(t)} \tag{4.35}$$

where $d\left[\sigma^2_\xi\left(\xi^{(0)}(t)\right)\right]^{(2)}/d\xi^{(0)}(t)$ is given by (R.9) as

$$\frac{d\left[\sigma^2_\xi\left(\xi^{(0)}(t)\right)\right]^{(2)}}{d\xi^{(0)}(t)} = \frac{2}{\xi^{(0)}(t)}\int_0^{\xi^{(0)}(t)} C^{(2)}_{Y\xi}(y,\xi^{(0)}(t))dy$$
$$-2\left(\frac{1}{\xi^{(0)}(t)}-\frac{b}{b\xi^{(0)}(t)+H-a}\right)\left[\sigma^2_\xi\left(\xi^{(0)}(t)\right)\right]^{(2)} \tag{4.36}$$

The later implies

$$\frac{1}{2}\frac{d^2\left[\sigma_\xi^2\left(\xi^{(0)}(t)\right)\right]^{(2)}}{d\xi^{(0)}(t)^2} = -\frac{1}{\xi^{(0)}(t)^2}\int_0^{\xi^{(0)}(t)} C_{Y\xi}^{(2)}\left(y,\xi^{(0)}(t)\right)dy$$

$$+\frac{1}{\xi^{(0)}(t)}\frac{d}{d\xi^{(0)}(t)}\int_0^{\xi^{(0)}(t)} C_{Y\xi}^{(2)}(y,\xi^{(0)}(t))dy$$

$$+\left(\frac{1}{\xi^{(0)}(t)^2}-\frac{b^2}{\left(b\xi^{(0)}(t)+H-a\right)^2}\right)\left[\sigma_\xi^2\left(\xi^{(0)}(t)\right)\right]^{(2)}$$

$$-\left(\frac{1}{\xi^{(0)}(t)}-\frac{b}{b\xi^{(0)}(t)+H-a}\right)\frac{d\left[\sigma_\xi^2\left(\xi^{(0)}(t)\right)\right]^{(2)}}{d\xi^{(0)}(t)} \tag{4.37}$$

4.1.9 Direct solution

The one-dimensional version of (2.7)-(2.10) can also be solved by direct integration of (2.7).

Integrating the one-dimensional version of (2.7) once gives

$$K_D(z)\frac{\partial h(z,t)}{\partial z} = A \tag{4.38}$$

Integrating (4.38) again from 0 to z yields

$$h(z,t) = A\int_0^z \frac{1}{K_D(y)}dy + h(0,t) \tag{4.39}$$

From boundary condition (2.9) follows that

$$h(0,t)=H-a \tag{4.40}$$

Evaluating (4.39) at $z=\xi(t)$ and using boundary condition (2.10) we can find the constant A.

Then (4.39) can be written in final form as

$$h(z,t)=-\frac{b\xi(t)+H-a}{\int_0^{\xi(t)}\frac{1}{K_D(y)}dy}\int_0^{z}\frac{1}{K_D(y)}dy+H-a \tag{4.41}$$

The head gradient is found by taking the derivative of (4.41) with respect to z,

$$\frac{\partial h(z,t)}{\partial z}=-\frac{b\xi(t)+H-a}{\int_0^{\xi(t)}\frac{1}{K_D(y)}dy}\frac{1}{K_D(z)} \tag{4.42}$$

A one-dimensional version of the second boundary condition in (2.10) is

$$-K_D(z)\frac{\partial h(z,t)}{\partial z}\bigg|_{z=\xi}=\theta\frac{d\xi}{dt} \tag{4.43}$$

Evaluating (4.42) at the front and incorporating (4.43) yields

$$\theta\frac{d\xi(t)}{dt}=\frac{b\xi(t)+H-a}{\int_0^{\xi(t)}\frac{1}{K_D(y)}dy} \tag{4.44}$$

After some mathematical manipulations and integration an implicit expression for ξ as a function of time is obtained:

$$\frac{t}{\theta}=\int_0^{\xi(t)}\frac{\int_0^{x}\frac{1}{K_D(y)}dy}{bx+H-a}dx \tag{4.45}$$

Expression (4.45) was used to conduct Monte Carlo simulations.

In Appendix S we show that the moment expressions obtained in the previous paragraph using a "Green functions" approach can also be derived directly from equation (4.45).

4.2 Front propagation under a fixed head boundary condition in the absence of gravity

Here we consider horizontal flow driven by a constant head boundary at x=0. We prescribe constant head

h=H-a at x=0, (4.46)

while maintaining

$h = 0$ at $x = \xi(t)$. (4.47)

This is a special case of the problem described earlier, but now without the gravity term $-b\xi(t)$. Since $b = (\rho_D - \rho_w)/\rho_D$, it is obvious that gravity-free flow does not depend on density difference between the two fluids. Likewise, the propagation of a front formed by two fluids having equal densities does not depend on gravity.

4.2.1 Zero-order mean front position

The zero-order mean front position is obtained from (4.14) by setting b=0,

$$\frac{\theta}{K_G}\frac{d\xi^{(0)}(t)}{dt} = \frac{H-a}{\xi^{(0)}(t)} \tag{4.48}$$

or

$$\xi^{(0)}(t)=\sqrt{\frac{2(H-a)K_G}{\theta}}\sqrt{t} \tag{4.49}$$

4.2.2 Zero-order mean head and its gradient

From (4.18)-(4.19) the zero-order head and its gradient for gravity-free flow can be found:

$$h^{(0)}(x,t)=H-a-(H-a)\frac{x}{\xi^{(0)}(t)} \tag{4.50}$$

$$\frac{\partial h^{(0)}(x,t)}{\partial x}=-\frac{H-a}{\xi^{(0)}(t)} \tag{4.51}$$

4.2.3 Cross-covariance $C_{Y\xi}$

The expression (M.18) for cross-covariance $C_{Y\xi}^{(2)}$ (Appendix M) in the absence of gravity reduces to

$$C_{Y\xi}^{(2)}(x,t)=\frac{\sigma_Y^2 l_Y}{\xi^{(0)}}\int_0^x\left(e^{\frac{z-x}{l_Y}}-e^{-\frac{x}{l_Y}}\right)dy+\int_x^{\xi^{(0)}(t)}\left(2-e^{\frac{x-z}{l_Y}}-e^{-\frac{x}{l_Y}}\right)dy$$

$$=\frac{\sigma_Y^2 l_Y}{\xi^{(0)}(t)}\left\{e^{-\frac{x}{l_Y}}\int_0^x e^{\frac{z}{l_Y}}dz-xe^{-\frac{x}{l_Y}}+\left(2-e^{-\frac{x}{l_Y}}\right)\left(\xi^{(0)}(t)-x\right)-e^{\frac{x}{l_Y}}\int_x^{\xi^{(0)}(t)}e^{-\frac{z}{l_Y}}dz\right\}$$

$$=\frac{K_G\sigma_Y^2 l_Y}{\xi^{(0)}(t)}\left\{l_Y\left(1-e^{-\frac{x}{l_Y}}\right)+\left(2-e^{-\frac{x}{l_Y}}\right)\xi^{(0)}(t)-2x+l_Y\left(e^{-\frac{\xi^{(0)}(t)-x}{l_Y}}-1\right)\right\} \tag{4.52}$$

or finally,

$$C_{Y\xi}^{(2)}(x,t)=\sigma_Y^2 l_Y\left\{\frac{l_Y}{\xi^{(0)}(t)}\left(e^{-\frac{\xi^{(0)}(t)-x}{l_Y}}-e^{-\frac{x}{l_Y}}\right)+2\left(1-\frac{x}{\xi^{(0)}(t)}\right)-e^{-\frac{x}{l_Y}}\right\} \tag{4.53}$$

4.2.4 Residual flux

For b=0, (N.11) reduces to

$$r^{(2)}(x)=K_G\frac{\partial C_{Y\xi}^{(2)}(x,\xi^{(0)})}{\partial\xi^{(0)}}\frac{H-a}{\xi^{(0)}}-K_G\sigma_Y^2\frac{H-a}{\xi^{(0)}} \tag{4.54}$$

4.2.5 Front variance

The front variance for gravity-free flow is obtained from (4.23) as

$$\left[\sigma_\xi^2(t)\right]^{(2)}=\frac{2}{\left(\xi^{(0)}(t)\right)^2}\int_0^{\xi^{(0)}(t)}xg(x)dx \tag{4.55}$$

where

$$g(x)=\int_0^x C_{Y\xi}^{(2)}(y,x)dy \tag{4.56}$$

Substitution (4.53) into (4.56) yields

$$g(x)=\sigma_Y^2 l_Y\left\{\frac{l_Y}{x}\left(e^{-\frac{x}{l_Y}}\int_0^x e^{\frac{y}{l_Y}}dy-\int_0^x e^{-\frac{y}{l_Y}}dy\right)+2\left(x-\frac{1}{x}\int_0^x ydy\right)-\int_0^x e^{-\frac{y}{l_Y}}dy\right\}$$

$$=\sigma_Y^2 l_Y^2\left\{\frac{x}{l_Y}+e^{-\frac{x}{l_Y}}-1\right\} \tag{4.57}$$

Then

$$\left[\sigma_\xi^2(t)\right]^{(2)}=\frac{2\sigma_Y^2 l_Y^2}{\left(\xi^{(0)}(t)\right)^2}\int_0^{\xi^{(0)}(t)} x\left\{\frac{x}{l_Y}+e^{-\frac{x}{l_Y}}-1\right\}dx$$

$$=\frac{2\sigma_Y^2 l_Y^2}{\left(\xi^{(0)}(t)\right)^2}\left[\frac{\left(\xi^{(0)}(t)\right)^3}{3l_Y}+\int_0^{\xi^{(0)}(t)} xe^{-\frac{x}{l_Y}}dx-\frac{\left(\xi^{(0)}(t)\right)^2}{2}\right] \tag{4.58}$$

or, using Gradsteyn and Ryzhik (1994), Eq.2.322(6)

$$\left[\sigma_\xi^2(t)\right]^{(2)}=2\sigma_Y^2 l_Y^2\left(\frac{1}{3}\frac{\xi^{(0)}(t)}{l_Y}-\frac{1}{2}-\frac{l_Y}{\xi^{(0)}(t)}\left(1+\frac{l_Y}{\xi^{(0)}(t)}\right)e^{-\frac{\xi^{(0)}(t)}{l_Y}}+\left(\frac{l_Y}{\xi^{(0)}(t)}\right)^2\right) \tag{4.59}$$

4.2.6 Second-order mean front position

A second-order approximation of front position for gravity-free flow is obtained from (Q.2) with b=0,

$$\xi^{(0)}(t)\frac{d\bar{\xi}^{(2)}(t)}{d\xi^{(0)}(t)}+\bar{\xi}^{(2)}(t)$$
$$=-\frac{1}{2}\frac{d\left[\sigma_{\xi}^{2}(t)\right]^{(2)}}{d\xi^{(0)}(t)}+\xi^{(0)}(t)\frac{\sigma_{Y}^{2}}{2}+\frac{1}{K_G}\frac{\xi^{(0)}(t)}{H-a}\int_{0}^{\xi^{(0)}(t)}r^{(2)}(y)dy+C_{Y\xi}^{(2)}(\xi^{(0)},t) \tag{4.60}$$

Substituting the expression for residual flux (4.54) into (4.60) yields

$$\xi^{(0)}(t)\frac{d\bar{\xi}^{(2)}(t)}{d\xi^{(0)}(t)}+\bar{\xi}^{(2)}(t)=-\frac{1}{2}\frac{d\left[\sigma_{\xi}^{2}(t)\right]^{(2)}}{d\xi^{(0)}(t)}+\xi^{(0)}(t)\frac{\sigma_{Y}^{2}}{2}$$
$$+\int_{0}^{\xi^{(0)}}\frac{\partial C_{Y\xi}^{(2)}(y,\xi^{(0)})}{\partial\xi^{(0)}(t)}dy-\sigma_{Y}^{2}\xi^{(0)}(t)+C_{Y\xi}^{(2)}(\xi^{(0)},t) \tag{4.61}$$

After some mathematical manipulations,

$$\frac{d\left(\xi^{(0)}(t)\bar{\xi}^{(2)}(t)\right)}{d\xi^{(0)}(t)}=-\frac{1}{2}\frac{d\left[\sigma_{\xi}^{2}(t)\right]^{(2)}}{d\xi^{(0)}(t)}-\xi^{(0)}(t)\frac{\sigma_{Y}^{2}}{2}$$
$$+\frac{\partial}{\xi^{(0)}(t)}\int_{0}^{\xi^{(0)}}C_{Y\xi}^{(2)}(y,\xi^{(0)})dy \tag{4.62}$$

Substitution (4.59) and (4.53) into (4.62) gives the differential equation

$$\frac{d\left(\xi^{(0)}(t)\bar{\xi}^{(2)}(t)\right)}{d\xi^{(0)}(t)}=-\xi^{(0)}(t)\frac{\sigma_{Y}^{2}}{2}$$
$$+\sigma_{Y}^{2}l_{Y}^{2}\frac{\partial}{\partial\xi^{(0)}(t)}\left[\frac{2}{3}\frac{\xi^{(0)}(t)}{l_Y}-\frac{1}{2}+\frac{l_Y}{\xi^{(0)}(t)}\left(\frac{\xi^{(0)}(t)}{l_Y}+1+\frac{l_Y}{\xi^{(0)}(t)}\right)e^{-\frac{\xi^{(0)}(t)}{l_Y}}-\left(\frac{l_Y}{\xi^{(0)}(t)}\right)^{2}\right] \tag{4.63}$$

subject to $\bar{\xi}^{(2)}(0)=0$

Integration gives

$$\xi^{(0)}(t)\bar{\xi}^{(2)}(t)=-\frac{\sigma_{Y}^{2}}{4}\left(\xi^{(0)}(t)\right)^{2}$$
$$+\sigma_{Y}^{2}l_{Y}^{2}\left[\frac{2}{3}\frac{\xi^{(0)}(t)}{l_Y}-\frac{1}{2}+\left(1+\frac{l_Y}{\xi^{(0)}(t)}+\left(\frac{l_Y}{\xi^{(0)}(t)}\right)\right)e^{-\frac{\xi^{(0)}(t)}{l_Y}}-\left(\frac{l_Y}{\xi^{(0)}(t)}\right)^{2}\right] \tag{4.64}$$

or in final form

$$\frac{\bar{\xi}^{(2)}(t)}{l_Y} = -\frac{\sigma_Y^2}{4}\frac{\xi^{(0)}(t)}{l_Y}$$
$$+\frac{\sigma_Y^2 l_Y}{\xi^{(0)}(t)}\left[\frac{2}{3}\frac{\xi^{(0)}(t)}{l_Y} - \frac{1}{2} + \frac{l_Y}{\xi^{(0)}(t)}\left(\frac{\xi^{(0)}(t)}{l_Y} + 1 + \frac{l_Y}{\xi^{(0)}(t)}\right)e^{-\frac{\xi^{(0)}(t)}{l_Y}} - \left(\frac{l_Y}{\xi^{(0)}(t)}\right)^2\right] \tag{4.65}$$

4.2.7 Second–order mean head and its gradient

From (4.27) and (4.29) the second-order mean head and its gradient are obtained respectively as

$$\bar{h}^{(2)}(x,t) = -x\frac{H-a}{\xi^{(0)}(t)}\frac{d\bar{\xi}^{(2)}\left(\xi^{(0)}(t)\right)}{d\xi^{(0)}(t)} - x\frac{\sigma_Y^2}{2}\frac{H-a}{\xi^{(0)}(t)}$$
$$+\frac{H-a}{\xi^{(0)}(t)}\frac{\partial}{\partial\xi^{(0)}(t)}\left(\int_0^x C_{Y\xi}^{(2)}\left(y,\xi^{(0)}(t)\right)dy\right) \tag{4.66}$$

and

$$\frac{\partial\bar{h}^{(2)}(x,t)}{\partial x} = -\frac{H-a}{\xi^{(0)}(t)}\left(\frac{d\bar{\xi}^{(2)}\left(\xi^{(0)}(t)\right)}{d\xi^{(0)}(t)} + \frac{\sigma_Y^2}{2} - \frac{\partial C_{Y\xi}^{(2)}\left(x,\xi^{(0)}(t)\right)}{\partial\xi^{(0)}(t)}\right) \tag{4.67}$$

where from (4.53)

$$\frac{\partial C_{Y\xi}^{(2)}\left(x,\xi^{(0)}(t)\right)}{\partial\xi^{(0)}} = -\sigma_Y^2\left\{\frac{l_Y^2}{\left(\xi^{(0)}(t)\right)^2}\left(e^{-\frac{\xi^{(0)}(t)-x}{l_Y}} - e^{-\frac{x}{l_Y}}\right)\frac{l_Y}{\xi^{(0)}(t)}e^{-\frac{\xi^{(0)}(t)-x}{l_Y}} - 2\frac{xl_Y}{\left(\xi^{(0)}(t)\right)^2}\right\} \tag{4.68}$$

Then

$$\frac{\partial}{\partial \xi^{(0)}(t)}\left(\int_0^x C_{Y\xi}^{(2)}\left(y,\xi^{(0)}(t)\right)dy\right)=\int_0^x \frac{\partial C_{Y\xi}^{(2)}\left(y,\xi^{(0)}(t)\right)}{\partial \xi^{(0)}(t)}dy$$

$$=-\sigma_Y^2\left\{\frac{l_Y^2}{\left(\xi^{(0)}(t)\right)^2}\left(e^{-\frac{\xi^{(0)}(t)}{l_Y}}\int_0^x e^{\frac{y}{l_Y}}dy-\int_0^x e^{-\frac{y}{l_Y}}dy\right)+\frac{l_Y}{\xi^{(0)}(t)}e^{-\frac{\xi^{(0)}(t)}{l_Y}}\int_0^x e^{\frac{y}{l_Y}}dy-\frac{x^2 l_Y}{\left(\xi^{(0)}(t)\right)^2}\right\}$$

$$=-\sigma_Y^2 l_Y\left\{\frac{l_Y^2}{\left(\xi^{(0)}(t)\right)^2}\left(e^{-\frac{\xi^{(0)}(t)}{l_Y}}\left(e^{\frac{x}{l_Y}}-1\right)+e^{-\frac{x}{l_Y}}-1\right)+\frac{l_Y}{\xi^{(0)}(t)}e^{-\frac{\xi^{(0)}(t)}{l_Y}}\left(e^{\frac{x}{l_Y}}-1\right)-\frac{x^2}{\left(\xi^{(0)}(t)\right)^2}\right\} \quad (4.69)$$

From (4.65)

$$\frac{d\bar{\xi}^{(2)}(t)}{d\xi^{(0)}(t)}=-\frac{\sigma_Y^2}{4}+3\sigma_Y^2\frac{l_Y^4}{\left(\xi^{(0)}(t)\right)^4}$$

$$+\frac{\sigma_Y^2}{2}\frac{l_Y^2}{\left(\xi^{(0)}(t)\right)^2}-\sigma_Y^2\left(\frac{l_Y}{\xi^{(0)}(t)}+\frac{2l_Y^2}{\left(\xi^{(0)}(t)\right)^2}+\frac{3l_Y^3}{\left(\xi^{(0)}(t)\right)^3}+\frac{3l_Y^4}{\left(\xi^{(0)}(t)\right)^4}\right)e^{-\frac{\xi^{(0)}(t)}{l_Y}} \quad (4.70)$$

Note that the second-order head gradient is not a constant but a function of x.

4.2.8 Direct solution

The gravity-free solution for $\xi(t)$ is obtained from (4.45) with b=0

$$\frac{t}{\theta}=\frac{1}{H-a}\int_0^{\xi(t)}\left(\int_0^x\frac{1}{K_D(y)}dy\right)dx \quad (4.71)$$

4.3 Flux-driven front propagation

Consider a front driven by a constant flux Q at the boundary x=0, i.e.

$$K_D(x)\frac{\partial h(x)}{\partial x} = -Q \qquad x = 0 \tag{4.72}$$

while maintaining constant head at the front

$$h = -b\xi(t) \quad \text{at} \quad x = \xi(t) \tag{4.73}$$

The corresponding zero-order Green's function $G_K^{(0)} = K_G G$ satisfies the boundary conditions

$$\frac{\partial G_K^{(0)}(x,y)}{\partial x} = 0 \qquad x = 0 \tag{4.74}$$

$$G_K^{(0)}(x,y) = 0 \qquad x = l \qquad l > \xi \tag{4.75}$$

From (4.3) and (4.74) it follows that

$$\left.\frac{\partial G_K^{(0)}(x,y)}{\partial x}\right|_{x=0} = -\mathrm{H}(x-y) - (x-y)\delta(x-y) + \alpha(y)\big|_{x=0} = \alpha(y) \tag{4.76}$$

and $\alpha(y)$=0.

Evaluating the zero-order approximation of (4.3) at x=l subject to (4.75) gives

$$G_K^{(0)}(l,y) = -(l-y) + \beta(y) = 0 \tag{4.77}$$

and so $\beta(y) = l - y$. Hence to zero-order (4.3) becomes

$$G_K^{(0)}(x,y) = -(x-y)\mathrm{H}(x-y) + l - y \tag{4.78}$$

Recognizing from (4.78) that

$$G_K^{(0)}(\xi^{(0)}(t), x) = l - \xi^{(0)}(t) \tag{4.79}$$

$$G_K^{(0)}(0,x) = l - x \tag{4.80}$$

and from (4.1.2) that

$$\frac{\partial G_K^{(0)}(y,x)}{\partial y} = -\mathrm{H}(y-x) \tag{4.81}$$

$$\left.\frac{\partial G_K^{(0)}(y,x)}{\partial y}\right|_{y=\xi^{(0)}(t)} = -1 \tag{4.82}$$

we can rewrite (2.42) and (2.44) in one-dimension as

$$h^{(0)}(x,t) = -\frac{\theta V^{(0)}(t)}{K_G}\left(l-\xi^{(0)}(t)\right) - b\xi^{(0)}(t) + \frac{Q}{K_G}(l-x) \tag{4.83}$$

$$\begin{aligned}\overline{h}^{(2)}(x,t) = &-\frac{\sigma_Y^2}{2}\frac{Q}{K_G}(l-x) - \frac{\theta}{K_G}\left(\overline{V}^{(2)}(t) - \frac{\sigma_Y^2}{2}V^{(0)}(t)\right)\left(l-\xi^{(0)}(t)\right) - b\overline{\xi}^{(2)}(t) \\ &+C_{Y\xi}^{(2)}\left(\xi^{(0)}(t),\xi^{(0)}(t)\right)\frac{\partial h^{(0)}(y,t)}{\partial y} + \int_0^{\xi^{(0)}(t)} r^{(2)}(y,t)\frac{\partial G_K^{(0)}(y,x)}{\partial y}dy\end{aligned} \tag{4.84}$$

4.3.1 Zero-order mean front position

Evaluating (4.83) at $x = \xi$ and using boundary condition (4.73) gives

$$\theta V^{(0)}(t) = Q \tag{4.85}$$

where

$$V^{(0)}(t) = \frac{d\xi^{(0)}(t)}{dt} \tag{4.86}$$

Integrating subject to $\xi^{(0)}(0) = 0$ yields

$$\xi^{(0)}(t) = \frac{Q}{\theta}t \tag{4.87}$$

4.3.2 Zero-order mean head and its gradient

Substituting (4.85) into (4.83) gives

$$h^{(0)}(x,t) = -b\xi^{(0)}(t) + \frac{Q}{K_G}(\xi^{(0)}(t) - x) \tag{4.88}$$

and

$$\frac{\partial h^{(0)}(x,t)}{\partial x} = -\frac{Q}{K_G} \tag{4.89}$$

To find the second-order mean head and front position we need expressions for $C_{Y\xi}^{(2)}$ and $r^{(2)}(y,t)$.

4.3.3 Cross-covariance $C_{Y\xi}^{(2)} = \overline{Y'\xi'}^{(2)}$

Substituting (4.78) into the 1-D version of (2.27) and evaluating at $x = \xi^{(0)}$ gives

$$\begin{aligned} bC_{Y\xi}^{(2)}\left(z,\xi^{(0)}(t)\right) &= -\frac{Q}{K_G}\int_0^{\xi^{(0)}(t)} C_Y^{(2)}(z,y)\frac{\partial G_K^{(0)}\left(y;\xi^{(0)}(t)\right)}{\partial y}dy \\ &+\theta C_{YY'}^{(2)}(z,\xi^{(0)}(t))G_K^{(0)}\left(\xi^{(0)}(t),\xi^{(0)}(t)\right) \\ &-bC_{Y\xi}^{(2)}(z,\xi^{(0)}(t))\left.\frac{\partial G_K^{(0)}\left(y;\xi^{(0)}(t)\right)}{\partial y}\right|_{y=\xi^{(0)}(t)} \end{aligned} \tag{4.90}$$

From (4.81) it follows that

$$\int_0^{\xi^{(0)}(t)} C_Y^{(2)}(z,y)\frac{\partial G_K^{(0)}\left(y;\xi^{(0)}(t)\right)}{\partial y}dy =$$

$$-\int_0^{\xi^{(0)}(t)} C_Y^{(2)}(z,y)\mathrm{H}\left(y-\xi^{(0)}(t)\right)dy = 0 \tag{4.91}$$

Substituting (4.79) and (4.82) into (4.90) we obtain

$$C_{Y\xi}^{(2)}(z,\xi^{(0)}(t)) = \frac{\partial C_{Y\xi}^{(2)}(z,\xi^{(0)}(t))}{\partial t} = 0 \tag{4.92}$$

subject to

$$C_{Y\xi}^{(2)}(z,0) = 0 \tag{4.93}$$

From (4.92) and (4.93) it follows that

$$C_{Y\xi}^{(2)}\left(z,\xi^{(0)}(t)\right) = 0 \tag{4.94}$$

4.3.4 Residual flux

Substituting (4.89), (4.92) and (4.94) into the one-dimensional version of (2.26) gives

$$r^{(2)}(x,t) = -\frac{Q}{K_G}\int_0^{\xi^{(0)}(t)} C_Y^{(2)}(x,y)\frac{\partial^2 G_K^{(0)}(y,x)}{\partial y\partial x}dy \tag{4.95}$$

From (4.81)

$$\frac{\partial^2 G_K^{(0)}(y,x)}{\partial y\partial x} = \delta(x-y) \tag{4.96}$$

From here the residual flux is

$$r^{(2)}(x,t) = -\underline{Q}\sigma_Y^2 \tag{4.97}$$

4.3.5 Second-order mean front position

Evaluating (4.84) at $x = \xi$, using (4.73), (4.85), (4.86), (4.94) and analogy with (4.91) gives

$$\overline{V}^{(2)}(x,t) = 0 \tag{4.98}$$

Since

$\overline{V}^{(2)}(t) = \dfrac{d\overline{\xi}^{(2)}(t)}{dt}$ and $\overline{\xi}^{(2)}(0) = 0$, we find that

$$\overline{\xi}^{(2)}(t) = 0 \tag{4.99}$$

4.3.6 Second-order mean head and its gradient

Substitution of (4.85), (4.94), (4.97) and (4.98) into (4.84) yields

$$\overline{h}^{(2)}(x,t) = \frac{\sigma_Y^2}{2}\frac{\underline{Q}}{K_G}\left(x - \xi^{(0)}(t)\right) + \frac{r^{(2)}(y,t)}{K_G}\left[G_K^{(0)}(\xi^{(0)}(t),x) - G_K^{(0)}(0,x)\right] \tag{4.100}$$

It follows from (4.79), (4.80) and (4.97) that

$$\overline{h}^{(2)}(x,t) = \frac{\sigma_Y^2}{2}\frac{\underline{Q}}{K_G}\left(\xi^{(0)}(t) - x\right) \tag{4.101}$$

A second-order approximation of the mean head gradient is obtained by taking the derivative of (4.101) with respect to x.

$$\frac{\partial \bar{h}^{(2)}(x,t)}{\partial x} = -\frac{\sigma_Y^2}{2}\frac{Q}{K_G} \tag{4.102}$$

4.3.7 Velocity variance

From the one-dimensional version of (B.5) the first-order fluctuation of head is

$$\begin{aligned} h^{(1)}(x,t) &= -\frac{\theta}{K_G}V^{(1)}(t)G_K^{(0)}(\xi^{(0)}(t),x) \\ &+b\xi^{(1)}(t)\frac{\partial G_K^{(0)}(y,x)}{\partial y}\bigg|_{y=\xi^{(0)}(t)} \\ &-\int_0^{\xi^{(0)}(t)} Y'(y)\frac{\partial h^{(0)}(y,t)}{\partial y}\frac{\partial G_K^{(0)}(y,x)}{\partial y}dy \end{aligned} \tag{4.103}$$

Substituting (4.79), (4.81), (4.82) and (4.89) gives

$$\begin{aligned} h^{(1)}(x,t) &= -\frac{\theta}{K_G}V^{(1)}(t)\left(1-\xi^{(0)}(t)\right)-b\xi^{(1)}(t) \\ &-\frac{Q}{K_G}\int_0^{\xi^{(0)}(t)} Y'(y)\mathrm{H}(y-x)dy \end{aligned} \tag{4.104}$$

Evaluating (4.104) at the front and multiplying by $V^{(1)}(t)$ yields

$$\begin{aligned} -b\xi^{(1)}(x,t)V^{(1)}(t) &= -\frac{\theta}{K_G}V^{(1)}(t)V^{(1)}(t)\left(1-\xi^{(0)}(t)\right)-b\xi^{(1)}(t)V^{(1)}(t) \\ &-\frac{Q}{K_G}\int_0^{\xi^{(0)}(t)} Y'(y)V^{(1)}(t)\mathrm{H}(y-\xi)dy \end{aligned} \tag{4.105}$$

From the definition of the Heaviside function it follows that integral equals zero. Taking average of the rest of (4.105) gives

$$\sigma_{V}^{(2)}(t) = 0 \tag{4.106}$$

4.3.8 Front variance

Evaluating (4.104) at the front, multiplying by $\xi^{(1)}(t)$ and taking average gives

$$\sigma_{\xi}^{(2)}(t) = 0 \tag{4.107}$$

The fact that σ_{ξ}^{2}, σ_{V}^{2}, $\overline{\xi}^{(2)}(t)$, $\overline{V}^{(2)}(x,t)$ and cros-covariances associated with them are equal to zero follows directly from mass conservation arguments. Indeed, prescribing constant flux Q at the boundary requires that, with probability 1, the front propagates at a fixed deterministic velocity $V = \overline{V} = Q/\theta$. While trivial, this correspondence indicates that our averaged boundary-value problem is free of internal contradictions.

While the front moves through a random porous medium at deterministic velocity, the head and its gradient remain random.

4.3.9 Head gradient variance

The derivative of (4.103) with respect of x is

$$\frac{\partial h^{(1)}(x,t)}{\partial x} = -\frac{\theta}{K_G} V^{(1)}(t) \frac{\partial}{\partial x}\left(G_K^{(0)}(\xi^{(0)}(t),x)\right)$$
$$+b\xi^{(1)}(t)\frac{\partial}{\partial x}\left(\left.\frac{\partial G_K^{(0)}(y,x)}{\partial y}\right|_{y=\xi^{(0)}(t)}\right) \qquad (4.108)$$
$$-\int_0^{\xi^{(0)}(t)} Y'(y)\frac{\partial h^{(0)}(y,t)}{\partial y}\frac{\partial^2 G_K^{(0)}(y,x)}{\partial y \partial x}dy$$

Substituting (4.81), (4.82) and (4.96) into (4.108) yields

$$\frac{\partial h^{(1)}(x,t)}{\partial x} = -Y^{(1)}(x)\frac{\partial h^{(0)}(x,t)}{\partial x} \qquad (4.109)$$

Multiplying (4.109) by $\frac{\partial h^{(1)}(x,t)}{\partial x}$ and taking mean gives

$$\left[\sigma^2_{\partial h/\partial x}(x,t)\right]^{(2)} = r^{(2)}(x,t)\frac{\partial h^{(0)}(x,t)}{\partial x} \qquad (4.110)$$

or, using expressions (4.97) for the residual flux and (4.89) for the zero-order head gradient,

$$\left[\sigma^2_{\partial h/\partial x}\right]^{(2)} = \frac{Q^2\sigma_Y^2}{K_G} \qquad (4.111)$$

4.3.10 Comparison with direct analytical solution

We now compare the moment solutions, derived above, with corresponding exact solutions obtained by direct integration of (2.38).Integrating the one-dimensional version of (2.38) once gives

$$K_D(z)\frac{\partial h(z,t)}{\partial z} = A \qquad (4.112)$$

From the one-dimensional version of boundary condition (2.40) we find the constant $A = -Q$

Integrating (4.112) gives

$$h(z,t) = -Q\int_0^z \frac{dy}{K_D(y)} + h(0,t) \tag{4.113}$$

From the one-dimensional version of the first boundary condition in (2.41)

$$h(0,t) = -b\xi(t) + Q\int_0^z \frac{dy}{K_D(y)} \tag{4.114}$$

Then the exact expression for head is

$$h(z,t) = Q\int_z^{\xi(t)} \frac{dy}{K_D(y)} + a - b\xi(t) \tag{4.115}$$

From (4.112) it follows that front velocity $V=Q$. This corresponds exactly to our perturbation solution. Moreover, since V is deterministic, all its higher moments and cross-covariances are zero, $\sigma_V^2(t) = C_{KV}(x,t) = C_{hV}(x,t) \equiv 0$, which is in exact agreement with our perturbation solutions. A deterministic V implies deterministic dynamics of front movement,

$$\xi(t) = \frac{V}{\theta}t \tag{4.116}$$

From (4.112) it follows that the residual flux is given exactly by

$$r \equiv -\overline{K'(z)\frac{dh(z)}{dz}} = Q\frac{\overline{K'(z)}}{K(z)} = Q\frac{\overline{K - \overline{K(z)}}}{K(z)} = Q\left(1 - \overline{K(z)}\,\overline{\frac{1}{K(z)}}\right) = Q\left(1 - e^{\sigma_Y^2}\right) \tag{4.117}$$

Thus, indeed, $r^{(2)}(x,t) = -Q\sigma_Y^2$ given by (4.97) is true to second-order of approximation.

From (4.112)

$$\frac{\partial h(z,t)}{\partial z} = -\frac{Q}{K_D(z)} \tag{4.118}$$

Taking the mean of (4.118) gives

$$\frac{\partial \overline{h}(z,t)}{\partial z} = -\frac{Q}{K_G} e^{\sigma_Y^2} \tag{4.119}$$

Integrating (4.119) from z to $\xi(t)$ gives

$$\overline{h(z)} = \frac{Q_0}{K_G} e^{\frac{\sigma_Y^2}{2}} (\xi(t) - z) + a - b\xi(t) \tag{4.120}$$

Since in this case, $\xi(t) = \overline{\xi(t)} = \xi^{(0)}(t)$ $\overline{\xi}^{(2)} = \xi' \equiv 0$, (4.88) and (4.101) are indeed the zero- and second-order mean head approximations.

4.4. Flux-driven front in the absence of gravity

Here we consider horizontal flow driven by a constant flux. As mentioned earlier, moment expressions for gravity-free flow can be obtained from corresponding moment expressions for gravity flow by setting b=0.

For flux-driven front only the zero-order head depends on b and so on gravity. All other quantities are independent of b and thus similar for horizontal and vertical flows. This is not the case for a front with constant head boundary.

The expression for zero-order head can be obtained from (4.88) with b=0,

$$h^{(0)}(x,t) = \frac{Q}{K_G}(\xi^{(0)}(t) - x) \tag{4.121}$$

4.5 One - dimensional results and comparison with Monte Carlo simulations

4.5.1 Monte Carlo simulation

To test our moment equations, we compare their solutions to sample moments obtained from Monte Carlo solution. The principle of Monte Carlo simulation is straitforward. One treats log conductivity as a multivariate, Gaussian correlated random field with known statistical properties (mean, variance and correlation length). Each randomly generated realization of the hydraulic conductivity field is used to evaluate expressions (4.45) and (4.71) that are respectively solutions for "gravity" and "gravity-free" 1-D fronts driven by constant head. Each realization thus yields a random front position as a function of time. Unconditional random $Y(y) = \ln K(y)$ fields were generated by means of the Gaussian sequential simulator SGSIM (Deutsch and Journel, 1998).

Figure 4.1 shows the dimensionless time $K_G t / \theta l_Y$ needed for "gravity" front driven by constant head to reach dimensionless depth $L = \xi / l_Y$ equals to 10 for different realizations of Y. The time is seen to vary significantly for different realizations.

A statistical analysis of many such random solutions provides their mean and variance. The mean provides an optimum unbiased prediction of front position under uncertainty caused by unknown spatial variability of the hydraulic conductivity. The variance provides a measure of the corresponding predictive uncertainty.

Figures 4.2 and 4.3 show mean "gravity" 1-D front position driven by constant head, and its variance, versus the number of realizations for $\sigma_Y^2 = 1$ and $\sigma_Y^2 = 0.25$, respectively. We see that these sample statistics change with the number of realizations. The mean reaches a constant value much faster than the variance. The number of simulations required to obtain meaningful statistics increases with the variance of Y. There are no reliable criteria to assess the convergence of these Monte Carlo simulations.

4.5.2 Dynamic of one-dimensional mean front

Figures 4.4-4.6 show how head driven dimensionless mean front depth $L = \xi / I_Y$ increases with dimensionless time $K_G t / \theta I_Y$ as a function of σ_Y^2 for various flow parameters. MC denotes the results of 4000 Monte Carlo simulations and AN denotes the second-order analytical result $L^{[2]} = \left(\xi^{(0)} + \overline{\xi}^{(2)}\right) / I_Y$. Our analytical solution implies that for σ_Y^2 =0 the second-order mean front depth is $L^{[2]} = \xi^{(0)} / I_Y$, and $\xi^{(0)} / I_Y$ does not depend on the variance of Y.

Figure 4.4 describes gravity flow driven by constant head when b=0.5 and $(H - a)/bI_Y$ = 10 and Figure 4.5 when b=1 and $(H - a)/I_Y$ = 4. Note that $b = (\rho_D - \rho_W) / \rho_D$=1 represents an extreme case where $\rho_D \gg \rho_W$ or, more generally, where density of the driven fluid can be disregarded in comparison to that of the driving fluid. This extreme situation does not commonly arise in the context of a DNAPL front but does represent

well a wetting front where water drives air. We thus refer to a front with b=1 as a wetting front. Figure 4.6 displays gravity-free flow with $(H - a)/l_Y = 10$.

Figures 4.4-4.6 show that the zero-order analytical solution (corresponding to σ_Y^2=0) consistently overestimates the mean depth of the MC front. The second-order analytical solution is much closer to that obtained from Monte Carlo simulations and therefore more accurate. In all three cases accuracy is high for $\sigma_Y^2 = 0.25$ but deteriorates as σ_Y^2 increases. Mean front depth and its rate of advance diminish with increasing variance.

Figure 4.7 shows how the second-order approximation of dimensionless mean front depth $L^{[2]}$ increases with dimensionless time $K_G t / \theta l_Y$ as a function of $(H-a)/bl_Y$ for gravity flow driven by constant head when σ_Y^2=0.5 and b=0.5. Mean front depth and its rate of advance increase with $(H-a)/bl_Y$, i.e., increase with the driving head and decrease with the correlation length l_Y. The latter effect is amplified by the fact that dimensionless time also decreases as l_Y increases.

Figure 4.8 shows how $L^{[2]}$ increases with dimensionless time $K_G t / \theta l_Y$ as a function of b for gravity flow driven by constant head when σ_Y^2=0.5 and $(H-a)/l_Y$ =5. The larger is b (i.e., the density difference between driving and driven fluids), the faster does the front propagate. On the other hand, our analytical solution shows that in the absence of gravity, the front propagation rate is independent of density difference between the two fluids.

A one-dimensional front driven by a constant flux Q advances at a deterministic velocity Q/θ. Front velocity depends neither on density differences nor on gravity.

4.5.3 Front variance

Figures 4.9-4.11 show how dimensionless front variance σ_ξ^2 / l_Y^2 increases with dimensionless time $K_G t / \theta l_Y$ as a function of σ_Y^2 for various flow parameters.

Figure 4.9 describes gravity flow driven by constant head when b=0.5 and $(H - a)/bl_Y$ = 10. Figure 4.10 depicts variance of gravity wetting front driven by constant head when b=1 and $(H - a)/l_Y = 4$. Figure 4.11 displays gravity-free flow when $(H - a)/l_Y = 10$. The analytical solutions for front variance compare favorably with Monte Carlo results when $\sigma_Y^2 \le 0.5$ but deteriorate with time as σ_Y^2 increases in all but the gravity-free cases. Dimensionless gravity front variance appears to grow asymptotically in a near-linear fashion with dimensionless time, at a rate that increases with σ_Y^2. It follows from (4.59) that dimensionless gravity-free front variance grows in proportion to the square root of dimensionless time $\tilde{t}$,

$$\lim_{\tilde{t}\to\infty} \frac{\left[\sigma_\xi^2\right]^{(2)}}{l_Y^2} = 2\sigma_Y^2 \left(\sqrt{\frac{2(H-a)}{l_Y}} \frac{\sqrt{\tilde{t}}}{3} - \frac{1}{2} \right) \tag{4.122}$$

Under gravity and gravity-free flow the coefficient of variation $CV(t) = \sigma_\xi(t) / \bar{\xi}(t)$ (Figures 4.12 and 4.13, respectively) tends to zero with time, i.e., the standard deviation of front position $\sigma_\xi(t) = \sqrt{\sigma_\xi^2(t)}$ diminishes fast relative to mean growth rate. It follows

from (4.49) and (4.65) that in the absence of gravity the coefficient of variation obtained analytically goes to zero with time as $\sqrt{\frac{2}{3}}\frac{\sigma_Y}{\left[\frac{2(H-a)}{l_Y}\right]^{1/4} \tilde{t}^{1/4}\left(1-\frac{\sigma_Y^2}{4}\right)}$.

Figure 4.14 shows how dimensionless front variance σ_ξ^2 / l_Y^2 increases with dimensionless time $K_G t / \theta l_Y$ as a function of $(H-a)/bl_Y$ for gravity flow driven by constant head when σ_Y^2=0.5 and b=0.5. Figure 4.15 describes how dimensionless front variance increases with dimensionless time as a function of $(H-a)/l_Y$ for gravity-free flow driven by constant head when σ_Y^2=0.5. The dimensionless front variance increases with $(H-a)/l_Y$, i.e., increases with the driving head and diminishes with the correlation length l_Y. The latter effect is amplified by the fact that dimensionless time also decreases as l_Y increases. However, for a given dimensionless variance, the actual variance increases as l_Y^2.

Figure 4.16 shows how front variance σ_ξ^2 increases with normalized time $K_G t / \theta$ as a function of l_Y for gravity flow driven by constant head when $H-a$ = 0.1, σ_Y^2 = 1 and b = 0.5. Figure 4.17 describes how front variance increases with normalized time as a function of l_Y for gravity-free flow driven by constant head when $H-a$ = 0.1 and σ_Y^2 = 1. In both cases the front variance increases with l_Y.

Figure 4.18 illustrates how dimensionless front variance increases with dimensionless time as a function of b for gravity flow driven by constant head when σ_Y^2=0.5 and $(H-a)/l_Y$ =5. The front variance increases with b. The larger is the density difference between

driving and driven fluids the higher is the uncertainty associated with predicting the front position. For gravity-free flow, the front variance is independent of b.

A one-dimensional front driven by constant flux Q has zero variance.

4.5.4 Mean-pressure head gradient

As shown in Chapter 3, a front is stable when the gradient of pressure head immediately above it is negative (z pointing downward and pressure head increasing upward) and unstable when this gradient is positive. For instabilities to develop, the front must undergo some slight initial perturbation. In the case of randomly heterogeneous media, such perturbations are introduced (among other causes) by random variations in soil properties.

Figures 4.19, 4.20 and 4.21 show how the second-order approximation of mean pressure head gradient varies with dimensionless time as a function of σ_Y^2 for different sets of parameters. Figure 4.19 corresponds to gravity flow driven by constant head when b=0.5 and $(H - a)/bI_Y = 0.1$, Figure 4.20 to similar flow when b=1 and $(H - a)/bI_Y$ =0.1, and Figure 4.21 to gravity-free flow when $(H - a)/I_Y = 0.1$. In a homogeneous soil ($\sigma_Y^2 = 0$, hence second-order pressure head = 0) pressure gradient is represented by the zero-order solution. In Figures 4.20-4.21 the mean wetting front and gravity-free front remain stable in a homogeneous medium. The mean DNAPL front is initially stable but becomes unstable with time in Figure 4.19 regardless σ_Y^2. Heterogeneity is seen to have a destabilizing effect on the front under gravity. This effect increases rapidly to a peak at

early dimensionless time and then gradually dies out. In the gravity-free case, the front is always stable regardless of σ_Y^2. Theory and the figures indicate that the gradient of mean pressure head for gravity flow tends asymptotically to (1-*b*) with time. For gravity-free flow the gradient tends asymptotically to zero (constant pressure drop over increasing distance). That DNAPL fronts become unconditionally unstable with time is confirmed, among others, by the experimental work of Zhang and Smith (2001).

The gradient of mean pressure head for gravity flow $\frac{1}{\rho_D g}\frac{d\bar{p}}{dz}=1+\frac{d\bar{h}}{dz}$ driven by constant flux can be found from (4.89) and (4.102),

$$\frac{1}{\rho_D g}\frac{d\bar{p}}{dz}=1-\frac{Q}{K_G}(1+\frac{\sigma_Y^2}{2}) \tag{4.123}$$

and the gradient of mean pressure head for gravity-free flow $\frac{1}{\rho_D g}\frac{d\bar{p}}{dz}=\frac{d\bar{h}}{dz}$ driven by constant flux,

$$\frac{1}{\rho_D g}\frac{d\bar{p}}{dz}=-\frac{Q}{K_G}(1+\frac{\sigma_Y^2}{2}) \tag{4.124}$$

We can see that gravity-free front driven by constant flux is unconditionally stable (note that here we consider the case where $\mu_D \geq \mu_W$). A gravity front driven by constant flux is stable for $\frac{Q}{K_G}(1+\frac{\sigma_Y^2}{2})>1$ and unstable otherwise. It follows that heterogeneity has a stabilizing effect on gravity flow driven by constant flux.

The fact that gravity-free fronts driven by constant flux and by constant head remain stable is in full agreement with Saffman and Taylor (1958) who stated that such

displacements are stable to small deviations if motion is directed from the more viscous to the less viscous fluid, whatever are the relative densities of the fluids.

Figures 4.22-4.24 depict the influence of $(H - a)/I_Y$ on the gradient of mean pressure head, and on the onset of instability, for different types of flow. A DNAPL gravity front eventually becomes unstable for any $(H - a)/I_Y$ (Figure 4.22). For a mean wetting front to be stable, $(H - a)/I_Y$ must be sufficiently large (Figure 4.23). In both cases, the smaller is $(H - a)/I_Y$ the earlier does instability set in. A gravity-free front remains stable for all $(H - a)/I_Y$ (Figure 4.24).

An increase in the correlation scale I_Y has a destabilizing effect on the wetting front when $\sigma_Y^2 = 1$ and $(H - a)/I_Y = 0.1$ (Figure 4.25). DNAPL gravity front (Figure 4.26) and gravity-free fronts (Figure 4.27) remain unstable and stable, respectively, as correlation length increases.

Figure 4.28 shows that uncertainty in the prediction of mean pressure head gradient is largest at time zero, diminishes steeply at early time and more slowly at later time toward an asymptote that increases with σ_Y^2.

CHAPTER 5

TWO-DIMENSIONAL FRONT PROPAGATION

5.1 Displacement of water by low viscous DNAPL

In this chapter we consider two-dimensional displacement of water by a DNAPL in a horizontal channel of infinite length under a constant uniform flux maintained far behind the front (Fig. 5.1). DNAPL is either less viscous or more viscous than water. It was pointed by Saffman and Taylor (1958) that such displacement is "stable or unstable to small deviations according as the direction of motion is directed from the more viscous to less viscous fluid or vice versa, whatever the relative densities of the fluids, provided that the velocity is sufficiently large".

In Chapter 2 we described viscous DNAPL penetration below the water table by considering the water to remain static. Here we start by considering horizontal displacement of water by DNAPL whose viscosity is very small compared to that of water.

According to Darcy's law, water and DNAPL head gradients are given by

$$\nabla h_W(\mathbf{x}) = -\frac{\mathbf{q}_W(\mathbf{x})\mu_W}{k(x)\rho_W g} \tag{5.1}$$

and

$$\nabla h_D(\mathbf{x}) = -\frac{\mathbf{q}_D(\mathbf{x})\mu_D}{k(\mathbf{x})\rho_D g} \tag{5.2}$$

Since $\mu_D \ll \mu_W$ we can disregard the DNAPL head gradient relative to that of water and treat h_D as a constant. This allows us to focus solely on the motion of water.

The approach we follow was inspired by the work of Li *et al.* (1986) who studied Saffman-Taylor finger growth in a horizontal Hele-Shaw cell. Their equations (with capillary length d_0=0) are similar to (2.38)-(2.41) but disregard gravity and prescribe flux at $z = \infty$ rather than at z=0. Here z is the direction of motion of DNAPL and x is a direction perpendicular to the channel.

In terms of modified head $h = h_W - (P_D - P_E)/\rho_W g$, two-dimensional horizontal water flow in the porous medium is governed by

$$\mathbf{q}_W(\mathbf{x},t) = -K(\mathbf{x})\nabla h(\mathbf{x},t) \qquad \nabla\cdot\mathbf{q}_W(\mathbf{x}) = 0 \qquad \mathbf{x}\in\Omega,\ t>0 \tag{5.3}$$

$$\mathbf{n}(\mathbf{x},t)\cdot\mathbf{q}_W(\mathbf{x},t) = 0 \qquad \mathbf{x}\in walls \tag{5.4}$$

$$h(\mathbf{x},t) = 0 \qquad \mathbf{n}(\mathbf{x},t)\cdot\mathbf{q}_W(\mathbf{x},t) = \theta V_n(\mathbf{x},t) \qquad \mathbf{x}\in\gamma(t) \tag{5.5}$$

where $\mathbf{q}_W$ is Darcy flux of water, $h_W = P_W/\rho_W g$ is hydraulic head of water, P_D is DNAPL pressure and P_E is DNAPL entry pressure. Water flux through the channel is constant and related to front normal velocity via

$$\theta\int_{\gamma(t)} V_n(\mathbf{y},t)d\mathbf{y} = Q \tag{5.6}$$

This reflects the fact that water flow rate far down the channel is the same as at the front.

In analogy to (2.13), the above system of equations can be converted to an integral equation

$$h(\mathbf{x},t) = M + \theta \int_{\gamma(t)} V_n(\mathbf{y},t) G(\mathbf{x},\mathbf{y}) d\mathbf{y}$$
$$- \int_{\Omega(t)} K'(\mathbf{y}) \nabla_{\mathbf{y}} h(\mathbf{y},t) \bullet \nabla_{\mathbf{y}} G(\mathbf{x},\mathbf{y}) d\mathbf{y} \tag{5.7}$$

Here $M = \bar{M} + M'$ is a random constant that arises from condition (5.6) and Ω is the flow domain, occupied by water.

In analogy to (2.42) and (2.44) the leading-order approximations of (5.7) are

$$h^{(0)}(\mathbf{x},t) = M^{(0)} + \frac{\theta}{K_G} \int_{\gamma^{(0)}(t)} G_K^{(0)}(\mathbf{x},\mathbf{y}) V_n^{(0)}(\mathbf{y},t) d\mathbf{y} \tag{5.8}$$

and

$$\bar{h}^{[2]}(\mathbf{x},t) = M^{[2]} + \frac{\theta}{K_G} \int_{\gamma^{[2]}(t)} \left(\bar{V}_n^{[2]}(\mathbf{y},t) - \frac{\sigma_Y^2}{2} V_n^{(0)}(\mathbf{y},t) \right) G_K^{(0)}(\mathbf{x},\mathbf{y}) d\mathbf{y}$$
$$+ \int_{\Omega^{(0)}(t)} \mathbf{r}^{[2]}(\mathbf{y},t) \bullet \nabla_{\mathbf{y}} G_K^{(0)}(\mathbf{x},\mathbf{y}) d\mathbf{y} \tag{5.9}$$
$$+ \int_{\gamma^{(0)}(t)} C_{YY}^{[2]}(\mathbf{y},\mathbf{y}) \nabla h^{(0)}(\mathbf{y},t) \bullet \nabla_{\mathbf{y}} G_K^{(0)}(\mathbf{x},\mathbf{y}) d\mathbf{y}$$

Here the signs of integrals along the front have been reversed as compared to equations (2.42) and (2.44). This is so because the latter equations represent DNAPL flow behind the front, whereas (5.8)-(5.9) describe water flow ahead of the front. The outer normal vectors in these two cases point in opposite directions, causing a reversal of sign.

In the above $G_K^{(0)} = K_G G^{(0)}$ is a deterministic Green's function that satisfies (Kessler *et al.*, 1986)

$$\nabla_{\mathbf{y}}^2 G_K^{(0)}(\mathbf{x},\mathbf{y}) + \delta(\mathbf{x}-\mathbf{y}) = 0 \qquad \mathbf{y},\mathbf{x} \in \Omega_T \tag{5.10}$$

subject to

$$\mathbf{n}(\mathbf{x})\cdot\nabla_{\mathbf{x}}G_K^{(0)}(\mathbf{x},\mathbf{y})=0 \qquad \mathbf{x}\in walls \tag{5.11}$$

$$G_K^{(0)}(\mathbf{x},\mathbf{y})=0 \qquad z_{\mathbf{x}}\to-\infty \tag{5.12}$$

For two-dimensional symmetric flow in the (x, z) plane with half width of the channel $c=1$, $G_K^{(0)}$ is given by (Kessler *et al.*, 1986)

$$G_K^{(0)}(\mathbf{x},\mathbf{y})=-\frac{z_{\mathbf{x}}-z_{\mathbf{y}}+\left|z_{\mathbf{x}}-z_{\mathbf{y}}\right|}{4}-\frac{1}{4\pi}\ln\left(1-2e^{-\pi\left|z_{\mathbf{x}}-z_{\mathbf{y}}\right|}\cos\left[\pi\left(x_{\mathbf{x}}-x_{\mathbf{y}}\right)\right]+e^{-2\pi\left|z_{\mathbf{x}}-z_{\mathbf{y}}\right|}\right) \tag{5.13}$$

The zero and second order approximations of M, $M^{(0)}$ and $M^{[2]}$, arise from

$$\theta\int_{\gamma(t)}V_n^{(0)}(\mathbf{y},t)d\mathbf{y}=Q \tag{5.14}$$

and

$$\theta\int_{\gamma(t)}\bar{V}_n^{[2]}(\mathbf{y},t)d\mathbf{y}=Q. \tag{5.15}$$

respectively.

Evaluating (5.8) at the front yields

$$0=M^{(0)}+\frac{\theta}{K_G}\int_{\gamma^{(0)}(t)}G_K^{(0)}(\mathbf{x}_\gamma,\mathbf{y})V_n^{(0)}(\mathbf{y},t)d\mathbf{y} \tag{5.16}$$

Next we evaluate (5.9) at the front, expand the integral $\frac{\theta}{K_G}\frac{\sigma_\gamma^2}{2}\int_{\bar{\gamma}^{[2]}(t)}V_n^{(0)}(\mathbf{y},t)G_K^{(0)}(\mathbf{x},\mathbf{y})d\mathbf{y}$ about $\gamma^{(0)}$, and retain only the leading term. From (5.16) it follows that this term is $\frac{\theta}{K_G}\frac{\sigma_\gamma^2}{2}\int_{\gamma^{(0)}(t)}G_K^{(0)}(\mathbf{x}_\gamma,\mathbf{y})V_n^{(0)}(\mathbf{y},t)d\mathbf{y}=-\frac{\sigma_\gamma^2}{2}M^{(0)}$. Hence

$$0 = M^{[2]} + \frac{\sigma_Y^2}{2} M^{(0)} + \frac{\theta}{K_G} \int_{\gamma^{[2]}(t)} \bar{V}_n^{[2]}(\mathbf{y},t) G_K^{(0)}(\mathbf{x}_\gamma,\mathbf{y}) d\mathbf{y} + \int_{\Omega^{(0)}(t)} \mathbf{r}^{[2]}(\mathbf{y},t) \bullet \nabla_{\mathbf{y}} G_K^{(0)}(\mathbf{x}_\gamma,\mathbf{y}) d\mathbf{y}$$
$$+ \int_{\gamma^{(0)}(t)} C_{Y\gamma}^{[2]}(\mathbf{y},\mathbf{y}) \nabla h^{(0)}(\mathbf{y},t) \bullet \nabla_{\mathbf{y}} G_K^{(0)}(\mathbf{x}_\gamma,\mathbf{y}) d\mathbf{y} \tag{5.17}$$

where $\mathbf{x}_\gamma$ is position on $\gamma(t)$.

Operating on (5.7) with the stochastic differential operator $Y'(\mathbf{x})\nabla_{\mathbf{x}}$, taking ensemble mean, and retaining terms of order σ_Y^2 gives an expression for $\mathbf{r}(\mathbf{x},t)$ that is similar to (2.26),

$$r_x^{[2]}(\mathbf{x},t) = -\frac{\theta}{K_G} \int_{\gamma^{(0)}(t)} C_{YV}^{[2]}(\mathbf{x},\mathbf{y}) \frac{\partial G_K^{(0)}(\mathbf{x},\mathbf{y})}{\partial x_{\mathbf{x}}} d\mathbf{y}$$
$$+ \int_{\Omega^{(0)}(t)} C_Y^{[2]}(\mathbf{x},\mathbf{y}) \left(\frac{\partial h^{(0)}(\mathbf{y},t)}{\partial x_{\mathbf{y}}} \frac{\partial^2 G_K^{(0)}(\mathbf{x},\mathbf{y})}{\partial x_{\mathbf{y}} \partial x_{\mathbf{x}}} + \frac{\partial h^{(0)}(\mathbf{y},t)}{\partial z_{\mathbf{y}}} \frac{\partial^2 G_K^{(0)}(\mathbf{x},\mathbf{y})}{\partial z_{\mathbf{y}} \partial x_{\mathbf{x}}} \right) d\mathbf{y} \tag{5.18}$$

$$r_z^{[2]}(\mathbf{x},t) = -\frac{\theta}{K_G} \int_{\gamma^{(0)}(t)} C_{YV}^{[2]}(\mathbf{x},\mathbf{y}) \frac{\partial G_K^{(0)}(\mathbf{x},\mathbf{y})}{\partial z_{\mathbf{x}}} d\mathbf{y}$$
$$+ \int_{\Omega^{(0)}(t)} C_Y^{[2]}(\mathbf{x},\mathbf{y}) \left(\frac{\partial h^{(0)}(\mathbf{y},t)}{\partial x_{\mathbf{y}}} \frac{\partial^2 G_K^{(0)}(\mathbf{x},\mathbf{y})}{\partial x_{\mathbf{y}} \partial z_{\mathbf{x}}} + \frac{\partial h^{(0)}(\mathbf{y},t)}{\partial z_{\mathbf{y}}} \frac{\partial^2 G_K^{(0)}(\mathbf{x},\mathbf{y})}{\partial z_{\mathbf{y}} \partial z_{\mathbf{x}}} \right) d\mathbf{y} \tag{5.19}$$

Note that operating with the stochastic differential operator $Y'(\mathbf{x})\nabla_{\mathbf{x}}$ on random constant M gives zero, $Y'(\mathbf{x})\nabla_{\mathbf{x}} M = 0$.

The covariance C_{YV} is obtained by evaluating (5.7) at the front, multiplying by $Y'(\mathbf{x})$, taking average, and retaining terms of order σ_Y^2 (in analogy to Appendix D):

$$\frac{\theta}{K_G} \int_{\gamma^{(0)}(t)} C_{YV}^{[2]}(\mathbf{x},\mathbf{y}) G_K^{(0)}(\mathbf{x}_\gamma,\mathbf{y}) d\mathbf{y} + m_1(\mathbf{x}) = \int_{\Omega^{(0)}(t)} C_Y^{[2]}(\mathbf{x},\mathbf{y}) \nabla_{\mathbf{y}} h^{(0)}(\mathbf{y},t) \bullet \nabla_{\mathbf{y}} G_K^{(0)}(\mathbf{x}_\gamma,\mathbf{y}) d\mathbf{y} \tag{5.20}$$

where $m_1(\mathbf{x}) = \overline{MY'(\mathbf{x})}$ can be found from the condition

$$\int_{\gamma^{(0)}(t)} C_{YV}^{[2]}(\mathbf{x},\mathbf{y})d\mathbf{y} = 0 \tag{5.21}$$

The cross-covariance $C_{Y\gamma}$ can be found from the differential equation

$$C_{YV} = \frac{dC_{Y\gamma}}{dt} \tag{5.22}$$

and the initial condition

$$C_{Y\gamma}(t=0) = 0\,. \tag{5.23}$$

Given the shape of the front at some time t, its normal velocity $\overline{V}_n^{[i]}$, i=0, 2 is fully defined by equations (5.14)-(5.17).

We parameterize the zero- and second-order mean fronts by relative arc length $s^{[i]}$ (measured from finger tip and normalized by total arc length , $s_t^{[i]}$, from fingertip to base) and angles between the normal to the interface at $s^{[i]}$ and the z coordinate, $\alpha^{[i]}(s^{[i]})$. Given normal mean velocity $\overline{V}_n^{[i]}$ along the front, a new front position is calculated according to (R.C. Brower, 1983; Kessler, 1984).

$$\frac{d\alpha^{[i]}}{dt} = -\frac{1}{s_t^{[i]}}\frac{\partial \overline{V}_n^{[i]}}{\partial s^{[i]}} - \frac{1}{s_t^{[i]}}\frac{\partial \alpha^{[i]}}{\partial s^{[i]}}\left\{\int_0^{s^{[i]}} \frac{\partial \alpha^{[i]}(y)}{\partial y}\overline{V}_n^{[i]}(y)dy - s^{[i]}\int_0^1 \frac{\partial \alpha^{[i]}(y)}{\partial y}\overline{V}_n^{[i]}(y)dy\right\} \tag{5.24}$$

and

$$\frac{ds_t^{[i]}}{dt} = s_t^{[i]}\int_0^1 \frac{\partial \alpha^{[i]}(y)}{\partial y}\overline{V}_n^{[i]}(y)dy \tag{5.25}$$

Uncertainty in the predicted front position is quantified by the variance of its normal velocity. Evaluating (5.7) at some point $\mathbf{x}_\gamma$ along the front, multiplying by $V_n'(\mathbf{z}_\gamma)$, taking ensemble mean and retaining terms of order σ_Y^2 yields

$$0 = m_2(\mathbf{z}_\gamma) + \frac{\theta}{K_G}\int_{\gamma^{(0)}(t)} C_V^{[2]}(\mathbf{z}_\gamma,\mathbf{y})G_K^{(0)}(\mathbf{x}_\gamma,\mathbf{y})d\mathbf{y} - \int_{\Omega^{(0)}(t)} C_{YV}^{[2]}(\mathbf{z}_\gamma,\mathbf{y})\nabla_y h^{(0)}(\mathbf{y},t)\bullet\nabla_y G_K^{(0)}(\mathbf{x}_\gamma,\mathbf{y})d\mathbf{y} \tag{5.26}$$

where $m_2(\mathbf{z}_\gamma) = \overline{MV_n'(\mathbf{z}_\gamma)}$ arises from

$$\int_{\gamma^{(0)}(t)} C_V^{[2]}(\mathbf{z}_\gamma,\mathbf{y})d\mathbf{y} = 0 \tag{5.27}$$

5.2 Displacement of water by highly viscous DNAPL

Here we consider the same problem as before but with $\mu_D \gg \mu_W$. This allows us to disregard water head gradients and treat h_W as a constant, motion being restricted to DNAPL.

The problem is governed by

$$\mathbf{q}_D(\mathbf{x},t) = -K_D(\mathbf{x})\nabla h(\mathbf{x},t) \qquad \nabla\bullet\mathbf{q}_D(\mathbf{x}) = 0 \qquad \mathbf{x}\in\Omega,\ t>0 \tag{5.28}$$

$$\mathbf{n}(\mathbf{x},t)\bullet\mathbf{q}_D(\mathbf{x},t) = 0 \qquad \mathbf{x}\in walls \tag{5.29}$$

$$h(\mathbf{x},t) = 0 \qquad \mathbf{n}(\mathbf{x},t)\bullet\mathbf{q}_D(\mathbf{x},t) = \theta V_n(\mathbf{x},t) \qquad \mathbf{x}\in\gamma(t) \tag{5.30}$$

where $\mathbf{q}_D$ is Darcy's flux of DNAPL, K_D is DNAPL conductivity as defined in Chapter 2, and $h = P_D / \rho_D g - (P_E - P_0)/\rho_D g$ is modified DNAPL head . Mass conservation implies that

$$\theta \int_{\gamma(t)} V_n(\mathbf{y},t)d\mathbf{y} = Q \tag{5.31}$$

i. e., DNAPL flow rate at the front is equal to that at the far end of the channel.

Equations (5.28)-(5.30) are similar to (5.3)-(5.5), the former describing flow of DNAPL behind the front and the latter flow of water ahead of the front.

Hence integral equations describing front evolution based on (5.28)-(5.30) have similar forms to those based on (5.3)-(5.5) but with opposite sign in front of boundary integrals. It follows that

$$h(\mathbf{x},t) = M - \theta \int_{\gamma(t)} V_n(\mathbf{y},t)G(\mathbf{x},\mathbf{y})d\mathbf{y} \tag{5.32}$$

There also is a change in the 0^{th} Fourier component of the Green's function, which controls its behavior at infinity. To guarantee that DNAPL head increases linearly as $z_x \to -\infty$, the Green's function must vanish at $z_x \to +\infty$ (Kessler et al. 1986):

$$G_K(\mathbf{x},\mathbf{y}) = -\frac{z_y - z_x + |z_x - z_y|}{4} - \frac{1}{4\pi}\ln\left(1 - 2e^{-\pi|z_x - z_y|}\cos\left[\pi\left(x_x - x_y\right)\right] + e^{-2\pi|z_x - z_y|}\right) \tag{5.33}$$

The zero- and second-order mean DNAPL heads are

$$h^{(0)}(\mathbf{x},t) = M^{(0)} - \frac{\theta}{K_G}\int_{\gamma^{(0)}(t)} G_K^{(0)}(\mathbf{x},\mathbf{y})V_n^{(0)}(\mathbf{y},t)d\mathbf{y} \tag{5.34}$$

and

$$\overline{h}^{[2]}(\mathbf{x},t)=M^{[2]}+\frac{\sigma_Y^2}{2}M^{(0)}-\frac{\theta}{K_G}\int_{\gamma^{[2]}(t)}\overline{V}_n^{[2]}(\mathbf{y},t)G_K^{(0)}(\mathbf{x},\mathbf{y})d\mathbf{y}+\int_{\Omega^{(0)}}\mathbf{r}^{[2]}(\mathbf{y},t)\bullet\nabla_y G_K^{(0)}(\mathbf{x},\mathbf{y})d\mathbf{y}$$

$$-\int_{\gamma^{(0)}(t)}C_{Y\gamma}^{[2]}(\mathbf{y},\mathbf{y})\nabla h^{(0)}(\mathbf{y},t)\bullet\nabla_y G_K^{(0)}(\mathbf{x},\mathbf{y})d\mathbf{y} \tag{5.35}$$

where $M^{(0)}$ and $M^{[2]}$ are obtained from

$$\theta\int_{\gamma^{(0)}(t)}V_n^{(0)}(\mathbf{y},t)d\mathbf{y}=Q \tag{5.36}$$

and

$$\theta\int_{\gamma^{[2]}(t)}\overline{V}_n^{[2]}(\mathbf{y},t)d\mathbf{y}=Q. \tag{5.37}$$

respectively.

Zero- and second-order mean front evolutions are described by

$$0=M^{(0)}-\frac{\theta}{K_G}\int_{\gamma^{(0)}(t)}G_K^{(0)}(\mathbf{x}_\gamma,\mathbf{y})V_n^{(0)}(\mathbf{y})d\mathbf{y} \tag{5.38}$$

and

$$0=M^{[2]}+\frac{\sigma_Y^2}{2}M^{(0)}-\frac{\theta}{K_G}\int_{\gamma^{[2]}(t)}\overline{V}_n^{[2]}(\mathbf{y},t)G_K^{(0)}(\mathbf{x}_\gamma,\mathbf{y})d\mathbf{y}+$$

$$\int_{\Omega^{(0)}}\mathbf{r}^{[2]}(\mathbf{y},t)\bullet\nabla_y G_K^{(0)}(\mathbf{x}_\gamma,\mathbf{y})d\mathbf{y} \tag{5.39}$$

$$-\int_{\gamma^{(0)}(t)}C_{Y\gamma}^{[2]}(\mathbf{y},\mathbf{y})\nabla h^{(0)}(\mathbf{y},t)\bullet\nabla_y G_K^{(0)}(\mathbf{x}_\gamma,\mathbf{y})d\mathbf{y}$$

where $\mathbf{x}_\gamma$ is on $\gamma(t)$.

Components of the second-order residual flux vector are given by

$$r_x^{[2]}(\mathbf{x},t)=\frac{\theta}{K_G}\int_{\gamma^{(0)}(t)} C_{Y\Gamma'}^{[2]}(\mathbf{x},\mathbf{y})\frac{\partial G_K^{(0)}(\mathbf{x},\mathbf{y})}{\partial x_{\mathbf{x}}}d\mathbf{y}+$$
$$\int_{\Omega^{(0)}(t)} C_Y^{[2]}(\mathbf{x},\mathbf{y})\left(\frac{\partial h^{(0)}(\mathbf{y},t)}{\partial x_{\mathbf{y}}}\frac{\partial^2 G_K^{(0)}(\mathbf{x},\mathbf{y})}{\partial x_{\mathbf{y}}\partial x_{\mathbf{x}}}+\frac{\partial h^{(0)}(\mathbf{y},t)}{\partial z_{\mathbf{y}}}\frac{\partial^2 G_K^{(0)}(\mathbf{x},\mathbf{y})}{\partial z_{\mathbf{y}}\partial x_{\mathbf{x}}}\right)d\mathbf{y} \tag{5.40}$$

$$r_z^{[2]}(\mathbf{x},t)=\frac{\theta}{K_G}\int_{\gamma^{(0)}(t)} C_{Y\Gamma'}^{[2]}(\mathbf{x},\mathbf{y})\frac{\partial G_K^{(0)}(\mathbf{x},\mathbf{y})}{\partial z_{\mathbf{x}}}d\mathbf{y}$$
$$+\int_{\Omega^{(0)}(t)} C_Y^{[2]}(\mathbf{x},\mathbf{y})\left(\frac{\partial h^{(0)}(\mathbf{y},t)}{\partial x_{\mathbf{y}}}\frac{\partial^2 G_K^{(0)}(\mathbf{x},\mathbf{y})}{\partial x_{\mathbf{y}}\partial z_{\mathbf{x}}}+\frac{\partial h^{(0)}(\mathbf{y},t)}{\partial z_{\mathbf{y}}}\frac{\partial^2 G_K^{(0)}(\mathbf{x},\mathbf{y})}{\partial z_{\mathbf{y}}\partial z_{\mathbf{x}}}\right)d\mathbf{y} \tag{5.41}$$

The second-order cross-covariance $C_{Y\Gamma'}$ is obtained from

$$-\frac{\theta}{K_G}\int_{\gamma^{(0)}(t)} C_{Y\Gamma'}^{[2]}(\mathbf{x},\mathbf{y})G_K^{(0)}(\mathbf{x}_\gamma,\mathbf{y})d\mathbf{y}+m_1(\mathbf{x})=\int_{\Omega^{(0)}(t)} C_Y^{[2]}(\mathbf{x},\mathbf{y})\nabla_{\mathbf{y}}h^{(0)}(\mathbf{y},t)\bullet\nabla_{\mathbf{y}}G_K^{(0)}(\mathbf{x}_\gamma,\mathbf{y})d\mathbf{y}$$

(5.42)

where $m_1(\mathbf{x})=\overline{M'Y'(\mathbf{x})}$ is found from the condition

$$\int_{\gamma^{(0)}(t)} C_{Y\Gamma'}^{[2]}(\mathbf{x},\mathbf{y})d\mathbf{y}=0 \tag{5.43}$$

The cross-covariance $C_{Y\gamma}$ is determined from the differential equation

$$C_{Y\Gamma'}=\frac{dC_{Y\gamma}}{dt} \tag{5.44}$$

subject to the initial condition

$$C_{Y\gamma}(t=0)=0 \tag{5.45}$$

The variance of normal velocity is obtained from

$$0 = m_2(\mathbf{z}_\gamma) - \frac{\theta}{K_G}\int_{\gamma(t)} C_V^{[2]}(\mathbf{z}_\gamma,\mathbf{y})G_K^{(0)}(\mathbf{x}_\gamma,\mathbf{y})d\mathbf{y}$$
$$- \int_{\Omega^{(0)}(t)} C_{IV}^{[2]}(\mathbf{z}_\gamma,\mathbf{y})\nabla_{\mathbf{y}}h^{(0)}(\mathbf{y},t)\bullet\nabla_{\mathbf{y}}G_K^{(0)}(\mathbf{x}_\gamma,\mathbf{y})d\mathbf{y} \qquad (5.46)$$

where $m_2(\mathbf{z}_\gamma) = \overline{MV_n'(\mathbf{z}_\gamma)}$ follows from the condition

$$\int_{\gamma^{(0)}(t)} C_V^{[2]}(\mathbf{z}_\gamma,\mathbf{y})d\mathbf{y} = 0 \qquad (5.47)$$

5.3 Numerical results

Here we present numerical results describing displacement of water by low viscous DNAPL. Details of numerical solution are given in Appendix T .

5.3.1 DNAPL fingering in homogeneous soil

The zero-order approximation of the mean front satisfies a standard boundary-value problem with moving boundaries for a homogeneous medium with conductivity $K=K_G$. We found that a single perturbation of the front gives rise to a single smooth Saffman-Tailor type finger (Figure 5.3). Finger width equals half the width of the channel in perfect agreement with Saffman and Taylor (1958).

To check the stability and accuracy of our numerical solution we computed front positions for different numbers of discretization points and for different time step sizes. Figure 5.4 shows that when the number of discretization points increases from 25 to 40,

the finger shortens slightly but otherwise remains the same. The LSODE code allows controlling time step size by varying the relative error tolerance parameter (RTOL). Figure 5.5 shows that RTOL has only a small effect on finger shape and size.

Figure 5.6 shows the evolution of a dominant finger from the largest of three initial perturbations. This agrees in principle with experimental results by Tabeling et al. (1986) (Figure 5.7). This "shielding" effect disappears when the initial perturbations are uniform, resulting in uniform finger evolution (Figure 5.8).

Perturbation of a fingertip leads to splitting (Figure 5.9). This too agrees with the experimental results (Figure 5.10) of Tabeling et al. (1986).

5.3.2 Effect of heterogeneity

Heterogeneity and nonlocality of mean behavior manifest themselves solely in second- and higher-order terms. As was already mentioned, we computed second-order mean front evolution for $Y(x)$ having an exponential covariance function

$$C_Y\left(|\mathbf{x}-\mathbf{y}|\right)=\sigma_Y^2\exp\left(\frac{|z_x-z_y|}{l_z}\right) \tag{5.48}$$

where l_z is correlation length in the z direction. For simplicity, we take the correlation length in the x direction to be infinite. This is analogous to flow across a perfectly stratified medium.

To check our solution we start with the case where correlation length in the z direction is also infinite. This renders the conductivity a random constant. As flow is controlled by

a constant flux, the mean front does not depend on the random conductivity value. Figure 5.11 compares zero- and second-order mean front positions at various times, showing that they are identical except for what we consider to be numerical errors associated with the second-order solution (theoretically, the two solutions should be identical). These errors are seen to grow with time, causing a numerical splitting of the finger. We suspect that part of the error stems from our rudimentary schemes of domain integration and front velocity computation. Since both the domain and the front vary with time, employing higher-order numerical schemes might require an added amount of computational effort. To avoid this, we have opted for artificially smoothing the front normal velocity profile whenever it becomes rough. The results agreed closely with the zero-order solution.

Figure 5.12 shows second-order mean Saffman-Taylor fingers at different times for various σ_Y^2 (normalized correlation length l_z/c = 1). We see that random layering reduces mean finger propagation rate. The larger is the variance of conductivity, the slower does the finger propagate. Figure 5.13 shows that as the normalized correlation length l_z/c increases, the second-order mean Saffman-Taylor finger becomes longer.

Figure 5.14 indicates that velocity variance is highest at fingertip, which moves the fastest, and dies out toward the slower base of the finger, increasing with σ_Y^2. The velocity variance decreases as l_z/c increases (Figure 5.15).

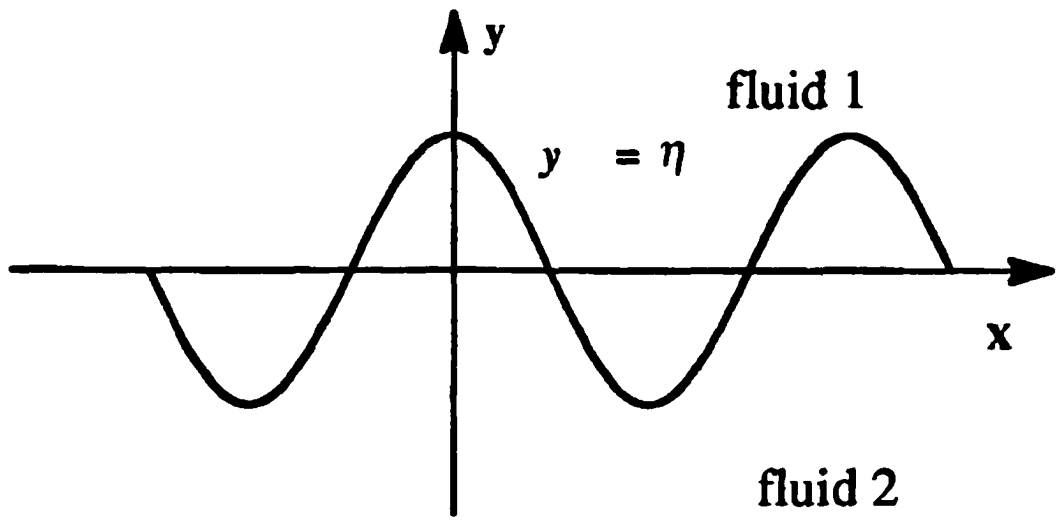

Figure 1.1. Wave like disturbance. After Chen et al. (1995).

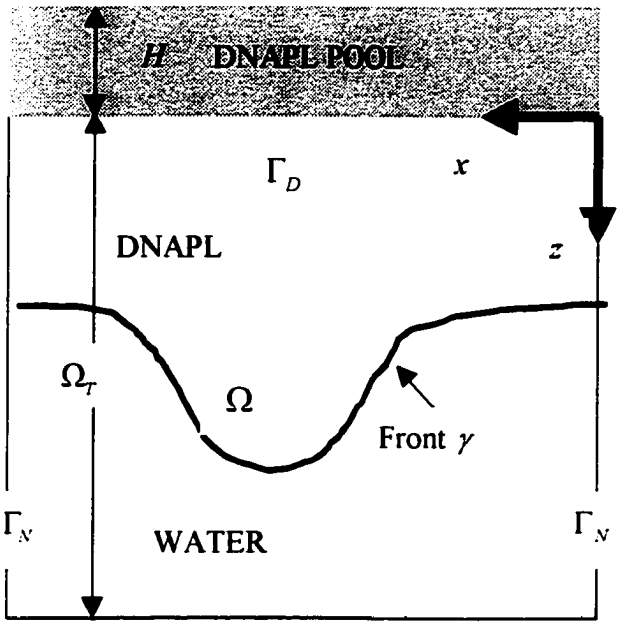

Figure 2.1. Flow domain Ω (DNAPL region). Green's function defined on Ω_T that consists of DNAPL region and region saturated with water, separated by front γ. Dirichlet boundary Γ_D with prescribed constant hydraulic head $h=H$. No-flow Neumann boundary Γ_N.

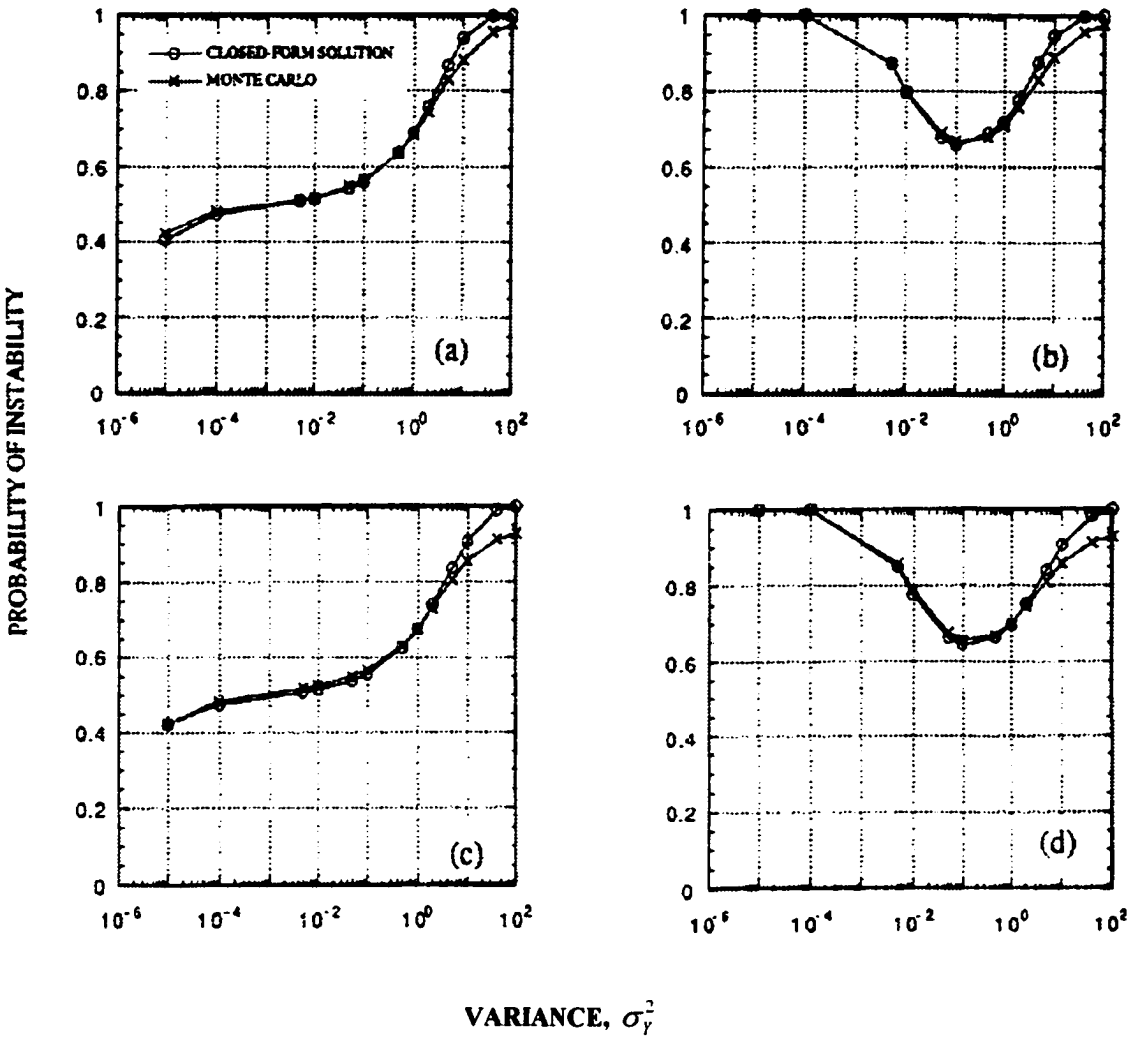

Figure 3.1. Probability of instability computed analytically and by Monte Carlo simulation at $L/I_Y = 40$ for (a) prescribed ψ_E with G_u = 0.00075, (b) prescribed ψ_E with G_u = -0.075, (c) random ψ_E with b = 8.16 $(m^3/d)^{1/2}$ and G_u = 0.00075, (d) random ψ_E with b = 8.16 $(m^3/d)^{1/2}$ and G_u = -0.075. After Chen and Neuman (1996).

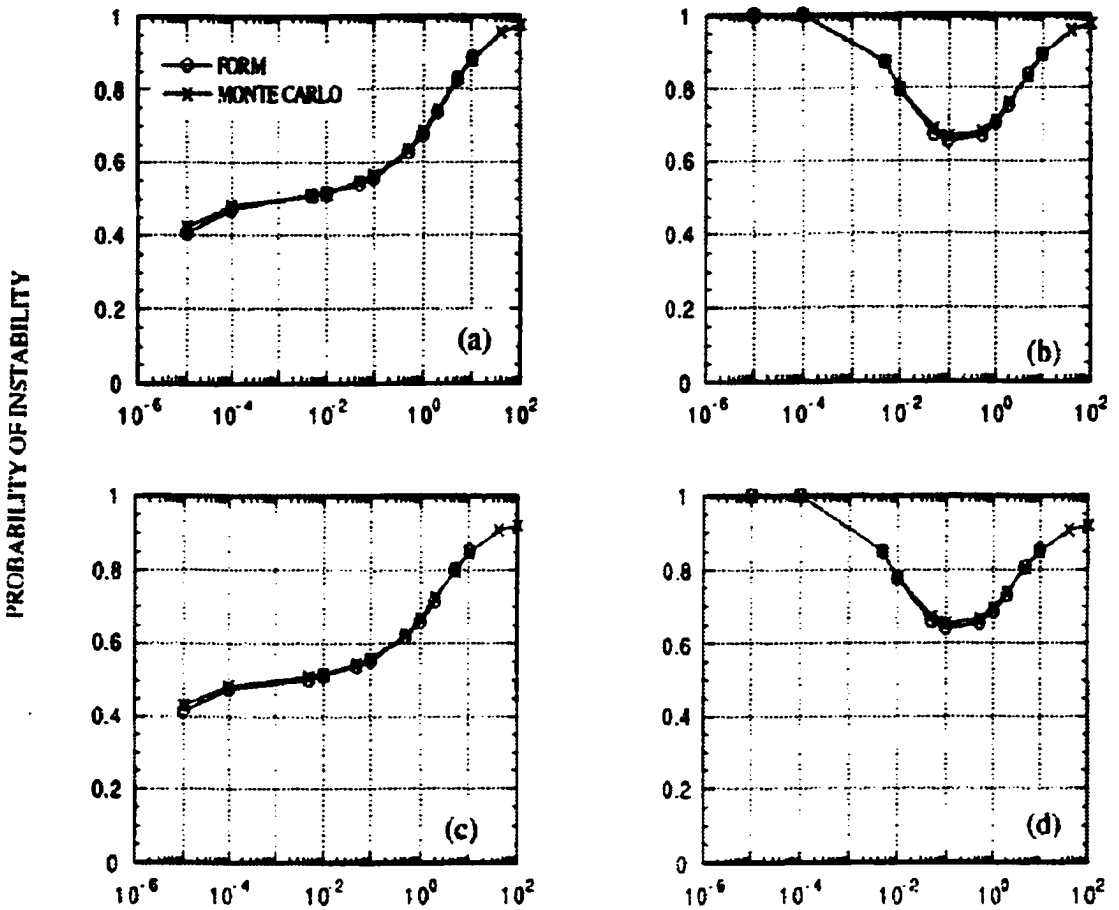

Figure 3.2. Probability of instability computed by first-order reliability method and Monte Carlo simulation at $L/I_Y = 40$ for (a) prescribed ψ_E with G_u = 0.00075, (b) prescribed ψ_E with G_u = -0.075, (c) random ψ_E with b = 8.16 $(m^3/d)^{1/2}$ and G_u = 0.00075, (d) random ψ_E with b = 8.16 $(m^3/d)^{1/2}$ and G_u = -0.075. After Chen and Neuman (1996).

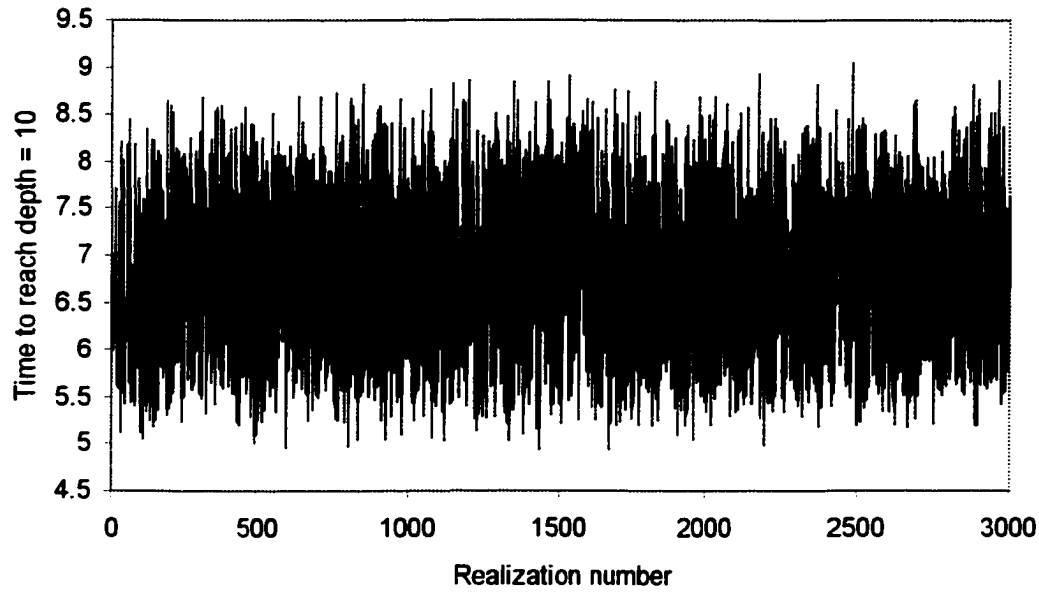

Figure 4.1. Dimensionless time needed for gravity front driven by constant head to reach dimensionless depth equals to 10 for different realizations of Y=ln$K$ field. b = 0.5, $(H\text{-}a)/bI_Y$ = 10, σ_Y^2 = 0.25.

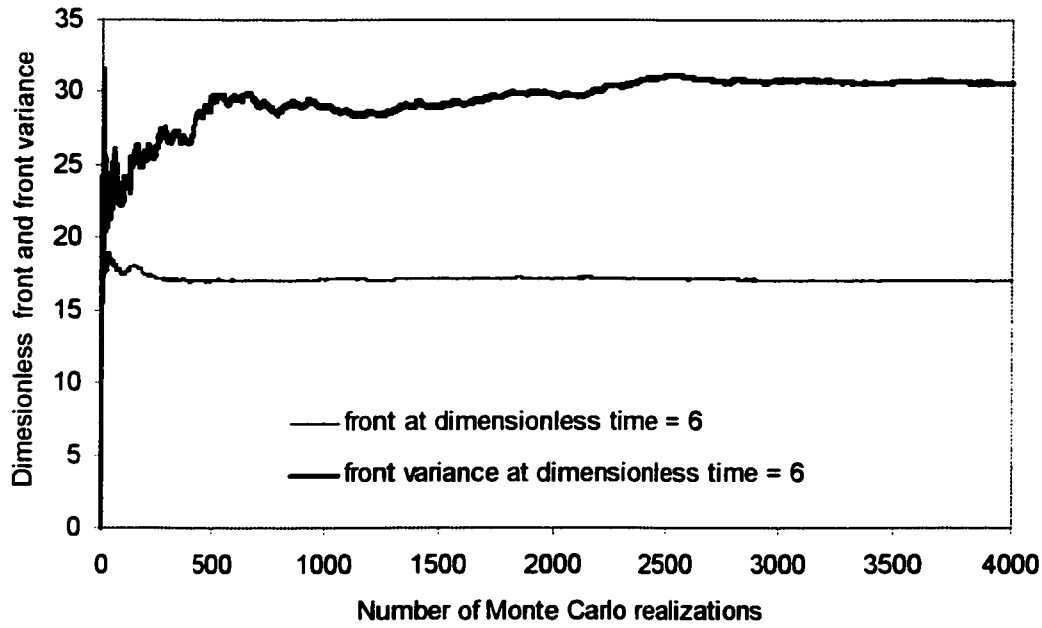

Figure 4.2. Mean 1-D front position and its variance versus number of realizations. Gravity flow driven by constant head. $b = 0.5$, $(H\text{-}a)/bI_Y = 10$, $\sigma_Y^2 = 1$.

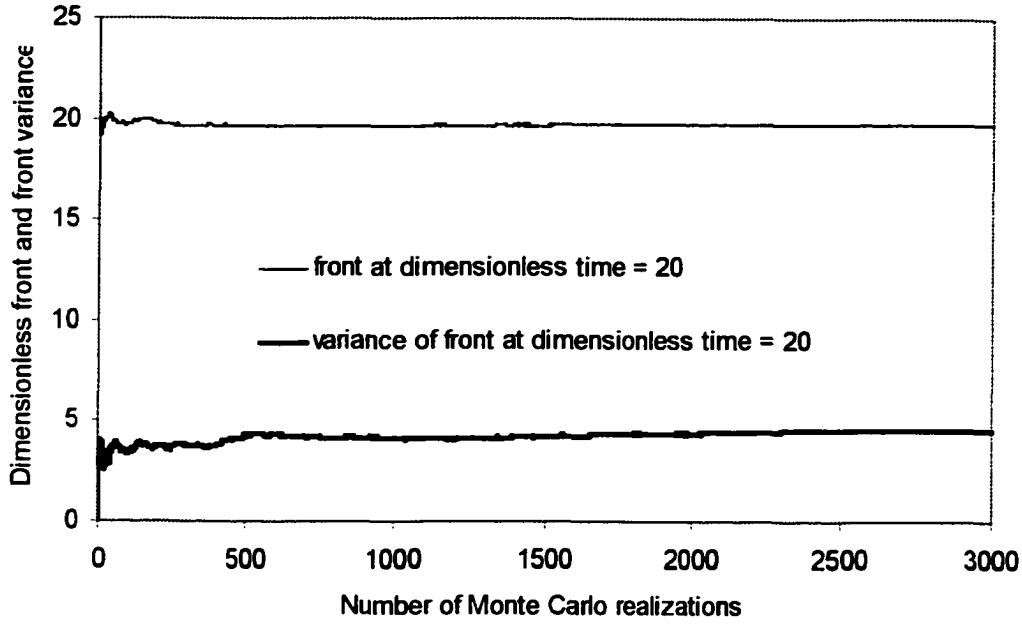

Figure 4.3. Mean 1-D front position and its variance versus number of realizations. Gravity flow driven by constant head. $b = 0.5$, $(H\text{-}a)/bl_Y = 10$, $\sigma_Y^2 = 0.25$.

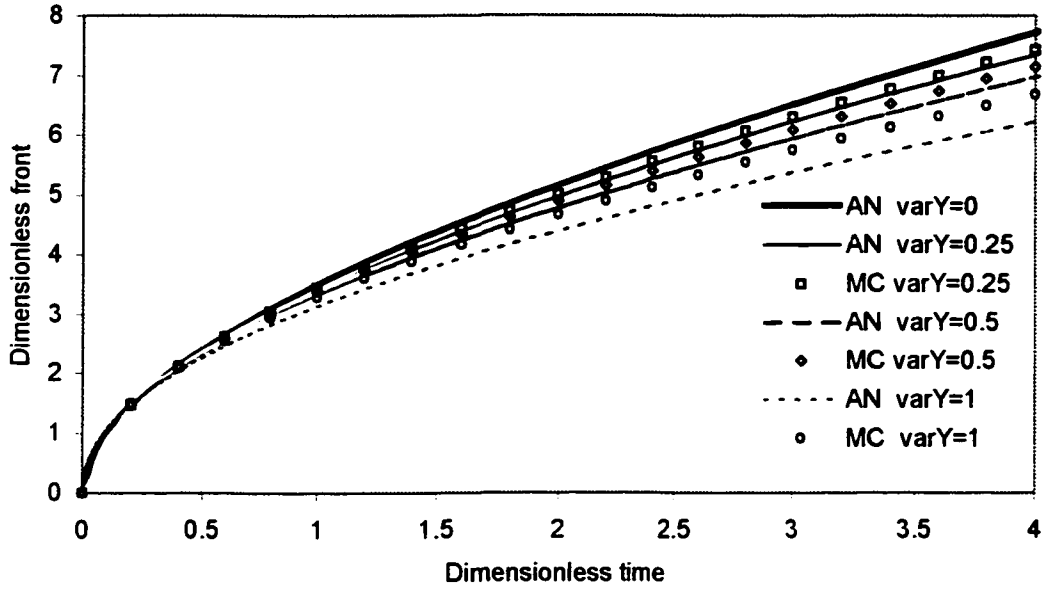

Figure 4.4. Dimensionless mean front position versus dimensionless time obtained analytically (AN) and with Monte Carlo simulations (MC) for different values of var$Y$ = σ_Y^2. Gravity flow driven by constant head. b = 0.5, $(H\text{-}a)/bI_Y$ = 10.

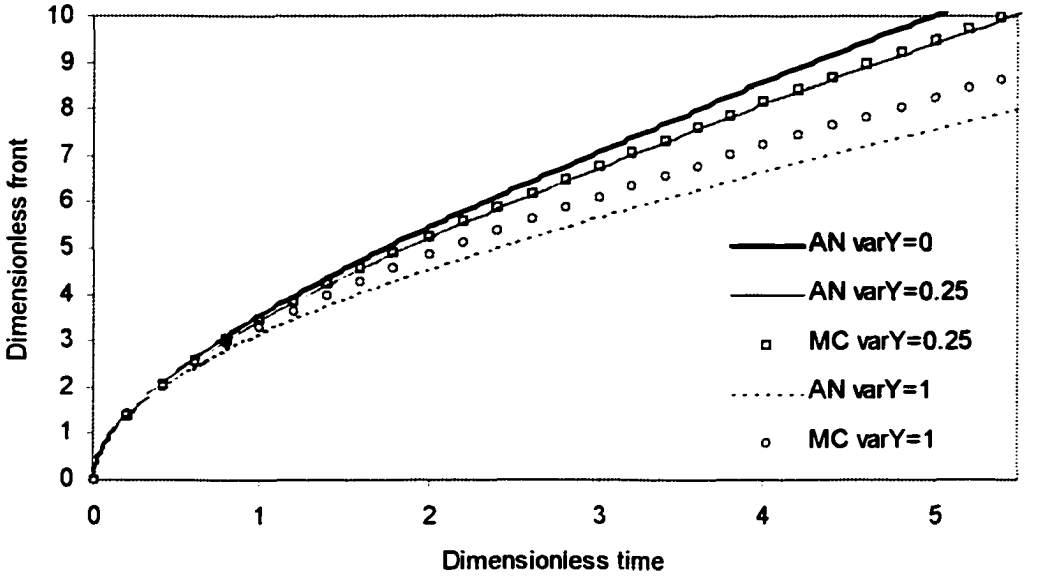

Figure 4.5. Dimensionless mean wetting front position versus dimensionless time obtained analytically (AN) and with Monte Carlo simulations (MC) for different values of var$Y=\sigma_Y^2$. Gravity flow driven by constant head. $b = 1$, $(H\text{-}a)/I_Y = 4$.

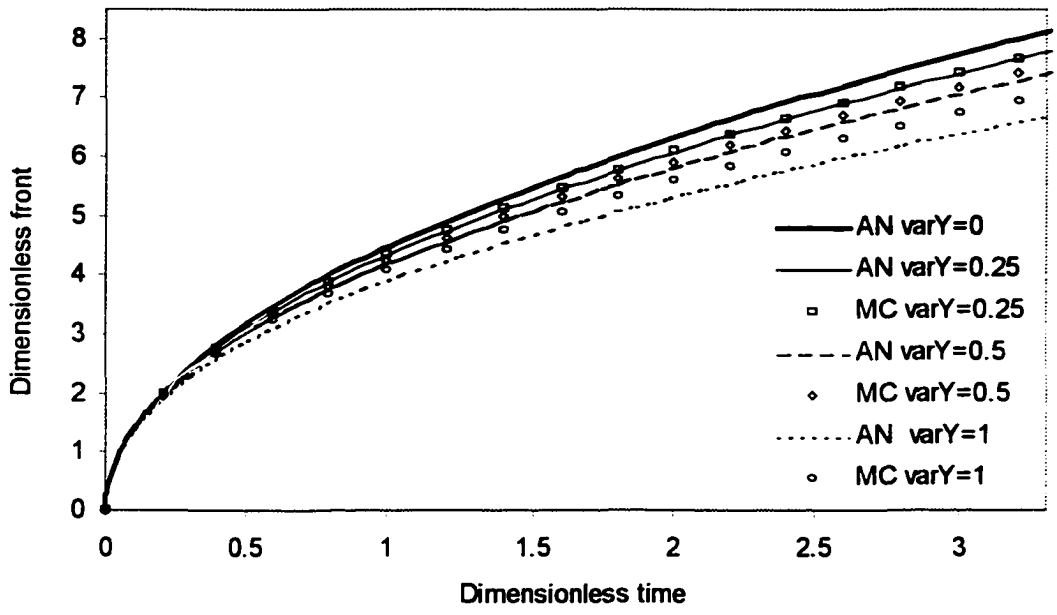

Figure 4.6. Dimensionless mean front position versus dimensionless time obtained analytically (AN) and with Monte Carlo simulations (MC) for different values of var$Y = \sigma_Y^2$. Gravity-free flow driven by constant head. $(H\text{-}a)/I_Y = 10$.

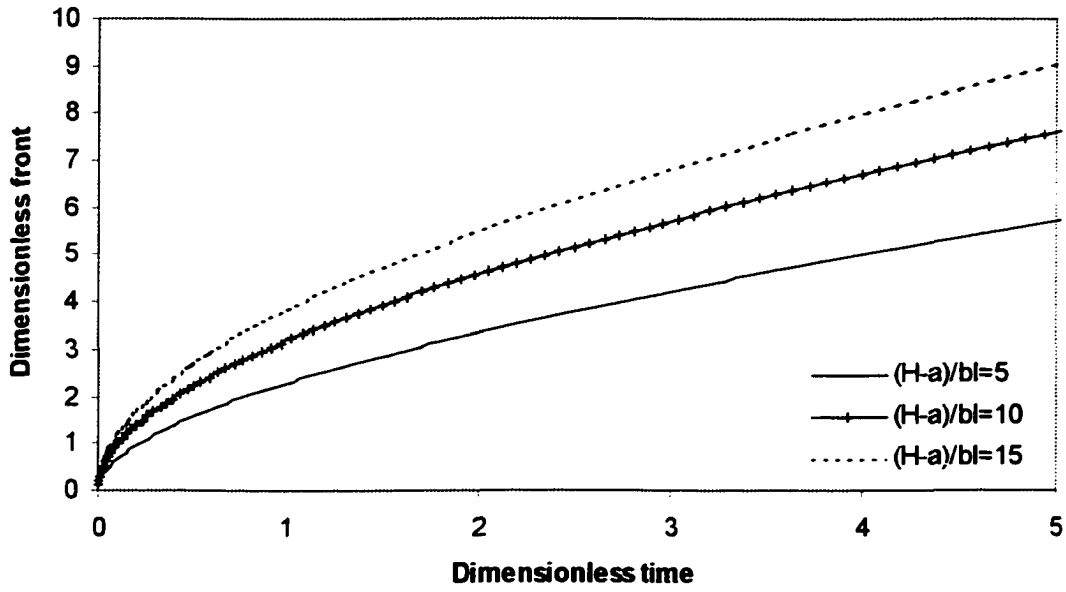

Figure 4.7. Dimensionless mean front position versus dimensionless time obtained analytically for different values of $(H\text{-}a)/bl_Y$. Gravity flow driven by constant head. b = 0.5, $\sigma_Y^2 = 0.5$.

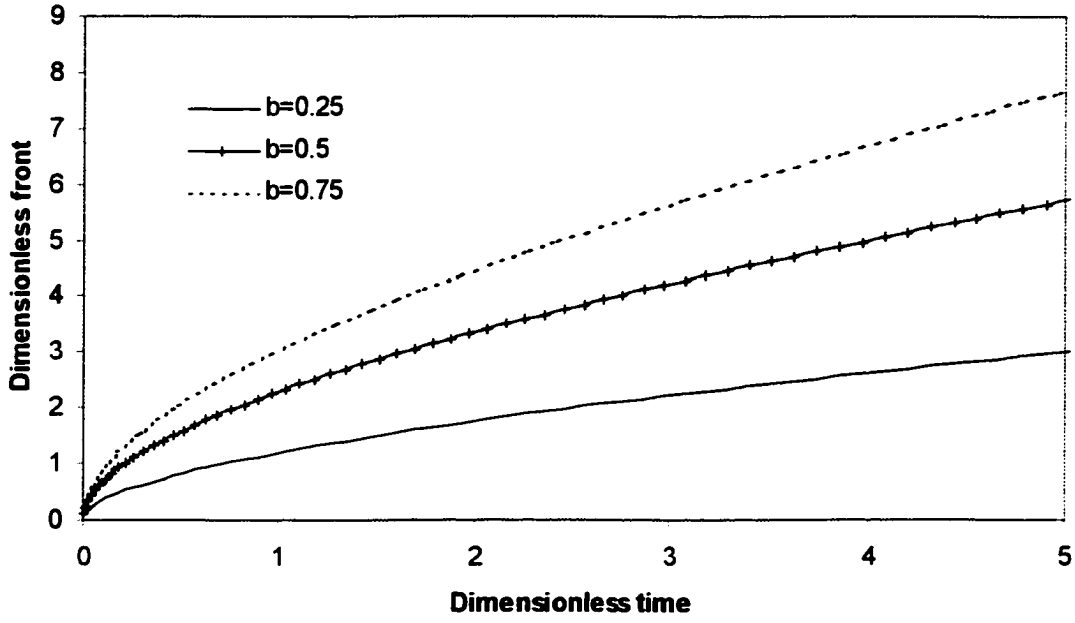

Figure 4.8. Dimensionless mean front position versus dimensionless time obtained analytically for different values of b. Gravity flow driven by constant head. $(H-a)/l_Y = 5$, $\sigma_Y^2 = 0.5$.

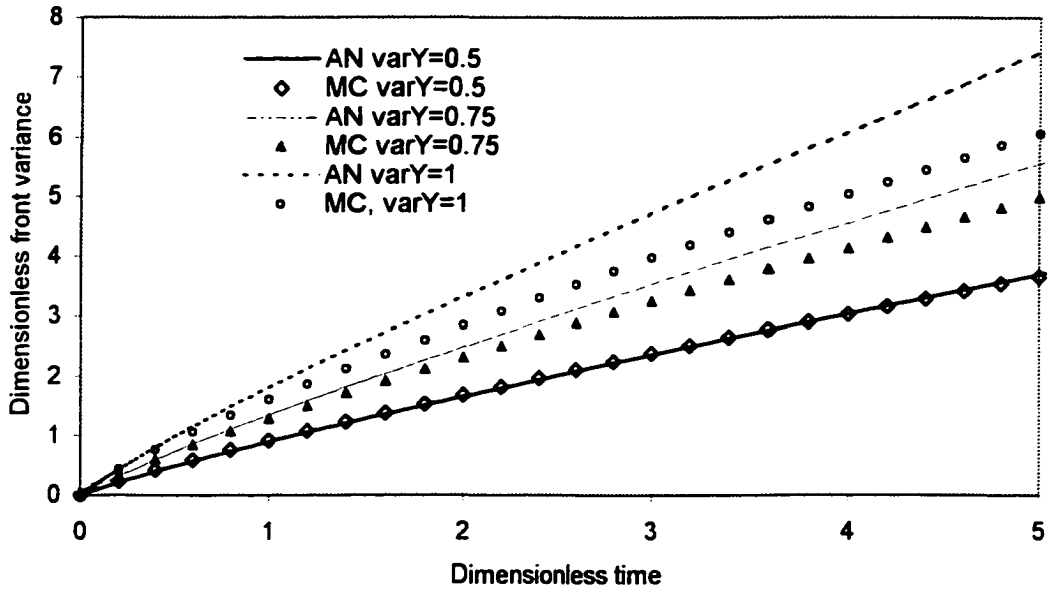

Figure 4.9. Dimensionless front variance versus dimensionless time obtained analytically (AN) and with Monte Carlo simulations (MC) for different values of var$Y$ = σ_Y^2. Gravity flow driven by constant head. b = 0.5, $(H\text{-}a)/bI_Y$ = 10.

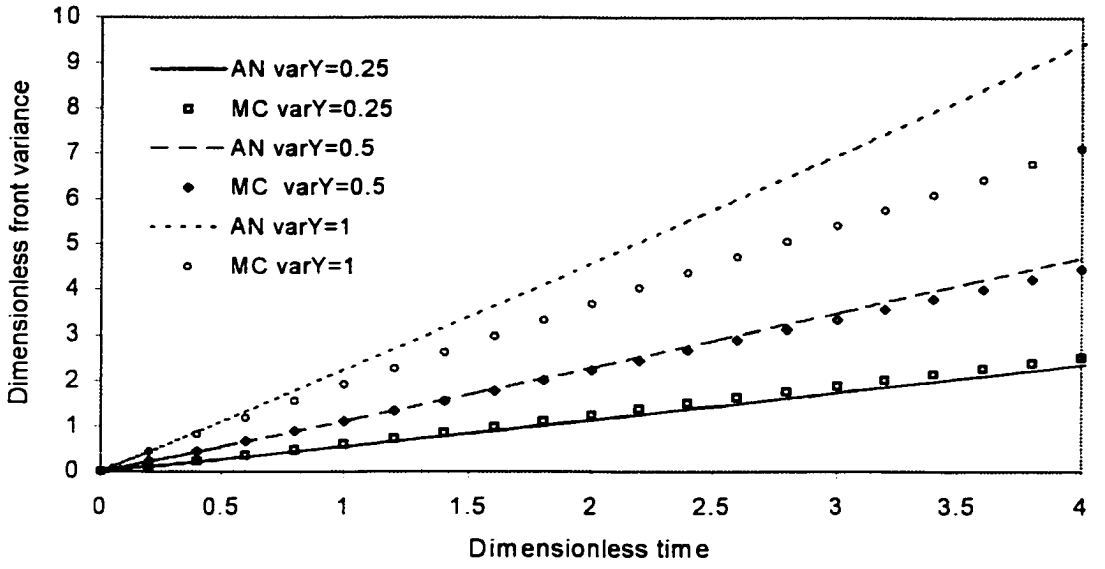

Figure 4.10. Dimensionless wetting front variance versus dimensionless time obtained analytically (AN) and with Monte Carlo simulations (MC) for different values of varY=σ_Y^2. Gravity flow driven by constant head. b=1, $(H-a)/I_Y$=4.

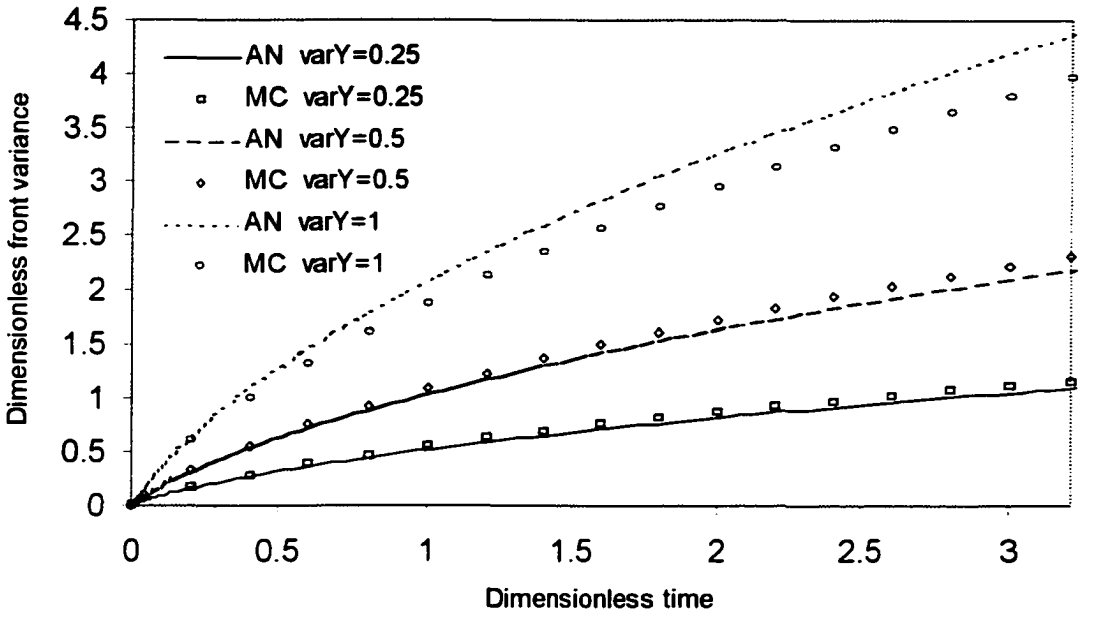

Figure 4.11. Dimensionless front variance versus dimensionless time obtained analytically (AN) and with Monte Carlo simulations (MC) for different values of var$Y$ = σ_Y^2. Gravity-free flow driven by constant head. $(H\text{-}a)/I_Y$= 10.

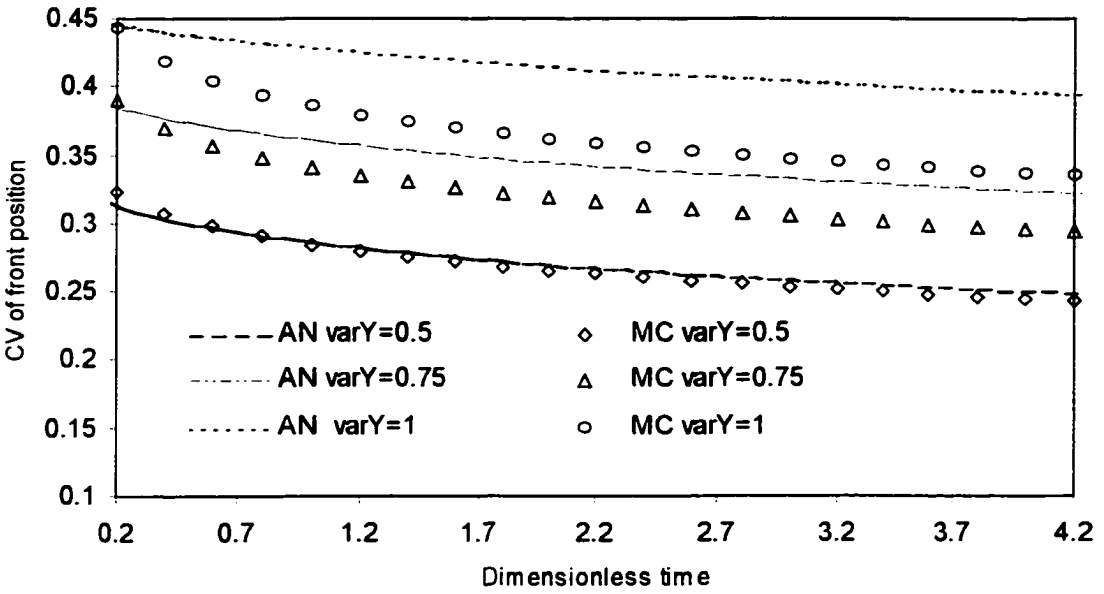

Figure 4.12. Coefficient of variance (CV) versus dimensionless time obtained analytically (AN) and with Monte Carlo simulations (MC) for different values of var$Y=\sigma_Y^2$. Gravity flow driven by constant head. $b = 0.5$, $(H\text{-}a)/bI_Y = 10$.

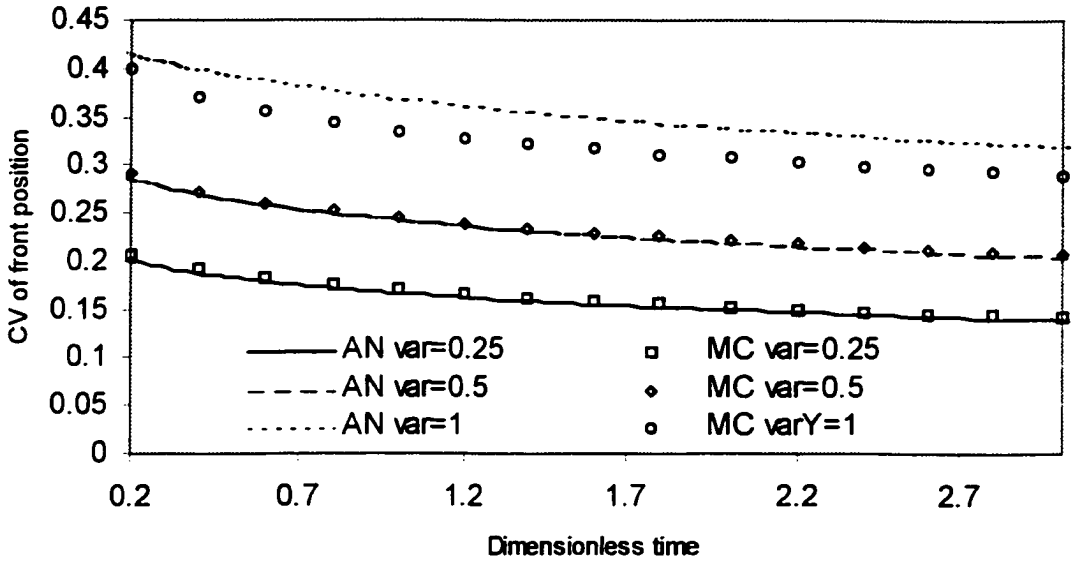

Figure 4.13. Coefficient of variation (CV) obtained analytically (AN) and with Monte Carlo simulations (MC) versus dimensionless time for different values of varY=σ_Y^2. Gravity-free flow driven by constant head. (H-a)/I_Y = 10.

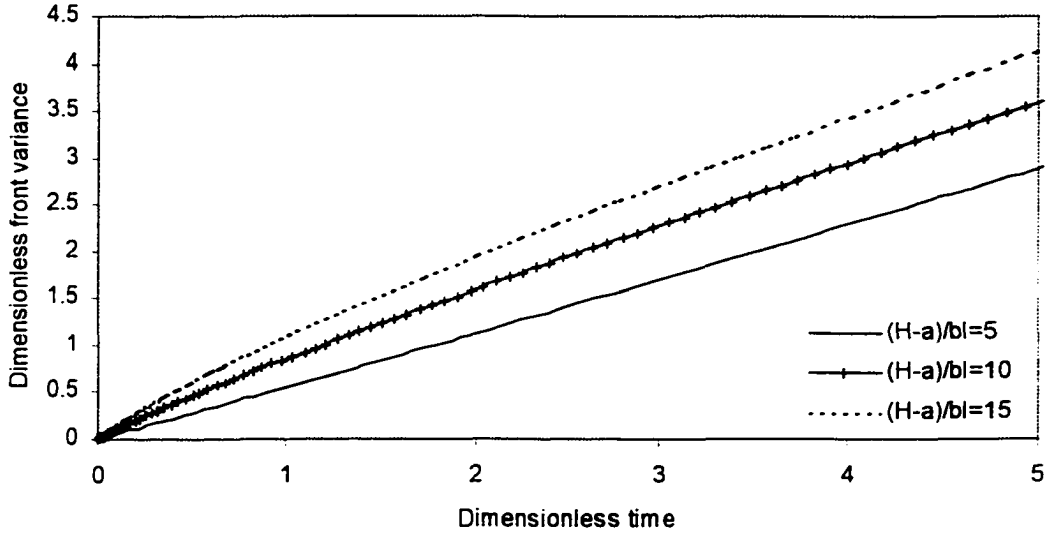

Figure 4.14. Dimensionless front variance versus dimensionless time obtained analytically for different values of $(H\text{-}a)/bl_Y$. Gravity flow driven by constant head. b = 0.5, $\sigma_Y^2 = 0.5$.

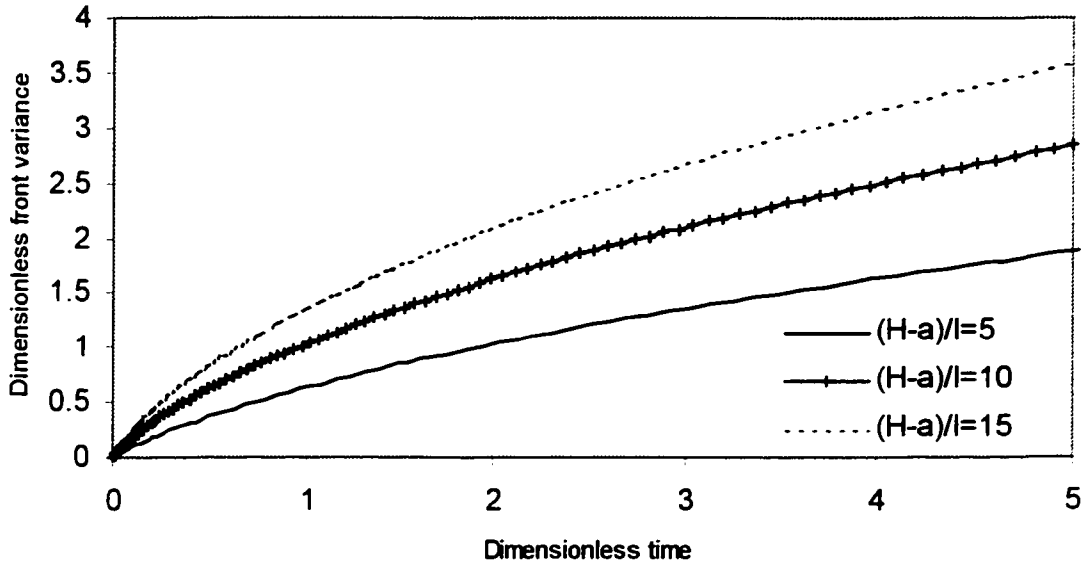

Figure 4.15. Dimensionless front variance versus dimensionless time obtained analytically for different values of $(H\text{-}a)/l_Y$. $\sigma_Y^2 = 0.5$. Gravity-free flow driven by constant head.

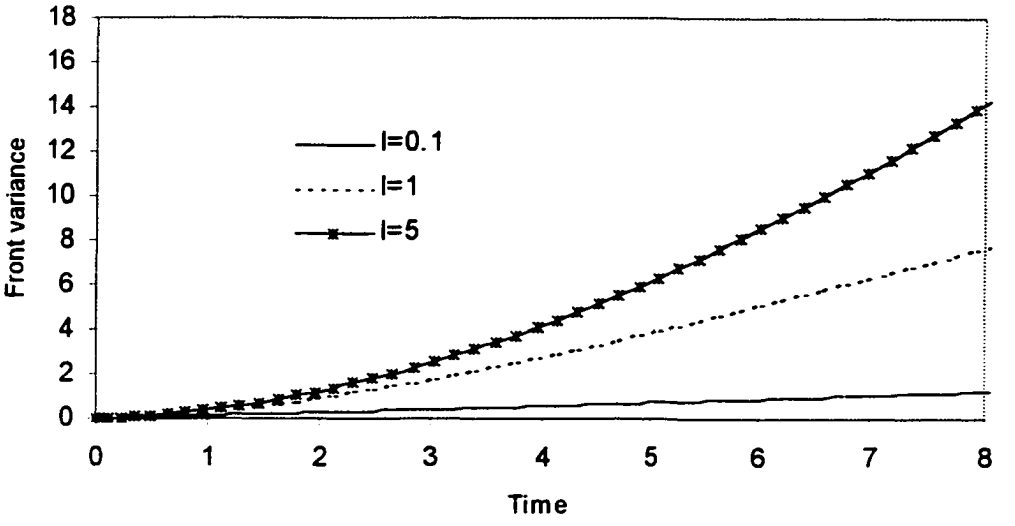

Figure 4.16. Front variance versus time obtained analytically for different l=l_Y. Gravity flow driven by constant head. H-a=0.1, b=0.5, σ_Y^2=1

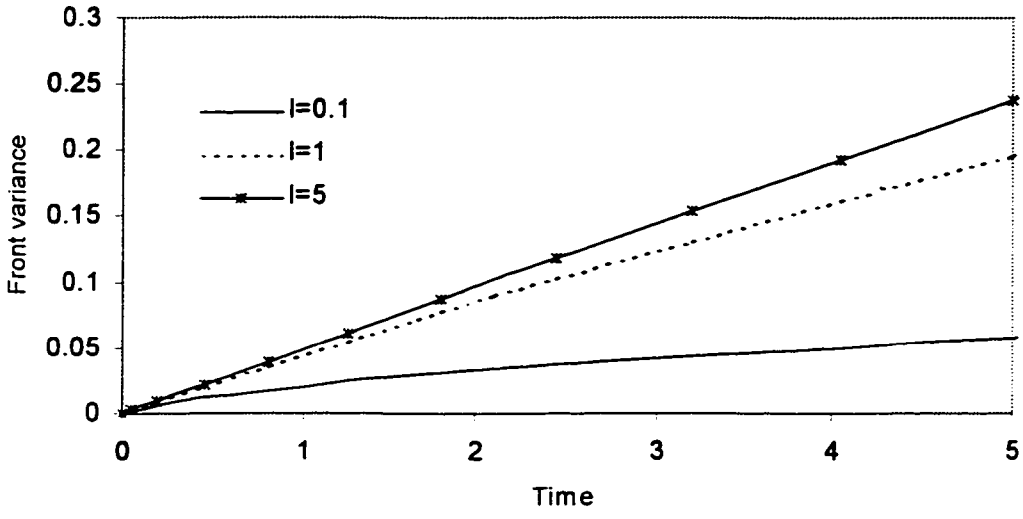

Figure 4.17. Front variance versus time obtained analytically for different l=l_Y. Gravity-free flow driven by constant head. H-a = 0.1, b = 0.5, σ_Y^2 = 1.

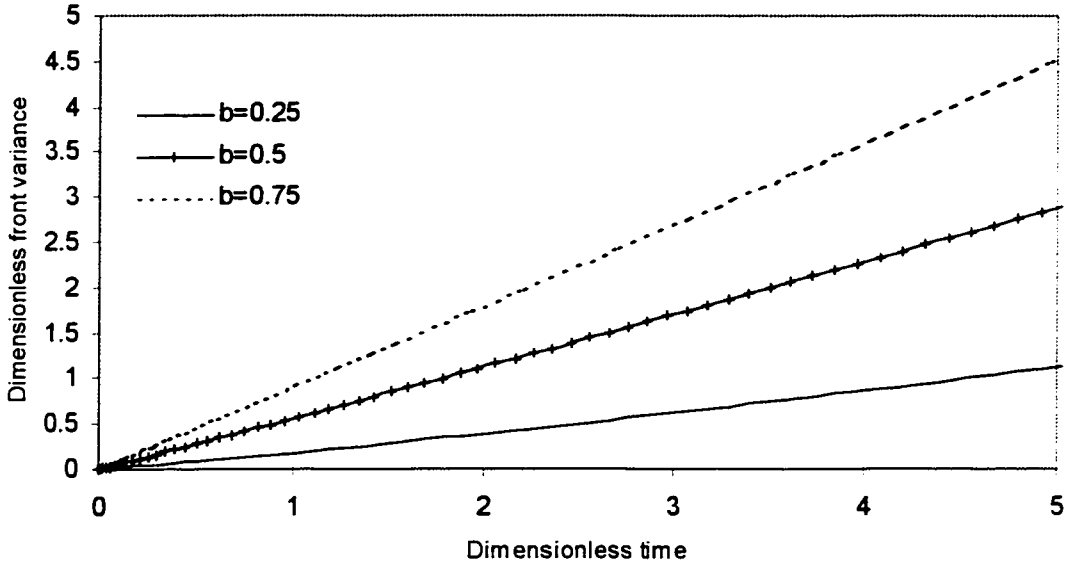

Figure 4.18. Dimensionless front variance versus dimensionless time obtained analytically for different values of b. Gravity flow driven by constant head. $(H\text{-}a)/l_Y = 5$, $\sigma_Y^2 = 0.5$.

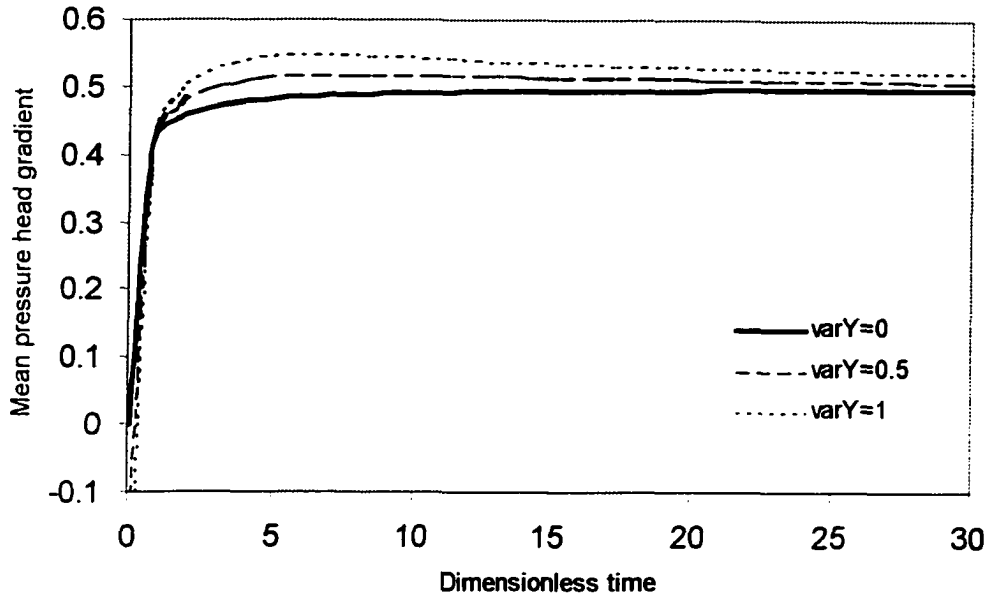

Figure 4.19. Mean pressure head gradient versus dimensionless time obtained analytically for different values of var$Y = \sigma_Y^2$. Gravity flow driven by constant head. b = 0.5, $(H\text{-}a)/bI_Y = 0.1$.

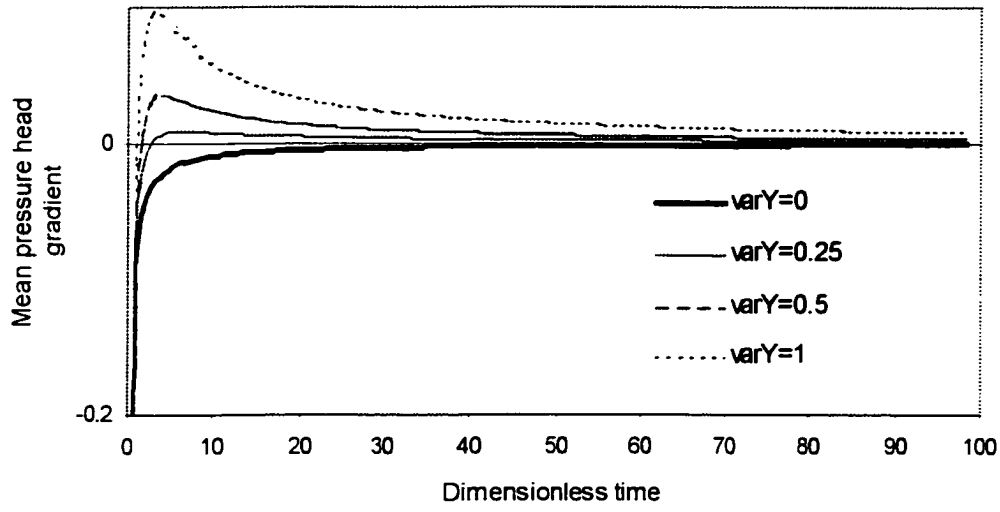

Figure 4.20. Mean pressure head gradient at wetting front versus dimensionless time calculated analytically for different values of var$Y=\sigma_Y^2$. Gravity flow driven by constant head. b=1, $(H-a)/l_Y$=0.1.

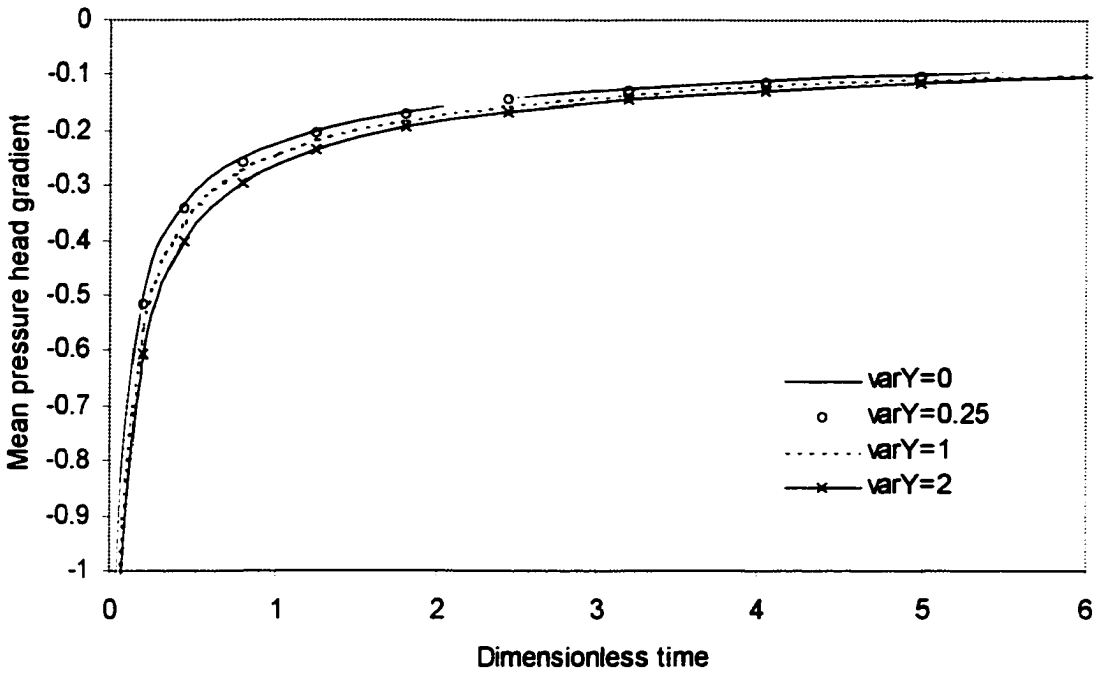

Figure 4.21. Mean pressure head gradient versus dimensionless time obtained analytically for different values of varY = σ_Y^2. Gravity-free flow driven by constant head. $(H\text{-}a)/l_Y = 0.1$.

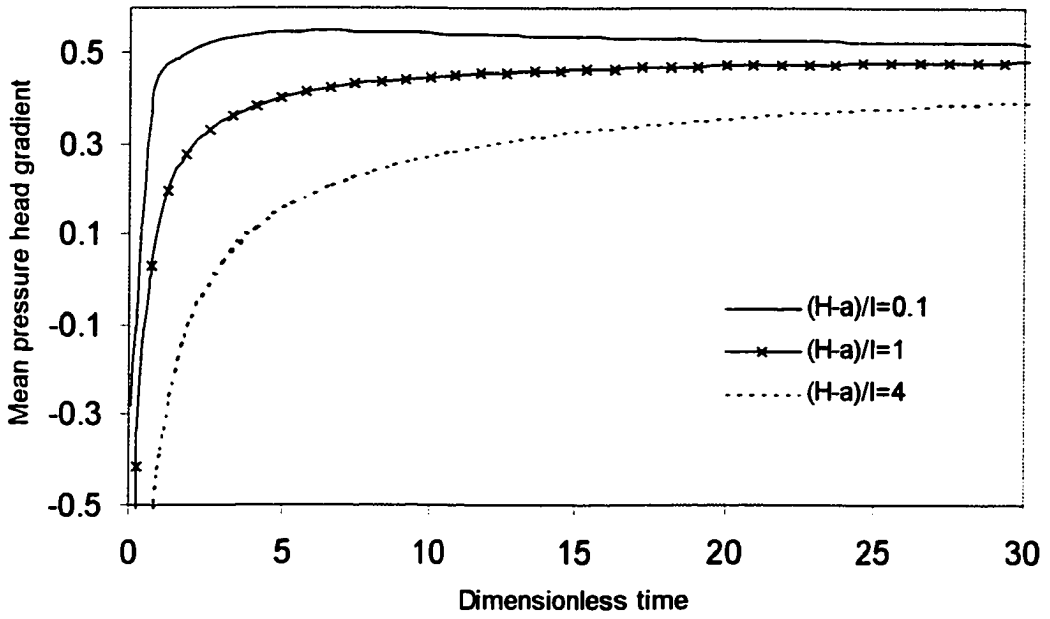

Figure 4.22. Mean pressure head gradient versus dimensionless time obtained analytically for different values of $(H\text{-}a)/bl_Y$. Gravity flow, driven by constant head. b = 0.5, $\sigma_Y^2 = 1$.

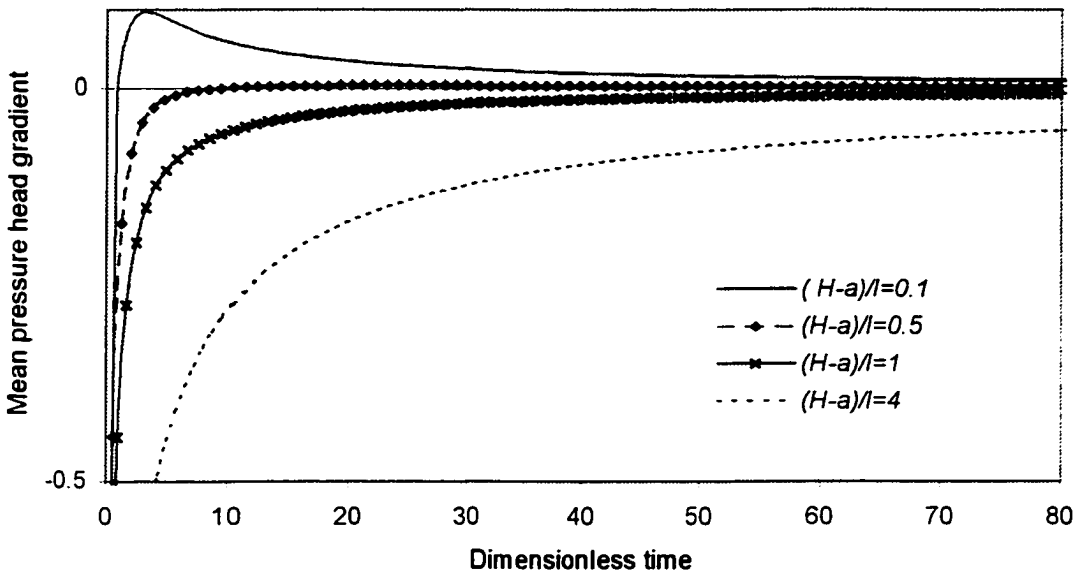

Figure 4.23. Mean pressure head gradient at wetting front versus dimensionless time calculated analytically for different values of $(H\text{-}a)/l_Y$. Gravity flow driven by constant head. b=1, $\sigma_Y^2 = 1$.

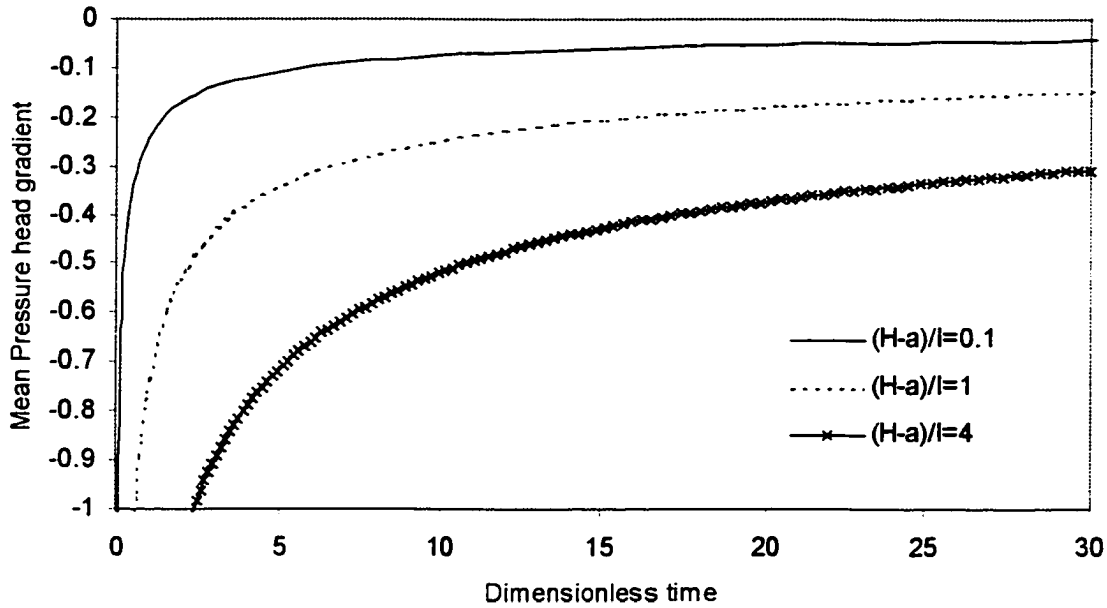

Figure 4.24. Mean pressure head gradient versus dimensionless time obtained analytically for different values of $(H\text{-}a)/l_Y$. Gravity-free flow driven by constant head. $\sigma_Y^2 = 1$.

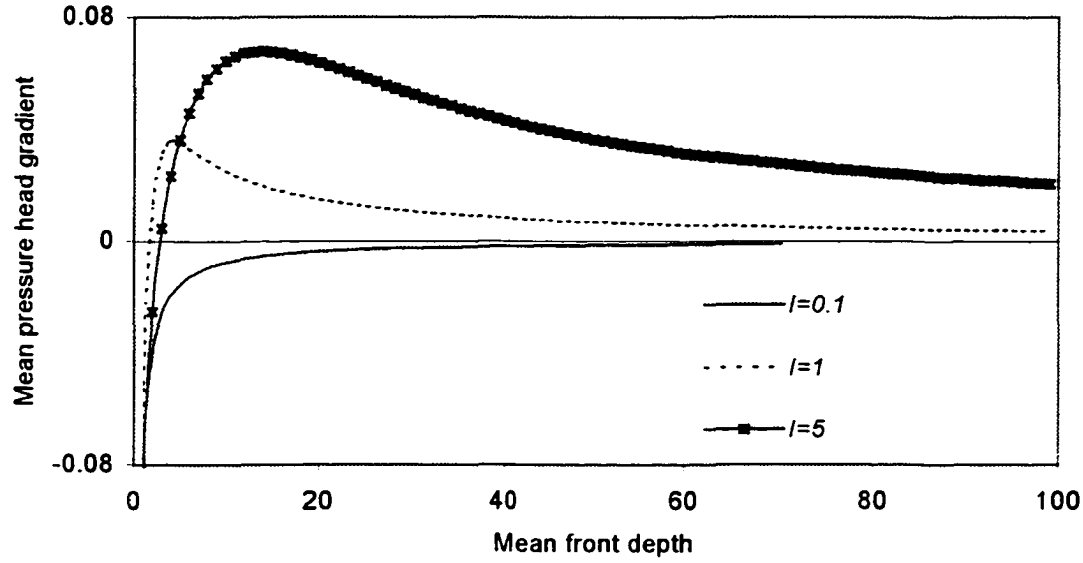

Figure 4.25. Mean pressure head gradient at wetting front versus mean front depth obtained analytically for different l_Y . Gravity flow driven by constant head. b=1, (H-a)/l_Y =0.1, $\sigma_Y^2 = 0.5$.

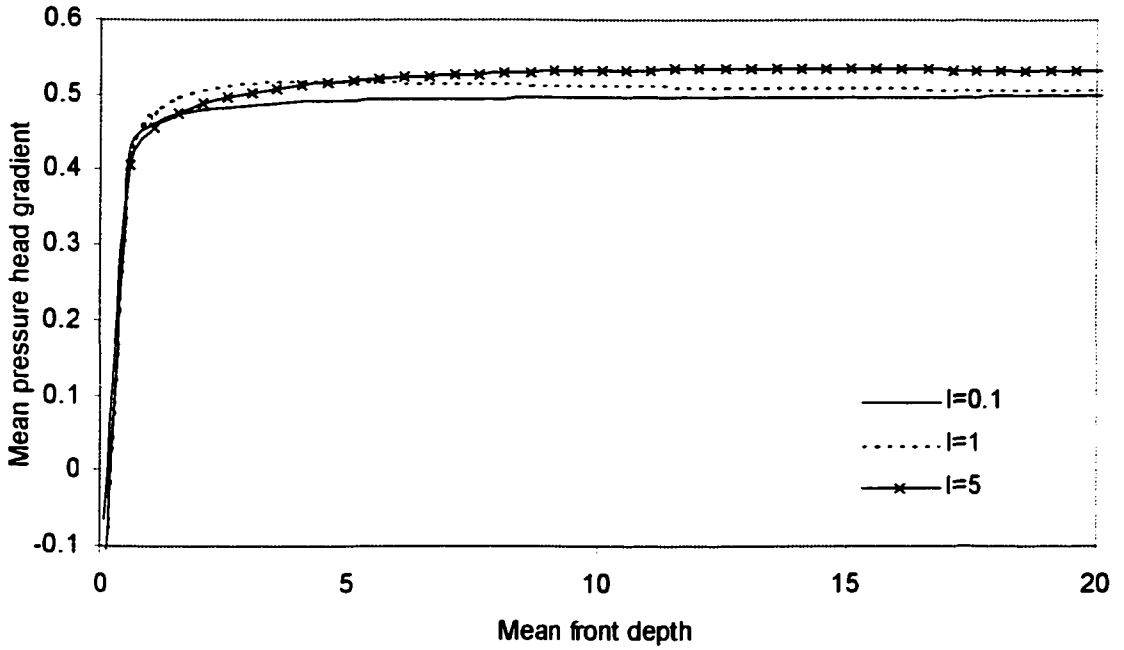

Figure 4.26. Mean pressure head gradient versus mean front depth obtained analytically for different l_Y. Gravity flow driven by constant head. $b = 0.5$, $(H\text{-}a)/b = 0.1$, $\sigma_Y^2 = 0.5$.

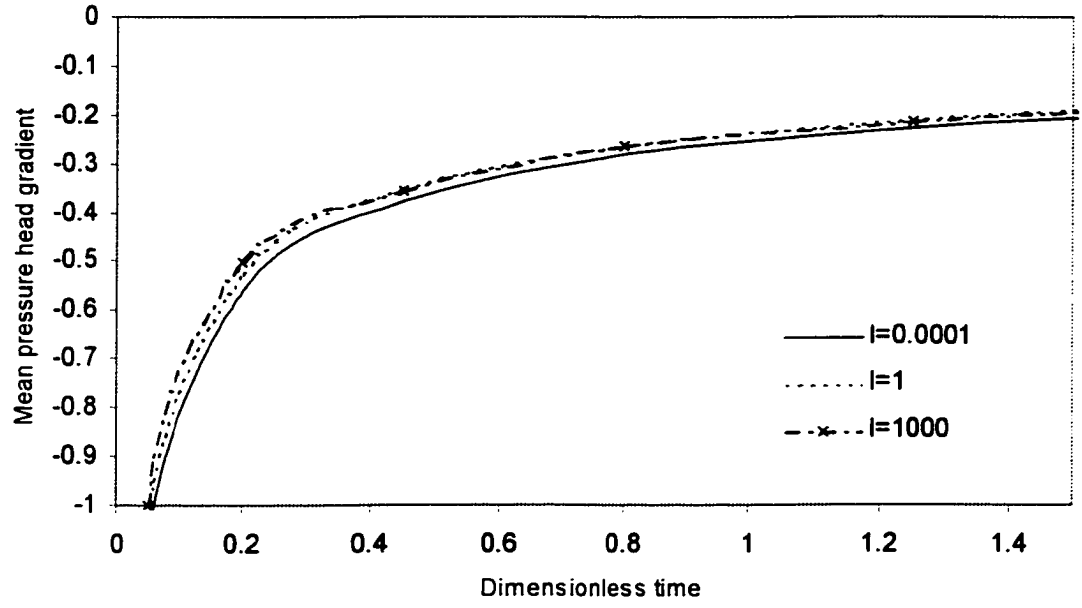

Figure 4.27. Mean pressure head gradient versus dimensionless time obtained analytically for different values of l_Y. $\sigma_Y^2 = 1$, H-$a = 0.1$. Gravity-free flow driven by constant head.

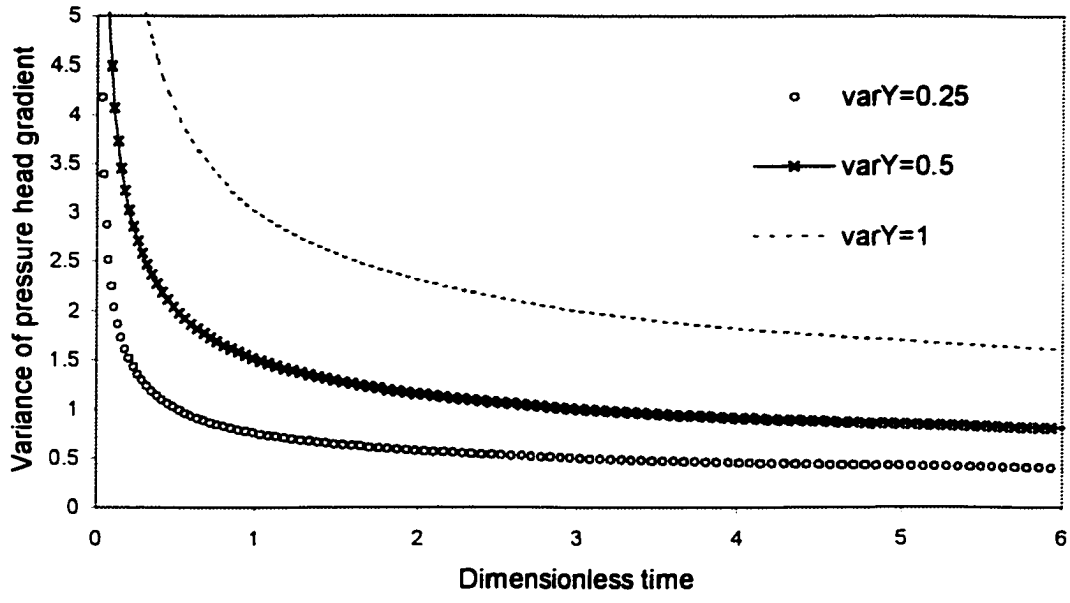

Figure 4.28. Variance of pressure head gradient at the wetting front obtained analytically versus dimensionless time for different values of varY=σ_Y^2. Gravity flow driven by constant head. b=1, $(H\text{-}a)/l_Y$=4.

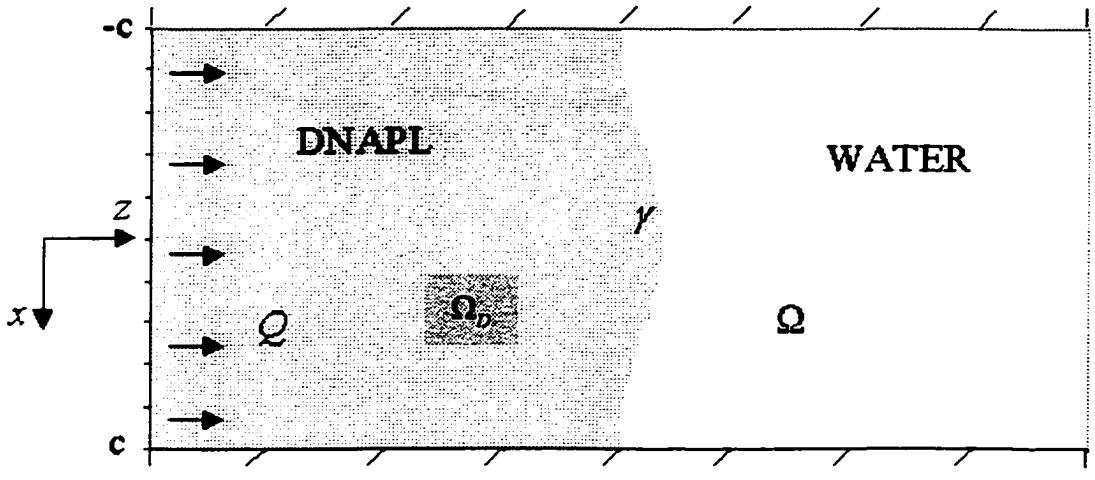

Figure 5.1. Flow domains Ω_D and Ω separated by sharp front γ. Green's function defined on both domains. Uniform flux prescribed far behind front. Impermeable walls located at $x = \pm c$.

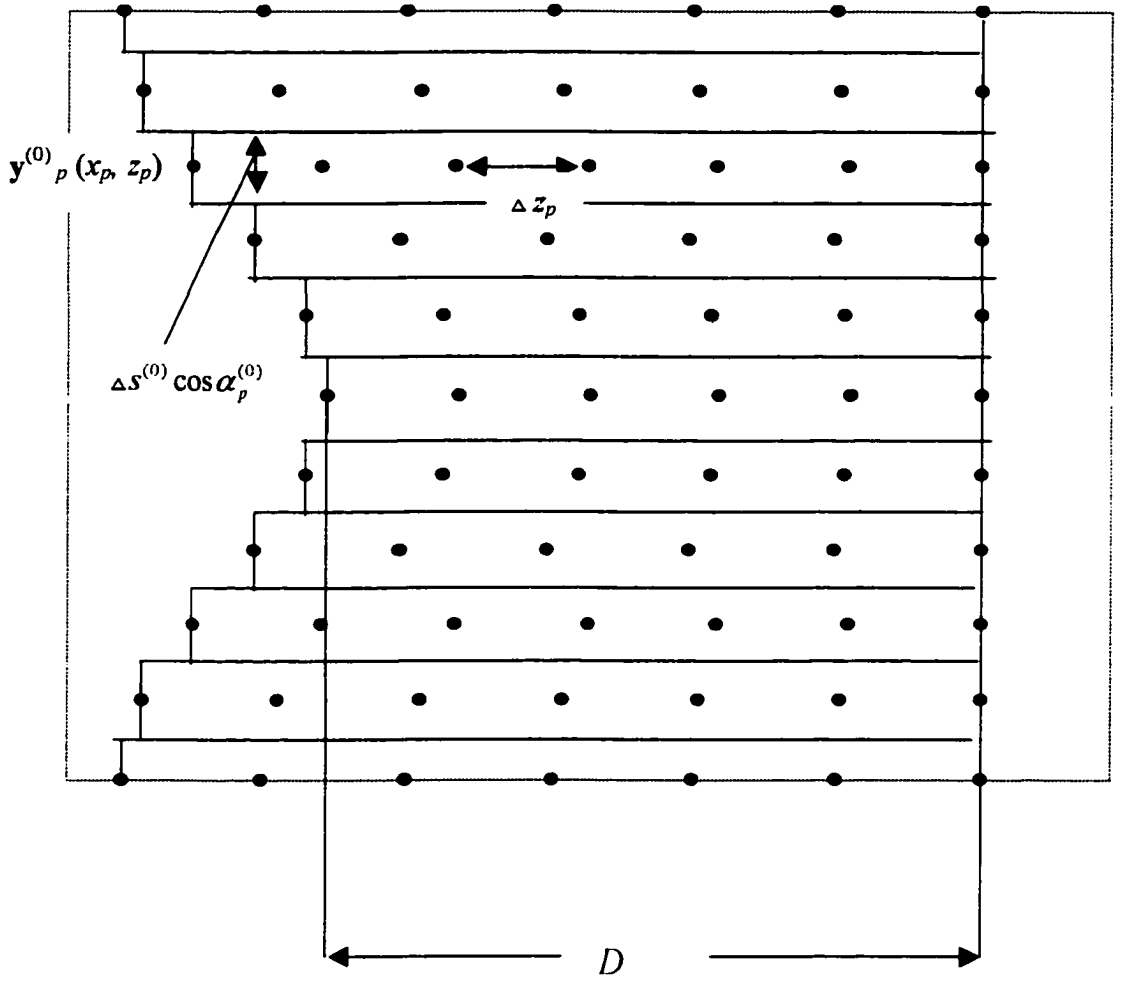

Figure 5.2. Discretization of domain of integration.

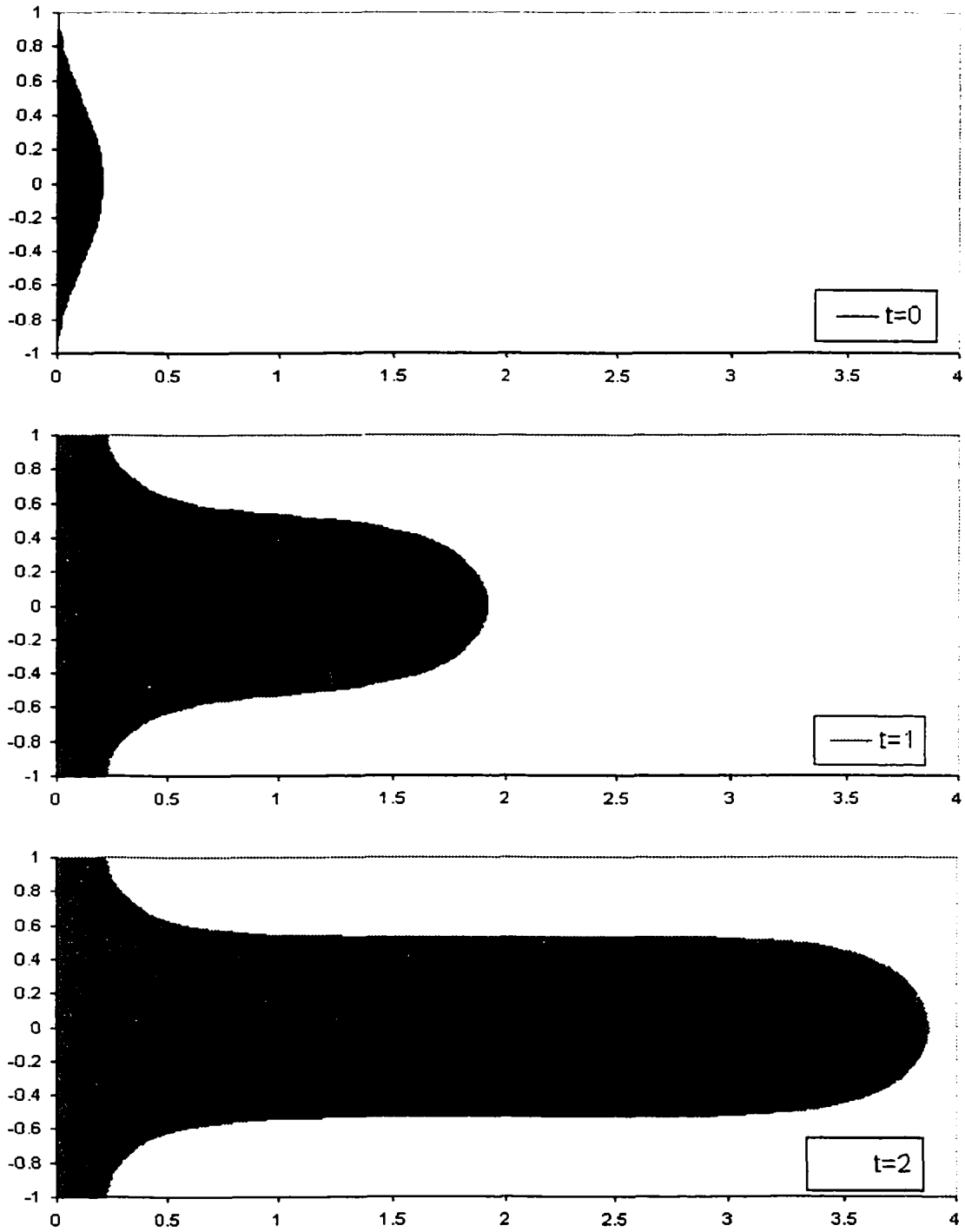

Figure 5.3. Zero-order mean finger growth with dimensionless time = $K_G t/\theta c$ driven by dimensionless flux $Q/2cK_G$ =1. x and z are normalized by c. Saffman-Taylor type finger resulting from a single perturbation.

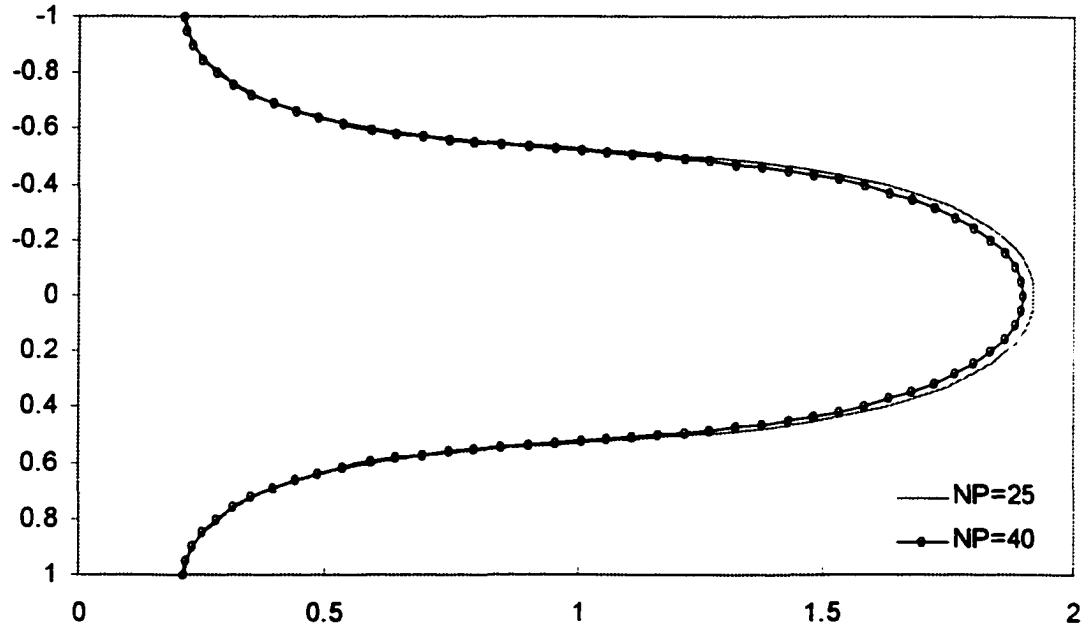

Figure 5.4. Zero-order Saffman-Taylor type fingers at dimensionless time $K_G t/\theta c = 1$ driven by dimesionless flux $Q/2cK_G = 1$ obtained with different number of discretization points (NP). x and z are normalized by c.

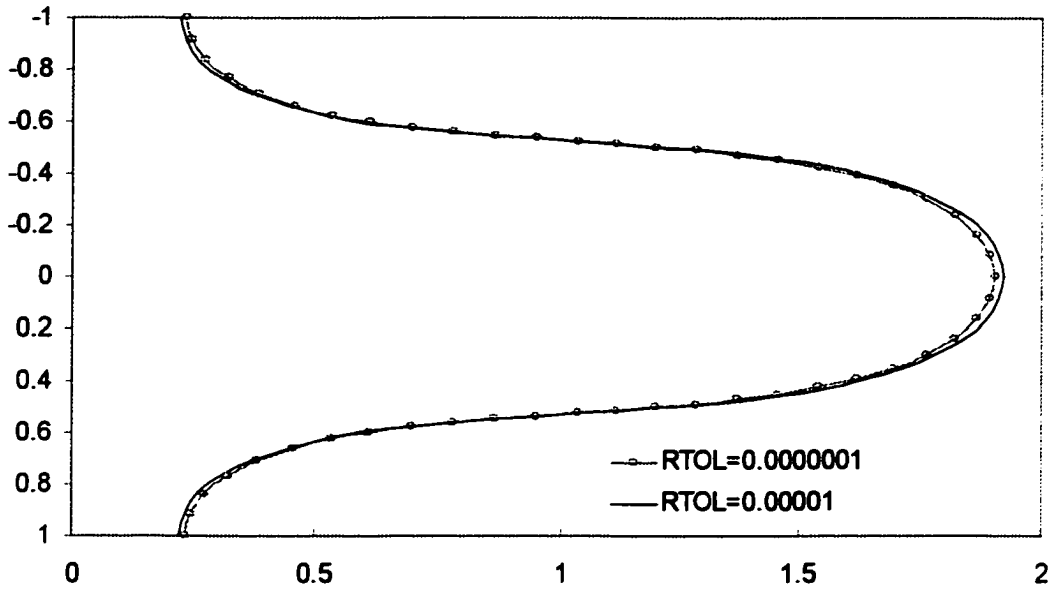

Figure 5.5. Zero-order Saffman-Taylor type fingers at dimensionless time $K_G t/\theta c = 1$ driven by dimesionless flux $Q/2cK_G = 1$ obtained with different parameter RTOL. x and z are normalized by c.

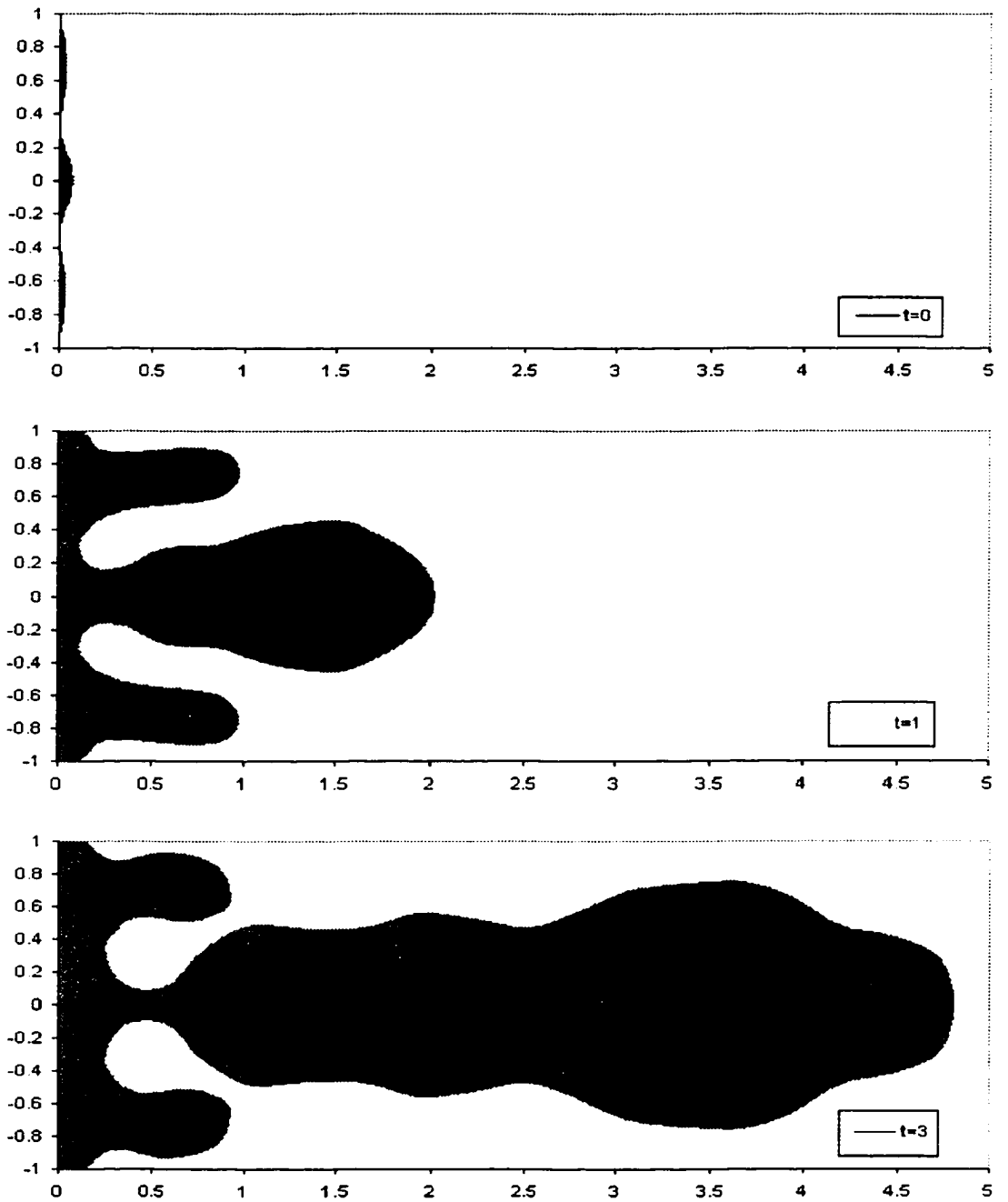

Figure 5.6. Zero-order mean finger growth with dimensionless time = $K_G t/\theta c$ driven by dimensionless flux $Q/2cK_G$ =1. x and z are normalized by c. Uneven initial perturbations give rise to dominant finger.

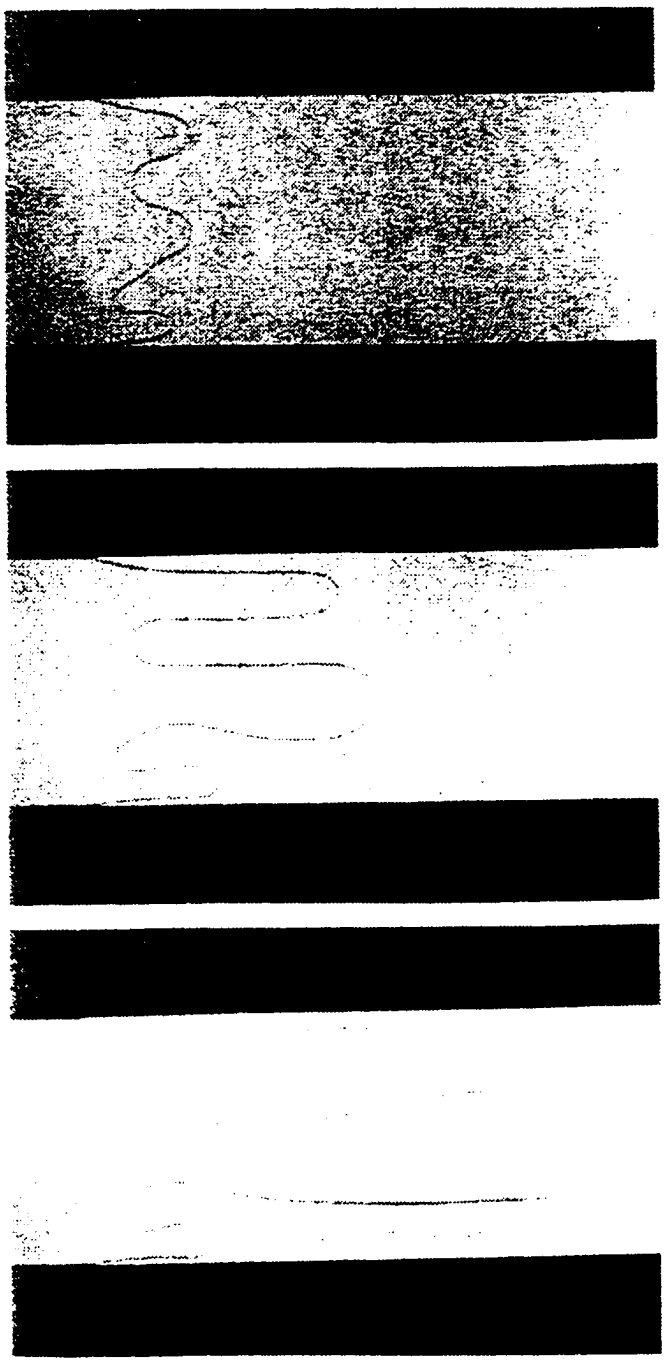

Figure 5.7. Developing of dominant finger. Oil penetrating glycerin. After Tabeling et al. 1986.

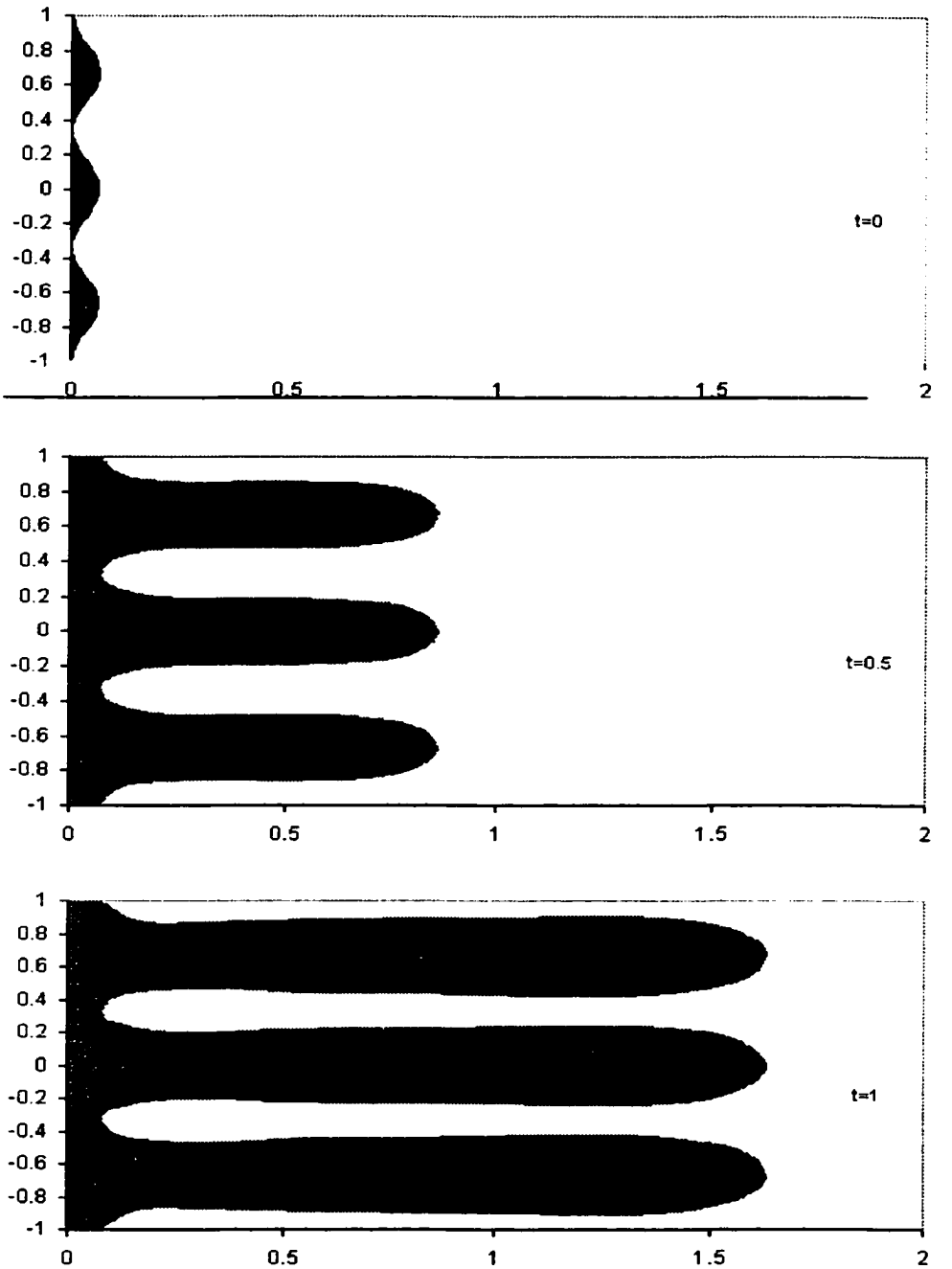

Figure 5.8. Zero-order mean fingers growth with dimensionless time = $K_G t/\theta c$ driven by dimensionless flux $Q/2cK_G$ =1. x and z are normalized by c. Multiple uniform perturbations grow into uniform fingers.

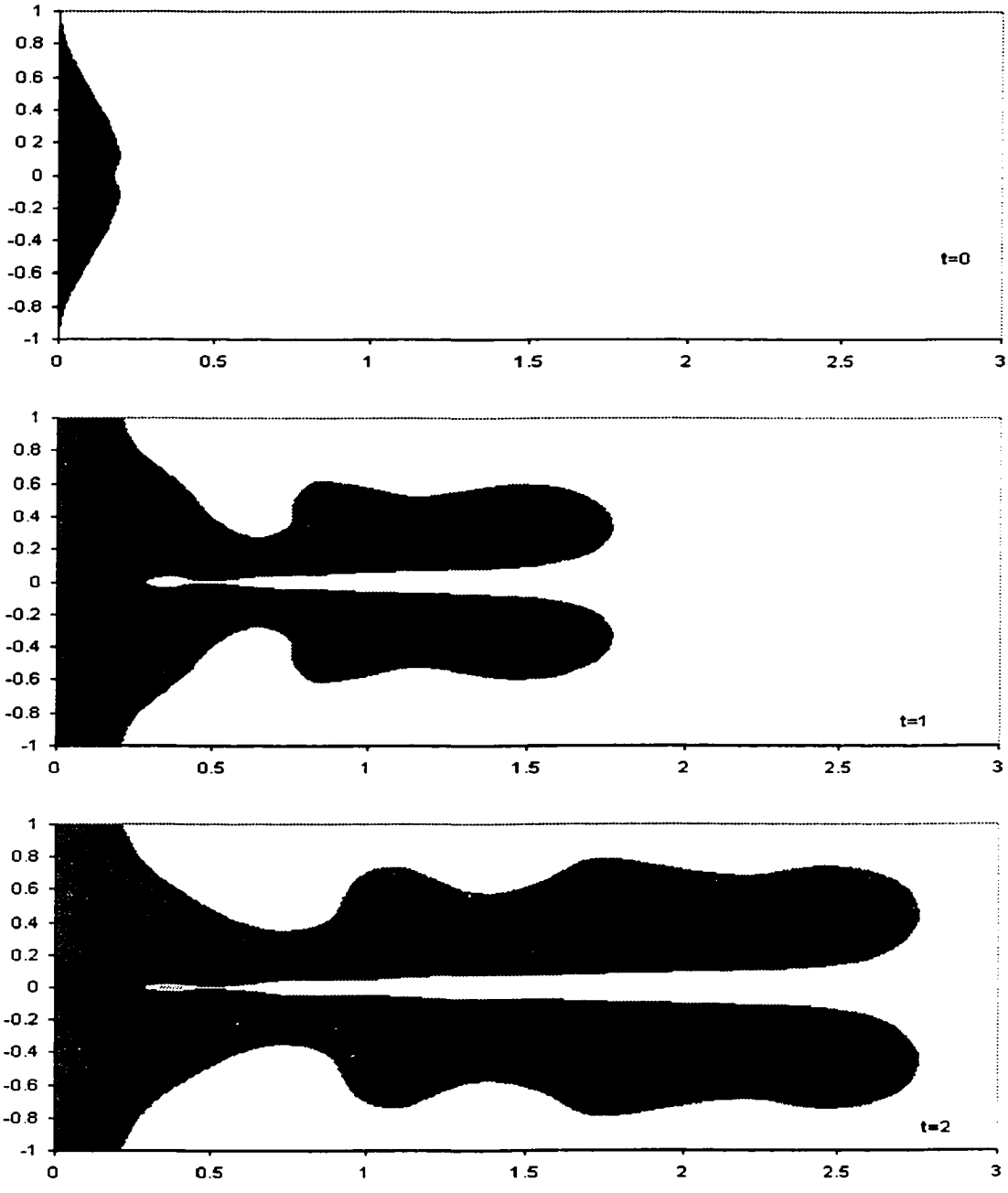

Figure 5.9. Zero-order mean finger growth with dimensionless time = $K_G t/\theta c$ driven by dimensionless flux $Q/2cK_G$ =1. x and z are normalized by c. Splitting of the finger as result of perturbation of the finger tip at t=0.

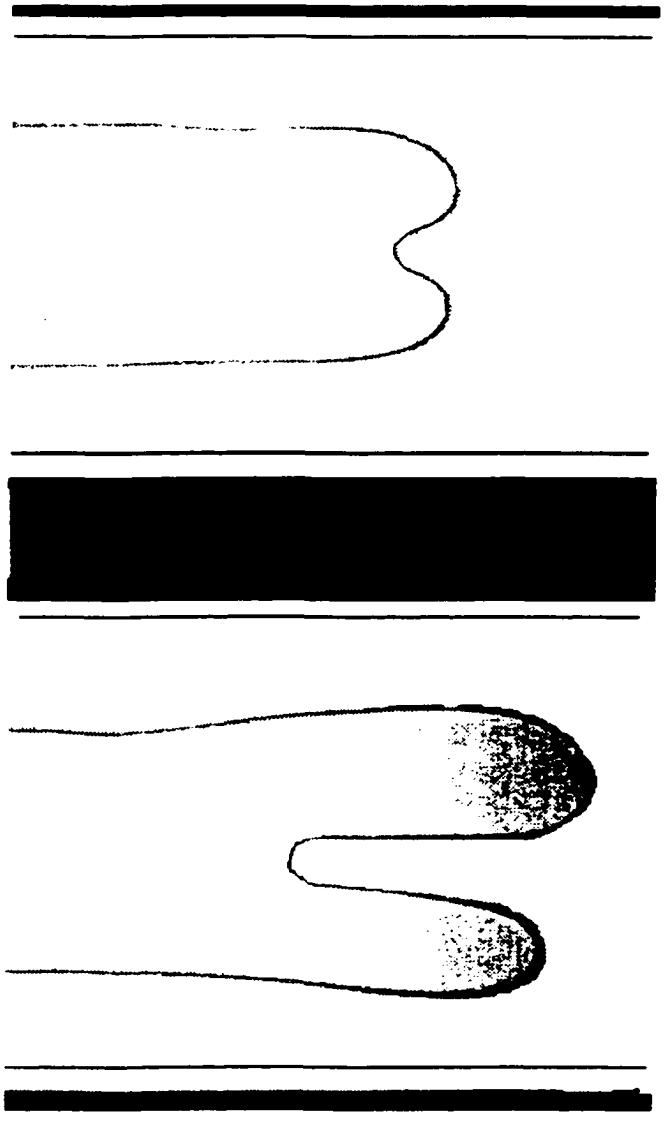

Figure 5.10. Finger of oil penetrating glycerin in Hele-Shaw cell. After Tabeling et al., 1986.

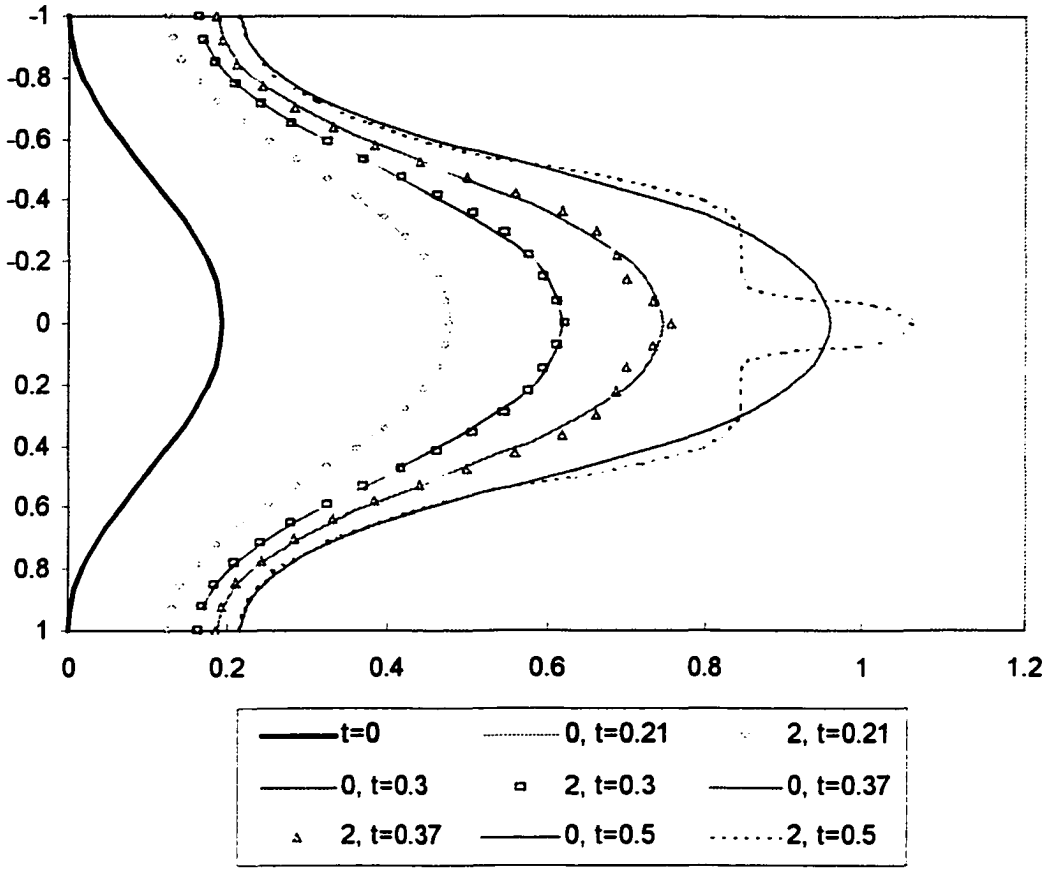

Figure 5.11. Zero- and second-order Saffman-Taylor mean finger growth with dimensionless time = $K_G t/\theta c$ driven by dimensionless flux $Q/2cK_G = 1$. x and z are normalized by c. $\sigma_Y^2 = 1$, $l_z/c = \infty$, $l_x = \infty$.

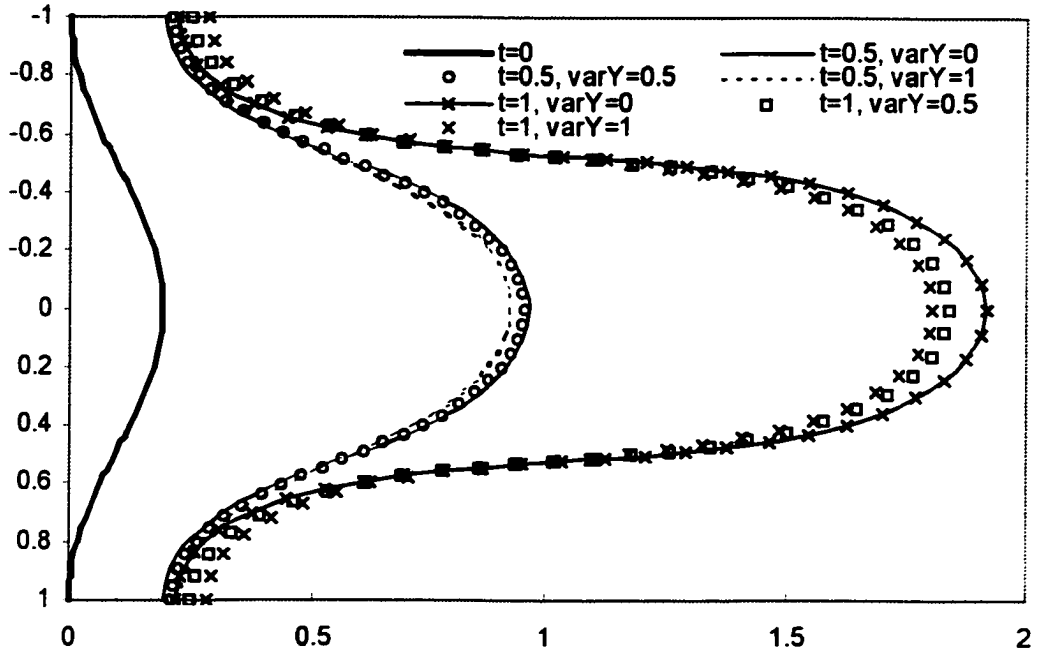

Figure 5.12. Second-order Saffman-Taylor type mean finger growth with dimensionless time = $K_G t/\theta c$ driven by dimensionless flux $Q/2cK_G = 1$ for different σ_Y^2 = varY. x and z are normalized by c. $l_z/c = 1$, $l_x = \infty$.

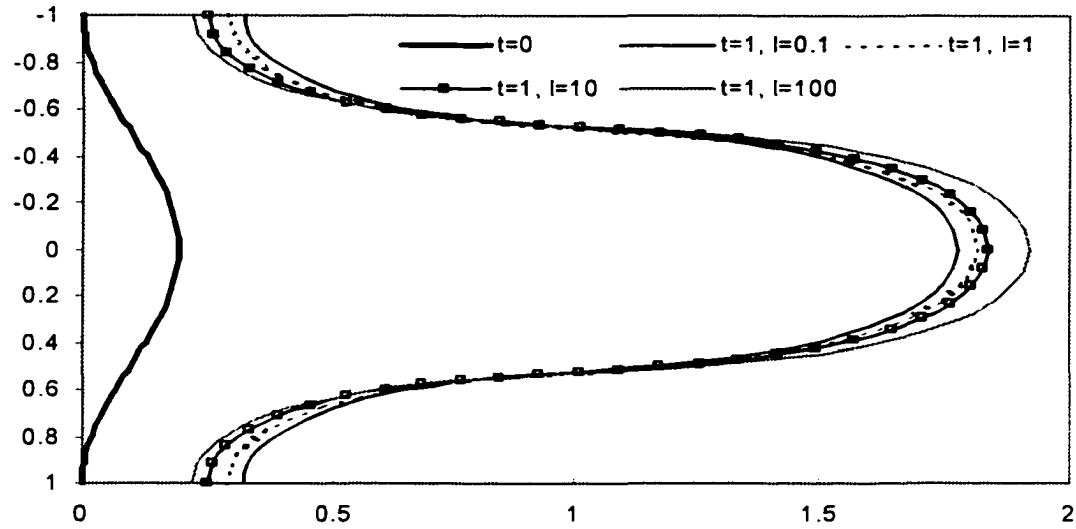

Figure 5.13. Second-order Saffman-Taylor type mean finger growth with dimensionless time = $K_G t/\theta c$ driven by dimensionless flux $Q/2cK_G$ =1 for different normalized correlation length l = l_z/c. x and z are normalized by c. σ_Y^2=1, $l_x = \infty$.

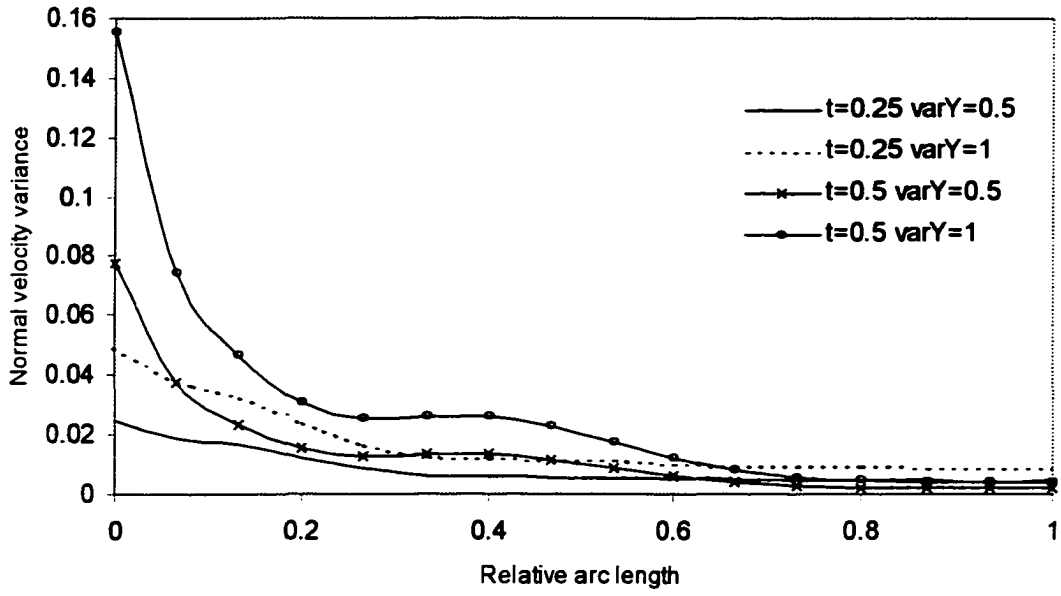

Figure 5.14. Dimensionless normal velocity variance = $\theta^2\left[\sigma_V^2\right]^{[2]} / K_G^2$ of a Saffman-Taylor type finger versus relative arc length as a function of dimensionless time = $K_G t/\theta c$ for different varY = σ_Y^2 . $Q/2cK_G = 1$, $l_z/c = 1$, $l_x=\infty$.

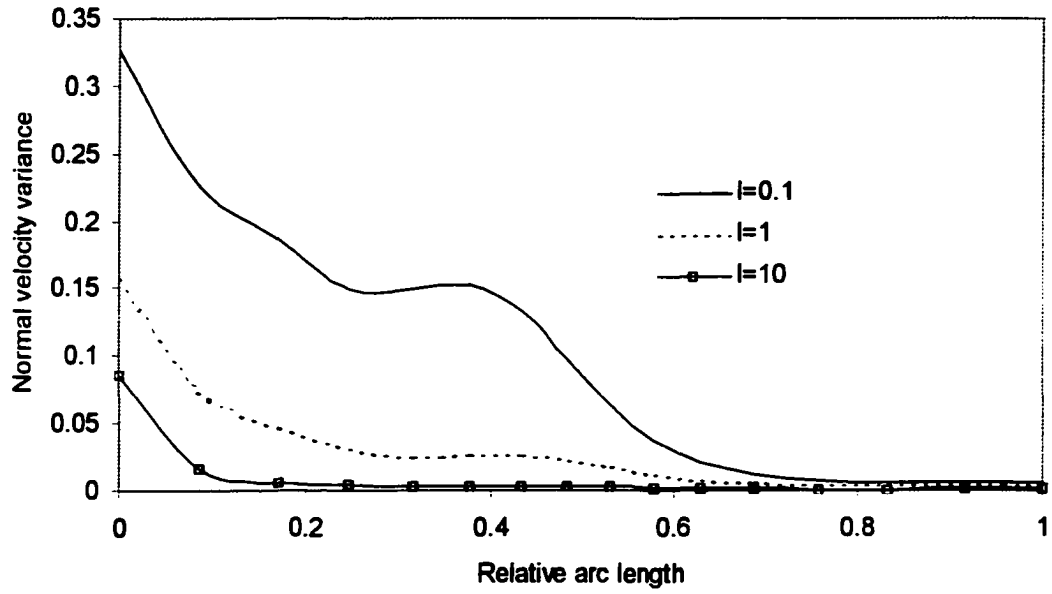

Figure 5.15 Dimensionless normal velocity variance = $\theta^2\left[\sigma_v^2\right]^{[2]} / K_G^2$ of a Saffman-Taylor type finger versus relative arc length as a function of normalized correlation length $l = l_z/c$ at $K_G t/\theta c = 0.5$. $\sigma_Y^2 = 1$, $Q/2cK_G = 1$, $l_x = \infty$.

CHAPTER 6

SUMMARY AND CONCLUSIONS

1. Based on the sharp front approximation we derived stochastic equations and boundary conditions that control DNAPL propagation in randomly heterogeneous saturated porous media. We found that they have similar form to those describing dynamics of a wetting front.
2. In line with Tartakovsky and Winter (2001) we proposed a new moment approach to the analysis of the above stochastic equations by converting them into integro-differential equations. Tartakovsky and Winter had approximated the domain and boundary of integration by their mean counterparts, resulting in what they termed a "leaner solution". Authors showed that this approximation introduces a systematic error in the prediction of mean front position. Upon treating the domain and boundary of integration as being random, we had obtained an additional second-order term in our equations for mean head (equations (2.25) and (2.44)), which eliminated the error.
3. Due to our choice of deterministic boundary conditions, the expressions for moments are formally the same for flow under prescribed head as for flow under prescribed flux. The difference between the two solutions stems from a difference in Green's functions.
4. The zero-order approximation of the mean hydraulic head, $h^{(0)}(\mathbf{x},t)$, satisfies a standard boundary-value problem with moving boundaries for a medium with

known properties, driven by a deterministic forcing term. Randomness, and nonlocality of the mean flow problem, manifest themselves solely in second-order (and higher) terms.

5. Our instability analysis implies that a DNAPL front is stable when the gradient of pressure head immediately above it is negative (the vertical coordinate z pointing downward and pressure head increasing upward) and unstable when this gradient is positive. We showed that a probabilistic analysis of wetting front instability due to Chen and Neuman (1996) applies to a DNAPL front.
6. We solved our moment equations analytically in one dimension and compared the results with Monte Carlo simulations. We found the result to be accurate for both mildly and moderately heterogeneous soils. Our analytical solution allows one to investigate the effect that the variance and spatial correlation scale of log hydraulic conductivity have on front behavior under the action of various forcing terms.
7. Our one-dimensional analysis demonstrates the advantages of our moment solution over Monte Carlo simulation. The number of Monte Carlo simulations necessary for convergence of the two leading moments to a stable result increases with heterogeneity (the variance of log conductivity). There generally is no assurance that stabilization takes place at the theoretical ensemble value. We nevertheless take the Monte Carlo solution to represent the true ensemble moments.
8. Our second-order front position is much closer to the one obtained from Monte Carlo simulation than the zero-order front position, which constantly overestimate Monte Carlo solution.

9. We found that a one-dimensional front driven by deterministic flux Q propagates at a fixed deterministic velocity Q/θ, θ being DNAPL content, so that front variance σ_ξ^2, velocity variance σ_V^2, second-order mean front position $\overline{\xi}^{(2)}(t)$, second-order mean front velocity $\overline{V}^{(2)}(x,t)$ and related cros-covariances are zero. While trivial (this result can be obtained directly from the mass-conservation principle), it indicates that our moment solution is free of internal contradictions. While the front moves through a random porous medium at a deterministic velocity the actual head and its gradient remain random.
10. We found that when one-dimensional flow is driven by constant head, heterogeneity reduces the mean front propagation rate regardless of gravity. Mean front depth and its rate of advance increase with $(H\text{-}a)/l_Y$, i.e., increase with the driving head and decrease with the correlation length l_Y. The latter effect is amplified by the fact that dimensionless time also decreases as l_Y increases. The larger is b (i.e., the density difference between driving and driven fluids), the faster does the one-dimensional gravity front propagate. In the absence of gravity, the front prorogation rate is independent of density difference between the two fluids.
11. The one-dimensional front variance increases with the log conductivity variance σ_Y^2, the driving head and the correlation length l_Y regardless of gravity. In the presence of gravity, the front variance increases also with b. The variance of a gravity-free front does not depend of b.

12. We found that gravity-free DNAPL fronts ($\mu_D >> \mu_W$) driven by either constant flux or constant head remain stable. This is in full agreement with Saffman and Taylor (1958) who stated that such displacements are stable to small deviations if motion is directed from the more viscous to the less viscous fluid, whatever are their relative densities.
13. A gravity DNAPL front driven by constant head is initially stable but becomes unstable with time regardless of σ_Y^2.
14. A gravity wetting front (b=1) can be stable or unstable depending on σ_Y^2 and (H - a)/l_Y. For a mean wetting front to be stable, (H - a)/l_Y must be sufficiently large. Increasing of σ_Y^2 has a destabilizing effect on the front under gravity. Change in correlation length does not have significant effect on the front.
15. A gravity DNAPL front driven by constant flux is stable for $\frac{Q}{K_G}(1+\frac{\sigma_Y^2}{2}) > 1$ and unstable otherwise. In other words, heterogeneity (increasing of σ_Y^2) has a stabilizing effect on gravity flow driven by constant flux. The one-dimensional moment solutions for DNAPL flow driven by constant flux do not depend on correlation length.
16. We solved our moment equations numerically in two dimensions. Our numerical solution reproduces known phenomena such as finger splitting and shielding in a homogeneous porous medium. It shows that (a) random layering reduces the mean

finger propagation rate and (b) the front velocity variance is highest at fingertip, increases with σ_Y^2 and decreases with spatial correlation.

17. Our results are of both theoretical and practical importance because in most soils, conductivity behaves as a correlated random field.

APPENDIX A

INTEGRAL EQUATION

From (2.7) follows the Second-Order Partial Differential Equation (PDE)

$$\nabla\left(K_D(\mathbf{x})\nabla h(\mathbf{x},t)\right)=0 \qquad \mathbf{x}\in\Omega \quad t\geq 0 \tag{A.1}$$

subject to boundary conditions

$$\frac{\partial h(\mathbf{x},t)}{\partial x_{\mathbf{x}}}=0 \qquad \mathbf{x}\in\Gamma_N \tag{A.2}$$

$$h(\mathbf{x})=H-a \qquad \mathbf{x}\in\Gamma_D \tag{A.3}$$

$$h(\mathbf{x},t)=-b\xi(x_{\mathbf{x}},y_{\mathbf{x}};t) \qquad z_{\mathbf{x}}=\xi(x_{\mathbf{x}},y_{\mathbf{x}};t) \quad (\text{or } \mathbf{x}\in\gamma), \quad t\geq 0 \tag{A.4}$$

$$-\mathbf{n}(\mathbf{x},t)\bullet\left(K_D(\mathbf{x})\nabla h(\mathbf{x},t)\right)=\theta V_n(\mathbf{x},t) \qquad z_{\mathbf{x}}=\xi(x_{\mathbf{x}},y_{\mathbf{x}};t) \quad (\text{or } \mathbf{x}\in\gamma), \quad t\geq 0 \tag{A.5}$$

$$\gamma=\gamma_0 \quad (\text{or } \xi(x,y,0)=\xi_0(x,y)) \qquad t=0 \tag{A.6}$$

The random field K_D is represented as

$$K_D(\mathbf{x})=\bar{K}(\mathbf{x})+K'(\mathbf{x}) \qquad \overline{K'}(\mathbf{x})=0 \tag{A.7}$$

Substituting (A.7) into (A.1), multiplying by G and integrating over Ω give

$$\int_{\Omega(t)}\nabla_{\mathbf{y}}\bullet\left[\bar{K}(\mathbf{y})\nabla_{\mathbf{y}}h(\mathbf{y},t)\right]G(\mathbf{y},\mathbf{x})d\mathbf{y}+\int_{\Omega(t)}\nabla_{\mathbf{y}}\bullet\left[K'(\mathbf{y})\nabla_{\mathbf{y}}h(\mathbf{y},t)\right]G(\mathbf{y},\mathbf{x})d\mathbf{y}=0 \tag{A.8}$$

where G is defined in (2.14)-(2.16)

Applying Green's formula to the first domain integral gives

$$\int_{\Gamma(t)} \bar{K}(\mathbf{y})\mathbf{n}(\mathbf{y},t)\bullet\nabla_{\mathbf{y}}h(\mathbf{y},t)G(\mathbf{y},\mathbf{x})d\mathbf{y} - \int_{\Omega(t)} \bar{K}(\mathbf{y})\nabla_{\mathbf{y}}h(\mathbf{y},t)\bullet\nabla_{\mathbf{y}}G(\mathbf{y},\mathbf{x})d\mathbf{y}$$
$$+ \int_{\Omega(t)} \nabla_{\mathbf{y}}\bullet\left[K'(\mathbf{y})\nabla_{\mathbf{y}}h(\mathbf{y},t)\right]G(\mathbf{y},\mathbf{x})d\mathbf{y} = 0 \qquad (A.9)$$

where **n** is an outward normal unit vector.

Applying Green's formula again gives

$$-\int_{\Omega(t)} h(\mathbf{y},t)\nabla_{\mathbf{y}}\bullet\left[\bar{K}(\mathbf{y})\nabla_{\mathbf{y}}G(\mathbf{y},\mathbf{x})\right]d\mathbf{y} =$$
$$\int_{\Gamma(t)} \left[\bar{K}(\mathbf{y})\mathbf{n}(\mathbf{y},t)\bullet\nabla_{\mathbf{y}}h(\mathbf{y},t)G(\mathbf{y},\mathbf{x}) - \bar{K}(\mathbf{y})h(\mathbf{y},t)\mathbf{n}(\mathbf{y},t)\bullet\nabla_{\mathbf{y}}G(\mathbf{y},\mathbf{x})\right]d\mathbf{y} \qquad (A.10)$$
$$+ \int_{\Omega(t)} \nabla_{\mathbf{y}}\bullet\left[K'(\mathbf{y})\nabla_{\mathbf{y}}h(\mathbf{y},t)\right]G(\mathbf{y},\mathbf{x})d\mathbf{y}$$

Incorporating (2.14) and applying Green's formula to the last integral give

$$\int_{\Omega(t)} h(\mathbf{y},t)\delta(\mathbf{y}-\mathbf{x})d\mathbf{y} =$$
$$+ \int_{\Gamma(t)} \left[\bar{K}(\mathbf{y})\mathbf{n}(\mathbf{y},t)\bullet\nabla_{\mathbf{y}}h(\mathbf{y},t)G(\mathbf{y},\mathbf{x}) - \bar{K}(\mathbf{y})h(\mathbf{y},t)\mathbf{n}(\mathbf{y},t)\bullet\nabla_{\mathbf{y}}G(\mathbf{y},\mathbf{x})\right]d\mathbf{y} \qquad (A.11)$$
$$+ \int_{\Gamma(t)} K'(\mathbf{y})\mathbf{n}(\mathbf{y},t)\bullet\nabla_{\mathbf{y}}h(\mathbf{y},t)G(\mathbf{y},\mathbf{x})d\mathbf{y} - \int_{\Omega(t)} K'(\mathbf{y})\nabla_{\mathbf{y}}h(\mathbf{y},t)\bullet\nabla_{\mathbf{y}}G(\mathbf{y},\mathbf{x})d\mathbf{y}$$

Incorporating boundary conditions and the definition of the delta function yields

$$h(\mathbf{x},t) = -(H-a)\int_{\Gamma_D} \bar{K}(\mathbf{y})\mathbf{n}(\mathbf{y})\bullet\nabla_{\mathbf{y}}G(\mathbf{y},\mathbf{x})d\mathbf{y}$$
$$-\int_{\gamma(t)} \left[\theta V_n(\mathbf{y},t)G(\mathbf{y},\mathbf{x}) - \bar{K}(\mathbf{y})b\xi(x_{\mathrm{y}},y_{\mathrm{y}};t)\mathbf{n}(\mathbf{y},t)\bullet\nabla_{\mathbf{y}}G(\mathbf{y},\mathbf{x})\right]d\mathbf{y} \qquad (A.12)$$
$$-\int_{\Omega(t)} K'(\mathbf{y})\nabla_{\mathbf{y}}h(\mathbf{y},t)\bullet\nabla_{\mathbf{y}}G(\mathbf{y},\mathbf{x})d\mathbf{y}$$

Note that the integral over the front is equivalent to the integral over the depth of the front as a function of x and y, because we defined front position in term of depth.

APPENDIX B

ZERO-, FIRST- AND SECOND ORDER APPROXIMATIONS OF MEAN HEAD

Zero-order approximations of mean head $h^{(0)}(x,t)$

To obtain a zero-order mean head approximation we substitute (2.20)-(2.22) in (2.13) and retain only terms of zero-order:

$$h^{(0)}(\mathbf{x},t) = -(H-a)\int_{\Gamma_D} K_G(\mathbf{y})\mathbf{n}(\mathbf{y})\bullet\nabla_{\mathbf{y}}G^{(0)}(\mathbf{y},\mathbf{x})d\mathbf{y} - \int_{\gamma^{(0)}(t)}\left[\theta V_n^{(0)}(\mathbf{y},t)G^{(0)}(\mathbf{y},\mathbf{x}) - K_G(\mathbf{y})b\xi^{(0)}(x_{\mathbf{y}},y_{\mathbf{y}};t)\mathbf{n}(\mathbf{y},t)\bullet\nabla_{\mathbf{y}}G^{(0)}(\mathbf{y},\mathbf{x})\right]d\mathbf{y} \tag{B.1}$$

where $G^{(0)}$ satisfies

$$\nabla_{\mathbf{y}}\bullet\left(K_G(\mathbf{y})\nabla_{\mathbf{y}}G^{(0)}(\mathbf{y},\mathbf{x})\right)+\delta(\mathbf{y}-\mathbf{x})=0 \qquad \mathbf{y},\mathbf{x}\in\Omega_T \tag{B.2}$$

subject to the boundary conditions

$$G^{(0)}(\mathbf{y},\mathbf{x})=0 \qquad \mathbf{y}\in\Gamma_D \tag{B.3}$$

$$\mathbf{n}(\mathbf{y})\bullet\nabla_{\mathbf{y}}G^{(0)}(\mathbf{y},\mathbf{x})=0 \qquad \mathbf{y}\in\Gamma_N \tag{B.4}$$

First-order approximations of head $h^{[1]}(x,t)$

A self-consistent representation of (2.13) in terms of the first-order head $h^{[1]}=h^{(0)}+h^{(1)}$ is

$$
\begin{aligned}
h^{[1]}(\mathbf{x},t) &= -(H-a)\int_{\Gamma_D} K_G(\mathbf{y})\mathbf{n}(\mathbf{y})\bullet\nabla_{\mathbf{y}}G^{(0)}(\mathbf{y},\mathbf{x})d\mathbf{y} \\
&-\theta\int_{\gamma^{[1]}(t)} V_n^{[1]}(\mathbf{y},t)G^{(0)}(\mathbf{y},\mathbf{x})d\mathbf{y} \\
&+b\int_{\gamma^{[1]}(t)} K_G(\mathbf{y})\xi^{[1]}(x_{\mathbf{y}},y_{\mathbf{y}},t)\mathbf{n}(\mathbf{y},t)\bullet\nabla_{\mathbf{y}}G^{(0)}(\mathbf{y},\mathbf{x})d\mathbf{y} \\
&-\int_{\Omega^{[1]}} K_G(\mathbf{y})Y'(\mathbf{y})\nabla_{\mathbf{y}}h^{(0)}(\mathbf{y},t)\bullet\nabla_{\mathbf{y}}G^{(0)}(\mathbf{y},\mathbf{x})d\mathbf{y}
\end{aligned}
\tag{B.5}
$$

Note that $G^{(1)}$ satisfies

$$
\nabla\bullet\left(K_G(\mathbf{y})\nabla G^{(1)}(\mathbf{y},\mathbf{x})\right)+\nabla\bullet\left(\overline{K}^{(1)}(\mathbf{y})\nabla G^{(0)}(\mathbf{y},\mathbf{x})\right)=0 \qquad \mathbf{y},\mathbf{x}\in\Omega_T \tag{B.6}
$$

subject to the boundary conditions

$$
G^{(1)}(\mathbf{y},\mathbf{x})=0 \qquad \mathbf{y}\in\Gamma_D \tag{B.7}
$$

$$
\mathbf{n}(\mathbf{y})\bullet\nabla_{\mathbf{y}}G^{(1)}(\mathbf{y},\mathbf{x})=0 \qquad \mathbf{y}\in\Gamma_N \tag{B.8}
$$

Since $\overline{K}^{(1)}\equiv 0$, $G^{(1)}$=0.

Note that the first-order mean head satisfies

$$
\nabla\left(K_G\nabla\overline{h}^{(1)}(\mathbf{x},t)\right)=0 \tag{B.9}
$$

$$
\overline{h}^{(1)}(\mathbf{x})=0 \qquad \mathbf{x}\in\Gamma_D \tag{B.10}
$$

$$
\frac{\partial\overline{h}^{(1)}(\mathbf{x},t)}{\partial x}=0 \qquad \mathbf{x}\in\Gamma_N \tag{B.11}
$$

$$
\overline{h}^{(1)}(\mathbf{x},t)=-b\overline{\xi}^{(1)} \qquad z_{\mathbf{x}}=\overline{\xi}^{(1)}(x_{\mathbf{x}},y_{\mathbf{x}},t) \tag{B.12}
$$

$$
-K_G\nabla\overline{h}^{(1)}(\mathbf{x},t)\bullet\mathbf{n}_{\overline{\gamma}^{(1)}}=\theta\frac{\partial\overline{\xi}^{(1)}(x_{\mathbf{x}},y_{\mathbf{x}};t)}{\partial t}\left(n_z\right)_{\overline{\gamma}^{(1)}} \qquad z_{\mathbf{x}}=\overline{\xi}^{(1)}(x_{\mathbf{x}},y_{\mathbf{x}};t) \tag{B.13}
$$

whose solution is $\overline{h}^{(1)}=0$ and $\overline{\xi}^{(1)}=0$.

Here $\mathbf{n}_{\gamma^{(1)}}$ is a unit vector to the front γ defined by $\bar{\xi}^{(1)}(x,y;t)$.

Second-order approximations of mean head $h^{[2]}(x,t)$

A self-consistent representation of (2.13) in terms of the second-order head $h^{[2]} = h^{(0)} + h^{(1)} + h^{(2)}$ is

$$h^{[2]}(\mathbf{x},t) = -(H-a)\int_{\Gamma_D}\left[K_G(\mathbf{y})(1+\frac{\sigma_Y^2}{2})\mathbf{n}(\mathbf{y},t)\bullet\nabla_{\mathbf{y}}G^{(0)}(\mathbf{y},\mathbf{x}) + K_G\mathbf{n}(\mathbf{y},t)\bullet\nabla_{\mathbf{y}}G^{(2)}(\mathbf{y},\mathbf{x})\right]d\mathbf{y}$$
$$-\theta\int_{\gamma^{[2]}(t)}\left(\left(V_n^{(0)}(\mathbf{y},t)+V_n^{(1)}(\mathbf{y},t)+V_n^{(2)}(\mathbf{y},t)\right)G^{(0)}(\mathbf{y},\mathbf{x})+V_n^{(0)}(\mathbf{y},t)G^{(2)}(\mathbf{y},\mathbf{x})\right)d\mathbf{y}$$
$$+b\int_{\gamma^{[2]}(t)}K_G(\mathbf{y})\left(\xi^{(0)}(x_{\mathbf{y}},y_{\mathbf{y}},t)+\xi^{(1)}(x_{\mathbf{y}},y_{\mathbf{y}},t)+\xi^{(2)}(x_{\mathbf{y}},y_{\mathbf{y}},t)\right)\mathbf{n}(\mathbf{y},t)\bullet\nabla_{\mathbf{y}}G^{(0)}(\mathbf{y},\mathbf{x})d\mathbf{y}$$
$$+b\int_{\gamma^{[2]}}K_G(\mathbf{y})\xi^{(0)}(x_{\mathbf{y}},y_{\mathbf{y}},t)\mathbf{n}(\mathbf{y},t)\bullet\nabla_{\mathbf{y}}G^{(2)}(\mathbf{y},\mathbf{x})d\mathbf{y}$$
$$+b\frac{\sigma_Y^2}{2}\int_{z=\xi^{[2]}}K_G(\mathbf{y})\xi^{(0)}(x_{\mathbf{y}},y_{\mathbf{y}},t)\mathbf{n}(\mathbf{y},t)\bullet\nabla_{\mathbf{y}}G^{(0)}(\mathbf{y},\mathbf{x})d\mathbf{y}$$

$$-\int_{\Omega^{[2]}}\left[K'^{(1)}(\mathbf{y})\left(\nabla_{\mathbf{y}}h^{(0)}(\mathbf{y},t)+\nabla_{\mathbf{y}}h^{(1)}(\mathbf{y},t)\right)+K'^{(2)}(\mathbf{y})\nabla_{\mathbf{y}}h^{(0)}(\mathbf{y},t)\right]\bullet\nabla_{\mathbf{y}}G^{(0)}(\mathbf{y},\mathbf{x})d\mathbf{y} \qquad \text{(B.14)}$$

where we define $K'^{(t)} = K^{(t)} - \bar{K}^{(t)}$.

$G^{(2)}$ satisfies

$$\nabla_{\mathbf{y}}\bullet\left(K_G(\mathbf{y})\nabla_{\mathbf{y}}G^{(2)}(\mathbf{y},\mathbf{x})\right)+\frac{\sigma_Y^2}{2}\nabla_{\mathbf{y}}\bullet\left(K_G(\mathbf{y})\nabla_{\mathbf{y}}G^{(0)}(\mathbf{y},\mathbf{x})\right)=0 \qquad \mathbf{y},\mathbf{x}\in\Omega_T \qquad \text{(B.15)}$$

subject to the boundary conditions

$$G^{(2)}(\mathbf{y},\mathbf{x})=0 \qquad \mathbf{y}\in\Gamma_D \qquad \text{(B.16)}$$

$$\mathbf{n}(\mathbf{y})\bullet\nabla_{\mathbf{y}}G^{(2)}(\mathbf{y},\mathbf{x})=0 \qquad \mathbf{y}\in\Gamma_N \tag{B.17}$$

Substitution of (B.2) into (B.15) gives

$$\nabla_{\mathbf{y}}\left(K_G(\mathbf{y})\nabla_{\mathbf{y}}G^{(2)}(\mathbf{y},\mathbf{x})\right)-\frac{\sigma_Y^2}{2}\delta(\mathbf{y}-\mathbf{x})=0 \tag{B.18}$$

It follows that

$$G^{(2)}=-\frac{\sigma_Y^2}{2}G^{(0)} \tag{B.19}$$

Combining terms in (B.14) yields

$$\begin{aligned}
h^{[2]}(\mathbf{x},t)=&-(H-a)\int_{\Gamma_D}\left[\bar{K}^{[2]}(\mathbf{y})\mathbf{n}(\mathbf{y},t)\bullet\nabla_{\mathbf{y}}G^{(0)}(\mathbf{y},\mathbf{x})+K_G(\mathbf{y})\mathbf{n}(\mathbf{y},t)\bullet\nabla_{\mathbf{y}}G^{(2)}(\mathbf{y},\mathbf{x})\right]d\mathbf{y}\\
&-\theta\int_{\gamma^{[2]}(t)}\left(V_n^{[2]}(\mathbf{y},t)G^{(0)}(\mathbf{y},\mathbf{x})+V_n^{(0)}(\mathbf{y},t)G^{(2)}(\mathbf{y},\mathbf{x})\right)d\mathbf{y}\\
&+b\int_{\gamma^{[2]}(t)}K_G(\mathbf{y})\xi^{[2]}(x_{\mathrm{y}},y_{\mathrm{y}},t)\mathbf{n}(\mathbf{y},t)\bullet\nabla_{\mathbf{y}}G^{(0)}(\mathbf{y},\mathbf{x})d\mathbf{y}\\
&+b\int_{\gamma^{[2]}(t)}K_G(\mathbf{y})\xi^{(0)}(x_{\mathrm{y}},y_{\mathrm{y}},t)\mathbf{n}(\mathbf{y},t)\bullet\nabla_{\mathbf{y}}G^{(2)}(\mathbf{y},\mathbf{x})d\mathbf{y}\\
&+b\frac{\sigma_Y^2}{2}\int_{\gamma^{[2]}(t)}K_G(\mathbf{y})\xi^{(0)}(x_{\mathrm{y}},y_{\mathrm{y}})\mathbf{n}(\mathbf{y},t)\bullet\nabla_{\mathbf{y}}G^{(0)}(\mathbf{y},\mathbf{x})d\mathbf{y}\\
&-\int_{\Omega^{[2]}(t)}\left[K'^{(1)}(\mathbf{y})\nabla_{\mathbf{y}}h^{[1]}(\mathbf{y},t)\bullet\nabla_{\mathbf{y}}G^{(0)}(\mathbf{y},\mathbf{x})+K'^{(2)}(\mathbf{y})\nabla_{\mathbf{y}}h^{(0)}(\mathbf{y},t)\bullet\nabla_{\mathbf{y}}G^{(0)}(\mathbf{y},\mathbf{x})\right]d\mathbf{y}
\end{aligned} \tag{B.20}$$

Substituting (B.19) into (B.20) gives

$$\begin{aligned}
h^{[2]}(\mathbf{x},t)=&-(H-a)\int_{\Gamma_D}K_G(\mathbf{y})\mathbf{n}(\mathbf{y},t)\bullet\nabla_{\mathbf{y}}G^{(0)}(\mathbf{y},\mathbf{x})d\mathbf{y}\\
&-\theta\int_{\gamma^{[2]}(t)}\left(V_n^{[2]}(\mathbf{y},t)G^{(0)}(\mathbf{y},\mathbf{x})-\frac{\sigma_Y^2}{2}V_n^{(0)}(\mathbf{y},t)G^{(0)}(\mathbf{y},\mathbf{x})\right)d\mathbf{y}\\
&+b\int_{\gamma^{[2]}(t)}K_G(\mathbf{y})\xi^{[2]}(x_{\mathrm{y}},y_{\mathrm{y}},t)\mathbf{n}(\mathbf{y},t)\bullet\nabla_{\mathbf{y}}G^{(0)}(\mathbf{y},\mathbf{x})d\mathbf{y}\\
&-\int_{\Omega^{[2]}(t)}\left(K'^{(1)}(\mathbf{y})\nabla_{\mathbf{y}}h^{[1]}(\mathbf{y},t)\bullet\nabla_{\mathbf{y}}G^{(0)}(\mathbf{y},\mathbf{x})+K'^{(2)}(\mathbf{y})\nabla_{\mathbf{y}}h^{(0)}(\mathbf{y},t)\bullet\nabla_{\mathbf{y}}G^{(0)}(\mathbf{y},\mathbf{x})\right)d\mathbf{y}
\end{aligned} \tag{B.21}$$

We rewrite the domain integral in (2.13) as

$$\int_{\Omega(t)} K'(\mathbf{y})\nabla_y h(\mathbf{y},t)\bullet\nabla_y G(\mathbf{y},\mathbf{x})d\mathbf{y} = \int_{\Gamma_D}\int_{0}^{\xi^{(0)}+\xi^{(1)}+..} K'(\mathbf{y})\nabla_y h(\mathbf{y},t)\bullet\nabla_y G(\mathbf{y},\mathbf{x})dz_y d\mathbf{y}$$

$$= \int_{\Gamma_D}\int_{0}^{\xi^{(0)}(t)} K'(\mathbf{y})\nabla_y h(\mathbf{y},t)\bullet\nabla_y G(\mathbf{y},\mathbf{x})d\mathbf{y} + \int_{\Gamma_D}\left(\xi^{(1)}+...\right)K'(\mathbf{y}_\xi)\nabla_{y_\xi} h(\mathbf{y}_\xi,t)\bullet\nabla_{y_\xi} G(\mathbf{y}_\xi,\mathbf{x})d\mathbf{y}_\xi + ...$$

$$= \int_{\Omega^{(0)}(t)} K'(\mathbf{y})\nabla_y h(\mathbf{y})\bullet\nabla_y G(\mathbf{y},\mathbf{x})d\mathbf{y} + \int_{\gamma^{(0)}(t)}\left(\xi^{(1)}+...\right)K'(\mathbf{y})\nabla_y h(\mathbf{y},t)\bullet\nabla_y G(\mathbf{y},\mathbf{x})d\mathbf{y} + ... \quad \text{(B.22)}$$

where $\mathbf{y}_\xi = \left(x_y, y_y, z=\xi^{(0)}(x_y,y_y)\right)^T$

Define $\xi'^{(t)} = \xi^{(t)} - \overline{\xi}^{(t)}$ and expand boundary integrals over $\xi^{[2]} = \overline{\xi}^{[2]} + \xi'^{(1)} + \xi'^{(2)}$ in Taylor series around $\overline{\xi}^{[2]}$, disregarding terms of order higher than 2. For example

$$\int_{\xi^{[2]}(x_y,y_y)\bullet\xi^{[2]}(x_y,y_y)} \theta V_n^{[2]}(\mathbf{y},t)G^{(0)}(\mathbf{y},\mathbf{x})d\mathbf{y}$$

$$= \int_{\xi^{[2]}(x_y,y_y)} \theta V_n^{[2]}(\mathbf{y},t)G^{(0)}(\mathbf{y},\mathbf{x})d\mathbf{y} + \left(\xi'^{(1)}+\xi'^{(2)}\right)\theta\overline{V}_n^{[2]}(\mathbf{y},t)G^{(0)}(\mathbf{y},\mathbf{x})_{z_y=\overline{\xi}^{(2)}(x_y,y_y,t)} + ... \quad \text{(B.23)}$$

From (2.19) it follows that $\overline{Y'}^{(2)} = \left(\overline{(Y')^2} - \sigma_Y^2\right)/2 = 0$.

Expanding (B.21) using (B.22)-(B.23) and averaging then gives

$$\overline{h}^{[2]}(\mathbf{x},t) = -(H-a)\int_{\Gamma_D} K_G(\mathbf{y})\mathbf{n}(\mathbf{y})\bullet\nabla_{\mathrm{y}}G^{(0)}(\mathbf{y},\mathbf{x})d\mathbf{y}$$

$$-\theta\int_{y^{[2]}(t)}\left(\overline{V}_n^{[2]}(\mathbf{y},t)G^{(0)}(\mathbf{y},\mathbf{x})-\frac{\sigma_Y^2}{2}V_n^{(0)}(\mathbf{y},t)G^{(0)}(\mathbf{y},\mathbf{x})\right)d\mathbf{y}$$

$$+b\int_{y^{[2]}(t)} K_G(\mathbf{y})\overline{\xi}^{[2]}(x_{\mathrm{y}},y_{\mathrm{y}},t)\mathbf{n}(\mathbf{y},t)\bullet\nabla_{\mathrm{y}}G^{(0)}(\mathbf{y},\mathbf{x})d\mathbf{y} \qquad \text{(B.24)}$$

$$+\int_{\Omega^{(0)}(t)} K_G(\mathbf{y})\mathbf{r}^{[2]}(\mathbf{y},t)\bullet\nabla_{\mathrm{y}}G^{(0)}(\mathbf{y},\mathbf{x})d\mathbf{y}$$

$$-\int_{y^{(0)}(t)} K_G(\mathbf{y})C_{YY}^{[2]}(\mathbf{y}^{(0)};x_{\mathrm{y}},y_{\mathrm{y}},t)\nabla_{\mathrm{y}}h^{(0)}(\mathbf{y}^{(0)},t)\bullet\nabla_{\mathrm{y}}G^{(0)}(\mathbf{y}^{(0)},\mathbf{x})d\mathbf{y}$$

where $\mathbf{r}^{(2)} = -\overline{Y'\nabla h'}^{(2)}$

APPENDIX C

SECOND ORDER APPROXIMATION OF RESIDUAL FLUX

To obtain $\mathbf{r}$ we operate on (B.5) with the stochastic differential operator $Y'^{(1)}(\mathbf{x})\nabla_{\mathbf{x}}$,

$$Y'(\mathbf{x})\nabla_{\mathbf{x}}h^{[1]}(\mathbf{x},t) = -(H-a)\int_{\Gamma_D} Y'(\mathbf{x})K_G(\mathbf{y})\mathbf{n}(\mathbf{y})\bullet\nabla_{\mathbf{y}}\nabla_{\mathbf{x}}G^{(0)}(\mathbf{y},\mathbf{x})d\mathbf{y}$$

$$-\int_{\gamma^{[1]}(t)} \left[\theta Y'(\mathbf{x})V_n^{[1]}(\mathbf{y},t)\nabla_{\mathbf{x}}G^{(0)}(\mathbf{y},\mathbf{x}) - Y'(\mathbf{x})K_G b\xi^{[1]}(x_{\mathrm{y}},y_{\mathrm{y}},t)\mathbf{n}(\mathbf{y},t)\bullet\nabla_{\mathbf{y}}\nabla_{\mathbf{x}}G^{(0)}(\mathbf{y},\mathbf{x})\right]d\mathbf{y}$$

$$-\int_{\Omega^{[1]}(t)} K_G(\mathbf{y})Y'(\mathbf{x})Y'(\mathbf{y})\nabla_{\mathbf{y}}h^{(0)}(\mathbf{y},t)\bullet\nabla_{\mathbf{y}}\nabla_{\mathbf{x}}G^{(0)}(\mathbf{y},\mathbf{x})d\mathbf{y} \tag{C.1}$$

Here we replace integrals over random domain and boundaries and domain with integrals over their zero-order equivalents. Tailor series expansions about the latter shows that by doing so we do not lose any second-order terms. Averaging (C.1) thus gives

$$\mathbf{r}(\mathbf{x},t)^{[2]} = \theta\int_{\gamma^{(0)}(t)} C^{[2]}_{YV_n}(\mathbf{x};\mathbf{y},t)\nabla_{\mathbf{x}}G^{(0)}(\mathbf{y},\mathbf{x})d\mathbf{y}$$

$$-b\int_{\gamma^{(0)}(t)} K_G(\mathbf{y})C^{[2]}_{Y\gamma}(\mathbf{x};\mathbf{y},t)\mathbf{n}(\mathbf{y},t)\bullet\nabla_{\mathbf{y}}\nabla_{\mathbf{x}}G^{(0)}(\mathbf{y},\mathbf{x})d\mathbf{y} \tag{C.2}$$

$$+\int_{\Omega^{(0)}(t)} K_G(\mathbf{y})C^{[2]}_{Y}(\mathbf{x},\mathbf{y})\nabla_{\mathbf{y}}h^{(0)}(\mathbf{y},t)\bullet\nabla_{\mathbf{y}}\nabla_{\mathbf{x}}G^{(0)}(\mathbf{y},\mathbf{x})d\mathbf{y}$$

APPENDIX D

SECOND ORDER APPROXIMATION OF COVARIANCE $C_{YY}^{[2]}(\mathbf{z};\mathbf{x}_\gamma,t)$

Evaluating (B.5) at the front and multiplying by $Y'(\mathbf{z})$ gives

$$\begin{aligned}
&-bY'(\mathbf{z})\xi^{[1]}(x_\mathrm{x},y_\mathrm{x},t) = -(H-a)\int_{\Gamma_D} Y'(\mathbf{z})K_G(\mathbf{y})\mathbf{n}(\mathbf{y})\bullet\nabla_\mathrm{y}G^{(0)}(\mathbf{y},\mathbf{x})d\mathbf{y}\\
&-\theta\int_{\gamma^{[1]}(t)} Y'(\mathbf{z})V_n^{[1]}(\mathbf{y},t)G^{(0)}(\mathbf{y},\mathbf{x})d\mathbf{y}\\
&+b\int_{\gamma^{[1]}(t)} K_G(\mathbf{y})Y'(\mathbf{z})\xi^{[1]}(x_\mathrm{y},y_\mathrm{y},t)\mathbf{n}(\mathbf{y},t)\bullet\nabla_\mathrm{y}G^{(0)}(\mathbf{y},\mathbf{x})d\mathbf{y}\\
&-\int_{\Omega^{[1]}} K_G(\mathbf{y})Y'(\mathbf{z})Y'(\mathbf{y})\nabla_\mathrm{y}h^{(0)}(\mathbf{y},t)\bullet\nabla_\mathrm{y}G^{(0)}(\mathbf{y},\mathbf{x})d\mathbf{y}
\end{aligned} \tag{D.1}$$

Replacing integrals over random domain and boundaries with integrals over their zero-order counterparts, taking average and retaining second-order terms yields an approximation for $C_{Y\gamma}=\overline{Y'\xi'}$

$$\begin{aligned}
&bC_{Y\gamma}^{[2]}(\mathbf{z};x_\mathrm{x},y_\mathrm{x},t) = \int_{\Omega^{(0)}(t)} K_G(\mathbf{y})C_Y^{[2]}(\mathbf{z},\mathbf{y})\nabla_\mathrm{y}h^{(0)}(\mathbf{y},t)\bullet\nabla_\mathrm{y}G^{(0)}\left(\mathbf{y};x_\mathrm{x},y_\mathrm{x},\xi(x_\mathrm{x},y_\mathrm{x},t)\right)d\mathbf{y}\\
&+\theta\int_{\gamma^{(0)}(t)} C_{YV_n}^{[2]}(\mathbf{z};\mathbf{y},t)G^{(0)}\left(\mathbf{y},x_\mathrm{x},y_\mathrm{x},\xi(x_\mathrm{x},y_\mathrm{x},t)\right)d\mathbf{y}\\
&-b\int_{\gamma^{(0)}(t)} K_G C_{Y\gamma}^{[2]}(\mathbf{z};\mathbf{y},t)\mathbf{n}(\mathbf{y},t)\bullet\nabla_\mathrm{y}G^{(0)}\left(\mathbf{y},x_\mathrm{x},y_\mathrm{x},\xi(x_\mathrm{x},y_\mathrm{x},t)\right)d\mathbf{y}
\end{aligned} \tag{D.2}$$

where

$$C_{YV_n} = \overline{Y'V_n'} = \frac{\partial C_{Y\gamma}}{\partial t}n_z \tag{D.3}$$

APPENDIX E

FRONT COVARIANCE

Evaluating (B.5) at the front and multiplying by $\xi^{(1)}(x_x, y_x; \tilde{t})$ gives

$$
\begin{aligned}
-b\xi^{(1)}(x_x, y_x; \tilde{t})\xi^{[1]}(x_x, y_x; t) &= -(H-a)\int_{\Gamma_D} \xi^{(1)}(x_x, y_x; \tilde{t}) K_G(\mathbf{y})\mathbf{n}(\mathbf{y})\cdot\nabla_y G^{(0)}(\mathbf{y}, \mathbf{x})d\mathbf{y} \\
&-\theta \int_{\gamma^{[1]}(t)} \xi^{(1)}(x_x, y_x; \tilde{t}) V_n^{[1]}(\mathbf{y}, t) G^{(0)}(\mathbf{y}, \mathbf{x})d\mathbf{y} \\
&+b \int_{\gamma^{[1]}(t)} K_G(\mathbf{y})\xi^{(1)}(x_x, y_x; \tilde{t})\xi^{[1]}(x_y, y_y; t)\mathbf{n}(\mathbf{y}, t)\cdot\nabla_y G^{(0)}(\mathbf{y}, \mathbf{x})d\mathbf{y} \\
&-\int_{\Omega^{[1]}} K_G(\mathbf{y})\xi^{(1)}(x_x, y_x; \tilde{t})Y'(\mathbf{y})\nabla_y h^{(0)}(\mathbf{y}, t)\cdot\nabla_y G^{(0)}(\mathbf{y}, \mathbf{x})d\mathbf{y}
\end{aligned}
\tag{E.1}
$$

Approximating it with integrals over zero-order domain and boundaries and averaging gives

$$
\begin{aligned}
bC_\gamma^{[2]}(x_x, y_x, \tilde{t}; x_x, y_x, t) &= \theta \int_{\gamma^{(0)}(t)} C_{\gamma V_n}^{[2]}(x_x, y_x, \tilde{t}; x_y, y_y, t) G^{(0)}\left(\mathbf{y}; x_x, y_x, \xi(x_x, y_x, t)\right)d\mathbf{y} \\
&-b \int_{\gamma^{(0)}(t)} K_G(\mathbf{y}) C_\gamma^{[2]}(x_x, y_x, \tilde{t}; x_y, y_y, t)\mathbf{n}(\mathbf{y}, t)\cdot\nabla_y G^{(0)}\left(\mathbf{y}; x_x, y_x, \xi(x_x, y_x, t)\right)d\mathbf{y} \\
&+\int_{\Omega^{(0)}(t)} K_G(\mathbf{y}) C_{Y\gamma}^{[2]}(\mathbf{y}; x_x, y_x, t)\nabla_y h^{(0)}(\mathbf{y}, t)\cdot\nabla_y G^{(0)}\left(\mathbf{y}; x_x, y_x, \xi(x_x, y_x, t)\right)d\mathbf{y}
\end{aligned}
\tag{E.2}
$$

where

$$
C_{\gamma V_n}(x, y, \tilde{t}; x_y, y_y, t) = \frac{\partial C_\gamma(x, y, \tilde{t}; x_y, y_y, t)}{\partial t} n_z(\mathbf{y}) \tag{E.3}
$$

APPENDIX F

HEAD VARIANCE

Multiply (B.5) by $h^{(1)}(\mathbf{x},t)$ to obtain

$$h^{(1)}(\mathbf{x},t)h^{[1]}(\mathbf{x},t) = -(H-a)\int_{\Gamma_D} h^{(1)}(\mathbf{x})K_G(\mathbf{y})\mathbf{n}(\mathbf{y})\bullet\nabla_{\mathbf{y}}G^{(0)}(\mathbf{y},\mathbf{x})d\mathbf{y}$$

$$-\theta\int_{\gamma^{[1]}(t)} h^{(1)}(\mathbf{x},t)V_n^{[1]}(\mathbf{y},t)G^{(0)}(\mathbf{y},\mathbf{x})d\mathbf{y}$$

$$+b\int_{\gamma^{[1]}(t)} K_G(\mathbf{y})h^{(1)}(\mathbf{x},t)\xi^{[1]}(x_{\mathrm{y}},y_{\mathrm{y}},t)\mathbf{n}(\mathbf{y},t)\bullet\nabla_{\mathbf{y}}G^{(0)}(\mathbf{y},\mathbf{x})d\mathbf{y} \qquad \text{(F.1)}$$

$$-\int_{\Omega^{[1]}} K_G(\mathbf{y})h^{(1)}(\mathbf{x},t)Y'(\mathbf{y})\nabla_{\mathbf{y}}h^{(0)}(\mathbf{y},t)\bullet\nabla_{\mathbf{y}}G^{(0)}(\mathbf{y},\mathbf{x})d\mathbf{y}$$

Approximating this using integrals over zero-order domain and boundaries and averaging gives

$$\left[\sigma_h^2(\mathbf{x},t)\right]^{[2]} = -\theta\int_{\gamma^{[1]}(t)} C_{hY'}^{[2]}\left(\mathbf{x};x_{\mathrm{y}},y_{\mathrm{y}},\xi^{(0)}(x_{\mathrm{y}},y_{\mathrm{y}},t)\right)G^{(0)}(\mathbf{y},\mathbf{x})d\mathbf{y}$$

$$+b\int_{\gamma^{(0)}(t)} K_G(\mathbf{y})C_{h\gamma}^{[2]}\left(\mathbf{x};x_{\mathrm{y}},y_{\mathrm{y}},\xi^{(0)}(x_{\mathrm{y}},y_{\mathrm{y}},t)\right)\mathbf{n}(\mathbf{y},t)\bullet\nabla_{\mathbf{y}}G^{(0)}(\mathbf{y},\mathbf{x})d\mathbf{y} \qquad \text{(F.2)}$$

$$-\int_{\Omega^{(0)}} K_G(\mathbf{y})C_{hY}^{[2]}(\mathbf{x},\mathbf{y})\nabla_{\mathbf{y}}h^{(0)}(\mathbf{y},t)\bullet\nabla_{\mathbf{y}}G^{(0)}(\mathbf{y},\mathbf{x})d\mathbf{y}$$

where

$$C_{hY_n'}^{[2]}\left(\mathbf{x};x_{\mathrm{y}},y_{\mathrm{y}},\xi^{(0)}(x_{\mathrm{y}},y_{\mathrm{y}},t)\right) = \frac{\partial C_{h\gamma}^{[2]}\left(\mathbf{x};x_{\mathrm{y}},y_{\mathrm{y}},\xi^{(0)}(x_{\mathrm{y}},y_{\mathrm{y}},t)\right)}{\partial t}n_z(\mathbf{y}) \qquad \text{(F.3)}$$

To obtain $C_{h\gamma}^{[2]}\left(\mathbf{x};x_{\mathrm{y}},y_{\mathrm{y}},\xi^{(0)}(x_{\mathrm{y}},y_{\mathrm{y}},t)\right)$ we multiply (B.5) by $\xi^{(1)}(x_z,y_z,t)$

$$h^{[1]}(\mathbf{x},t)\xi^{(1)}(x_z,y_z,t)=-(H-a)\int_{\Gamma_D}\xi^{(1)}(x_z,y_z,t)K_G(\mathbf{y})\mathbf{n}(\mathbf{y})\bullet\nabla_y G^{(0)}(\mathbf{y},\mathbf{x})d\mathbf{y}$$

$$-\theta\int_{\gamma^{(0)}(t)}\xi^{(1)}(x_z,y_z,t)V_n^{[1]}(\mathbf{y},t)G^{(0)}(\mathbf{y},\mathbf{x})d\mathbf{y}$$

$$+b\int_{\gamma^{(0)}(t)}K_G(\mathbf{y})\xi^{(1)}(x_z,y_z,t)\xi^{[1]}(x_y,y_y,t)\mathbf{n}(\mathbf{y},t)\bullet\nabla_y G^{(0)}(\mathbf{y},\mathbf{x})d\mathbf{y} \qquad \text{(F.4)}$$

$$-\int_{\Omega^{(0)}(t)}K_G(\mathbf{y})\xi^{(1)}(x_z,y_z,t)Y'(\mathbf{y})\nabla_y h^{(0)}(\mathbf{y},t)\bullet\nabla_y G^{(0)}(\mathbf{y},\mathbf{x})d\mathbf{y}$$

Approximating with integrals over zero-order domain and boundaries and averaging gives

$$C_{h\gamma}^{[2]}\left(\mathbf{x},x_z,y_z,\xi^{(0)}(x_z,y_z,t)\right)=$$

$$-\theta\int_{\gamma^{(0)}(t)}C_{\xi V_n}^{[2]}\left(x_z,y_z,t;x_y,y_y,t\right)G^{(0)}(\mathbf{y},\mathbf{x})d\mathbf{y}$$

$$+b\int_{\gamma^{(0)}(t)}K_G(\mathbf{y})C_{\gamma}^{[2]}\left(x_z,y_z,t;x_y,y_y,t\right)\mathbf{n}(\mathbf{y},t)\bullet\nabla_y G^{(0)}(\mathbf{y},\mathbf{x})d\mathbf{y} \qquad \text{(F.5)}$$

$$-\int_{\Omega^{(0)}}K_G(\mathbf{y})C_{Y\gamma}^{[2]}(\mathbf{y},t;x_z,y_z,t)\nabla_y h^{(0)}(\mathbf{y},t)\bullet\nabla_y G^{(0)}(\mathbf{y},\mathbf{x})d\mathbf{y}$$

Multiplying (B.5) by $Y'(\mathbf{z})$ gives

$$h^{[1]}(\mathbf{x})Y'(\mathbf{z})=-(H-a)\int_{\Gamma_D}Y'(\mathbf{z})K_G(\mathbf{y})\mathbf{n}(\mathbf{y})\bullet\nabla_y G^{(0)}(\mathbf{y},\mathbf{x})d\mathbf{y}$$

$$-\theta\int_{\gamma^{(0)}(t)}Y'(\mathbf{z})V_n^{[1]}(\mathbf{y},t)G^{(0)}(\mathbf{y},\mathbf{x})d\mathbf{y}$$

$$+b\int_{\gamma^{(0)}(t)}K_G(\mathbf{y})Y'(\mathbf{z})\xi^{[1]}(x_y,y_y,t)\mathbf{n}(\mathbf{y},t)\bullet\nabla_y G^{(0)}(\mathbf{y},\mathbf{x})d\mathbf{y} \qquad \text{(F.6)}$$

$$-\int_{\Omega^{(0)}(t)}K_G(\mathbf{y})Y'(\mathbf{z})Y'(\mathbf{y})\nabla_y h^{(0)}(\mathbf{y},t)\bullet\nabla_y G^{(0)}(\mathbf{y},\mathbf{x})d\mathbf{y}$$

Approximating with integrals over zero-order domain and boundaries and averaging gives

$$C_{hY}^{[2]}(\mathbf{x},\mathbf{z}) =$$

$$-\theta \int_{\gamma^{(0)}(t)} C_{YV_n}^{[2]}(\mathbf{z};x_y,y_y,t)G^{(0)}(\mathbf{y},\mathbf{x})d\mathbf{y}$$

$$+b \int_{\gamma^{(0)}(t)} K_G(\mathbf{y})C_{Y\gamma}^{[2]}(\mathbf{z};x_y,y_y,t)\mathbf{n}(\mathbf{y},t)\bullet\nabla_y G^{(0)}(\mathbf{y},\mathbf{x})d\mathbf{y} \qquad \text{(F.7)}$$

$$-\int_{\Omega^{(0)}} K_G(\mathbf{y})C_Y^{[2]}(\mathbf{z},\mathbf{y})\nabla_y h^{(0)}(\mathbf{y},t)\bullet\nabla_y G^{(0)}(\mathbf{y},\mathbf{x})d\mathbf{y}$$

APPENDIX G

CRITERION FOR INSTABILITY

Darcy's law above the front can be written as

$$q_D = -\frac{k(z)}{\mu_D}\frac{d}{dz}(P_D + z\rho_D g) \qquad -L \le z \le 0 \tag{G.1}$$

Integrating from 0 to z:

$$q_D \mu_D \int_0^z \frac{dz}{k(z)} = -\left[P_D(z) + z\rho_D g - P_0 - (\rho_D - \rho_w)Hg\right] \tag{G.2}$$

Evaluating at $z = -L$:

$$q_D \mu_D \int_0^{-L} \frac{dz}{k(z)} = -\left[P_E + L\rho_w g_w - L\rho_D g - (\rho_D - \rho_w)Hg\right] \tag{G.3}$$

Dividing (G.2) by (G.3) and solving for $P_D(z)$:

$$P_D(z) = P_0 + (\rho_D - \rho_w)Hg - z\rho_D g + \frac{\int_0^z \frac{dz}{k(z)}}{\int_0^{-L} \frac{dz}{k(z)}}\left[P_E - L(\rho_D - \rho_w)g - (\rho_D - \rho_w)Hg\right] \tag{G.4}$$

Pressure head gradient G immediately above front:

$$G \equiv \frac{1}{\rho_D g}\frac{dP_D}{dz}_{z=-L} = \frac{1}{k(-L)\int_0^{-L} \frac{dz}{k(z)}}\left[\frac{P_E}{\rho_D g} - (1 - \frac{\rho_w}{\rho_D})(L + H)\right] - 1 \tag{G.5}$$

Let $\psi_E \equiv \frac{P_E}{\rho_D g}$ and $\psi \equiv \frac{P_D}{\rho_D g}$ denote respectively entry and DNAPL pressure heads.

Define a new variable $\xi = -z$:

$$G = \frac{1}{k(L)\int_0^L \frac{d\xi}{k(\xi)}}\left[-\psi_E + (1-\frac{\rho_w}{\rho_D})(L+H)\right] - 1 \qquad \text{(G.6)}$$

In the case of uniform k:

$$G_u = \frac{H}{L}(1-\frac{\rho_w}{\rho_D}) - \frac{\rho_w}{\rho_D} - \frac{\psi_E}{L} \qquad \text{(G.7)}$$

Let ψ' be pressure head in the perturbed field and Ψ the perturbation:

$$\Psi = \psi' - \psi \qquad \text{(G.8)}$$

Substituting (G.8) into (2.1) yields

$$\nabla\left(k(z)\nabla\Psi\right) = 0 \qquad \text{(G.9)}$$

With boundary condition:

$$z = 0 \ldots\ldots \Psi = 0 \qquad \text{(G.10)}$$

$$z = -L \qquad \Psi = -\left[G + \frac{M^2 T}{\Delta\theta\rho_D g}\right]\varepsilon(t)Sin(nx+\tau)Sin(my+\delta) \qquad \text{(G.11)}$$

where T is effective surface tension,

$$\mathrm{M}^2 = n^2 + m^2, \qquad \text{(G.12)}$$

and

$$\Delta\theta = \theta_s - \theta_r = \theta \qquad \text{(G.13)}$$

Let the horizontal front $z = -L(t)$ at time t_0 be perturbed:

$$z(x,y,t) = -L + \varsigma = -L + \varepsilon(t)\sin(nx+\tau)\sin(my+\delta) \qquad \text{(G.14)}$$

ς - perturbation of front

$$\varsigma = \varepsilon(t)\sin(nx+\tau)\sin(my+\delta) \qquad \text{(G.15)}$$

$$\psi'(z)\Big|_{-L} = \psi(z+\varsigma)\Big|_{-L} = \psi(z)\Big|_{-L} + \frac{\partial\psi}{\partial z}\Big|_{-L}\varsigma = \psi(z)\Big|_{-L} + G\varsigma \tag{G.16}$$

$$\Psi_1 = \psi'(-L) - \psi(-L) = G\varsigma \tag{G.17}$$

$$\Psi_2 = \Delta\psi_E = \frac{T}{(\rho_D - \rho_w)g}\left(\frac{\partial^2\varsigma}{\partial x^2} + \frac{\partial^2\varsigma}{\partial y^2}\right) = -\frac{TM^2}{(\rho_D - \rho_w)g}\varsigma \tag{G.18}$$

$$z = -L \qquad \Psi = \Psi_1 + \Psi_2 = -\left(G + \frac{TM^2}{(\rho_D - \rho_w)g}\right)\varsigma \tag{G.19}$$

Solution of (G.9) subject to (G.10) and (G.11) is:

$$\Psi = -\left(G + \frac{TM^2}{(\rho_D - \rho_w)g}\right)\varsigma\Omega(z) \tag{G.20}$$

where $\Omega(z)$ is the solution of

$$\frac{1}{k(z)}\frac{\partial}{\partial z}\left(k(z)\frac{d\Omega}{dz}\right) - M^2\Omega = 0 \tag{G.21}$$

$$\begin{aligned} &z = 0 \text{.....} \Omega = 0 \\ &z = -L \text{.....} \Omega = 1 \end{aligned} \tag{G.22}$$

It can be shown that, for $k(z) \geq 0$, $\Omega(z)$ is monotonic decreasing.

Let $\Phi = -\frac{d\Omega}{dz}$, hence $\Phi \geq 0$

According to Darcy's law, the undisturbed wetting front velocity, u, is given by

$$u = \frac{k(z)\rho_D g}{\mu_D \theta}\left(-\frac{\partial\psi}{\partial z} + 1\right) \tag{G.23}$$

Velocity of the front in the perturbed field, u' :

$$u' = \frac{k(z)\rho_D g}{\mu_D \theta}\left(-\frac{\partial\psi'}{\partial z} + 1\right) \tag{G.24}$$

Perturbation velocity, $v = u' - u$:

$$v = \frac{k(z)\rho_D g}{\mu_D \theta}\left(-\frac{\partial}{\partial z}(\psi' - \psi)\right) \tag{G.25}$$

or

$$v = -\frac{k(z)\rho_D g}{\mu_D \theta}\frac{\partial}{\partial z}(\Psi) \tag{G.26}$$

Substituting (G.20) into (G.26) yields

$$v = -\frac{k(z)\rho_D g}{\mu_D \theta}\left(G + \frac{TM^2}{\theta(\rho_D - \rho_w)g}\right)\varepsilon \sin(nx + \tau)\sin(my + \delta)\Phi \tag{G.27}$$

Recalling that $\varsigma = \varepsilon(t)\sin(nx + \tau)\sin(my + \delta)$ - perturbation of front, the perturbed velocity v can be written as:

$$v = \frac{\partial \varsigma}{\partial t} = \frac{\partial \varepsilon}{\partial t}\sin(nx + \tau)\sin(my + \delta) \tag{G.28}$$

Combining (G.27) and (G.28) yields:

$$\frac{\partial \varepsilon}{\partial t} = -\frac{k(z)\rho_D g}{\mu_D \theta}\left(G + \frac{TM^2}{\theta(\rho_D - \rho_w)g}\right)\varepsilon(t)\Phi \tag{G.29}$$

Equation (G.29) is subject to the condition $\varepsilon(t_0) = \varepsilon_0$, so that the required solution is

$$t \geq t_0 \qquad \varepsilon(t) = \varepsilon_0 \exp\left(\int_{t_0}^{t} \vartheta dt\right) \tag{G.30}$$

with

$$\vartheta = -\frac{k(z)\rho_D g}{\mu_D \theta}\left(G + \frac{TM^2}{\theta(\rho_D - \rho_w)g}\right)\Phi \tag{G.31}$$

In general, we should treat ϑ as a function of time in Eq. (G.30)

Finally we have:

$$\frac{d\varepsilon}{dt} = \vartheta(t)\varepsilon(t) \tag{G.32}$$

Note that $\varepsilon(t_0) = \varepsilon_0 > 0$, because ε is small positive amplitude, it is clear that the front is unstable when $\vartheta > 0$ and stable otherwise.

As $k(z)$, ρ_D, g, θ, M^2, Φ and $(\rho_D - \rho_w)$ are inherently positive, a necessary criterion for instability is

$$G < 0 \tag{G.33}$$

or

$$\frac{1}{k(L)\int_0^L \frac{d\xi}{k(\xi)}}\left[-(\psi_E + \Delta\psi_w) + (L+H)(1-\frac{\rho_w}{\rho_D})\right] - 1 < 0 \tag{G.34}$$

that a sufficient condition for instability is:

$$M < M_c = \sqrt{-\frac{\theta(\rho_D - \rho_w)gG}{T}} \tag{G.35}$$

To determine the wave number, M_m , for the most unstable disturbance, Philip proposed the approximation

$$\varsigma \propto M \tag{G.36}$$

which he had shown holds when M is large compared with the reciprocal of L in uniform media. Here M_m corresponds to maximum ϑ, ϑ_m:

$$\frac{d\vartheta}{dM} = \frac{k(z)\rho_D g}{\mu_D \theta}\left(G + \frac{3M^2 T}{\theta(\rho_D - \rho_w)g}\right) = 0 \tag{G.37}$$

or

$$M_m = \frac{M_c}{\sqrt{3}} \tag{G.38}$$

APPENDIX F

PROBABILITY OF INSTABILITY

We can express permeability field as

$$k(z) = e^{Y(z)} = e^{\bar{Y}} e^{Y'(z)} \tag{H.1}$$

Substituting into the expression (3.6) for G gives

$$\begin{aligned} G &= \frac{1}{e^{\bar{Y}} e^{Y'(L)} \int_0^L \frac{d\xi}{e^{\bar{Y}} e^{Y'(\xi)}}} \left[-\psi_E + (1 - \frac{\rho_w}{\rho_D})(L+H) \right] - 1 \\ &= \frac{G_u + 1}{\Gamma \Sigma} - 1 \end{aligned} \tag{H.2}$$

where $G_u = \dfrac{H(1-\frac{\rho_w}{\rho_D}) - L\frac{\rho_w}{\rho_D} - \psi_E}{L}$, (H.3)

$$\Gamma = e^{Y'(L)}, \tag{H.4}$$

$$\Sigma = \frac{1}{L} \int_0^L e^{-Y'(\xi)} d\xi \tag{H.5}$$

$$\psi_E = P_E / \rho_D g \tag{H.6}$$

G_u represents G in uniform medium.

By assumption Y' is a zero-mean Gaussion random function having probability density

$$f(Y') = \frac{1}{\sqrt{2\pi}\sigma_y} \exp\left(-\frac{Y'^2}{2\sigma_y^2} \right) \tag{H.7}$$

Then,

$$\bar{\Gamma} = \overline{e^{Y'(L)}} = \frac{1}{\sqrt{2\pi}\sigma_y} \int_{-\infty}^{\infty} e^{Y'(L)} e^{-Y'^2/2\sigma_y^2} dY' = e^{\sigma_y^2/2} \tag{H.8}$$

It was shown by Chen and Neuman (1996) that $\overline{\Sigma} = \overline{\Gamma}$.

Variances of Γ and Σ can be found as

$$\sigma_\Gamma^2 = \overline{\left(e^{Y'(L)} - e^{\sigma_y^2/2}\right)^2} = \overline{e^{2Y'(L)} - 2e^{Y'(L)}e^{\sigma_y^2/2} + e^{\sigma_y^2}}$$

$$= e^{2\sigma_y^2} - 2\left\langle e^{Y'(L)}\right\rangle e^{\sigma_y^2/2} + e^{\sigma_y^2} = e^{\sigma_y^2}\left[e^{\sigma_y^2} - 1\right] \tag{H.9}$$

and

$$\sigma_\Sigma^2 = \frac{2e^{\sigma_y^2}}{L^2}\int_0^L (L-\xi)(e^{C_Y(\xi)} - 1)d\xi \tag{H.10}$$

In mildly heterogeneous soil with $\sigma_y^2 << 1$, (H.10) is given to first order in σ_y^2 by:

$$\sigma_\Sigma^2 \approx 2\left(1+\sigma_y^2\right)\sigma_y^2 A \tag{H.11}$$

where

$$A = \frac{I_Y}{L} + \frac{\left(e^{-L/I_Y} - 1\right)I_Y^2}{L^2} \tag{H.12}$$

and

$$\sigma_\Gamma^2 = (1+\sigma_y^2)\sigma_y^2 \tag{H.13}$$

Hence, the normalized variance of Σ is

$$\frac{\sigma_\Sigma^2}{\sigma_\Gamma^2} = 2A \tag{H.14}$$

(H.14) depends solely on L/I_Y. For larger σ_y^2, it depends on this parameter as well.

When L/I_Y >40, the magnitude of the normalized variance of Σ is less than 0.05.

Therefore, fluctuations in Σ can be safely disregarded in comparison to those in Γ, and Σ can be safely approximated by its mean, $\overline{\Sigma}$. It is therefore possible to evaluate $P(G<0)$ in closed form.

1. Closed form solution for $L/l_Y > 40$

Set $\Sigma = \overline{\Sigma} = \exp(\frac{\sigma_Y^2}{2})$, and start by treating ψ_E as constant; later it will be taken to vary at random.

$G_u = \frac{H}{L}(1-\frac{\rho_w}{\rho_D}) - \frac{\rho_w}{\rho_D} - \frac{\psi_E}{L}$ is the pressure head gradient behind DNAPL in a uniform medium.

We define a front to be uniformly stable if $G_u \geq 0$, and uniformly unstable if $G_u < 0$.

Since $\Gamma\Sigma > 0$, $G_u \leq -1$ implies $G < 0$, and the front is unstable with probability one.

For $G_u > -1$, we invoke the mean ergodic hypothesis for large L/l_Y. We can rewrite (H.2) as:

$$G + 1 = \frac{G_u + 1}{\Gamma\Sigma} \tag{H.15}$$

Then

$$\Gamma = \frac{G_u + 1}{(G+1)\Sigma} \tag{H.16}$$

and

$$\Gamma^{-1} = \frac{(G+1)\Sigma}{G_u + 1} \approx \frac{(G+1)e^{\sigma_Y^2/2}}{G_u + 1} \tag{H.17}$$

$$\ln\left[\frac{(G+1)e^{\sigma_y^2/2}}{G_u+1}\right] \approx -\ln\Gamma \equiv -Y'(L) \tag{H.18}$$

Note that G<0 is equivalent to:

$$\frac{G_u+1}{\Gamma\Sigma} - 1 < 0 \tag{H.19}$$

$$\Gamma^{-1} < \frac{\Sigma}{G_u+1} \approx \frac{e^{\sigma_y^2/2}}{G_u+1} \tag{H.20}$$

$$-Y' < \frac{1}{2}e^{\sigma_y^2} - \ln(G_u+1) \tag{H.21}$$

Hence,

$$P(G<0) = P[-Y' < \frac{1}{2}\sigma_y^2 - \ln(G_u+1)] \tag{H.22}$$

As $Y'(L)$ is zero-mean normal, its probability is the same as of $-Y'(L)$, and we can rewrite (H.22) as:

$$P[-Y' < \frac{1}{2}\sigma_y^2 - \ln(G_u+1)] = \int_{-\infty}^{\frac{1}{2}\sigma_y^2 - \ln(G_u+1)} p(Y')dY' =$$

$$= \frac{1}{\sqrt{2\pi}\sigma_y} \int_{-\infty}^{\frac{1}{2}\sigma_y^2 - \ln(G_u+1)} \exp(-\frac{Y'^2}{2\sigma_y^2})dY' \tag{H.23}$$

Under the change of variable $\frac{Y'^2}{2\sigma_y^2} = x^2$, $dx = \frac{dY'}{\sqrt{2}\sigma_y}$ (H.23) can be rewritten as:

$$P(G<0) = \frac{1}{\sqrt{\pi}} \int_{-\infty}^{\left(\frac{1}{2}\sigma_y^2 - \ln(G_u+1)\right)/\sqrt{2}\sigma_y} \exp(-x^2)dx = \frac{1}{2}\left[1 + erf\left(\left[\frac{1}{2}\sigma_y^2 - \ln(G_u+1)\right]/\sqrt{2}\sigma_y\right)\right]$$

or

$$P(G<0)=\frac{1}{2}\left(1+erf\left[\frac{\sigma_y}{2\sqrt{2}}-\frac{\ln(G_u+1)}{\sqrt{2}\sigma_y}\right]\right) \tag{H.24}$$

Next we allow $\psi_c = \psi_E$ to vary randomly as:

$$\psi_c(z)=-bk^{-1/2}(z) \tag{H.25}$$

where $b=-\psi_c^* k^{*1/2}$, ψ^*, k^* are reference values.

Then for G we will have

$$G=\left(\frac{b}{L}k(L)^{-1/2}+G_E+1\right)\frac{1}{k(L)\frac{1}{L}\int_0^L\frac{1}{k(\xi)}d\xi}-1=$$

$$=\left(\frac{b}{L}k(L)^{-1/2}+G_E+1\right)\frac{1}{k(L)B}-1 \tag{H.26}$$

where

$$B=\frac{1}{L}\int_0^L\frac{1}{k(\xi)}d\xi=\frac{1}{L}\int\exp\left[-\left(\overline{Y}+Y'(\xi)\right)\right]d\xi\approx\overline{B}=\exp(-\overline{Y}+\frac{\sigma_Y^2}{2}) \tag{H.27}$$

and

$$G_E=\frac{H}{L}(1-\frac{\rho_w}{\rho_D})-\frac{\rho_w}{\rho_D} \tag{H.28}$$

If we define $G'=-Bk(L)G$, then $G<0$ is equivalent to $G'>0$.

$$G'=Bk-\frac{b}{L}\frac{1}{\sqrt{k}}-(G_E+1) \tag{H.29}$$

$$\frac{dG'}{dK}=B+\frac{b}{L}k^{-1.5}>0 \quad (B,b,L \text{ and } k>0) \tag{H.30}$$

and

$$\lim_{k\to 0} G' = -\infty; \quad \lim_{k\to\infty} G' = +\infty \tag{H.31}$$

So G' increases monotonically from negative to positive infinity, passing through zero at some K_0. Then

$$P(G<0) = P(G'>0) = P(k>K_0) = P(\ln k > \ln K_0), \tag{H.32}$$

where $\ln k \equiv Y(\overline{Y}, \sigma_Y^2)$, and probability of instability is easily obtained once K_0 is known.

K_0 is obtained as the non-negative root of

$$G' = BK - \frac{b}{L}\frac{1}{\sqrt{k}} - (G_E + 1) \tag{H.33}$$

$$K_0 = \begin{cases} (\sqrt[3]{P+\sqrt{Q}} + \sqrt[3]{P-\sqrt{Q}})^2, & \text{if } Q>0 \\ (\sqrt[3]{P+\sqrt{Qi}} + \sqrt{P-\sqrt{Qi}})^2, & \text{if } Q<0 \end{cases} \tag{H.34}$$

where $P=b/(2LB)$, $Q = \dfrac{b^2}{4L^2B^2} - \dfrac{(G_E+1)^3}{27B^3}$

2. Reliability solution for $L/l_Y < 40$

If $L/\lambda_Y < 40$, Σ may vary significantly about the mean. This situation is conveniently handled by means of reliability theory (Chen and Neuman, 1996).

According to the first-order reliability method FORM, one can express the probability of instability as

$$P = 1 - \Phi(\delta), \tag{H.35}$$

where Φ is cumulative normal distribution function, δ is reliability index defined as $\delta = \mu_g / \sigma_g$. μ_g and σ_g are the mean and standard deviation of a performance function $g(x)$, that is less than zero, by definition, in the case of instability.

We shall concern ourselves below with the parameter

$$\tilde{k} = \frac{1}{L}\int_0^L \frac{1}{k(\xi)} d\xi \tag{H.36}$$

It has been shown by Chen and Neuman that it is reasonable to treat $\tilde{Y} = \ln \tilde{k}$ as being normal within our range of analysis with mean and variance given as

$$\bar{\tilde{Y}} = \ln\left(\frac{\bar{\tilde{k}}}{\left(\sigma_{\tilde{k}}^2 / \bar{\tilde{k}}^2 + 1\right)^{1/2}} \right) \tag{H.37}$$

$$\sigma_{\tilde{Y}}^2 = \ln\left(\sigma_{\tilde{k}}^2 / \bar{\tilde{k}}^2 + 1\right), \tag{H.38}$$

where

$$\bar{\tilde{k}} = e^{-\bar{Y} + \sigma_{\tilde{Y}}^2} \tag{H.39}$$

and

$$\sigma_{\tilde{k}}^2 = \frac{2e^{-2\bar{Y} + \sigma_{\tilde{Y}}^2}}{L^2} \int_0^L (L - \xi)(e^{C_Y(\xi)} - 1) d\xi \tag{H.40}$$

The cross-correlation coefficient is given by

$$\rho = \frac{C_{Y\tilde{Y}}}{\sigma_Y \sigma_{\tilde{Y}}} \tag{H.41}$$

where

$$C_{Y\tilde{Y}} = \ln(e^{-\sigma_Y^2} C_{K\tilde{K}} + 1) \tag{H.42}$$

and

$$C_{K\tilde{k}} = \frac{1}{L} e^{\sigma_{\tilde{Y}}^2} \int_0^L \left(e^{-C_Y(\xi)} - 1 \right) d\xi \tag{H.43}$$

When $\sigma_{\tilde{Y}}^2 << 1$, this can be approximated by

$$C_{K\tilde{k}} \approx -\frac{\sigma_Y^2 (1+\sigma_{\tilde{Y}}^2) l_Y}{L} (1 - e^{-L/l_Y}) \tag{H.44}$$

Chen and Neuman have shown that when the capillary pressure at the wetting front is prescribed one can define g as

$$g = \ln(1+G) = \ln(1+G_u) - Y(L) - \tilde{Y} \tag{H.45}$$

and FORM yields an exact solution

$$\delta = \frac{\ln(1+G_u) - \mu_Y - \mu_{\tilde{Y}}}{\sqrt{\sigma_Y^2 + \sigma_{\tilde{Y}}^2 + 2\rho\sigma_Y\sigma_{\tilde{Y}}}} \tag{H.46}$$

APPENDIX I

ONE-DIMENSIONAL GREEN'S FUNCTION

The Green's function satisfies equation

$$\frac{\partial^2 G_K(x,y)}{\partial x^2} + \delta(x-y) = 0 \qquad 0 \le x, \qquad y \le l \tag{I.1}$$

Integrating (I.1) from 0 to x one time gives:

$$\frac{\partial G_K(x,y)}{\partial x} + \mathrm{H}(x-y) - \alpha(y) = 0 \tag{I.2}$$

where H(x-y) is the Heaviside function:

$$\frac{\partial \mathrm{H}(x-y)}{\partial x} = \delta(x-y) \tag{I.3}$$

Integrating again leads to

$$G_K(x,y) = -(x-y)\mathrm{H}(x-y) + \alpha(y)x + \beta(y) \tag{I.4}$$

where the integral of the Heaviside function is:

$$\int_0^x \mathrm{H}(z-y)dz = \int_0^x (z-y)'\mathrm{H}(z-y)dz = (z-y)\mathrm{H}(z-y)\Big|_{z=0}^{z=x} - \int_0^x (z-y)\mathrm{H}'(z-y)dz$$

$$= (x-y)\mathrm{H}(x-y) - \int_0^x (z-y)\delta(z-y)dz = (x-y)\mathrm{H}(x-y) - (z-y)\Big|_{z=y}$$

$$= (x-y)\mathrm{H}(x-y) \tag{I.5}$$

APPENDIX J

FRONT PROPAGATION EQUATION

The 1-D version of (2.13) is

$$h(x,t) = -\frac{\theta}{\bar{K}} V(\xi,t) G_K(\xi,x) + b\xi(t) \frac{\partial G_K(y,x)}{\partial y}\bigg|_{y=\xi(t)} + (H-a) \frac{\partial G_K(y,x)}{\partial y}\bigg|_{y=0} - \frac{1}{\bar{K}} \int_0^{\xi(t)} K'(y) \frac{\partial h(y,t)}{\partial y} \frac{\partial G_K(y,x)}{\partial y} dy \tag{J.1}$$

Evaluating it at $x = \xi$ gives

$$-b\xi(t) = -\frac{\theta}{\bar{K}} V(\xi,t) G_K(\xi,\xi) + b\xi(t) \frac{\partial G_K(y,\xi)}{\partial y}\bigg|_{y=\xi(t)} + (H-a) \frac{\partial G_K(y,\xi)}{\partial y}\bigg|_{y=0} - \frac{1}{\bar{K}} \int_0^{\xi(t)} K'(y) \frac{\partial h(y,t)}{\partial y} \frac{\partial G_K(y,\xi)}{\partial y} dy \tag{J.2}$$

From (4.1.2) and (4.11) it follows that

$$G_K(\xi,\xi) = \frac{l-\xi(t)}{l} \xi(t) \tag{J.3}$$

$$\frac{\partial G_K(y,x)}{\partial y} = -\mathrm{H}(y-x) + \frac{l-x}{l} \tag{J.4}$$

$$\frac{\partial G_K(y,x)}{\partial y}\bigg|_{y=\xi(t)} = -1 + \frac{l-x}{l} \qquad \frac{\partial G_K(y,x)}{\partial y}\bigg|_{y=0} = \frac{l-x}{l} \tag{J.5}$$

Hence (J.2) becomes

$$-b\xi(t) = -\frac{\theta V(\xi,t)}{\bar{K}} \frac{l-\xi(t)}{l} \xi(t) - b\xi(t) + b\xi(t) \frac{l-\xi(t)}{l} + (H-a) \frac{l-\xi(t)}{l} - \frac{l-\xi(t)}{l} \frac{1}{\bar{K}} \int_0^{\xi} K'(y) \frac{\partial h(y,t)}{\partial y} dy \tag{J.6}$$

By virtue of (2.11) $V(\xi,t) = d\xi(t)/dt$ and so

$$0 = \theta \frac{d\xi(t)}{dt}\xi(t) + \bar{K}\left[a - H - b\xi(t)\right] + \int_0^{\xi(t)} K'(y)\frac{\partial h(y,t)}{\partial y}dy \qquad \text{(J.7)}$$

APPENDIX K

ZERO-ORDER FRONT AS FUNCTION OF TIME

Rewrite (4.14) as

$$\frac{K_G}{\theta}dt = \frac{\xi^{(0)}}{b\xi^{(0)} + H - a}d\xi^{(0)} \tag{K.1}$$

Integrate subject to zero-initial condition:

$$\frac{K_G}{\theta}t = \int_0^{\xi^{(0)}} \frac{\xi^{(0)}}{b\xi^{(0)} + H - a}d\xi^{(0)}$$

$$= \frac{1}{b}\int_0^{\xi^{(0)}} \left(1 - \frac{H-a}{b\xi^{(0)} + H - a}\right)d\xi^{(0)} = \frac{1}{b}\left(\xi^{(0)} - \frac{H-a}{b}\ln\frac{b\xi^{(0)} + H - a}{H - a}\right) \tag{K.2}$$

APPENDIX L

MEAN HEAD

From (4.2.1)-(4.2.5), Appendix 4.2

$$h(x,t) = -\frac{\theta V}{\bar{K}} G_K(\xi,x) + b\xi(t)\left.\frac{\partial G_K(y,x)}{\partial y}\right|_{y=\xi} + (H-a)\left.\frac{\partial G_K(y,x)}{\partial y}\right|_{y=0} - \frac{1}{\bar{K}}\int_0^{\xi(t)} K'(y)\frac{\partial h(y,t)}{\partial y}\frac{\partial G_K(y,x)}{\partial y}dy \tag{L.1}$$

$$G_K(\xi,x) = -(\xi - x) + \frac{l-x}{l}\xi \tag{L.2}$$

$$\frac{\partial G_K(y,x)}{\partial y} = -\mathrm{H}(y-x) + \frac{l-x}{l} \tag{L.3}$$

$$\left.\frac{\partial G_K(y,x)}{\partial y}\right|_{y=\xi} = -1 + \frac{l-x}{l} \qquad \left.\frac{\partial G_K(y,x)}{\partial y}\right|_{y=0} = \frac{l-x}{l} \tag{L.4}$$

Hence (L.1) becomes

$$h(x,t) = \frac{\theta V}{\bar{K}}(\xi - x) - \frac{\theta V}{\bar{K}}\frac{l-x}{l}\xi - b\xi + b\xi\frac{l-x}{l} + (H-a)\frac{l-x}{l} + \frac{1}{\bar{K}}\int_0^{\xi} K'(y)\frac{\partial h(y,t)}{\partial y}\mathrm{H}(y-x)dy - \frac{1}{\bar{K}}\frac{l-x}{l}\int_0^{\xi} K'(y)\frac{\partial h(y,t)}{\partial y}dy \tag{L.5}$$

Considering (4.12)

$$h(x,t) = \frac{\theta V}{\bar{K}}(\xi - x) - b\xi + \frac{1}{\bar{K}}\int_0^{\xi} K'(y)\frac{\partial h(y,t)}{\partial y}\mathrm{H}(y-x)dy \tag{L.6}$$

or,

$$h(x,t)=\frac{\theta V}{\bar{K}}(\xi-x)-b\xi+\frac{1}{\bar{K}}\int_0^x K'(y)\frac{\partial h(y,t)}{\partial y}\mathrm{H}(y-x)dy$$
$$+\frac{1}{\bar{K}}\int_x^{\xi} K'(y)\frac{\partial h(y,t)}{\partial y}\mathrm{H}(y-x)dy \tag{L.7}$$

or,

$$h(x,t)=\frac{\theta V}{\bar{K}}(\xi-x)-b\xi+\frac{1}{\bar{K}}\int_x^{\xi} K'(y)\frac{\partial h(y,t)}{\partial y}dy \tag{L.8}$$

Expanding the integral around $\bar{\xi}$ gives

$$h(x,t)=\frac{\theta}{\bar{K}}\frac{d\xi}{dt}(\xi-x)-b\xi+\frac{1}{\bar{K}}\int_x^{\bar{\xi}} K'(y)\frac{\partial h(y,t)}{\partial y}dy+\frac{1}{\bar{K}}\xi' K'(\bar{\xi})\frac{\partial h(y,t)}{\partial y}\bigg|_{y=\bar{\xi}} \tag{L.9}$$

Taking the mean gives the mean head,

$$\bar{h}(x,t)=\frac{\theta}{\bar{K}}\frac{d\bar{\xi}}{dt}(\bar{\xi}-x)+\frac{\theta}{2\bar{K}}\frac{d\sigma_\xi^2}{dt}-b\bar{\xi}$$
$$-\frac{1}{\bar{K}}\int_x^{\bar{\xi}} r(y)dy+\frac{K_G}{\bar{K}}C_{Y\xi}(\bar{\xi},\bar{\xi})\frac{\partial \bar{h}(y,t)}{\partial y}\bigg|_{y=\bar{\xi}} \tag{L.10}$$

where $\sigma_\xi^2=\overline{\xi'\xi'}$

The zero-order approximation of head is

$$h^{(0)}(x,t)=\frac{\theta}{K_G}\frac{d\xi^{(0)}}{dt}(\xi^{(0)}-x)-b\xi^{(0)} \tag{L.11}$$

or by virtue of (4.14)

$$h^{(0)}(x,t)=\frac{b\xi^{(0)}+H-a}{\xi^{(0)}}(\xi^{(0)}-x)-b\xi^{(0)} \tag{L.12}$$

or,

$$h^{(0)}(x,t) = H - a - \left(b\xi^{(0)} + H - a\right)\frac{x}{\xi^{(0)}} \tag{L.13}$$

Note that $\frac{1}{\overline{K}} = \frac{1}{K_G}\frac{1}{1+\sigma_Y^2/2+\ldots} = \frac{1}{K_G}\left(1-\frac{\sigma_Y^2}{2}+\ldots\right)$.

Then the second order approximation is

$$\begin{aligned}\bar{h}^{(2)}(x,t) = {} & \frac{\theta}{K_G}\frac{d\bar{\xi}^{(2)}}{dt}(\xi^{(0)}-x) + \frac{\theta}{K_G}\frac{d\xi^{(0)}}{dt}\bar{\xi}^{(2)} - \frac{\theta}{K_G}\frac{\sigma_Y^2}{2}\frac{d\xi^{(0)}}{dt}(\xi^{(0)}-x) \\ & + \frac{\theta}{2K_G}\frac{d\left[\sigma_\xi^2\right]^{(2)}}{dt} - b\bar{\xi}^{(2)} - \frac{1}{K_G}\int_x^{\xi^{(0)}} r^{(2)}(y)dy + C_{Y\xi}^{(2)}(\xi^{(0)},\xi^{(0)})\left.\frac{\partial h^{(0)}(y,t)}{\partial y}\right|_{y=\xi^{(0)}}\end{aligned} \tag{L.14}$$

Substitution of (4.14) and (4.15) into (L.14) gives

$$\bar{h}^{(2)}(x,t) = -x\frac{b\xi^{(0)}+H-a}{\xi^{(0)}}\frac{d\bar{\xi}^{(2)}}{d\xi^{(0)}} + x\frac{\sigma_Y^2}{2}\frac{b\xi^{(0)}+H-a}{\xi^{(0)}} + \frac{1}{K_G}\int_0^x r^{(2)}(y,t)dy \tag{L.15}$$

APPENDIX M

CROSS-COVARIANCE $C_{Y\xi}$

Multiplying (4.13) by K' gives,

$$0 = -\theta\xi\frac{d\xi}{dt}K'(x) - (a - b\xi)\bar{K}K'(x) + H\bar{K}K'(x) - \int_0^{\bar{\xi}} K'(y)K'(x)\frac{dh(y)}{dy}dy - \xi' K'(\bar{\xi})K'(x)\frac{dh(y)}{dy}\bigg|_{y=\bar{\xi}} \tag{M.1}$$

Taking the mean and retaining second-order terms gives,

$$0 = -\theta\xi^{(0)}\frac{\partial C_{Y\xi}^{(2)}(x,t)}{\partial t} - \theta\frac{d\xi^{(0)}}{dt}C_{Y\xi}^{(2)}(x,t) + bC_{Y\xi}^{(2)}(x,t) - K_G\int_0^{\xi^{(0)}} C_Y^{(2)}(x,y)\frac{\partial h^{(0)}(y,t)}{\partial y}dy \tag{M.2}$$

Substituting (4.19) for $\frac{\partial h^{(0)}(y,t)}{\partial y}$ gives an equation for $C_{Y\xi}^{(2)}$,

$$\theta\xi^{(0)}\frac{\partial C_{Y\xi}^{(2)}(x,t)}{\partial t} + \left(\theta\frac{d\xi^{(0)}}{dt} - K_G b\right)C_{Y\xi}^{(2)}(x,t) = K_G\left(b + \frac{H-a}{\xi^{(0)}}\right)\int_0^{\xi^{(0)}} C_Y^{(2)}(x,y)dy \tag{M.3}$$

Since $\frac{\partial C_{Y\xi}}{\partial t} = \frac{\partial C_{Y\xi}}{\partial \xi^{(0)}}\frac{d\xi^{(0)}}{dt}$, this becomes

$$\theta\xi^{(0)}\frac{\partial C_{Y\xi}^{(2)}(x,\xi^{(0)})}{\partial \xi^{(0)}}\frac{d\xi^{(0)}}{dt} + \left(\theta\frac{d\xi^{(0)}}{dt} - K_G b\right)C_{Y\xi}^{(2)}(x,\xi^{(0)}) = K_G\left(b + \frac{H-a}{\xi^{(0)}}\right)\int_0^{\xi^{(0)}} C_Y^{(2)}(x,y)dy \tag{M.4}$$

or

$$\theta\xi^{(0)}\frac{\partial C_{Y\xi}^{(2)}(x,\xi^{(0)})}{\partial\xi^{(0)}}+\left(\theta-K_G b\frac{dt}{d\xi^{(0)}}\right)C_{Y\xi}^{(2)}(x,\xi^{(0)})$$
$$=\frac{dt}{d\xi^{(0)}}K_G\left(b+\frac{H-a}{\xi^{(0)}}\right)\int_0^{\xi^{(0)}}C_Y^{(2)}(x,y)dy \tag{M.5}$$

From (4.14) $\frac{dt}{d\xi^{(0)}}=\frac{\theta}{K_G}\frac{\xi^{(0)}}{b\xi^{(0)}+H-a}$. Substituting into (M.5) yields

$$\xi^{(0)}\frac{\partial C_{Y\xi}^{(2)}(x,\xi^{(0)})}{\partial\xi^{(0)}}+\left(1-b\frac{\xi^{(0)}}{b\xi^{(0)}+H-a}\right)C_{Y\xi}^{(2)}(x,\xi^{(0)})$$
$$=\int_0^{\xi^{(0)}}C_Y^{(2)}(x,y)dy \tag{M.6}$$

or

$$\frac{\partial C_{Y\xi}^{(2)}\left(x,\xi^{(0)}\right)}{\partial\xi^{(0)}}+P\left(\xi^{(0)}\right)C_{Y\xi}^{(2)}\left(x,\xi^{(0)}\right)=R\left(x,\xi^{(0)}\right) \tag{M.7}$$

subject to initial conditions:

$$C_{Y\xi}^{(2)}(x,0)=0 \tag{M.8}$$

where $P\left(\xi^{(0)}\right)=\left(\frac{1}{\xi^{(0)}}-\frac{b}{b\xi^{(0)}+H-a}\right)=\frac{H-a}{\xi^{(0)}\left(b\xi^{(0)}+H-a\right)}$ (M.9)

and $R\left(x,\xi^{(0)}\right)=\frac{1}{\xi^{(0)}}\int_0^{\xi^{(0)}}C_Y^{(2)}(x,y)dy$ (M.10)

The solution of (M.7)-(M.10) is

$$C_{Y\xi}^{(2)}\left(x,\xi^{(0)}\right)=e^{-\int P(\xi^{(0)})d\xi^{(0)}}\int_0^{\xi^{(0)}}R(x,y)e^{\int P(z)dz}dy \tag{M.11}$$

where

$$-\int P(\xi^{(0)})d\xi^{(0)} = \ln\frac{b\xi^{(0)}+H-a}{\xi^{(0)}} \quad \text{and} \quad \int_{y} P(z)dz = \ln\frac{y}{by+H-a} \tag{M.12}$$

We can rewrite (M.11) as

$$C^{(2)}_{Y\xi}\left(x,\xi^{(0)}\right) = e^{\ln\frac{b\xi^{(0)}+H-a}{\xi^{(0)}}} \int_{0}^{\xi^{(0)}} \frac{1}{y}\left\{\int_{0}^{y} C^{(2)}_{Y}(x,z)dz\right\} e^{\ln\frac{y}{by+H-a}}dy \tag{M.13}$$

or

$$\frac{\xi^{(0)}C^{(2)}{}_{Y\xi}(x,t)}{b\xi^{(0)}+H-a} = \int_{0}^{x}\frac{\int_{0}^{y} C^{(2)}_{Y}(x,z)dz}{by+H-a}dy + \int_{x}^{\xi^{(0)}}\frac{\int_{0}^{y} C^{(2)}_{Y}(x,z)dz}{by+H-a}dy \tag{M.14}$$

Setting

$$C_{Y}(x,z) = \sigma_{Y}^{2}\exp\left(-\frac{|x-z|}{l_{Y}}\right) \tag{M.15}$$

we obtain for $x > y$

$$\int_{0}^{y} C^{(2)}_{Y}(x,z)dz = \sigma_{Y}^{2}\int_{0}^{y}\exp\left(-\frac{x-z}{l_{Y}}\right)dz = \sigma_{Y}^{2}l_{Y}\left(e^{\frac{y-x}{l_{Y}}} - e^{-\frac{x}{l_{Y}}}\right) \tag{M.16}$$

and for $x \le y$

$$\int_{0}^{y} C^{(2)}_{Y}(x,z)dz = \sigma_{Y}^{2}\int_{0}^{x}\exp\left(-\frac{x-z}{l_{Y}}\right)dz + \sigma_{Y}^{2}\int_{x}^{y}\exp\left(\frac{x-z}{l_{Y}}\right)dz = \sigma_{Y}^{2}l_{Y}\left(2-e^{\frac{x-y}{l_{Y}}} - e^{-\frac{x}{l_{Y}}}\right) \tag{M.17}$$

Substituting (M.16) and (M.17) into (M.14) gives

$$\frac{\xi^{(0)}}{b\xi^{(0)}+H-a}\frac{1}{\sigma_{Y}^{2}l_{Y}}C^{(2)}_{Y\xi}(x,t) = \int_{0}^{x}\frac{e^{\frac{y-x}{l_{Y}}} - e^{-\frac{x}{l_{Y}}}}{by+H-a}dy + \int_{x}^{\xi^{(0)}}\frac{2-e^{\frac{x-y}{l_{Y}}} - e^{-\frac{x}{l_{Y}}}}{by+H-a}dy \tag{M.18}$$

where

$$\int_0^x \frac{e^{\frac{y-x}{l_Y}} - e^{-\frac{x}{l_Y}}}{by+H-a}dy = \frac{e^{\frac{H-a-bx}{bl_Y}}}{b}\int_0^x \frac{e^{\frac{by+H-a}{bl_Y}}}{by+H-a}d(by+H-a) - \frac{e^{-\frac{x}{l_Y}}}{b}\ln\frac{bx+H-a}{H-a}$$

$$= \frac{e^{\frac{H-a-bx}{bl_Y}}}{b}\left\{Ei\left(\frac{bx+H-a}{bl_Y}\right) - Ei\left(\frac{H-a}{bl_Y}\right)\right\} - \frac{e^{-\frac{x}{l_Y}}}{b}\ln\frac{bx+H-a}{H-a} \qquad \text{(M.19)}$$

and

$$\int_x^{\xi^{(0)}} \frac{2-e^{\frac{x-y}{l_Y}} - e^{-\frac{x}{l_Y}}}{by+H-a}dy = \frac{2-e^{-\frac{x}{l_Y}}}{b}\ln\frac{b\xi^{(0)}+H-a}{bx+H-a} - \frac{e^{\frac{bx+H-a}{bl_Y}}}{b}\int_x^{\xi^{(0)}} \frac{e^{-\frac{by+H-a}{bl_Y}}}{by+H-a}d(by+H-a)$$

$$= \frac{2-e^{-\frac{x}{l_Y}}}{b}\ln\frac{b\xi^{(0)}+H-a}{bx+H-a} - \frac{e^{\frac{bx+H-a}{bl_Y}}}{b}\left\{Ei\left(-\frac{b\xi^{(0)}+H-a}{bl_Y}\right) - Ei\left(-\frac{bx+H-a}{bl_Y}\right)\right\} \qquad \text{(M.20)}$$

where $Ei(\alpha y) = \int \frac{e^{\alpha y}}{y}dy$ is the exponential integral (Gradshteyn and Ryzhik, 1994, p.113, 2.325).

Then

$$\frac{\xi^{(0)}}{b\xi^{(0)}+H-a}\frac{1}{\sigma_Y^2 l_Y}C_{Y\xi}^{(2)}(x,t)$$

$$= \frac{1}{b}e^{-\frac{bx+H-a}{bl_Y}}\left\{Ei\left(\frac{bx+H-a}{bl_Y}\right) - Ei\left(\frac{H-a}{bl_Y}\right)\right\} - \frac{1}{b}e^{-\frac{x}{l_Y}}\ln\frac{bx+H-a}{H-a}$$

$$+ \frac{\left(2-e^{-x/l_Y}\right)}{b}\ln\frac{b\xi^{(0)}+H-a}{bx+H-a} - \frac{1}{b}e^{\frac{bx+H-a}{bl_y}}\left\{Ei\left(-\frac{b\xi^{(0)}+H-a}{bl_y}\right) - Ei\left(-\frac{bx+H-a}{bl_y}\right)\right\}$$

(M.21)

or

$$C_{Y\xi}^{(2)}(x,\xi^{(0)}) = \sigma_Y^2 l_Y \frac{b\xi^{(0)} + H - a}{b\xi^{(0)}} \cdot$$

$$\left[e^{-\frac{bx+H-a}{bl_Y}} \left\{ Ei\left(\frac{bx+H-a}{bl_Y} \right) - Ei\left(\frac{H-a}{bl_Y} \right) \right\} - e^{-\frac{x}{l_Y}} \ln \frac{bx+H-a}{H-a} \right.$$

$$\left. + \left(2 - e^{-x/l_Y} \right) \ln \frac{b\xi^{(0)} + H - a}{bx+H-a} - e^{\frac{bx+H-a}{bl_y}} \left\{ Ei\left(-\frac{b\xi^{(0)} + H - a}{bl_y} \right) - Ei\left(-\frac{bx+H-a}{bl_y} \right) \right\} \right]$$

(M.22)

APPENDIX N

RESIDUAL FLUX

Operate on (J.1) with $K'(x)d/dx$:

$$\bar{K}K'(x)\frac{\partial h(x,t)}{\partial x} = -\theta V K'(x)\frac{\partial G_K(\xi,x)}{\partial x} + \bar{K}b\xi K'(x)\frac{\partial}{\partial x}\left[\left.\frac{\partial G_K(y,x)}{\partial y}\right|_{y=\xi}\right]$$
$$+\bar{K}HK'(x)\frac{\partial}{\partial x}\left[\left.\frac{\partial G_K(y,x)}{\partial y}\right|_{y=0}\right] - \int_0^{\xi(t)} K'(y)K'(x)\frac{\partial h(y,t)}{\partial y}\frac{\partial^2 G_K(y,x)}{\partial y \partial x}dy \qquad \text{(N.1)}$$

From (I.4)

$$G_K(\xi,x) = x - \xi + \frac{l-x}{l}\xi \qquad \text{(N.2)}$$

From (J.4)

$$\frac{\partial^2 G_K(y,x)}{\partial y \partial x} = \delta(y-x) - \frac{1}{l} \qquad \text{(N.3)}$$

From (J.5)

$$\frac{\partial}{\partial x}\left[\left.\frac{\partial G_K(y,x)}{\partial y}\right|_{y=\xi}\right] = -\frac{1}{l} \quad \text{and} \quad \frac{\partial}{\partial x}\left[\left.\frac{\partial G_K(y,x)}{\partial y}\right|_{y=0}\right] = -\frac{1}{l} \qquad \text{(N.4)}$$

Substituting (J.4), (J.5), (N.2), (N.3) and (N.4) into (N.1) yields

$$\bar{K}K'(x)\frac{\partial h(x,t)}{\partial x} = -\theta V K'(x)\left(1-\frac{\xi}{l}\right) - \frac{1}{l}\bar{K}b\xi K'(x)$$
$$-\frac{1}{l}\bar{K}HK'(x) - K'(x)K'(x)\frac{\partial h(x,t)}{\partial y} + \frac{1}{l}\int_0^{\xi} K'(y)K'(x)\frac{\partial h(y,t)}{\partial y}dy \qquad \text{(N.5)}$$

Expand the integral around $\bar{\xi}$ and recall that $V = \frac{d\xi}{dt}$

$$\bar{K}K'(x)\frac{\partial h(x,t)}{\partial x} = -\theta\frac{d\bar{\xi}}{dt}K'(x)\left(1-\frac{\bar{\xi}}{l}\right)-\frac{1}{l}\bar{K}b\bar{\xi}K'(x)$$
$$-\frac{1}{l}\bar{K}HK'(x)-K'(x)K'(x)\frac{\partial h(x,t)}{\partial y}+\frac{1}{l}\int_0^{\bar{\xi}}K'(y)K'(x)\frac{\partial h(y,t)}{\partial y}dy \qquad \text{(N.6)}$$
$$+\frac{\xi'}{l}K'(\bar{\xi})K'(x)\frac{\partial h(y,t)}{\partial y}\bigg|_{y=\bar{\xi}}$$

or,

$$\bar{K}K'(x)\frac{\partial \bar{h}(x,t)}{\partial x}+\bar{K}K'(x)\frac{\partial h'(x,t)}{\partial x} =$$
$$-\theta\frac{d\bar{\xi}}{dt}K'(x)-\theta\frac{d\xi'}{dt}K'(x)+\theta\frac{d\bar{\xi}}{dt}K'(x)\frac{\xi'}{l}+\theta\frac{d\xi'}{dt}K'(x)\frac{\bar{\xi}}{l}$$
$$+\theta\frac{d\bar{\xi}}{dt}K'(x)\frac{\bar{\xi}}{l}+\theta\frac{d\xi'}{dt}K'(x)\frac{\xi'}{l}$$
$$-\frac{1}{l}\bar{K}b\bar{\xi}K'(x)-\frac{1}{l}\bar{K}b\xi'K'(x) \qquad \text{(N.7)}$$
$$-\frac{1}{l}\bar{K}HK'(x)-K'(x)K'(x)\frac{\partial \bar{h}(x,t)}{\partial x}-K'(x)K'(x)\frac{\partial h'(x,t)}{\partial x}$$
$$+\frac{1}{l}\int_0^{\bar{\xi}}K'(y)K'(x)\frac{\partial \bar{h}(y,t)}{\partial y}dy+\frac{1}{l}\int_0^{\bar{\xi}}K'(y)K'(x)\frac{\partial h'(y,t)}{\partial y}dy$$
$$+\frac{\xi'}{l}K'(\bar{\xi})K'(x)\frac{\partial \bar{h}(y,t)}{\partial y}\bigg|_{y=\bar{\xi}}+\frac{\xi'}{l}K'(\bar{\xi})K'(x)\frac{\partial h'(y,t)}{\partial y}\bigg|_{y=\bar{\xi}}$$

Taking the mean and retaining only second-order terms yields

$$r^{(2)}(x,t) = \theta\frac{\partial C_{Y\xi}^{(2)}}{\partial t}-\theta\frac{\partial C_{Y\xi}^{(2)}}{\partial t}\frac{\xi^{(0)}}{l}-\theta\frac{d\xi^{(0)}}{dt}\frac{C_{Y\xi}^{(2)}}{l}+\frac{1}{l}K_G bC_{Y\xi}^{(2)}$$
$$+K_G\sigma_Y^2\frac{\partial h^{(0)}(x,t)}{\partial x}-\frac{1}{l}K_G\int_0^{\xi^{(0)}}C_Y^{(2)}(y,x)\frac{\partial h^{(0)}(y,t)}{\partial y}dy \qquad \text{(N.8)}$$

Substitution (4.19) and (4.20) into (N.8) gives

$$r^{(2)}(x,t) = \theta\frac{\partial C_{Y\xi}^{(2)}(x,t)}{\partial t}-K_G\sigma_Y^2\frac{b\xi^{(0)}+H-a}{\xi^{(0)}} \qquad \text{(N.9)}$$

Upon change of variable,

$$r^{(2)}(x,t)=\theta\frac{\partial C_{Y\xi}^{(2)}(x,\xi^{(0)})}{\partial\xi^{(0)}}\left[\frac{dt}{d\xi^{(0)}}\right]^{-1}-K_G\sigma_Y^2\frac{b\xi^{(0)}+H-a}{\xi^{(0)}} \tag{N.10}$$

or by virtue of (4.14)

$$r^{(2)}(x,t)=K_G\frac{\partial C_{Y\xi}^{(2)}(x,\xi^{(0)})}{\partial\xi^{(0)}}\frac{b\xi^{(0)}+H-a}{\xi^{(0)}}-K_G\sigma_Y^2\frac{b\xi^{(0)}+H-a}{\xi^{(0)}} \tag{N.11}$$

From (M.7)-(M.9) we find that

$$\frac{\partial C_{Y\xi}^{(2)}\left(x,\xi^{(0)}\right)}{\partial\xi^{(0)}}=-\frac{H-a}{\xi^{(0)}\left(b\xi^{(0)}+H-a\right)}C_{Y\xi}^{(2)}\left(x,\xi^{(0)}\right)+\frac{1}{\xi^{(0)}}\int_0^{\xi^{(0)}}C_Y^{(2)}(x,y)dy \tag{N.12}$$

The integral is given by (M.17) as

$$\int_0^{\xi^{(0)}}C_Y^{(2)}(x,z)dz=\sigma_Y^2 l_Y\left(2-e^{\frac{x-\xi^{(0)}}{l_Y}}-e^{-\frac{x}{l_Y}}\right) \tag{N.13}$$

Substituting (M.22) and (N.13) into (N.12) yields

$$\frac{\partial C_{Y\xi}^{(2)}(x,\xi^{(0)})}{\partial\xi^{(0)}}=-\frac{\sigma_Y^2 l_Y}{b}\frac{H-a}{\left(\xi^{(0)}\right)^2}\cdot$$

$$\left[e^{-\frac{bx+H-a}{bl_Y}}\left\{Ei\left(\frac{bx+H-a}{bl_Y}\right)-Ei\left(\frac{H-a}{bl_Y}\right)\right\}-e^{-\frac{x}{l_Y}}\ln\frac{bx+H-a}{H-a}\right.$$

$$\left.+\left(2-e^{-x/l_Y}\right)\ln\frac{b\xi^{(0)}+H-a}{bx+H-a}-e^{\frac{bx+H-a}{bl_y}}\left\{Ei\left(-\frac{b\xi^{(0)}+H-a}{bl_y}\right)-Ei\left(-\frac{bx+H-a}{bl_y}\right)\right\}\right]$$

$$+\sigma_Y^2 l_Y\frac{2-e^{-x/l_Y}-e^{x-\xi^{(0)}}}{\xi^{(0)}} \tag{N.14}$$

APPENDIX O

FRONT VARIANCE

Multiply (4.13) by ξ',

$$0=\theta\xi\frac{d\xi}{dt}\xi'-b\bar{K}\xi\xi'+(H-a)\bar{K}\xi' +\int_0^{\bar{\xi}}K'(y)\xi'\frac{\partial h(y,t)}{\partial y}dy+\xi'K'(\bar{\xi})\xi'\frac{\partial h(y,t)}{\partial y}\bigg|_{y=\bar{\xi}} \tag{O.1}$$

Take the mean and retrain the second-order terms only,

$$0=\theta\xi^{(0)}\overline{\frac{d\xi'}{dt}\xi'}^{(2)}+\theta\frac{d\xi^{(0)}}{dt}\left[\sigma_\xi^2(t)\right]^{(2)} -K_G b\left[\sigma_\xi^2(t)\right]^{(2)}+K_G\int_0^{\xi^{(0)}}C_{Y\xi}^{(2)}(y,\xi^{(0)})\frac{\partial h^{(0)}(y,t)}{\partial y}dy \tag{O.2}$$

or

$$0=\frac{\theta}{2}\xi^{(0)}\frac{d\left[\sigma_\xi^2(t)\right]^{(2)}}{dt}+\theta\frac{d\xi^{(0)}}{dt}\left[\sigma_\xi^2(t)\right]^{(2)} -K_G b\left[\sigma_\xi^2(t)\right]^{(2)}+K_G\int_0^{\xi^{(0)}}C_{Y\xi}^{(2)}(y,\xi^{(0)})\frac{\partial h^{(0)}(y,t)}{\partial y}dy \tag{O.3}$$

Substituting (4.19) yields

$$\frac{\theta}{2K_G}\xi^{(0)}\frac{d\left[\sigma_\xi^2(t)\right]^{(2)}}{dt}+\left(\frac{\theta}{K_G}\frac{d\xi^{(0)}}{dt}-b\right)\left[\sigma_\xi^2(t)\right]^{(2)} =\frac{b\xi^{(0)}+H-a}{\xi^{(0)}}\int_0^{\xi^{(0)}}C_{Y\xi}^{(2)}(y,\xi^{(0)})dy \tag{O.4}$$

Upon change of variable $\frac{d\sigma_\xi^2}{dt}=\frac{d\sigma_\xi^2}{d\xi^{(0)}}\frac{d\xi^{(0)}}{dt}$ we get

$$\frac{\theta}{2K_G}\xi^{(0)}\frac{d\left[\sigma_\xi^2(t)\right]^{(2)}}{d\xi^{(0)}}\frac{d\xi^{(0)}}{dt}+\left(\frac{\theta}{K_G}\frac{d\xi^{(0)}}{dt}-b\right)\left[\sigma_\xi^2(t)\right]^{(2)}$$
$$=\frac{b\xi^{(0)}+H-a}{\xi^{(0)}}\int_0^{\xi^{(0)}}C_{Y\xi}^{(2)}(y,\xi^{(0)})dy \tag{O.5}$$

or

$$\frac{\theta}{2K_G}\xi^{(0)}\frac{d\left[\sigma_\xi^2(t)\right]^{(2)}}{d\xi^{(0)}}+\left(\frac{\theta}{K_G}-b\frac{dt}{d\xi^{(0)}}\right)\left[\sigma_\xi^2(t)\right]^{(2)}$$
$$=\frac{dt}{d\xi^{(0)}}\frac{b\xi^{(0)}+H-a}{\xi^{(0)}}\int_0^{\xi^{(0)}}C_{Y\xi}^{(2)}(y,\xi^{(0)})dy \tag{O.6}$$

From (4.14) $\frac{dt}{d\xi^{(0)}}=\frac{\theta}{K_G}\frac{\xi^{(0)}}{b\xi^{(0)}+H-a}$ and so

$$\frac{1}{2}\xi^{(0)}\frac{d\left[\sigma_\xi^2(t)\right]^{(2)}}{d\xi^{(0)}}+\left(1-b\frac{\xi^{(0)}}{b\xi^{(0)}+H-a}\right)\left[\sigma_\xi^2(t)\right]^{(2)}$$
$$=\int_0^{\xi^{(0)}}C_{Y\xi}^{(2)}(y,\xi^{(0)})dy \tag{O.7}$$

or

$$\frac{d\left[\sigma_\xi^2(t)\right]^{(2)}}{d\xi^{(0)}}+P\left(\xi^{(0)}\right)\left[\sigma_\xi^2(t)\right]^{(2)}=R\left(\xi^{(0)}\right) \tag{O.8}$$

subject to boundary condition

$$\left[\sigma_\xi^2(0)\right]^{(2)}=0 \tag{O.9}$$

where $P\left(\xi^{(0)}\right)=\frac{2}{\xi^{(0)}}-\frac{2b}{b\xi^{(0)}+H-a}$ (O.10)

and $R\left(\xi^{(0)}\right)=\frac{2}{\xi^{(0)}}\int_0^{\xi^{(0)}}C_{Y\xi}^{(2)}(y,\xi^{(0)})dy$ (O.11)

The solution of this equation is

$$\left[\sigma_{\xi}^{2}(t)\right]^{(2)} = e^{-\int P(\xi^{(0)})d\xi^{(0)}} \int_{0}^{\xi^{(0)}} \left(e^{\int P(x)dx} \frac{2}{x} \int_{0}^{x} C_{Y\xi}^{(2)}(y,x)dy \right) dx \tag{O.12}$$

where

$$-\int P(\xi^{(0)}) = -2\ln\xi^{(0)} + 2\ln\left(b\xi^{(0)} + H - a\right) = \ln\left(\frac{b\xi^{(0)} + H - a}{\xi^{(0)}}\right)^{2} \tag{O.13}$$

Substitution of (O.13) into (O.12) gives

$$\left[\sigma_{\xi}^{2}(t)\right]^{(2)} = e^{\ln\left(\frac{b\xi^{(0)}+H-a}{\xi^{(0)}}\right)^{2}} \int_{0}^{\xi^{(0)}} \left(e^{-\ln\left(\frac{bx+H-a}{x}\right)^{2}} \frac{2}{x} \int_{0}^{x} C_{Y\xi}^{(2)}(y,x)dy \right) dx \tag{O.14}$$

or

$$\left[\sigma_{\xi}^{2}(t)\right]^{(2)} = 2\left(\frac{b\xi^{(0)}(t) + H - a}{\xi^{(0)}(t)}\right)^{2} \int_{0}^{\xi^{(0)}(t)} \frac{x\int_{0}^{x} C_{Y\xi}^{(2)}(y,x)dy}{\left(bx + H - a\right)^{2}} dx \tag{O.15}$$

APPENDIX P

INTEGRAL OF $C_{Y\xi}^{(2)}$

Rewrite expression (M.22) for $C_{Y\xi}^{(2)}$:

$$C_{Y\xi}^{(2)}(x,\xi^{(0)}) = \sigma_Y^2 l_Y \frac{b\xi^{(0)} + H - a}{b\xi^{(0)}} \bullet$$

$$\left[e^{-\frac{bx+H-a}{bl_Y}} \left\{ Ei\left(\frac{bx+H-a}{bl_Y} \right) - Ei\left(\frac{H-a}{bl_Y} \right) \right\} - e^{-\frac{x}{l_Y}} \ln\left(bx+H-a\right) + e^{-\frac{x}{l_Y}} \ln\left(H-a\right) \right.$$

$$+2\ln\left(b\xi^{(0)}+H-a\right) - 2\ln\left(bx+H-a\right)$$

$$-e^{-x/l_Y} \ln\left(b\xi^{(0)}+H-a\right) + e^{-x/l_Y} \ln\left(bx+H-a\right) \qquad \text{(P.1)}$$

$$\left. -e^{\frac{bx+H-a}{bl_y}} \left\{ Ei\left(-\frac{b\xi^{(0)}+H-a}{bl_y} \right) - Ei\left(-\frac{bx+H-a}{bl_y} \right) \right\} \right]$$

or

$$C_{Y\xi}^{(2)}(x,\xi^{(0)}) = \sigma_Y^2 l_Y \frac{b\xi^{(0)} + H - a}{b\xi^{(0)}} \bullet$$

$$\left[e^{-\frac{bx+H-a}{bl_Y}} \left\{ Ei\left(\frac{bx+H-a}{bl_Y} \right) - Ei\left(\frac{H-a}{bl_Y} \right) \right\} + e^{-\frac{x}{l_Y}} \ln \frac{H-a}{bl_Y} \right.$$

$$+2\ln\left(\frac{b\xi^{(0)}+H-a}{bl_y} \right) - 2\ln\left(\frac{bx+H-a}{bl_y} \right)$$

$$-e^{-x/l_Y} \ln\left(\frac{b\xi^{(0)}+H-a}{bl_y} \right) \qquad \text{(P.2)}$$

$$\left. -e^{\frac{bx+H-a}{bl_y}} \left\{ Ei\left(-\frac{b\xi^{(0)}+H-a}{bl_y} \right) - Ei\left(-\frac{bx+H-a}{bl_y} \right) \right\} \right]$$

The integral of (P.2) is

$$\int_0^x C_{Y\xi}^{(2)}(y,\xi^{(0)})dy = \sigma_Y^2 l_Y \frac{b\xi^{(0)}+H-a}{b\xi^{(0)}} \cdot$$

$$\left[\int_0^x e^{-\frac{by+H-a}{bl_Y}} Ei\left(\frac{by+H-a}{bl_Y}\right)dy \quad (I)\right.$$

$$-Ei\left(\frac{H-a}{bl_Y}\right)\int_0^x e^{-\frac{by+H-a}{bl_Y}}dy \quad (II)$$

$$+\ln\frac{H-a}{bl_Y}\int_0^x e^{-\frac{y}{l_Y}}dy \quad (III)$$

$$+2\ln\frac{b\xi^{(0)}+H-a}{bl_Y}x \quad (IV)$$

$$-2\int_0^x \ln\frac{by+H-a}{bl_Y}dy \quad (V)$$

$$-\ln\frac{b\xi^{(0)}+H-a}{bl_Y}\int_0^x e^{-y/l_Y}dy \quad (VI)$$

$$-Ei\left(-\frac{b\xi^{(0)}+H-a}{bl_y}\right)\int_0^x e^{\frac{by+H-a}{bl_y}}dy \quad (VII)$$

$$\left.+\int_0^x e^{\frac{by+H-a}{bl_y}} Ei\left(-\frac{by+H-a}{bl_y}\right)dy\right] \quad (VIII)$$

(P.3)

Integral (I)

$$(I) = l_Y\int_0^x e^{-\frac{by+H-a}{bl_Y}} Ei\left(\frac{by+H-a}{bl_Y}\right)d\frac{by+H-a}{bl_Y} \quad \text{(P.4)}$$

Let $z = -\dfrac{by+H-a}{bl_Y}$, then

$$(I) = -l_Y \int_{-\frac{H-a}{bl_Y}}^{-\frac{bx+H-a}{bl_Y}} e^z Ei(-z)dz \tag{P.5}$$

integrating by parts gives

$$(I) = -l_Y e^z Ei(-z)\Big|_{-\frac{H-a}{bl_Y}}^{-\frac{bx+H-a}{bl_Y}} + l_Y \int_{-\frac{H-a}{bl_Y}}^{-\frac{bx+H-a}{bl_Y}} e^z \frac{e^{-z}}{z} dz$$

$$= -l_Y e^{-\frac{bx+H-a}{bl_Y}} Ei\left(\frac{bx+H-a}{bl_Y}\right) + l_Y e^{-\frac{H-a}{bl_Y}} Ei\left(\frac{H-a}{bl_Y}\right) + l_Y \ln\frac{bx+H-a}{bl_Y} - l_Y \ln\frac{H-a}{bl_Y} \tag{P.6}$$

Integral (II)

$$(II) = -Ei\left(\frac{H-a}{bl_Y}\right)(-l_Y)\left(e^{-\frac{H-a}{bl_Y}} - e^{-\frac{H-a}{bl_Y}}\right)$$

$$= l_Y Ei\left(\frac{H-a}{bl_Y}\right)e^{-\frac{bx+H-a}{bl_Y}} - l_Y Ei\left(\frac{H-a}{bl_Y}\right)e^{-\frac{H-a}{bl_Y}} \tag{P.7}$$

Integral (III)

$$(III) = -l_Y \ln\frac{H-a}{bl_Y} e^{-\frac{x}{l_Y}} + l_Y \ln\frac{H-a}{bl_Y} \tag{P.8}$$

Integral (V)

$$(V) = -2\int_0^x \ln\frac{by+H-a}{bl_Y}dy$$

$$= -2\int_0^x \ln(by+H-a)dy + 2\ln(bl_y)x$$

$$= -\frac{2}{b}\{(by+H-a)[\ln(by+H-a)-1]\}\Big|_0^x + 2\ln(bl_y)x$$

$$= -2\frac{bx+H-a}{b}[\ln(bx+H-a)-1] + 2\frac{H-a}{b}[\ln(H-a)-1] + 2\ln(bl_y)x$$

$$= -2\frac{bx+H-a}{b}\ln(bx+H-a) + 2\frac{H-a}{b}\ln(H-a) + 2x + 2\ln(bl_y)\left(\frac{bx+H-a}{b} - \frac{H-a}{b}\right)$$

$$= -2\frac{bx+H-a}{b}\ln\frac{bx+H-a}{bl_y} + 2\frac{H-a}{b}\ln\frac{H-a}{bl_y} + 2x \qquad \text{(P.9)}$$

Integral (VI)

$$(VI) = -\ln\frac{b\xi^{(0)}+H-a}{bl_Y}(-l_Y)\left(e^{-x/l_Y}-1\right)$$

$$= l_Y\ln\frac{b\xi^{(0)}+H-a}{bl_Y}e^{-x/l_Y} - l_Y\ln\frac{b\xi^{(0)}+H-a}{bl_Y} \qquad \text{(P.10)}$$

Integral (VII)

$$(VII) = -l_Y Ei\left(-\frac{b\xi^{(0)}+H-a}{bl_y}\right)e^{\frac{bx+H-a}{bl_y}} + l_Y Ei\left(-\frac{b\xi^{(0)}+H-a}{bl_y}\right)e^{\frac{H-a}{bl_y}} \qquad \text{(P.11)}$$

Integral $(VIII)$

$$(VIII) = l_Y\int_0^x e^{\frac{by+H-a}{bl_y}}Ei\left(-\frac{by+H-a}{bl_y}\right)d\frac{by+H-a}{bl_y} \qquad \text{(P.12)}$$

Let $z = \dfrac{by + H - a}{bl_Y}$, then

$$(VIII) = l_Y \int_{\frac{H-a}{bl_Y}}^{\frac{bx+H-a}{bl_Y}} e^{z} Ei(-z) dz \qquad \text{(P.13)}$$

integrating by parts gives

$$(VIII) = l_Y e^{z}\, Ei(-z)\Big|_{\frac{H-a}{bl_Y}}^{\frac{bx+H-a}{bl_Y}} - l_Y \int_{\frac{H-a}{bl_Y}}^{\frac{bx+H-a}{bl_Y}} e^{z} \frac{e^{-z}}{z} dz$$

$$= l_Y e^{\frac{bx+H-a}{bl_Y}} Ei\left(-\frac{bx+H-a}{bl_Y}\right) - l_Y e^{\frac{H-a}{bl_Y}} Ei\left(-\frac{H-a}{bl_Y}\right) \qquad \text{(P.14)}$$
$$- l_Y \ln\frac{bx+H-a}{bl_Y} + l_Y \ln\frac{H-a}{bl_Y}$$

Finally

$$\int_0^x C_{YL}^{(2)}(y,\xi^{(0)})dy = \sigma_Y^2 l_Y^2 \frac{b\xi^{(0)}+H-a}{b\xi^{(0)}} \cdot$$

$$-e^{-\frac{bx+H-a}{bl_Y}} Ei\left(\frac{bx+H-a}{bl_Y}\right)+e^{-\frac{H-a}{bl_Y}} Ei\left(\frac{H-a}{bl_Y}\right)$$

$$+\ln\frac{bx+H-a}{bl_Y}-\ln\frac{H-a}{bl_Y}$$

$$+Ei\left(\frac{H-a}{bl_Y}\right)e^{-\frac{bx+H-a}{bl_Y}}-Ei\left(\frac{H-a}{bl_Y}\right)e^{-\frac{H-a}{bl_Y}}$$

$$-\ln\frac{H-a}{bl_Y}e^{-\frac{x}{l_Y}}+\ln\frac{H-a}{bl_Y}$$

$$+2\ln\frac{b\xi^{(0)}+H-a}{bl_Y}\frac{x}{l_Y}$$

$$-2\frac{bx+H-a}{bl_y}\ln\frac{bx+H-a}{bl_y}+2\frac{H-a}{bl_y}\ln\frac{H-a}{bl_y}+2\frac{x}{l_y}$$

$$+\ln\frac{b\xi^{(0)}+H-a}{bl_Y}e^{-x/l_Y}-\ln\frac{b\xi^{(0)}+H-a}{bl_Y}$$

$$-Ei\left(-\frac{b\xi^{(0)}+H-a}{bl_y}\right)e^{\frac{bx+H-a}{bl_y}}+Ei\left(-\frac{b\xi^{(0)}+H-a}{bl_y}\right)e^{\frac{H-a}{bl_y}}$$

$$+e^{\frac{bx+H-a}{bl_Y}}Ei\left(-\frac{bx+H-a}{bl_Y}\right)-e^{\frac{H-a}{bl_Y}}Ei\left(-\frac{H-a}{bl_Y}\right)$$

$$-\ln\frac{bx+H-a}{bl_Y}+\ln\frac{H-a}{bl_Y} \qquad \text{(P.15)}$$

or

$$\int_0^x C_{Y\xi}^{(2)}(y,\xi^{(0)})dy = \sigma_Y^2 l_r^2 \frac{b\xi^{(0)}+H-a}{b\xi^{(0)}} \cdot$$

$$\left[-e^{-\frac{bx+H-a}{bl_Y}} Ei\left(\frac{bx+H-a}{bl_Y}\right) + Ei\left(\frac{H-a}{bl_Y}\right) e^{\frac{bx+H-a}{bl_Y}} \right.$$

$$-\ln\frac{H-a}{bl_Y} e^{-\frac{x}{l_Y}} + 2\ln\frac{b\xi^{(0)}+H-a}{bl_Y}\frac{x}{l_Y}$$

$$-2\frac{bx+H-a}{bl_y}\ln\frac{bx+H-a}{bl_y} + 2\frac{H-a}{bl_y}\ln\frac{H-a}{bl_y} + 2\frac{x}{l_y}$$

$$+\ln\frac{b\xi^{(0)}+H-a}{bl_Y} e^{-x/l_Y} - \ln\frac{b\xi^{(0)}+H-a}{bl_Y}$$

$$-Ei\left(-\frac{b\xi^{(0)}+H-a}{bl_y}\right) e^{\frac{bx+H-a}{bl_y}} + Ei\left(-\frac{b\xi^{(0)}+H-a}{bl_y}\right) e^{\frac{H-a}{bl_y}}$$

$$\left. +e^{\frac{bx+H-a}{bl_Y}} Ei\left(-\frac{bx+H-a}{bl_Y}\right) - e^{\frac{H-a}{bl_Y}} Ei\left(-\frac{H-a}{bl_Y}\right) + \ln\frac{H-a}{bl_Y} \right] \qquad \text{(P.16)}$$

Note that the integral from 0 to $\xi^{(0)}$ is

$$\int_0^{\xi^{(0)}} C_{Y\xi}^{(2)}(y,\xi^{(0)})dy = \sigma_Y^2 l_r^2 \frac{b\xi^{(0)}+H-a}{b\xi^{(0)}} \cdot$$

$$\left[-e^{-\frac{b\xi^{(0)}+H-a}{bl_Y}} Ei\left(\frac{b\xi^{(0)}+H-a}{bl_Y}\right) + Ei\left(\frac{H-a}{bl_Y}\right) e^{-\frac{b\xi^{(0)}+H-a}{bl_Y}} \right.$$

$$-\ln\frac{H-a}{bl_Y} e^{-\frac{\xi^{(0)}}{l_Y}} - 2\frac{H-a}{bl_y}\ln\frac{b\xi^{(0)}+H-a}{bl_y} + 2\frac{H-a}{bl_y}\ln\frac{H-a}{bl_y} + 2\frac{\xi^{(0)}}{l_y}$$

$$+\ln\frac{b\xi^{(0)}+H-a}{bl_Y} e^{-\bar{\gamma}^{(0)} l_Y} - \ln\frac{b\xi^{(0)}+H-a}{bl_Y}$$

$$\left. +Ei\left(-\frac{b\xi^{(0)}+H-a}{bl_y}\right) e^{\frac{H-a}{bl_y}} - e^{\frac{H-a}{bl_Y}} Ei\left(-\frac{H-a}{bl_Y}\right) + \ln\frac{H-a}{bl_Y} \right] \qquad \text{(P.17)}$$

APPENDIX Q

SECOND-ORDER MEAN FRONT POSITION

We can rewrite (4.15), using (4.14) and (4.19), as

$$\xi^{(0)}\frac{d\bar{\xi}^{(2)}}{d\xi^{(0)}}+\left(1-\frac{b\xi^{(0)}}{b\xi^{(0)}+H-a}\right)\bar{\xi}^{(2)} = \frac{\xi^{(0)}}{b\xi^{(0)}+H-a}\left[\begin{array}{l} -\dfrac{\theta}{2K_G}\dfrac{d\left[\sigma_\xi^2\right]^{(2)}}{dt}+\left(b\xi^{(0)}+H-a\right)\dfrac{\sigma_Y^2}{2} \\ +\dfrac{1}{K_G}\displaystyle\int_0^{\xi^{(0)}} r^{(2)}(y,t)dy+C_{Y\xi}^{(2)}(\xi^{(0)},t)\frac{b\xi^{(0)}+H-a}{\xi^{(0)}} \end{array}\right] \tag{Q.1}$$

or, using (4.14) again,

$$\xi^{(0)}\frac{d\bar{\xi}^{(2)}}{d\xi^{(0)}}+\left(1-\frac{b\xi^{(0)}}{b\xi^{(0)}+H-a}\right)\bar{\xi}^{(2)} = -\frac{1}{2}\frac{d\left[\sigma_\xi^2\right]^{(2)}}{d\xi^{(0)}}+\xi^{(0)}\frac{\sigma_Y^2}{2}+\frac{1}{K_G}\frac{\xi^{(0)}}{b\xi^{(0)}+H-a}\int_0^{\xi^{(0)}} r^{(2)}(y,t)dy+C_{Y\xi}^{(2)}(\xi^{(0)},t) \tag{Q.2}$$

The residual flux is given by (4.22) as

$$r^{(2)}(y)=K_G\frac{\partial C_{Y\xi}^{(2)}(y,\xi^{(0)})}{\partial\xi^{(0)}}\frac{b\xi^{(0)}+H-a}{\xi^{(0)}}-K_G\sigma_Y^2\frac{b\xi^{(0)}+H-a}{\xi^{(0)}} \tag{Q.3}$$

An expression for front variance is given by (O.7) as

$$\frac{d\left[\sigma_\xi^2\right]^{(2)}}{d\xi^{(0)}}=\frac{2}{\xi^{(0)}}\int_0^{\xi^{(0)}} C_{Y\xi}^{(2)}(y,\xi^{(0)})dy-\frac{2}{\xi^{(0)}}\frac{H-a}{b\xi^{(0)}+H-a}\left[\sigma_\xi^2\right]^{(2)} \tag{Q.4}$$

Substituting (Q.3) and (Q.4) into (Q.2) gives

$$\xi^{(0)}\frac{d\bar{\xi}^{(2)}}{d\xi^{(0)}}+\left(1-\frac{b\xi^{(0)}}{b\xi^{(0)}+H-a}\right)\bar{\xi}^{(2)}$$
$$=-\frac{1}{\xi^{(0)}}\int_0^{\xi^{(0)}}C_{Y\xi}^{(2)}(y,\xi^{(0)})dy+\frac{1}{\xi^{(0)}}\frac{H-a}{b\xi^{(0)}+H-a}\left[\sigma_\xi^2\right]^{(2)}-\xi^{(0)}\frac{\sigma_Y^2}{2} \qquad \text{(Q.5)}$$
$$+\int_0^{\xi^{(0)}}\frac{\partial C_{Y\xi}^{(2)}(y,\xi^{(0)})}{\partial\xi^{(0)}}dy+C_{Y\xi}^{(2)}(\xi^{(0)},t)$$

Note that

$$\int_0^{\xi^{(0)}}\frac{\partial C_{Y\xi}^{(2)}(y,\xi^{(0)})}{\partial\xi^{(0)}}dy=\frac{d}{d\xi^{(0)}}\left(\int_0^{\xi^{(0)}}C_{Y\xi}^{(2)}(y,\xi^{(0)})dy\right)-C_{Y\xi}^{(2)}(\xi^{(0)},\xi^{(0)}) \qquad \text{(Q.6)}$$

Substitution gives

$$\frac{d\bar{\xi}^{(2)}(t)}{d\xi^{(0)}(t)}+\left(\frac{1}{\xi^{(0)}(t)}-\frac{b}{b\xi^{(0)}(t)+H-a}\right)\bar{\xi}^{(2)}(t)$$
$$=-\frac{1}{\left(\xi^{(0)}(t)\right)^2}\int_0^{\xi^{(0)}}C_{Y\xi}^{(2)}(y,\xi^{(0)}(t))dy+\frac{1}{\left(\xi^{(0)}(t)\right)^2}\frac{H-a}{b\xi^{(0)}(t)+H-a}\left[\sigma_\xi^2\right]^{(2)}-\frac{\sigma_Y^2}{2} \qquad \text{(Q.7)}$$
$$+\frac{1}{\xi^{(0)}(t)}\frac{d}{d\xi^{(0)}(t)}\left(\int_0^{\xi^{(0)}}C_{Y\xi}^{(2)}(y,\xi^{(0)}(t))dy\right)$$

or

$$\frac{d\bar{\xi}^{(2)}\left(\xi^{(0)}(t)\right)}{d\xi^{(0)}(t)}+P\left(\xi^{(0)}(t)\right)\bar{\xi}^{(2)}\left(\xi^{(0)}(t)\right)=R\left(\xi^{(0)}(t)\right) \qquad \text{(Q.8)}$$

where

$$P\left(\xi^{(0)}(t)\right)=\frac{1}{\xi^{(0)}(t)}-\frac{b}{b\xi^{(0)}(t)+H-a} \qquad \text{(Q.9)}$$

and

$$R\left(\xi^{(0)}(t)\right) = -\frac{1}{\left(\xi^{(0)}(t)\right)^2}\int_0^{\xi^{(0)}} C_{Y\xi}^{(2)}(y,\xi^{(0)}(t))dy + \frac{1}{\left(\xi^{(0)}(t)\right)^2}\frac{H-a}{b\xi^{(0)}(t)+H-a}\left[\sigma_\xi^2\right]^{(2)} - \frac{\sigma_Y^2}{2}$$

$$+\frac{1}{\xi^{(0)}(t)}\frac{d}{d\xi^{(0)}(t)}\left(\int_0^{\xi^{(0)}} C_{Y\xi}^{(2)}(y,\xi^{(0)}(t))dy\right) \qquad \text{(Q.10)}$$

Then

$$\overline{\xi}^{(2)} = e^{-\int P(\xi^{(0)})d\xi^{(0)}}\int_0^{\xi^{(0)}} e^{\int P(x)dx}R(x)dx \qquad \text{(Q.11)}$$

where

$$-\int P(\xi^{(0)}) = -\ln\xi^{(0)} + \ln\left(b\xi^{(0)}+H-a\right) = \ln\frac{b\xi^{(0)}+H-a}{\xi^{(0)}} \qquad \text{(Q.12)}$$

Substitution of (Q.12) into (Q.11) gives

$$\overline{\xi}^{(2)}\left(\xi^{(0)}(t)\right) = \frac{b\xi^{(0)}(t)+H-a}{\xi^{(0)}(t)}\int_0^{\xi^{(0)}(t)}\frac{xR(x)}{bx+H-a}dx \qquad \text{(Q.13)}$$

In terms of dimensionless quantities $\tilde{\gamma}^{(0)} = \xi^{(0)}/l_Y$ and $d = \frac{H-a}{bl_Y}$ (P.17) reads as

$$\int_0^{\tilde{\gamma}^{(0)}} C_{Y\xi}^{(2)}(y,\tilde{\gamma}^{(0)})dy = \sigma_Y^2 l_Y^2\frac{\tilde{\gamma}^{(0)}+d}{\tilde{\gamma}^{(0)}} \bullet$$

$$\left[-e^{-\tilde{\gamma}^{(0)}-d}\,Ei\left(\tilde{\gamma}^{(0)}+d\right) + Ei(d)e^{-\tilde{\gamma}^{(0)}-d} - \ln d e^{-\tilde{\gamma}^{(0)}}\right.$$

$$+2d\ln d + 2\tilde{\gamma}^{(0)} + \ln\left(\tilde{\gamma}^{(0)}+d\right)\left(e^{-\tilde{\gamma}^{(0)}} - 2d - 1\right)$$

$$\left.+Ei\left(-\tilde{\gamma}^{(0)}-d\right)e^d - e^d Ei(-d) + \ln d\right] \qquad \text{(Q.14)}$$

Then the derivative (Q.14) is

$$\frac{d}{d\tilde{\gamma}^{(0)}}\int_0^{\tilde{\gamma}^{(0)}} C_{\gamma\xi}^{(2)}(y,\tilde{\gamma}^{(0)})dy = -\sigma_\gamma^2 l_r^2 \frac{d}{\left(\tilde{\gamma}^{(0)}\right)^2} \bullet$$

$$\left[-e^{-\tilde{\gamma}^{(0)}-d}\, Ei\left(\tilde{\gamma}^{(0)}+d\right)+Ei\left(d\right)e^{-\tilde{\gamma}^{(0)}-d} \quad -\ln d e^{-\tilde{\gamma}^{(0)}}\right.$$

$$+2\tilde{\gamma}^{(0)}+\ln\left(\tilde{\gamma}^{(0)}+d\right)\left(e^{-\tilde{\gamma}^{(0)}}-2d-1\right)$$

$$\left.+Ei\left(-\tilde{\gamma}^{(0)}-d\right)e^{d} \quad -e^{d}Ei\left(-d\right)+2d\ln d+\ln d\right]$$

$$+\sigma_\gamma^2 l_r^2 \frac{\tilde{\gamma}^{(0)}+d}{\tilde{\gamma}^{(0)}} \bullet$$

$$\left[e^{-\tilde{\gamma}^{(0)}-d}\, Ei\left(\tilde{\gamma}^{(0)}+d\right)-\frac{1}{\tilde{\gamma}^{(0)}+d} -Ei\left(d\right)e^{-\tilde{\gamma}^{(0)}-d} \quad +\ln d e^{-\tilde{\gamma}^{(0)}}\right.$$

$$\left.+2+\frac{e^{-\tilde{\gamma}^{(0)}}-2d-1}{\tilde{\gamma}^{(0)}+d}-\ln\left(\tilde{\gamma}^{(0)}+d\right)e^{-\tilde{\gamma}^{(0)}}+\frac{e^{-\tilde{\gamma}^{(0)}}}{\tilde{\gamma}^{(0)}+d}\right] \qquad \text{(Q.15)}$$

APPENDIX R

VARIANCE OF HEAD GRADIENT AT THE FRONT

Subtracting the mean from the kinematic front condition $-K(x)\partial h/\partial x = \theta d\xi/dt$ leaves

$$-K'(\xi)\frac{\partial \bar{h}(x,t)}{\partial x}\bigg|_{x=\xi} - \bar{K}(\xi)\frac{\partial h'(x,t)}{\partial x}\bigg|_{x=\xi} - K'(\xi)\frac{\partial h'(x,t)}{\partial x}\bigg|_{x=\xi} - r(\xi) = \theta\frac{d\xi'}{dt} \tag{R.1}$$

Multiplying by $\dfrac{\partial h'}{\partial x}$, averaging and retaining only second-order terms gives

$$r^{(2)}(\xi^{(0)})\frac{\partial h^{(0)}}{\partial x}\bigg|_{x=\xi^{(0)}} - K_G\left[\sigma^2_{dh/dx}(\xi^{(0)})\right]^{(2)} = \theta\frac{\partial^2 C^{(2)}_{h\xi}(x,t)}{\partial x\partial t}\bigg|_{x=\xi^{(0)}} \tag{R.2}$$

Multiplying (R.1) by ξ', taking average and retaining only second-order terms leads to

$$-K_G C^{(2)}_{Y\xi}(x,t)\frac{\partial h^{(0)}(x,t)}{\partial x} - K_G\frac{\partial C^{(2)}_{h\xi}(x,t)}{\partial x} = \frac{\theta}{2}\frac{d\left[\sigma^2_\xi\right]^{(2)}}{dt} \tag{R.3}$$

Substituting this into (R.2) gives an expression for the variance of head gradient,

$$\begin{aligned} K_G\left[\sigma^2_{\partial h/\partial x}(\xi^{(0)})\right]^{(2)} &= r^{(2)}(\xi^{(0)})\frac{\partial h^{(0)}(x,t)}{\partial x}\bigg|_{x=\xi^{(0)}} \\ &+\theta\frac{\partial}{\partial t}\left(C^{(2)}_{Y\xi}(x,t)\frac{\partial h^{(0)}(x,t)}{\partial x} + \frac{\theta}{2K_G}\frac{d\left[\sigma^2_\xi\right]^{(2)}}{dt}\right)\bigg|_{x=\xi^{(0)}} \end{aligned} \tag{R.4}$$

or, by virtue of (4.14),

$$\begin{aligned} K_G\left[\sigma^2_{\partial h/\partial x}(\xi^{(0)})\right]^{(2)} &= r^{(2)}(\xi^{(0)})\frac{\partial h^{(0)}}{\partial x}\bigg|_{x=\xi^{(0)}} \\ &+\frac{b\xi^{(0)}+H-a}{\xi^{(0)}}\frac{d}{d\xi^{(0)}}\left(K_G C^{(2)}_{Y\xi}(x,\xi^{(0)})\frac{\partial h^{(0)}}{\partial x} + \frac{K_G}{2}\frac{d\left[\sigma^2_\xi\right]^{(2)}}{d\xi^{(0)}}\frac{b\xi^{(0)}+H-a}{\xi^{(0)}}\right)\bigg|_{x=\xi^{(0)}} \end{aligned} \tag{R.5}$$

or, by virtue of (4.19),

$$K_G\left[\sigma^2_{\partial h/\partial x}(\xi^{(0)})\right]^{(2)} = -r^{(2)}(\xi^{(0)})\frac{b\xi^{(0)}+H-a}{\xi^{(0)}}$$
$$+\frac{b\xi^{(0)}+H-a}{\xi^{(0)}}\frac{d}{d\xi^{(0)}}\left(-K_G C^{(2)}_{Y\xi}(x,\xi^{(0)})\frac{b\xi^{(0)}+H-a}{\xi^{(0)}}+\frac{K_G}{2}\frac{d\left[\sigma^2_\xi\right]^{(2)}}{d\xi^{(0)}}\frac{b\xi^{(0)}+H-a}{\xi^{(0)}}\right)\Bigg|_{x=\xi^{(0)}} \tag{R.6}$$

Substitution expression (4.22) for the residual flux gives

$$\left[\sigma^2_{\partial h/\partial x}(\xi^{(0)})\right]^{(2)} = -\left(\frac{b\xi^{(0)}+H-a}{\xi^{(0)}}\right)^2\frac{\partial C^{(2)}_{Y\xi}(x,\xi^{(0)})}{\partial\xi^{(0)}}\Bigg|_{x=\xi^{(0)}}+\sigma^2_Y\left(\frac{b\xi^{(0)}+H-a}{\xi^{(0)}}\right)^2$$
$$-\left(\frac{b\xi^{(0)}+H-a}{\xi^{(0)}}\right)^2\frac{\partial C^{(2)}_{Y\xi}(x,\xi^{(0)})}{\partial\xi^{(0)}}\Bigg|_{x=\xi^{(0)}}+\frac{b\xi^{(0)}+H-a}{\xi^{(0)}}\frac{H-a}{\left(\xi^{(0)}\right)^2}C^{(2)}_{Y\xi}(\xi^{(0)},\xi^{(0)}) \tag{R.7}$$
$$+\frac{1}{2}\left(\frac{b\xi^{(0)}+H-a}{\xi^{(0)}}\right)^2\frac{d^2\left[\sigma^2_\xi\right]^{(2)}}{d\xi^{(0)2}}-\frac{1}{2}\frac{b\xi^{(0)}+H-a}{\xi^{(0)}}\frac{H-a}{\left(\xi^{(0)}\right)^2}\frac{d\left[\sigma^2_\xi\right]^{(2)}}{d\xi^{(0)}}$$

or

$$\left[\sigma^2_{\partial h/\partial x}\left(\xi^{(0)}(t)\right)\right]^{(2)} = -2\left(\frac{b\xi^{(0)}(t)+H-a}{\xi^{(0)}(t)}\right)^2\frac{\partial C^{(2)}_{Y\xi}(x,\xi^{(0)}(t))}{\partial\xi^{(0)}}\Bigg|_{x=\xi^{(0)}}+\sigma^2_Y\left(\frac{b\xi^{(0)}(t)+H-a}{\xi^{(0)}(t)}\right)^2$$
$$+\frac{b\xi^{(0)}(t)+H-a}{\xi^{(0)}(t)}\frac{H-a}{\left(\xi^{(0)}(t)\right)^2}C^{(2)}_{Y\xi}(\xi^{(0)}(t),\xi^{(0)}(t))$$
$$+\frac{1}{2}\left(\frac{b\xi^{(0)}(t)+H-a}{\xi^{(0)}(t)}\right)^2\frac{d^2\left[\sigma^2_\xi\left(\xi^{(0)}(t)\right)\right]^{(2)}}{d\xi^{(0)}(t)^2} \tag{R.8}$$
$$-\frac{1}{2}\frac{b\xi^{(0)}(t)+H-a}{\xi^{(0)}(t)}\frac{H-a}{\left(\xi^{(0)}(t)\right)^2}\frac{d\left[\sigma^2_\xi\left(\xi^{(0)}(t)\right)\right]^{(2)}}{d\xi^{(0)}(t)}$$

From (4.16) and (4.14) it follows that

$$\frac{d\left[\sigma_{\xi}^{2}\left(\xi^{(0)}(t)\right)\right]^{(2)}}{d\xi^{(0)}(t)}=\frac{2}{\xi^{(0)}(t)}\int_{0}^{\xi^{(0)}}C_{Y\xi}^{(2)}(y,\xi^{(0)}(t))dy$$
$$-2\left(\frac{1}{\xi^{(0)}(t)}-\frac{b}{b\xi^{(0)}(t)+H-a}\right)\left[\sigma_{\xi}^{2}\left(\xi^{(0)}(t)\right)\right]^{(2)} \qquad \text{(R.9)}$$

The second derivative of front variance is

$$\frac{1}{2}\frac{d^{2}\left[\sigma_{\xi}^{2}\left(\xi^{(0)}(t)\right)\right]^{(2)}}{d\xi^{(0)}(t)^{2}}=-\frac{1}{\xi^{(0)}(t)^{2}}\int_{0}^{\xi^{(0)}(t)}C_{Y\xi}^{(2)}\left(y,\xi^{(0)}(t)\right)dy$$
$$+\frac{1}{\xi^{(0)}(t)}\frac{d}{d\xi^{(0)}(t)}\int_{0}^{\xi^{(0)}(t)}C_{Y\xi}^{(2)}(y,\xi^{(0)}(t))dy \qquad \text{(R.10)}$$
$$+\left(\frac{1}{\xi^{(0)}(t)^{2}}-\frac{b^{2}}{\left(b\xi^{(0)}(t)+H-a\right)^{2}}\right)\left[\sigma_{\xi}^{2}\right]^{(2)}-\left(\frac{1}{\xi^{(0)}(t)}-\frac{b}{b\xi^{(0)}(t)+H-a}\right)\frac{d\left[\sigma_{\xi}^{2}\right]^{(2)}}{d\xi^{(0)}(t)}$$

APPENDIX S

MOMENT EQUATIONS OBTAINED BY AVERAGING OF ANALYTICAL SOLUTION

We can rewrite (4.45) as

$$\frac{t}{\theta}=\int_0^{\xi}\frac{\int_0^x \frac{dy}{\bar{K}+K'(y)}}{bx+H-a}dx=\frac{1}{\bar{K}}\int_0^{\xi}\frac{\int_0^x \frac{dy}{1+K'(y)/\bar{K}}}{bx+H-a}dx \tag{S.1}$$

Taylor series expansion of $\frac{1}{1+K'/\bar{K}}$ about 1 gives

$$\frac{1}{1+K'/\bar{K}}=1-\frac{K'}{\bar{K}}+\left(\frac{K'}{\bar{K}}\right)^2+.... \tag{S.2}$$

Substitution of (S.2) into (S.1) yields

$$\frac{t}{\theta}=\frac{1}{\bar{K}}\int_0^{\xi}\frac{x}{bx+H-a}dx-\frac{1}{\bar{K}^2}\int_0^{\xi}\frac{\int_0^x K'(y)dy}{bx+H-a}dx+\frac{1}{\bar{K}^3}\int_0^{\xi}\frac{\int_0^x K'^2(y)dy}{bx+H-a}dx+... \tag{S.3}$$

Expanding about $\bar{\xi}$ yields

$$\frac{t}{\theta}=\frac{1}{\bar{K}}\int_0^{\bar{\xi}+\xi'}\frac{x}{bx+H-a}dx-\frac{1}{\bar{K}^2}\int_0^{\bar{\xi}+\xi'}\frac{\int_0^x K'(y)dy}{bx+H-a}dx+\frac{1}{\bar{K}^3}\int_0^{\bar{\xi}+\xi'}\frac{\int_0^x K'^2(y)dy}{bx+H-a}dx+...$$

$$= \frac{1}{\overline{K}} \int_0^{\overline{\xi}} \frac{x}{bx+H-a} dx + \frac{1}{\overline{K}} \frac{\overline{\xi}}{b\overline{\xi}+H-a} \xi' + \frac{1}{\overline{K}} \frac{H-a}{\left(b\overline{\xi}+H-a\right)^2} \frac{(\xi')^2}{2}$$

$$- \frac{1}{\overline{K}^2} \int_0^{\overline{\xi}} \frac{\int_0^x K'(y)dy}{bx+H-a} dx - \frac{1}{\overline{K}^2} \frac{\int_0^{\overline{\xi}} K'(y)dy}{b\overline{\xi}+H-a} \xi' \qquad \text{(S.4)}$$

$$+ \frac{1}{\overline{K}^3} \int_0^{\overline{\xi}} \frac{\int_0^x K'^2(y)dy}{bx+H-a} dx + \frac{1}{\overline{K}^3} \frac{\int_0^{\overline{\xi}} K'^2(y)dy}{b\overline{\xi}+H-a} \xi' + \ldots$$

Taking the mean of (S.4)

$$\frac{t}{\theta} = \frac{1}{\overline{K}} \int_0^{\overline{\xi}} \frac{x}{bx+H-a} dx + \frac{1}{\overline{K}} \frac{H-a}{\left(b\overline{\xi}+H-a\right)^2} \frac{\overline{\xi'\xi'}}{2}$$

$$- \frac{1}{\overline{K}^2} \frac{\int_0^{\overline{\xi}} \overline{K'(y)\xi'} dy}{b\overline{\xi}+H-a} + \frac{1}{\overline{K}^3} \int_0^{\overline{\xi}} \frac{\int_0^x \overline{K'^2}(y)dy}{bx+H-a} dx + \ldots \qquad \text{(S.5)}$$

Expanding (S.5) in power of σ_Y, noting that $\overline{\xi}^{(1)} = 0$ (from 2.24) and

$$\frac{1}{\overline{K}} = \frac{1}{K_G} \frac{1}{1+\sigma_Y^2/2+\ldots} = \frac{1}{K_G}\left(1 - \frac{\sigma_Y^2}{2} + \ldots\right), \qquad \text{(S.6)}$$

and retaining up to second order terms:

$$\frac{t}{\theta} = \frac{1}{K_G} \int_0^{\xi^{(0)}} \frac{x}{bx+H-a} dx + \frac{1}{K_G} \frac{\xi^{(0)}}{b\xi^{(0)}+H-a} \overline{\xi}^{(2)} + \frac{1}{K_G} \frac{H-a}{\left(b\xi^{(0)}+H-a\right)^2} \frac{\left[\sigma_\xi^2\right]^{(2)}}{2}$$

$$- \frac{1}{K_G} \frac{\int_0^{\xi^{(0)}} C_{Y\xi}(y,\xi^{(0)})dy}{b\xi^{(0)}+H-a} + \frac{\sigma_Y^2}{2K_G} \int_0^{\xi^{(0)}} \frac{x}{bx+H-a} dx \qquad \text{(S.7)}$$

Collecting terms of the same order gives expressions for zero- and second-order mean front positions:

$$\frac{t}{\theta}=\frac{1}{K_G}\int_0^{\xi^{(0)}}\frac{x}{bx+H-a}dx=\frac{1}{K_G}\frac{1}{b}\left(\xi^{(0)}-\frac{H-a}{b}\ln\frac{b\xi^{(0)}+H-a}{H-a}\right) \tag{S.8}$$

and

$$\bar{\xi}^{(2)}=\frac{1}{\xi^{(0)}}\int_0^{\xi^{(0)}}C_{Y\xi}(y,\xi^{(0)})dy-\frac{\sigma_Y^2}{2}\frac{b\xi^{(0)}+H-a}{\xi^{(0)}}\int_0^{\xi^{(0)}}\frac{x}{bx+H-a}dx$$
$$-\frac{H-a}{\xi^{(0)}\left(b\xi^{(0)}+H-a\right)}\frac{\left[\sigma_\xi^2\right]^{(2)}}{2} \tag{S.9}$$

or

$$\bar{\xi}^{(2)}=\frac{1}{\xi^{(0)}}\int_0^{\xi^{(0)}}C_{Y\xi}^{(2)}(y,\xi^{(0)})dy-\frac{H-a}{\xi^{(0)}\left(b\xi^{(0)}+H-a\right)}\frac{\left[\sigma_\xi^2\right]^{(2)}}{2}$$
$$-\frac{\sigma_Y^2}{2}\frac{b\xi^{(0)}+H-a}{b\xi^{(0)}}\left(\xi^{(0)}-\frac{H-a}{b}\ln\frac{b\xi^{(0)}+H-a}{H-a}\right) \tag{S.10}$$

Expression (S.8) is the same as (4.17). Correspondence between (S.10) and (4.25)-(4.26) is discussed later.

Covariance $C_{Y\xi}$

Subtraction of (S.5) from (S.4) gives

$$0=\frac{1}{\overline{K}}\frac{\overline{\xi}}{b\overline{\xi}+H-a}\xi'-\frac{1}{\overline{K}^2}\int_0^{\overline{\xi}}\frac{\int_0^x K'(y)dy}{bx+H-a}dx-\frac{1}{\overline{K}^2}\frac{\int_0^{\overline{\xi}}K'(y)\xi'dy}{b\overline{\xi}+H-a}$$
$$+\frac{1}{\overline{K}^3}\int_0^{\overline{\xi}}\frac{\int_0^x K'^2(y)dy}{bx+H-a}dx+\frac{1}{\overline{K}^2}\frac{\int_0^{\overline{\xi}}\overline{K'(y)\xi'}dy}{b\overline{\xi}+H-a}-\frac{1}{\overline{K}^3}\int_0^{\overline{\xi}}\frac{\int_0^x\overline{K'^2(y)}dy}{bx+H-a}dx \qquad \text{(S.11)}$$
$$+\frac{1}{\overline{K}}\frac{H-a}{\left(b\overline{\xi}+H-a\right)^2}\frac{\left(\xi'\right)^2}{2}-\frac{1}{\overline{K}}\frac{H-a}{\left(b\overline{\xi}+H-a\right)^2}\frac{\sigma_\xi^2}{2}+\ldots$$

Multiplying by $K'(z)$, taking mean and retaining terms to second order yields

$$\frac{\xi^{(0)}C_{Y\xi}^{(2)}(z,t)}{b\xi^{(0)}+H-a}=\int_0^{\xi^{(0)}}\frac{\int_0^x C_Y^{(2)}(z,y)dy}{bx+H-a}dx \qquad \text{(S.12)}$$

This is the same as (M.14) in Appendix M.

Front variance

Multiplying (S.11) by ξ', taking ensemble mean and retaining terms to second-order gives

$$\left[\sigma_\xi^2\right]^{(2)}=\frac{b\xi^{(0)}+H-a}{\xi^{(0)}}\int_0^{\xi^{(0)}}\frac{\int_0^x C_{Y\xi}^{(2)}(y,t)dy}{bx+H-a}dx \qquad \text{(S.13)}$$

It can be demonstrated numerically that (S.13) is identical to (4.23).

Second-order mean front position

Substituting (S.13) into (S.10) gives

$$\bar{\xi}^{(2)} = \frac{1}{\xi^{(0)}} \int_0^{\xi^{(0)}} C_{Y\xi}^{(2)}(y, \xi^{(0)}) dy - \frac{H-a}{2\left(\xi^{(0)}\right)^2} \int_0^{\xi^{(0)}} \frac{\int_0^x C_{Y\xi}^{(2)}(y,t) dy}{bx + H - a} dx$$
$$- \frac{\sigma_Y^2}{2} \frac{b\xi^{(0)} + H - a}{b\xi^{(0)}} \left(\xi^{(0)} - \frac{H-a}{b} \ln \frac{b\xi^{(0)} + H - a}{H-a} \right) \qquad \text{(S.14)}$$

where $\int_0^{\xi^{(0)}} C_{Y\xi}(y, \xi^{(0)}) dy$ is given by (4.24).

It can be demonstrated numerically that (S.14) is identical to (4.25)-(4.26).

APPENDIX T

NUMERICAL SOLUTION

We compute front propagation for a medium having log conductivity $Y(\mathbf{x})$ with constant mean and exponential covariance function

$$C_Y\left(|\mathbf{x}-\mathbf{y}|\right)=\sigma_Y^2 \exp\left(\sqrt{\frac{(x_x-x_y)^2}{l_x^2}+\frac{(z_x-z_y)^2}{l_z^2}}\right) \tag{T.1}$$

where l_x and l_z are correlation lengths in the x and z directions, respectively. Due to symmetric boundary conditions the front is symmetric with respect to the z axis.

For simplicity, we set $l_x=\infty$ which renders all second moments to be symmetric (e. g. $C_{YV}(\mathbf{x};x_y,z_y t)=C_{YV}(\mathbf{x};-x_y,z_y t)$).

To parameterize the front we select $N+1$ nodal points at equal arclength separations running from p=0 at the tip (located along the channel axis where x=0) to $p = N$ at the wall of the channel (where x=c, c being half width of the channel). We define a midpoint j to lie midway between p - 1 and p so that j runs from 1 to N. Our dependent variables are defined at j, $\alpha_j^{[t]}=\alpha^{[t]}(s_j^{[t]})$. The corresponding coordinates $x_p^{[t]}$ and $z_p^{[t]}$ are given by

$$x_p^{[t]}=x_{p-1}^{[t]}+\Delta s^{[t]}\cos\alpha_p^{[t]} \qquad p=1,\ldots N \tag{T.2}$$

$$z_p^{[t]}=z_{p-1}^{[t]}-\Delta s^{[t]}\sin\alpha_p^{[t]} \qquad p=1,\ldots N \tag{T.3}$$

subject to $x_0^{[t]}$=0 and $x_N^{[t]}$=c.

Computation of zero-order front position

To calculate zero-order front position we use a modified code originally written by D. Kessler. We start by solving (5.16) for the normalized normal velocities $v^{(0)}(\mathbf{x}_p,t)=\frac{\theta}{K_G}V_n^{(0)}(\mathbf{x}_p,t)$, p = 0,...N. To do so, we approximate (5.16) using the trapezoidal rule according to

$$\sum_{p=-N}^{N} G_K^{(0)}(\mathbf{y}_n^{(0)},\mathbf{y}_p^{(0)})v^{(0)}(\mathbf{y}_p^{(0)})\Delta s^{(0)}+M^{(0)}=0 \qquad \text{for } n=-N,\ldots N \tag{T.4}$$

From symmetry $v(\mathbf{y}_p)=v(\mathbf{y}_{-p})$ and we can reduce the number of unknowns in (T.4):

$$G_K^{(0)}(\mathbf{y}_n,\mathbf{y}_0)v^{(0)}(\mathbf{y}_0,t)\Delta s^{(0)}+\sum_{p=1}^{N}\left[G_K^{(0)}(\mathbf{y}_n,\mathbf{y}_p)+G_K^{(0)}(\mathbf{y}_n,\mathbf{y}_{-p})\right]v^{(0)}(\mathbf{y}_t,t)\Delta s^{(0)}+M^{(0)}=0$$

for n =0,...N (T.5)

The system (T.5) includes N +2 unknowns ($v(s_p,t)$, p=0...N and $M^{(0)}$) but only N+1 equations. An additional equation is obtained from condition (5.14),

$$\sum_{p=0}^{N} v^{(0)}(\mathbf{y}_p^{(0)},t)\Delta s^{(0)}=\tilde{Q} \tag{T.6}$$

where $\tilde{Q}=\frac{Q}{2cK_G}$ is dimensionless flow rate.

After computing $v^{(0)}(\mathbf{y}_p)$, discretizing (5.24) allows us to calculate $\frac{d\alpha_j^{(0)}}{dt}$, $j=1,\ldots, N$ and solve for $\alpha_j^{(0)}$ by a predictor corrector method. We do so by using the LSODE code that is part of the SLATEC package (A. C. Hindmarsh, 1980). LSODE uses a backward differentiation scheme. Based on a newly determined $\alpha_j^{(0)}$ we compute a new zero-order front position using (T.2) and (T.3).

Calculating second-order velocity requires computing the residual flux $\mathbf{r}$, $\nabla h^{(0)}$ and cros-covariances C_{YV}, C_{YY}, as well as domain integrals associated with these terms.

Computation of $\nabla h^{(0)}$

Head gradients are obtained explicitly from (5.8) as

$$\frac{\partial h^{(0)}(\mathbf{x},t)}{\partial x_{\mathbf{x}}} = \sum_{p=-N}^{N} \frac{\partial G_K^{(0)}(\mathbf{x},\mathbf{y}_p)}{\partial x_{\mathbf{x}}} v^{(0)}(\mathbf{y}_p,t)\Delta s^{(0)} \tag{T.7}$$

$$\frac{\partial h^{(0)}(\mathbf{x},t)}{\partial y_{\mathbf{x}}} = \sum_{p=-N}^{N} \frac{\partial G_K^{(0)}(\mathbf{x},\mathbf{y}_p)}{\partial y_{\mathbf{x}}} v^{(0)}(\mathbf{y}_p,t)\Delta s^{(0)} \tag{T.8}$$

Computation of cross-covariance $C_{YV}(\mathbf{x},\mathbf{x}_\gamma)$

$C_{YV}(\mathbf{x},\mathbf{x}_\gamma)$ represents cross-covariance between Y at any point $\mathbf{x}$ in the domain occupied by water and normal velocity at any point $\mathbf{x}_\gamma$ on the front. For any point $\mathbf{x}$ there are $2N+1$ discrete $C_{YV}(\mathbf{x},\mathbf{x}_i)$ values.

Discretization of (5.20) gives

$$\sum_{p=-N}^{N} C_{Yv}^{[2]}(\mathbf{x},\mathbf{y}_p)G_K^{(0)}(\mathbf{y}_n,\mathbf{y}_p)\Delta s^{(0)} + m_1(\mathbf{x})$$
$$= \sum_{p=-N}^{N}\sum_{k=0}^{K_p} C_Y^{[2]}(\mathbf{x},\mathbf{y}_{pk})\left(\nabla_y h^{(0)}(\mathbf{y},t)\bullet\nabla_y G_K^{(0)}(\mathbf{y}_n,\mathbf{y})\right)\Big|_{\mathbf{y}=\mathbf{y}_{pk}} \Delta z_p \Delta s^{(0)}\cos\alpha_p^{(0)} \qquad n=-N,\ldots N \qquad \text{(T.9)}$$

where $C_{Yv}^{[2]}(\mathbf{x},\mathbf{y}) = \dfrac{\theta}{K_G} C_{YV}^{[2]}(\mathbf{x},\mathbf{y})$, $\alpha_0^{(0)} = 0$, K_p=integer[$(D\text{-}z_p)$ / $\Delta s^{(0)}$], $\Delta z_p = (D\text{-}z_p)/ K_p$ for $k \neq 0$ or K_p and Δz_p =0.5 $(D\text{-}z_p)$ / K_p otherwise, $\mathbf{y}_{pk}=[x_p,\ z_p+k\Delta z_p]^T$ and $\mathbf{y}_p=[x_p\ ,\ z_p]^T$ (Figure 5.2).

(T.9) is a system of $2N+1$ equations in $2N+2$ unknowns. An additional equation is obtained from condition (5.21),

$$\sum_{p=-N}^{N} C_{Yv}^{[2]}(\mathbf{x},\mathbf{y}_p)\Delta s^{(0)} = 0 \qquad \text{(T.10)}$$

Under the assumption $l_x = \infty$, the number of unknowns in (T.9) reduces to $N+2$ due to symmetry.

Computation of residual flux

Knowing the zero-order head gradient and second-order cross-covariance $C_{Yv}^{[2]}(\mathbf{x},\mathbf{x}_t)$, the residual flux is calculated explicitly from

$$r_x^{[2]}(\mathbf{x},t) = -\sum_{p=-N}^{N} C_{Yv}^{[2]}(\mathbf{x},\mathbf{y}_p)\frac{\partial G_K^{(0)}(\mathbf{x},\mathbf{y}_p)}{\partial x_x}\Delta s^{(0)}$$
$$+\sum_{p=-N}^{N}\sum_{k=0}^{K_p} C_Y^{[2]}(\mathbf{x},\mathbf{y}_{pk})\left(\frac{\partial h^{(0)}(\mathbf{y},t)}{\partial x_y}\frac{\partial^2 G_K^{(0)}(\mathbf{x},\mathbf{y})}{\partial x_y \partial x_x}+\frac{\partial h^{(0)}(\mathbf{y},t)}{\partial z_y}\frac{\partial^2 G_K^{(0)}(\mathbf{x},\mathbf{y})}{\partial z_y \partial x_x}\right)_{\mathbf{y}=\mathbf{y}_{pk}} \Delta z_p \Delta s^{(0)}\cos\alpha_p^{(0)} \qquad \text{(T.11)}$$

$$r_z^{[2]}(\mathbf{x},t) = -\sum_{p=-N}^{N} C_{Yv}^{[2]}(\mathbf{x},\mathbf{y})\frac{\partial G_K^{(0)}(\mathbf{x},\mathbf{y}_p)}{\partial z_{\mathbf{x}}}\Delta s^{(0)}$$
$$+\sum_{p=-N}^{N}\sum_{k=0}^{K_p} C_Y^{[2]}(\mathbf{x},\mathbf{y}_{pk})\left(\frac{\partial h^{(0)}(\mathbf{y},t)}{\partial x_{\mathbf{y}}}\frac{\partial^2 G_K^{(0)}(\mathbf{x},\mathbf{y})}{\partial x_{\mathbf{y}}\partial z_{\mathbf{x}}}+\frac{\partial h^{(0)}(\mathbf{y},t)}{\partial z_{\mathbf{y}}}\frac{\partial^2 G_K^{(0)}(\mathbf{x},\mathbf{y})}{\partial z_{\mathbf{y}}\partial z_{\mathbf{x}}}\right)_{\mathbf{y}=\mathbf{y}_{pk}}\Delta z_p \Delta s^{(0)}\cos\alpha_p^{(0)} \tag{T.12}$$

Computation of second-order front position

We start by solving equation (5.17) for the second-order mean normalized normal velocities $v^{[2]} = \frac{\theta}{K_G}\bar{V}_n^{[2]}$ at the front,

$$M^{[2]} + v^{[2]}(\mathbf{y}_0^{[2]})G_K^{(0)}(\mathbf{y}_n^{[2]},\mathbf{y}_0^{[2]})\Delta s^{[2]}$$
$$+\sum_{p=1}^{N} v^{[2]}(\mathbf{y}_p^{[2]},t)\left(G_K^{(0)}(\mathbf{x}_n^{[2]},\mathbf{y}_{-p}^{[2]})+G_K^{(0)}(\mathbf{x}_n^{[2]},\mathbf{y}_p^{[2]})\right)\Delta s^{[2]}$$
$$=-\sum_{p=-N}^{N}\sum_{k=0}^{K_p}\left[\mathbf{r}^{[2]}(\mathbf{y},t)\bullet\nabla_{\mathbf{y}}G_K^{(0)}(\mathbf{y}_n^{[2]},\mathbf{y})\right]_{\mathbf{y}=\mathbf{y}_{pk}^{(0)}}\Delta z_t \Delta s^{(0)}\cos\alpha_p^{(0)} \qquad \text{for } n=0,\ldots N \tag{T.13}$$
$$-\sum_{p=-N}^{N} C_{Y\gamma}^{[2]}(\mathbf{y}_p^{(0)},\mathbf{y}_p^{(0)})\left[\nabla h^{(0)}(\mathbf{y},t)\bullet\nabla_{\mathbf{y}}G_K^{(0)}(\mathbf{y}_n^{[2]},\mathbf{y})\right]_{\mathbf{y}=\mathbf{y}_p^{(0)}}\Delta s^{(0)} - \frac{\sigma_Y^2}{2}M^{(0)}$$

and

$$\sum_{p=0}^{N} v^{[2]}(\mathbf{y}_p^{[2]})\Delta s^{[2]} = \tilde{Q} \tag{T.14}$$

This is a system of N+2 equations in N+2 unknowns ($v^{[2]}(\mathbf{y}_p)$, p=0,...N, and $M^{[2]}$). Solving it for $v^{[2]}$ allows us to compute second-order front positions in the same way as we did for the zero-order front.

Computation of normal velocity variance

Discretization of equations (5.26) and (5.27) gives a system of $2N+2$ equations for the second-order normalized normal velocity covariance $C_v^{[2]} = \frac{\theta^2}{K_G^2} C_V^{[2]}$ between point $\mathbf{y}_l$ and any point $\mathbf{y}_i$ at the front, i=-N,...N:

$$m_2(\mathbf{y}_l^{(0)}) + \sum_{p=-N}^{N} C_v^{[2]}(\mathbf{y}_l^{(0)}, \mathbf{y}_p^{(0)}) G^{(0)}(\mathbf{y}_n^{(0)}, \mathbf{y}_p^{(0)}) \Delta s^{(0)} \qquad n=-N,\ldots N$$
$$= \sum_{i=-N}^{N} \sum_{k=0}^{K_i} C_{Yv}^{[2]}(\mathbf{y}_l^{(0)}, \mathbf{y}_{pk}^{(0)}) \left[\nabla_y h^{(0)}(\mathbf{y}, t) \bullet \nabla_y G^{(0)}(\mathbf{y}_n^{(0)}, \mathbf{y}) \right]_{\mathbf{y}=\mathbf{y}_{pk}^{(0)}} \Delta z_p^{(0)} \Delta s^{(0)} \cos\alpha_p^{(0)} \qquad \text{(T.15)}$$

and

$$\sum_{p=-N}^{N} C_v^{[2]}\left(\mathbf{y}_l^{(0)}, \mathbf{y}_p^{(0)}\right) \Delta s^{(0)} = 0 \qquad \text{(T.16)}$$

Setting l=i yields the variance of normal front velocity at point $\mathbf{y}_l$. To compute variances of normal velocity at all nodes along the front we need to solve the above system for l=0,...N. Under the assumption that $l_x = \infty$, $C_v(\mathbf{y}_l, \mathbf{y}_p) = C_v(\mathbf{y}_l, \mathbf{y}_{-p})$ and the number of unknowns in (T.15) reduces to N+2.

REFERENCES

Brower, R. C., D. A. Kessler, J. Koplic and H. Levine, Geometrical approach to moving-interface dynamics, Phys. Rev. Lett., 51, 1111-1114, 1983.

Chang, W.L., Biggar, J.W. and Nielsen, D.R., Fractal description of wetting front instability in layered soils. Water Resour. Res., 30, 125-132, 1994.

Chen, G., M. Taniguchi, and S. P. Neuman, An Overview of Instability and Fingering During Immiscible Groundwater Flow in Porous and Fractured Media, NUREG/CR-6308, prepared for U. S. Nuclear Regulatory Commission, Washington, D. C., May, 1995.

Chen, G. and S. P. Neuman, Wetting front instability in randomly stratified soils, Phys. Fluids A, 8(2), 353-369, 1996.

Chuoke, R. L., P. van Meurs, and C. van der Poel, The instability of slow, immiscible, viscous liquid-liquid displacements in permeable media, Trans. AIME, 216, 188-194, 1959.

Christakos, G., D. T. Hristopulos, Stochastic radon operators in porous media hydrodynamics, Quarterly of Applied Mathematics, 55 (1), 89-112, 1997.

de Rooij, G. H., Modeling fingered flow of water in soils owing to wetting front instability: a review, Journal of Hydrology, v. 231-232, 277-294, 2000.

Dagan, G., Flow and transport in porous formations, springer Verlag, New York, 1989.

Du, X., T. Yao, W. D. Stone, J. M. H. Hendrickx, Stability analysis of the unsaturated water flow equation 1. Mathematical derivation, Water Resour. Res., 37(7), 1869-1874, 2001.

Gau, H.-S., Liu, C.-W. and Tsao, Y.-S., Stochastic analysis of immiscible displacement in porous media, Adv. Water Resour, 21, 605-615, 1998.

Glass, R. J. J.-Y. Parlange, and T.S. Steehuis, Immiscible displacements in porous media: Stability analysis of three-dimensional, axissymetric disturbance with application to gravity-driven wetting front instability, Water Resour. Res., 27, 1947-1956, 1991.

Glass, R. J., S. H. Conrad and W. Peplinski, Gravity-destabilized nonwetting phase invasion in macroheterogeneous porous media: Experimental observations of invasion dynamics and scale analysis, Water Resour. Res., 36(11), 3121-3137, 2000.

Glass, R. J., S. H. Conrad and L. Yarrington, Gravity-destabilized nonwetting phase invasion in macroheterogeneous porous media: Near-pore-scale macro modified invasion percolation simulation of experiments, Water Resour. Res., 37(5), 1197-1207, 2001.

Gradshteyn, I. S. and I. M. Ryzhik, Table of integrals, series, and products: Fifth edition, Academic press, San Diego, 1994.

Green, W. H. and G. A. Ampt, Studies in soil physics, I. The flow of air and water through soil, J. Agr. Sci., 4, 1-24, 1911.

Guadagnini, A. and S. P. Neuman, Nonlocal and localized analyses of conditional mean steady state flow in bounded, randomly nonuniform domains 1. Theory and computational approach, Water Resour. Res., 35 (10), 2999-3018, 1999.

Gupta, S. P., and R. A. Greenkorn, An experimental study of immiscible displacement with an unfavorable mobility ratio in porous media, Water Resour. Res., 10, 371-374, 1974.

A. C. Hindmarsh, Association for Computing Machinery (ACM) – Signum Newsletter 15,10-17, 1980.

Hollenbeck, K. J. and K. H. Jensen, Experimental evidence of randomness and nonuniqueness in unsaturated outflow experiments designed for hydraulic parameter estimation, Water Resour. Res., 34(4), 595-602 1998.

Indelman, P., Averaging of unsteady flows in heterogeneous media of stationary conductivity, J. Fluid Mech., 310, 39-60, 1996.

Kasteel, R., I. Forrer, H. Flühler, K. Roth, Solute transport estimated by field- and laboratory-determined hydraulic parameters, Proceedings of the International Workshop on Characterization and Measurement of the Hydraulic Properties of Unsaturated Porous Media, Riverside, CA, 1997, edited by M. T. van Genuchten, F. J. Leij, and L. Wu, 1485-1494, Univ. of Calif. Riverside, 1999.

D. Kessler, J. Koplic and H. Levine, Numerical simulation of two-dimensional snowflake growth, Physical Review A, 30(5), 2820-2823, 1984.

Kessler, D., J. Koplic and H. Levine, Dendritic growth in the channel, Physical Review A, 34(6), 4980-4987, 1986.

Li, G., D. Kessler and L.Sender, Sidebranching of the Saffman-Taylor finger, Physical Review A, 34(4), 3535-3538, 1986.

Longino, B. L. and B. H. Kuper, Nonwetting phase retention and mobilization in rock fractures, Water Resour. Res., 35(7), 2085-2093, 1999.

Maxworthy, T., The nonlinear growth of a gravitational unstable interface in a Hele-Shaw cell, J. Fluid Mech., 177, 207-232, 1987.

Mineev-Weinstein and Selvina Dawson, Class of nonsingular solutions for Laplacian pattern formation, Physical Review E, Vol. 50, 1, 24-27, July 1994.

Mortensen, A. P., R. J. Glass, K. Hollenbeck, K. H. Jensen, Visualization of microscale phase displacement processes in retention and outflow experiments: Nonuniqueness of unsaturated flow properties, Water Resour. Res., 37(6), 1627-1640, 2001.

Neuman, S. P., Gas leakage through fractures from storage cavities below the water table due to interface instability, Research report, 1982.

Neuman, S.P., Role of Geostatistics in Subsurface Hydrology, 787-816 in Geostatistics for Natural Resources Characterization, Part 2, edited by G. Verly, M. David, A.G. Journal, and A. Marechal., D. Reidel Publ. Co., Dordrecht, Holland, 1984.

Neuman, S. P. and S. Orr, Prediction of steady-state flow in nonuniform geologic media by conditional moments – exact nonlocal formalism, effective conductivities, and weak approximation, Water Resour. Res., 29 (2), 341-364, 1993.

Nizovtsev, V.V., O. V. Panchenko and R. G. Garifullin, , Investigation into the instability of water front under satiation of a modeled ground. Eurasian Soil Sci, 31, 149-152, 1998.

Pankow, J. F. and J. A. Cherry, Dense chlorinated solvents and others DNAPLs in Groundwater Waterlow press, Portland, Oregon, 1996.

Park, C. –W. and G. M. Homsy, The instability of long fingersin Hele-Shaw flows, Phys. Fluids, 28, 1983-1585, 1985.

Pierre, Dynamics of curved fronts, Academic Press, San Diego, 1988.

Philip J. R., Stability analysis of infiltration, Soil Sci. Soc. Amer. Proc., 39, 1042-1053, 1975.

Raats, P. A., Unstable wetting fronts in uniform and non-uniform soils, Soil Sci. Soc. Am. Proc., 37, 681-685, 1973.

Saffman P.G. and G.I. Taylor, The penetration of a fluid into a porous medium or Hele-Shaw cell containing a more viscous fluid, Proc. Roy. Soc. London, Ser. A, 245, 312-320, 1958.

Schwille, F., Dense chlorinated Solvents, Lewis Publishers, Chelsea, Michigan, 1988.

Shariati, M. and Y.C. Yortsos, Stability of miscible displacements across stratified porous media, Phys. Fluids, 13(8), 1, 2001.

Sililo OTN, Tellam J.H., Fingering in unsaturated zone flow: A qualitative review with laboratory experiments on heterogeneous systems, Ground Water, 38 (6), 864-871 2000.

Smith, J. E., Z. F. Zhang, Determining effective interfacial tension and predicting finger spacing for DNAPL penetration into water-saturated porous media, J Contam. Hydrol. 48 (1-2), 167-183, 2001.

Stolte, J., J. I. Freijer, W. Bouten, C. Dirksen, J. M. Halbertsma, J. C. van Dam, J. A. van den berg, G. J. Veerman, J. H. M. Wösten, Comparison of six methods to determine unsaturated soil hydraulic conductivity, Soil Sci. Soc. Am. J., 58 1596-1603 1994.

Tartakovsky, D. M. and S. P. Neuman, Transient effective hydraulic conductivities under slowly and rapidly varying mean gradients in bounded three-dimensional random media, Water Resour. Res., 34(1), 21-32, 1998.

Tartakovsky, D. M., Stochastic modeling of heterogeneous phreatic aquifers, Water Resour. Res. 35(12), 3941-3945 DEC 1999.

Tartakovsky, D. M. and C. L. Winter, Dynamics of free surfaces in random porous media, SIAM Journal of Applied Math., 61(6), 1857-1876, 2001.

Zhang, D., Stochastic methods for flow in porous media. Coping with uncertainties, Academic Press, San Diego, 2002.

Zhang, Z. F. and J. E. Smith, The velocity of DNAPL fingering in water-saturated porous media: laboratory experiments and a mobile-immobile-zone model, J Contam. Hydrol. 49(3-4), 335-353, 2001.

van Dam, J. C., J. N. M. Stricker, P. Droogers, Inverse method to determine soil hydraulic functions from multistep outflow experiments, Soil Sci. Soc. Am. J., 58, 647-652, 1994.
Wang, Z., J. Feyen and C. J. Ritsema, Susceptibility and predictability of conditions for preferential flow, Water Resour. Res., 34(9), 2169-2182, 1998.

Wang, Z., J. Feyen and D. E. Elrick, Prediction of fingering in porous media. Water Resour. Res., 34(9), 2183-2190, 1998.

Winter, C. L., C. M. Newman and S. P. Neuman, A perturbation expansion for diffusion in random velocity-field, SIAM Journal on Applied Mathematics, 44(2), 411-424, 1984.

Yao T, Hendrickx JMH Stability analysis of the unsaturated water flow equation 2. Experimental verification, Water Resour. Res., 37(7), 1875-1881, 2001.

Yeh, T. C. J., Stochastic modeling of groundwater flow and solute transport in aquifers, Hydrological Processes, 6, 369-395, 1992.

Yortsos, Y.C. and A. B. Huang, Linear-stability analysis of immiscible displacement: Part 1—Simple basic flow profiles, SPE Reservoir Engng, 378-390, 1986.